Oxygen-sensitive Regulation of Na,K-ATPase in Rat Heart

Dissertation

zur

Erlangung der naturwissenschaftlichen Doktorwürde

(Dr. sc. nat)

vorgelegt der

Mathematisch-Naturwissenschaftlichen Fakultät

der

Universität Zürich

von

Sergey Sergeevich Yakushev

aus

Russland

Promotionskomitee

Prof. Dr. Max Gassmann (Vorsitz)

PD Dr. Anna Yu. Bogdanova (Leitung der Dissertation)

Prof. Dr. Carsten Wagner

Prof. Dr. Kaethi Geering

Zürich, 2012

Table of Contents

Abreviations

AKAP	A-kinase anchoring protein
AngII	Angiotensin II
AP-1	Activator protein 1
AV node	Atrioventricular node
BH4	Tetrahydrobiopterin
BLASTP	Basic Local Alignment Search Tool Protein
CaMK	Ca^{2+}/calmodulin-dependent Protein Kinase
CBF	Coronary Blood Flow
CTS	Cardiotonic Steroids
DG	Diacylglycerol
ECG	Electrocardiogram
EGFR	Epidermal Growth Factor Receptor
eNOS	Endothelial Nitric Oxide Synthase
ERK1/2	Extracellular Signal-Regulated Kinase 1/2
ESL	External Sarcolemma
FSTL1	Follistatin-like 1
GPx	Glutathione Peroxidase
GRX1	Glutaredoxin 1
GSH	Reduced Glutathione
GSNO	Nitrosylated Glutathione
GSSG	Oxidized Glutathione
iNOS	Inducible Nitric Oxide Synthase
IP3	Inositol Triphosphate
ITC	Isothermal Titration Calorimetry
L-NAME	N^G-Nitro-L-Arginine Methyl Ester
LTCC	L-Type Calcium Channel
MALDI	Matrix-Assisted Laser Desorption/Ionization Time-Of-Flight Mass Spectroscopy
MAPK	Mitogen Activated Protein Kinase
MEK	Mitogen Activated Protein Kinase Kinase
mtNOS	Mitochondrial Nitric Oxide Synthase
NAK	Na,K-ATPase
NCX	Na/Ca-exchanger
NF-kappaB	Nuclear Factor Kappa-light-chain-enhancer of activated B-cells
NHE	Na/H-exchanger
nNOS	Neuronal Nitric Oxide Synthase
NO	Nitric Oxide
NOS	Nitric Oxide Synthase
PAX	Paired Box Gene
PI3K	Phosphoinositide 3-Kinase
PKA	Protein Kinase A
PKG	Protein Kinase G
PLB	Phospholamban
PLC	Phospholipase C
PLM	Phospholemman
PMCA	Plasma Membrane Ca^{2+} -ATPase
Raf	Rapidly Accelerated

	Fibrosarcoma Kinase
Ras	Rat Sarcoma small GTPase
RNS	Reactive Nitrogen Species
ROS	Reactive Oxygen Species
SERCA	Sarcoplasmic/Endoplasmic Reticulum Calcium ATPase
SOD	Superoxide Dismutase
SR	Sarcoplamic Reticulum
Src	Sarcoma Tyrosine Kinase
TT	Transversal Tubuli
UCP	Uncoupling Protein
WI	Work Index
XO	Xanthine Oxidase

Summary

Responsible for about 20% of total ATP expenditure in the heart, the Na,K-ATPase sustains the transmembrane Na^+/K^+ gradients that generate action potentials. Furthermore, this enzyme actively participates in the regulation of contractile force as it is functionally coupled to the Na^+/Ca^{2+} exchanger.

Local or global hypoxia causes acute changes in the myocardial function. Oxygen-induced regulation of the Na,K-ATPase activity in the heart is of particular importance for successful adaptation to hypoxia. Indirect evidence suggests that the enzyme does not respond to changes in O_2 availability, but to resulting shifts in the tissue redox state and nitric oxide production[1-3][1-3]. In the heart Na,K-ATPase is composed of the catalytic α- (α1 and α2), regulatory β-subunit and phospholemman. Whereas modulation of the enzyme activity in response to S-glutathionylation of the β-subunit has been reported, possible involvement of the 23 cysteines of the α-subunit in oxygen-induced regulation of the enzyme has not been addressed. This study was designed to assess hypoxia-induced reversible thiol modifications (S-nitrosylation and S-glutathionylation) in the catalytic α-subunit and associate them with the changes in hydrolytic activity of Na,K-ATPase in response to deoxygenation. We have monitored the hypoxia-induced changes in nitric oxide availability, tissue redox status, thiol modifications of the α-subunit and the concomitant alterations in Na,K-ATPase activity in the Wistar rat heart. We have also analyzed the role of thiol modifications in adaptation of the heart to hypoxia and compared hypoxia tolerant (Blind subterranean mole rat Spalax) and hypoxia sensitive (Norwegian rat) animals. We found that Na,K-ATPase in Wistar rat myocardium shows a profound sensitivity to oxygen availability. Oxygen-induced regulation of the Na,K-ATPase in Wistar rat heart is NO- and redox-dependent and is mediated through thiol modifications of the catalytic subunit.

We have detected the presence of basal and regulatory S-glutathionylation sites in the α-subunit of the Na,K-ATPase. Binding of glutathione to the Cys454, 458, 459 and Cys244 was associated with complete inhibition of the enzyme. The inhibitory

action of S-glutathionylation was caused by occlusion of the adenine nucleotide binding site by glutathione.

Na,K-ATPase function in *Spalax* myocardium is preserved during hypoxic exposure. Lack of inhibitory response of Na,K-ATPase to hypoxia in *Spalax* heart was associated with the absence of hypoxia-induced changes is redox state.

Taken together this work shows molecular mechanism of inhibition of Na,K-ATPase in Wistar rat heart in response to hypoxia. This mechanism is triggered by the decrease in NO production and tissue oxidation and involves occlusion of the adenine nucleotide binding site by glutathionylation of cystine residues in the catalytic subunit of the enzyme.

Zusammenfassung

Die Na,K-ATPase ist ein oligomerisches Membranprotein das verantwortlich für den zellulären transmembranen Natrium und Kalium Ionentransport ist. Im Herzen ist sie am Aufbau des Aktionspotential beteiligt und reguliert die Schlagkraft. Zudem spielt die Na,K-ATPase eine wichtige Rolle in der zellulären Reaktion des Herzens bei Sauerstoffunterversorgung (Hypoxie). Es gibt jedoch Hinweise, dass dieses Enzyms nicht direkt durch die Sauerstoffkonzentration gesteuert wird sondern durch eine Änderung des Redoxstatus im Gewebe und durch die Produktion von Stickstoffmonoxid.

Es wurde gezeigt, dass die Enzymaktivität durch eine Redoxmodifikation von Cysteinen an der β-Untereinheit moduliert werden kann, dennoch gibt es diesbezüglich keine Untersuchungen an der α-Untereinheit, die 23 Cysteine enthält. Das Ziel dieser Doktorarbeit war zu prüfen, ob eine Hypoxie Cysteinmodifikationen in der α-Untereinheit der Na,K-ATPase induziert und ob diese mögliche Modifikation die Funktion des Enzyms im hypoxischen Myokard beeinflusst. Folgende Parameter wurden unter hypoxischen Bedingungen im Myokard untersucht: Stickstoff-Monoxid Verfügbarkeit, Redoxstatus des Gewebes, Cysteinmodifikationen der α-Untereinheit der Na,K-ATPase bei gleichzeitigen Aktivitätsmessungen des Enzyms.

Zudem wurde die Rolle der Cysteinmodifikationen bei der Adaptation des Herzens an hypoxische Bedingungen untersucht, und im Vergleich bei hypoxietoleranten und hypoxieempfindlichen Tieren betrachtet.

Wir konnten zeigen, dass die Na,K-ATPase in Wistar Rattenherzen sehr empfindlich auf die Verfügbarkeit von Sauerstoff reagiert. Die sauerstoffabhängige Regulation des Enzyms ist abhängig vom Redoxstatus des Gewebes und der Cysteinmodifiktionen der α-Untereinheit. Die Bindung von Glutathion an die Cysteine 454, 458, 459 und 244 verursacht eine Blockierung der ATP-Bindungsstelle und führt zu einer Inaktivierung der Na,K-ATPase.

Interessanterweise war die Funktion der Na,K-ATPase bei hypoxietoleranten Tieren unter Hypoxie nicht beeinträchtigt, da sich der Redoxstatus des Gewebes bei diesen Tieren unter hypoxischen Bedingungen nicht ändert.
Zusammenfassend beschäftigt sich diese Studie mit den molekularen Mechanismen der Inhibierung der Na,K-ATPase in Wistar Rattenherzen unter hypoxischen Bedingungen. Dieser Mechanismus ist durch eine Gewebeoxidierung und eine verminderte NO-Bildung gesteuert, was eine Glutathionylierung der Cysteine in der katalytischen Untereinheit des Enzyms bewirkt, wodurch Adenin-Nukleotid-Bindingsstellen blockiert werden.

Introduction

1. Na,K-ATPase: structure, isoforms, composition, cycle of functioning

The Na,K-ATPase belongs to the family of P-type ATPases (Table 1) that are responsible for building and maintenance of electrochemical gradients in the living organisms.

Table 1. P-type ATPase family (adopted from [4])

Family	Bacteria	Archaea	Fungi	Plants	Invertebrates	Vertebrates	Specificity	Function
PIa	★	★					$(K^+)^a$	Turgor pressure regulation
PIb	★	★	★	★	★	★	Cu^+, Cu^{2+}, Ag^+, Cd^{2+}, Zn^{2+}, Pb^{2+}, Co^{2+}	Detoxification, trace element homeostasis
PIIa	★	★	★	★	★	★	Ca^{2+}, Mn^{2+} (incl. SERCA)	Ca^{2+} transport, signaling, muscle relaxation, trace element homeostasis
PIIb			★	★	★	★	Ca^{2+} (incl. PMCA)	Ca^{2+} transport (plasma membrane), signaling
PIIc			★		★	★	Na^+/K^+, H^+/K^+	Plasma membrane potential, kidney function, stomach acidification
PIId			★		★		Na^+, Ca^{2+}	Unknown
PIIIa	★	★	★	★			H^{+b}	Plasma membrane potential, pH homeostasis
PIIIb	★						$(Mg^{2+})^c$	Unknown
PIV			★	★	★	★	Phospholipids	Lipid transport, lipid-bilayer asymmetry
PV			★	★	★	★	Unknown	Unknown

Source: P-type ATPase Database; http://traplabs.dk/patbase/.

a Through concerted function of a K^+ conducting KdpA subunit.

b Occurrence in bacteria detected by a novel sequence analysis tool (B. Pedersen, unpublished data).

c Mg^{2+} transport has not been demonstrated.

Na,K-ATPase is composed of two obligatory subunits α (catalytic) and β (regulatory), which form αβ heterodimer or some higher order oligomer $(\alpha\beta)_n$ [5]. Although the α-subunit provides catalytic functions (it contains ATP binding site, phosphorylation and dephosphorylation domains and ion transport pore, Figure 1), hydrolytic activity of the enzyme is minimal in the absence of β-subunit.
In some tissues Na,K-ATPase is found as a heterotrimer with α-, β-subunits and FXYD subunit, the latter mediating additional fine-tuning of the enzyme activity [6].

1.1 Alpha-subunit structure and catalytic cycle of the enzyme

Na,K-ATPase uses the energy of hydrolysis of 1 ATP molecule to transport 2 K^+ into the cell and 3 Na^+ out of the cell.
The catalytic subunit of Na,K-ATPase conducts ATP binding and hydrolysis as well as binding and translocation of ions across plasma membrane. This cyclic activity is associated with large conformational changes as the enzyme shuttles between two distinct enzymatic states: The E1 state is characterized by the high-affinity for Na^+ whereas the affinity of Na,K-ATPase to Na^+ in E2 state is low. The two states are introduced in Alberts Post model (Figure 2) of the Na,K-ATPase function to describe a sequence of formation and breakdown of a phosphoenzyme intermediate, coupled to the binding, occlusion, translocation and release of ions.
In the E2 state, ATP is bound at the N domain of the catalytic α-subunit. The N-domain shown in pink in Figure 1 contains motifs that form the hydrophobic ATP binding pocket. The N-domain sequence alignment analysis within the group of PII-family ATPases (see Table 1) reveals five residues that are strictly conserved: Lys501, Gly502, Ala503, Glu505 and Cys511. These amino acids are essential for nucleotide binding [7]. ATP binding to the N domain stimulates an E2-to-E1 transition. Since the crystal structure is only available for the E2 state of the Na,K-ATPase [8], the localization of amino acid residues in the E1 state is still deduced based on a crystal structure of the homologous Ca^{2+} pump.
The transmembrane α-helixes M1-M6 form the membrane transport core highlighted in light blue in Figure 1, contains 2 K^+ binding sites, which overlap with

2 out of 3 Na^+ binding sites. Transmembrane helixes M7-M10 form intramembrane helix cluster marked in purple in Figure 1 provides support for the two centrally placed ion binding sites at the transmembrane core and possibly harbors a charge translocation module and a binding site for the third Na^+ ion. In the E1 state, Na^+ ions are bound to the α-subunit.

The ATP phosphate groups reach towards the P (phosphorylation, kinase) domain shown in dark blue in Figure 1 with conserved Asp369, to which the γ-phosphate of the ATP molecule is transferred. Phosphorylation of the α-subunit results in the formation of E1P state. The following conformational changes in cytosolic domains cause movement of M1 and M2 helixes within the transport core towards the cytoplasmic site, so the bound Na^+ ions are occluded inside the cytoplasmic half-channel (a gated channel structure that spans approximately half of the membrane bilayer and leads to a central binding site).

Structural K^+ binding site (shown in in Figure 1) is a part of the P-domain. Binding of one K^+ to it facilitates the docking of the A domain during catalysis and dephosphorylation of the α-subunit.

The A (anchor or actuator) domain shown in yellow in Figure 1 conducts dephosphorylation of the P domain. Conformational changes provided by the movement of this domain lead to the opening of a wide half-channel from the extracellular side of the membrane. The resulting E2P state promotes release of three occluded Na^+ ions into the extracellular space and binding of two K^+ to the enzyme. Upon binding of K^+ ions, dephosphorylation of P-domain occurs catalyzed by the TGE motif of A-domain (shown in Figure 1), bringing the enzyme into the E2 state. In this state K^+ ions are occluded within the pore. Binding of the ATP molecule stimulates E2 to E1 transition and release of K^+ ions into the cytosol [9]. Mg^{2+} is essential for all phosphate transfer reactions and for the E1P to E2P conversion in Na,K-ATPase [10]. The above-mentioned events known as Alberts-Post cycle are summarized schematically in Figure 2 [11].

Under optimal conditions in purified enzyme preparations the overall reaction rate can reach ~10000 cycles/min [12]. However, under physiological conditions, the local ATP availability limits the rate to 1500-5000 cycles/min [13].

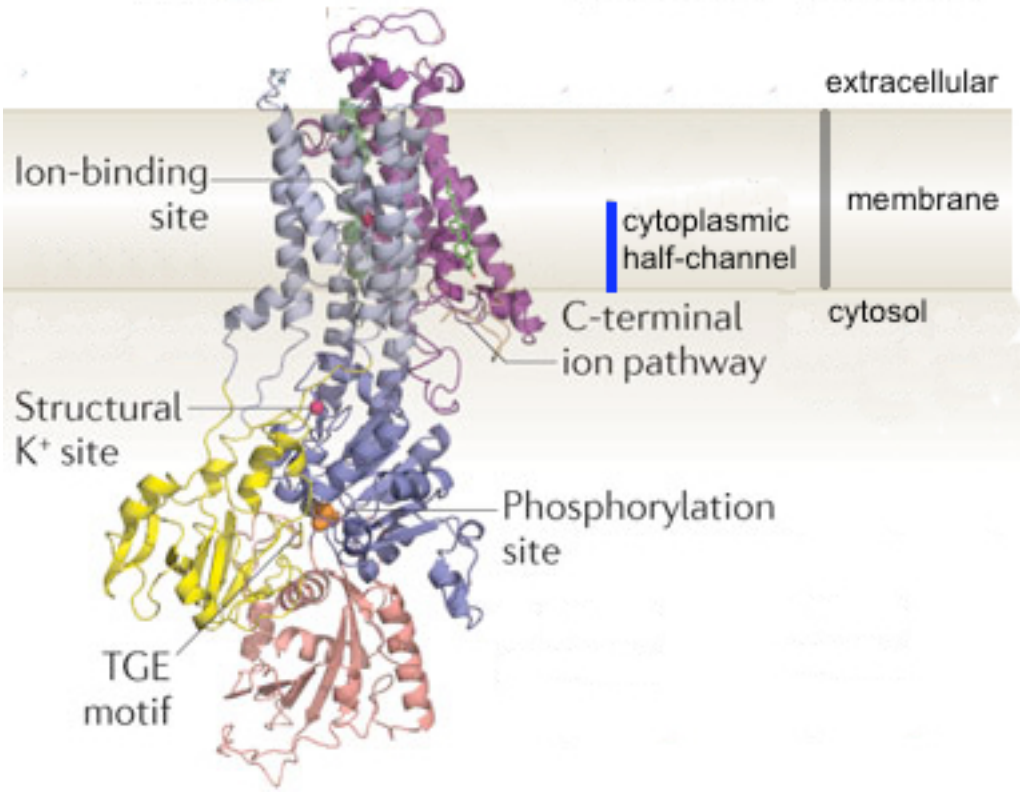

Figure 1. The domain organization of α-subunit of Na,K-ATPase. Pink – N domain, light blue – membrane transport core, purple - intramembrane helix cluster, dark blue – P domain, yellow – A domain [9].

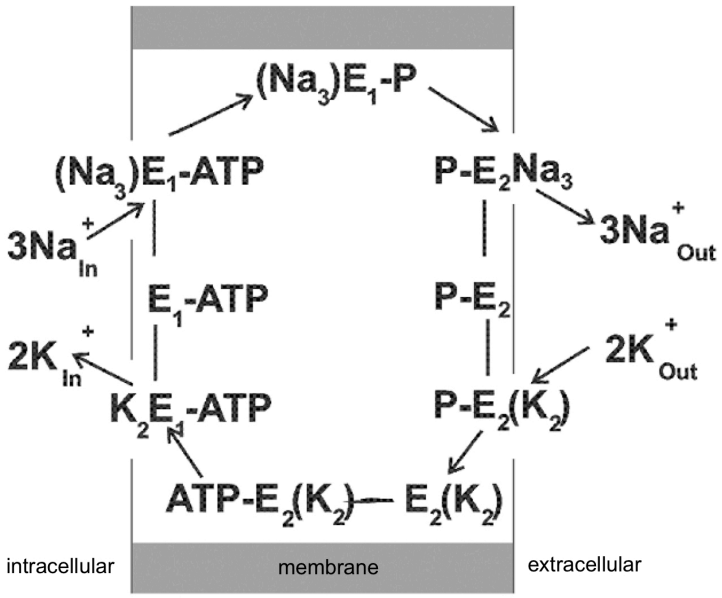

Figure 2. The Albers-Post reaction cycle (adopted from [14]). E1-ATP – E1 state of the enzyme with bound ATP, E1-P – phosphorylated E1 state, P-E2 – phosphorylated E2 state. For detail description see text.

1.2 Beta-subunit

This subunit contains one transmembrane helix. Most of the mass of the protein is exposed to the extracellular space and the N-terminal segment situated in the cytoplasm. The extracellular part of the subunit contains three sites of N-glycosylation and three S-S bridges between cysteines. The S-S bridges and N-glycosylation sites are highly conserved in all species [15].

Orientation of both folded α- and β-subunits in the membrane is shown in Figure 3. The transmembrane region of β-subunit is twisted around intramembrane helix cluster of the α-subunit interacting with M7 helix of the latter.

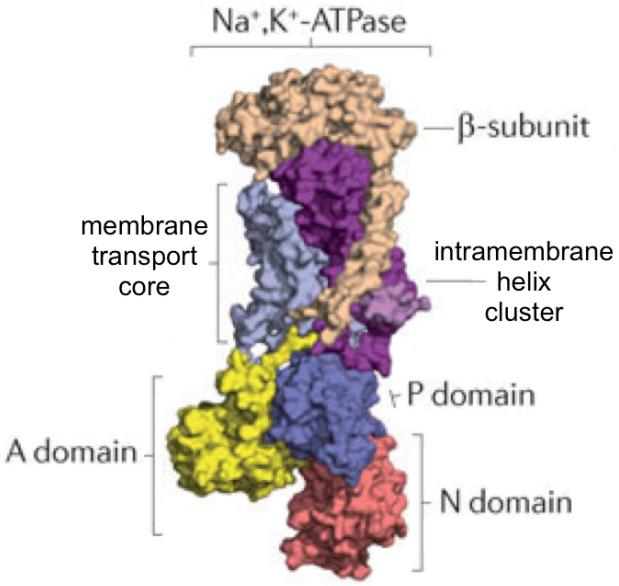

Figure 3. Orientation of folded α- and β-subunit in structure of Na,K-ATPase, from [9].

Interaction of its transmembrane helix with M7 helix of α-subunit facilitate the formation of transmembrane segment structures that are crucial for the interaction of the membrane transport domain with K^+, thus contributing to the assembly of K^+ binding site [9]. Recent findings reveal that redox-sensitive modifications of cysteines of β-subunit affect the catalytic subunit function (discussed in the section "Regulation of Na,K-ATPase activity") [16].

The β-subunit is important for translocation of its heterodimer with catalytic subunit of the Na,K-ATPase to the membrane [17-22]. Furthermore, β-subunit participates in formation of $(\alpha\beta)_n$ oligomers [23].

1.3 FXYD subunit

This subunit is presented in mammals with 7 members, including phospholemman (PLM, or FXYD1) specific for the heart tissue. This small (7-14 kDa) protein mainly contains one transmembrane domain and its intracellular C-terminus is involved in interaction with αβ dimer. Most FXYD proteins act as tissue-specific modulators of the Na,K-ATPase function, their interaction with the Na-pump changes the enzyme affinity to Na^+, K^+ or ATP [24, 25].

1.4 Phylogeny of α- and β-subunits

Four isoforms of the α- and three of the β-subunits have been identified, their phylogenetic trees are shown in Figure 4 A and B.

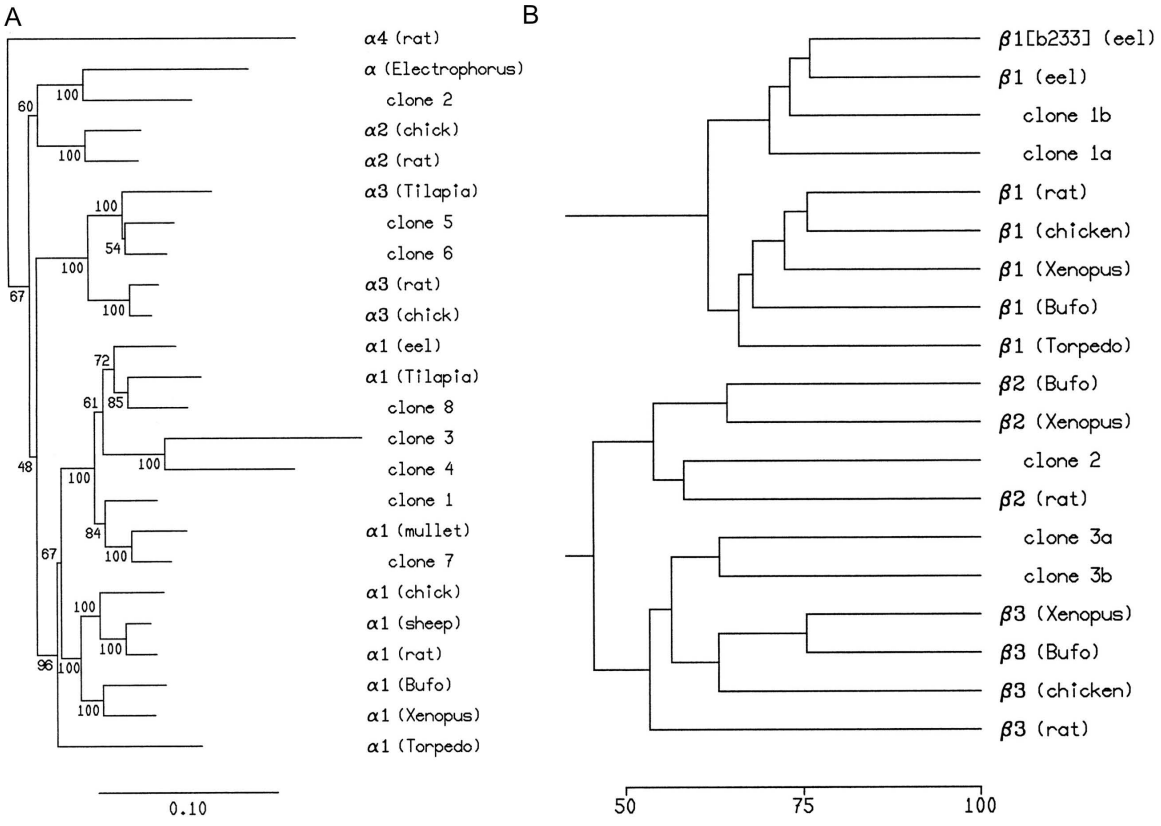

Figure 4. *A.* Phylogenetic analysis of vertebrate Na,K-ATPase α-subunits. Consensus tree generated using the distance matrix method with the scale of evolutionary distances below. Numbers at each branch point indicate percent support from bootstrap analysis. Na,K-ATPase α-subunit sequences were obtained from SwissProt or GenBank: rat α1 (atn_rat), α2 (atn2_rat), α3 (atn3_rat), and α4 (AAB81285); chicken α1 (atn1_chick), α2 (atn2_chick), and α3 (atn3_chick); sheep α1 (atn1_sheep); Bufo marinus α1 (atn1_bufma); Xenopus laevis α1 (atn1_xenla); European eel α1 (atna_angan); Tilapia mossambica α1(AAD11455) and α3 (AAF75108); mullet α1 (atna_catco); Torpedo californica α1 (atna_torca) . *B.* Sequence relatedness of Na,K-ATPase β-subunits. Dendrogram of amino acid sequence similarity was constructed using the PILEUP program. The scale at the bottom indicated percent identity between β-subunits. Sequences were obtained from SwissProt or GenBank: European eel β1 (atnb_angan) and β1 isoform b233 (CAB85586); rat β1 (atnb_rat), β2 (atnc_rat), and β3 (atnd_rat); chicken β1 (atnb_chick) and β3 (atnd_chick); Xenopus laevis β1 (AAA82967), β2 (CAC08235), and β3 (atnd_xenla), Bufo marinus β1 (atnb_bufma), β2 (atnc_bufma), and β3 (atnd_bufma); Torpedo californica β1 (atnb_torca) [26].

In humans, four isoforms of the Na,K-ATPase α-subunit have been identified: α1 is the predominant and ubiquitously expressed isoform, α2 is mainly expressed in skeletal, heart and smooth muscle, as well as in brain, lung and adipose tissue, and α3 is primarily expressed by neurons and heart cells. Isoform α4 is expressed only in testes where it contributes to the mobility of spermatozoa.

Of three isoforms of the β-subunit β1 is found in most tissues and is thought to form a ubiquitously expressed α1β1 Na,K-ATPase complex. Beta2 is predominantly expressed by neurons and, to some degree, by heart cells in rats, and β3 is expressed in testes and has also been detected in neurons during early brain development in *Xenopus laevis* [9]. Figure 5 illustrates amino acid homology among the different α and β isoforms.

Although combination of four α and three β isoforms can potentially result in twelve αβ isozymes, only six of them are described. These isozymes vary in their affinities for Na^+, K^+, ATP and ouabain (specific inhibitor of Na,K-ATPase) (Tables 2 and 4) and display different reaction kinetics [27, 28]. Differences in their affinities for substrates and inhibitors as well as stringent tissue-specific expression pattern and sub-cellular localisation of different isoforms of the α- and β-polypeptides under various physiological conditions are essential in adapting cellular Na,K-ATPase

activity to specific physiological requirements, providing plasticity in function and responses to stress [29].

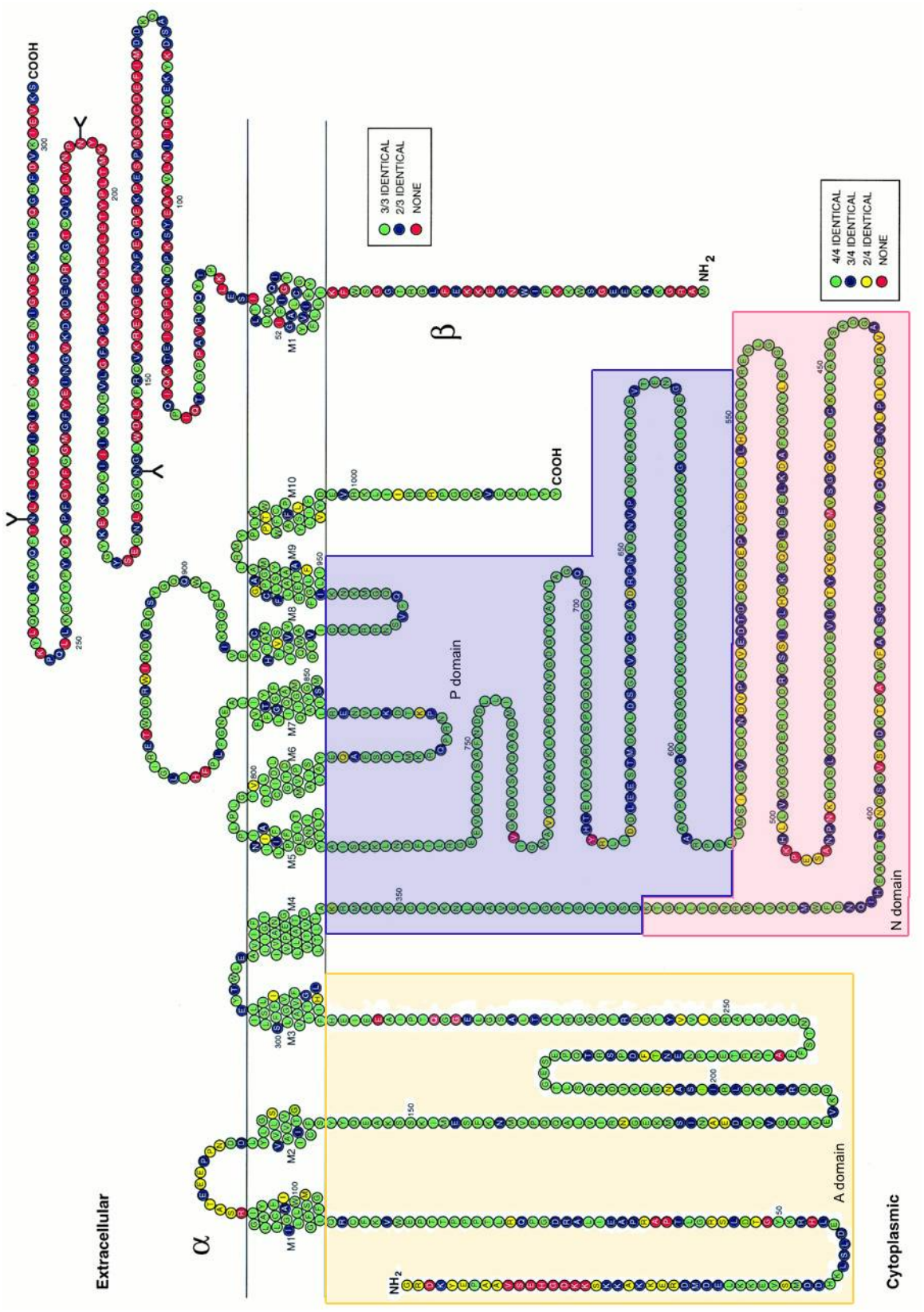

Figure 5. Scheme of the membrane topology of the α- and β-isoforms of the Na-K-ATPase. Sequences of rat α1- and β1-isoforms are shown. Residues color-coding indicates the amino acid homology among the different α-isoforms (α1, α2, α3, and α4) or β-isoforms (β1, β2, and β3) [29].

2. Na,K-ATPase: role in the heart functioning, isoform specialization, localization and distribution in cardiac tissue

2.1 Na,K-ATPase and energy consumption

Several studies have been performed to estimate the contribution of the Na,K-ATPase into the energy turnover in different types of tissues including the myocardium. Direct measurements in the beating heart are hard to perform because inhibition of Na,K-ATPase with cardiac glycosides is known to stimulate respiration of the cells [30, 31]. However, extrapolation of the observations on oxygen consumption [32], analysis of energy transfer with ^{32}P NMR spectroscopy of perfused heart [33], and mathematical simulations of ATP metabolism in cardiac excitation–contraction coupling [34] suggest that in the contracting heart at rest Na,K-ATPase requires 1-5% of total energy turnover [35], where the actomyosin ATPase, Ca-ATPase and protein synthesis require 40-50%, 15-30% and ~3%, respectively [32, 35].

2.2 Na,K-ATPase and ion handling

Main physiological outcome of Na,K-ATPase function is creation of a transmembrane Na^+/K^+ gradient critical for maintenance of resting membrane potential and cell volume [36]. Once generated, Na^+ gradient is used as a driving force for secondary-active uptake of amino acids, sugars and other organic molecules [37].

An adult heart is built up of different types of cells: of which ~30% are cardiomyocytes, ~64% are fibroblasts, and ~6% represent other cell types (i.e. vascular tissue cells, neurons etc.) [38]. Action potential and contractile function of cardiomyocytes are supported by Na,K-ATPase maintaining the resting membrane

potential and influencing Na^+ content in the "fuzzy space", controlling thereby the Ca^{2+} homeostasis [39]. Maintenance of Na^+/K^+ gradient is carried out in the heart by 3 isozymes of Na,K-ATPase α1, α2 and α3.

2.3 Isoform specialization, localization and distribution of Na,K-ATPase in cardiomyocytes

Na,K-ATPase content in the heart tissue was estimated to be ~2200 pmol/g wet weight [40, 41]. The proportion of different isoforms of the catalytic α-subunit, presented in the heart is ~74% α1, ~25% α2 and 1% α3 [42]. In cardiomyocytes α2-subunit is ~ 4.5-fold more abundant in t-tubes (TT) than in the external sarcolemma (ESL), whereas α1-isoform is practically uniformly distributed between the TT and ESL (Figure 6) [42-45].

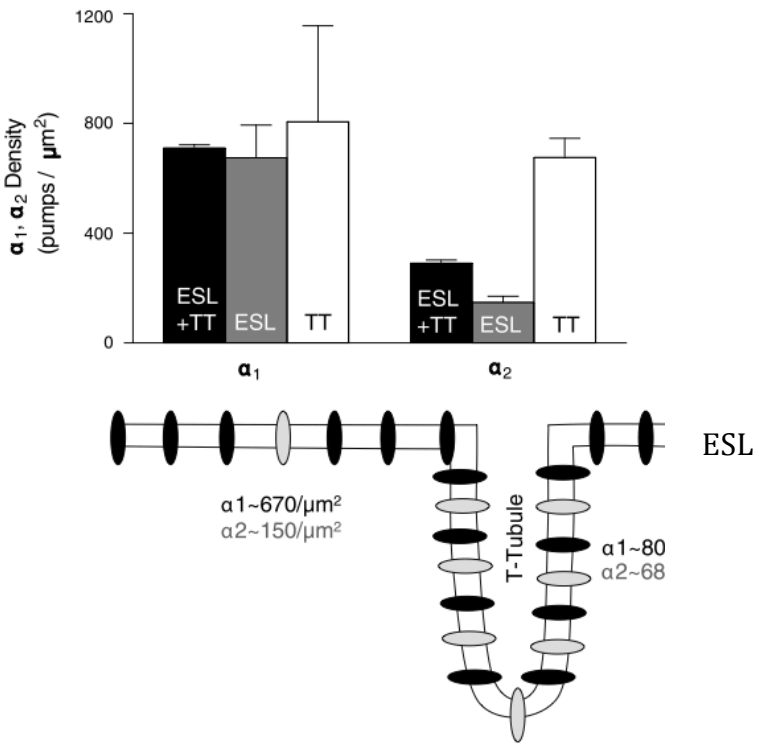

Figure 6. Distribution of α-subunit isoforms in T-tubes and external sarcolemma (ESL) of cardiomyocyte [43].

Na,K-ATPase in TT of rat cardiomyocytes colocalizes with Na^+/Ca^{2+} exchanger [46]. Targeting of both transporters to the TT is coordinated by ankyrin B [47]. In addition, Na^+/Ca^{2+} exchanger in the cardiomyocytes is shown to share the FXYD1 subunit with Na,K-ATPase, and phosphorylation of FXYD1 results in activation of Na,K-ATPase and inhibition of Na^+/Ca^{2+} exchanger [48]. Experiments with mouse models, lacking either α1 or α2 isoforms in the heart, showed that Na-pump units containing the α2- but not the α1-subunit are in control of Na^+ content in the fuzzy space of cardiomyocytes, intracellular region of restricted diffusion, dyadic cleft space, bordered by the sarcolemmal membrane on one side and the junctional sarcoplasmic reticulum membrane on the opposing side (Figure 7).

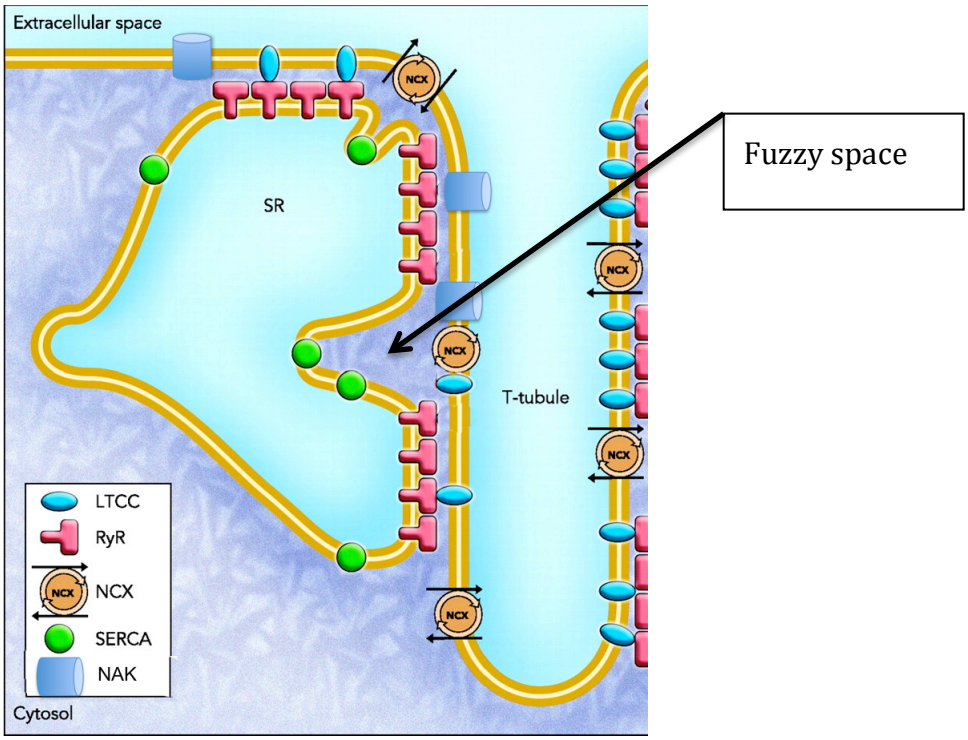

Figure 7. Schematically presented fuzzy space. SR – sarcoplasmic reticulum, LTCC – L-type Ca^{2+} channel, NCX – Na^+/Ca^{2+} exchanger, RyR - Ryanodine receptor, SERCA – Ca-ATPase, NAK – Na,K-ATPase (adopted from [49]).

Sodium content in fuzzy space can modulate Ca^{2+} influx via reverse Na^+/Ca^{2+} exchanger (NCX) [50, 51]. In rodent heart the α2 isoform, has a higher sensitivity to cardiac glycosides, compared to α1 [52]. This results in the selective inhibition of the activity of α2 isoform and fine modulation of Ca^{2+} homeostasis and contractility of rodent heart by endogenous ouabain-like factors (cardiac glycosides) [53].

Positive inotropic effect has been shown to follow selective inhibition of α2 isoform in mouse heart [54].

3. Cardiac glycosides and cardiac Na,K-ATPase

3.1 Cardiac glycosides and ion handling

Cardiac glycosides are specific inhibitors of Na,K-ATPase [55]. This family of compounds contains over 200 members. These substances may be generally divided into exogenous (poisons of different plants: Strophanthus, Digitalis etc. [56]) and endogenous ones (cardiotonic steroids: ouabain, marinobufagenin, bufalin, etc.[57]). All of the compounds interact with a specific, high affinity binding site for cardiac glycosides on the extracellular part of the catalytic subunit of the Na,K-ATPase [58]. Of note sensitivity of the enzyme to certain cardiac glycosides depends on isoform of Na,K-ATPase. Differential affinity of the Na,K-ATPase isozymes is illustrated in Table 2 [29].

Table 2 Sensitivity of different rat Na,K-ATPase isozymes to ouabain [29].

Isozyme	**Ouabain Inhibition K_i, M**
α1 β1	$4.3 \pm 1.9 \times 10^{-5}$
α2 β1	$1.7 \pm 0.1 \times 10^{-7}$
α2 β2	$1.5 \pm 0.2 \times 10^{-7}$
α3 β1	$3.1 \pm 0.3 \times 10^{-8}$
α3 β2	$4.7 \pm 0.4 \times 10^{-8}$

Na,K-ATPase isozymes of a rat and other rodents are known for the pronounced (orders of magnitude) difference in affinities to ouabain and other cardiotonic steroids between the α1β and α2/α3β heterodimers. Although present, this

difference in sensitivity to cardiotonic steroids is much less conspicuous in Na,K-ATPase of other species [59-62].

Inhibition of Na,K-ATPase in cardiomyocytes results in a transient increase in the intracellular Na^+, which causes activation of the Na^+/Ca^{2+} exchange system and Ca^{2+} uptake from the extracellular medium. These Ca^{2+} ions are taken up into the sarcoplasmic reticulum by sarcoplasmic Ca-ATPase (SERCA2A). Elevation of Ca^{2+} content in the sarcoplasmic reticulum stores results in augmentation of contractile force and to an increase in cardiac output [63]. Uncontrolled up-regulation of Ca^{2+} uptake may cause formation of necrotic lesions in the heart due to "Ca^{2+} overload" making therapeutic use of cardiotonic steroids rather dangerous [64].

Mechanism of action of cardiac glycosides on Ca^{2+} levels and the resulting inotropic effect is schematically presented in Figure 8.

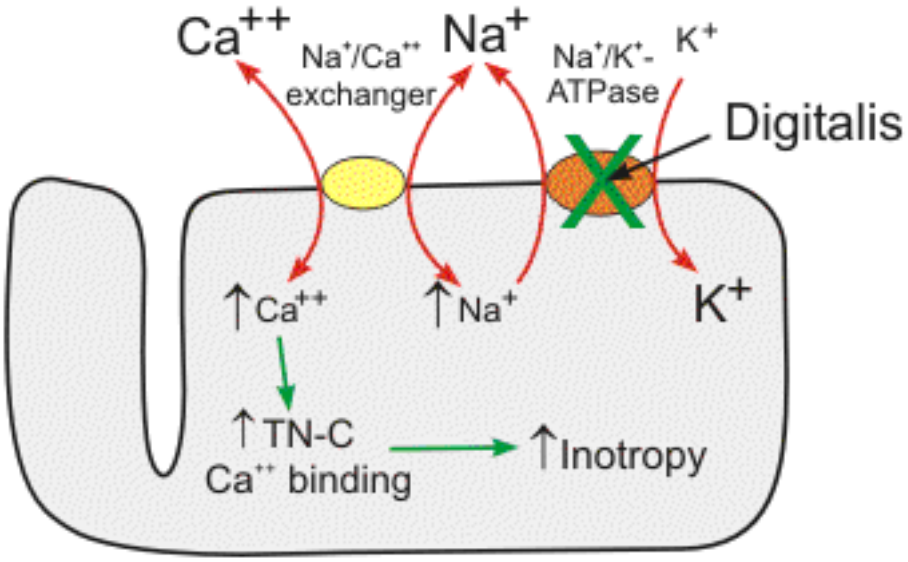

Figure 8. By inhibiting the Na/K-ATPase, cardiac glycosides cause elevation in Na^+ content in the "fuzzy space". This then leads to calcium uptake via the reversed Na^+/Ca^{2+} exchange system. The rise in intracellular Ca^{2+} is taken up by the sarcoplasmic reticulum via sarcoplasmic Ca-ATPase. Because of the elevated Ca^{2+} content in the sarcoplasmic reticulum, more Ca^{2+} can be released when the cardiomyocyte is stimulated, thereby making more calcium available to bind to troponin-C (TN-C). Thereby contractile force is increased [65].

Secondary to increased intracellular Ca^{2+}, are the effect of digitalis on the excitation generation and propagation in the heart. The changes in ECG observed in response

to digitalis administration reveal reduction in conduction rate through the AV node [66]. With the suppression of Na,K-ATPase activity comes a reduction in the ability of the conductive tissues to maintain their resting transmembrane potential of -80 to -90mv. Suppression of the Na,K-ATPase causes gradual depolarization due to the loss of transmembrane Na^+/K^+ gradients. As depolarization reaches a threshold level the excitability of the conduction tissues rises. Repolarization remains incomplete and firing occurs prematurely (phase 4 in Figure 9). At the ECG the changes in excitation propagation caused by digitalis treatment are manifested as an inversion of T-wave and a shorter R-T interval and a net positive chronotropic effect [67].

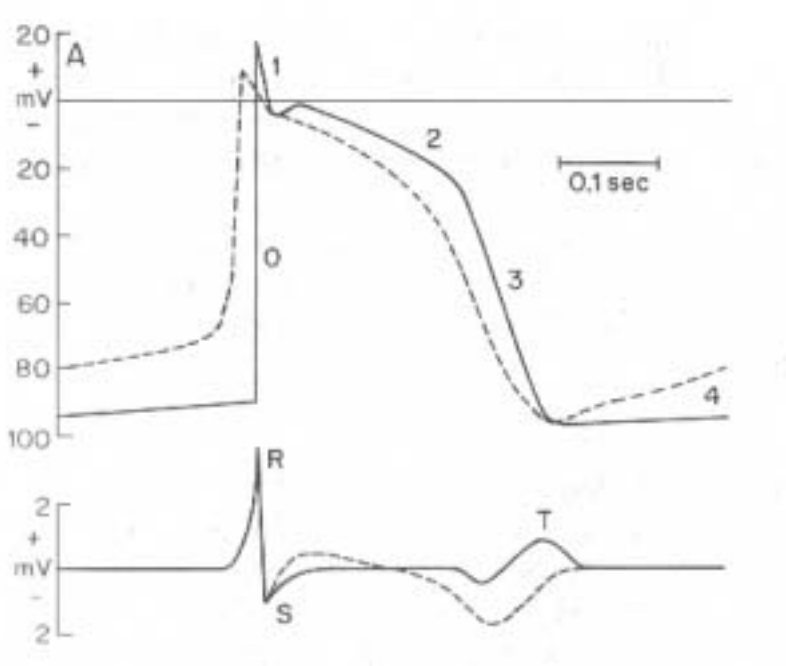

Figure 9. Unipolar recording of a transmembrane action potential from a Purkinje fiber (upper panel) and ECG (lower panel). Control conditions are traced with a solid line, digitalized tissue with dashed line [68].

3.2 Cardiac glycosides and Na,K-ATPase as a signaling molecule

At present role of cardiac glycosides is not limited to that of blockers of active transport of cations. At picomolar to nanomolar concentrations these compounds are suggested to act as hormones using Na,K-ATPase as a receptor. Binding of low doses of cardiac glycosides to the ATPase triggers assembly of a signaling protein complex and generation of downstream signaling cascade. A number of

investigations show, that cardiac glycosides regulate endocytosis of Na,K-ATPase [69], control growth of cardiomyocytes, participate in gene regulation and Ca^{2+} signaling [70, 71].

Interaction of cardiac glycosides with Na,K-ATPase results in recruitment of SRC-kinase/ epidermal growth factor receptor complex [72], and other interacting partners and activation of multiple signal pathways, which include PLC/IP3/CICR, PI3K, PLC/DG/PKC/Raf/MEK/ERK1/2, and Ras/Raf/MEK/ERK1/2 pathways. In several cell types direct interaction with PI3K [73] was observed.
The schematic representation of the action of cardiac glycosides is shown in Figure 10.

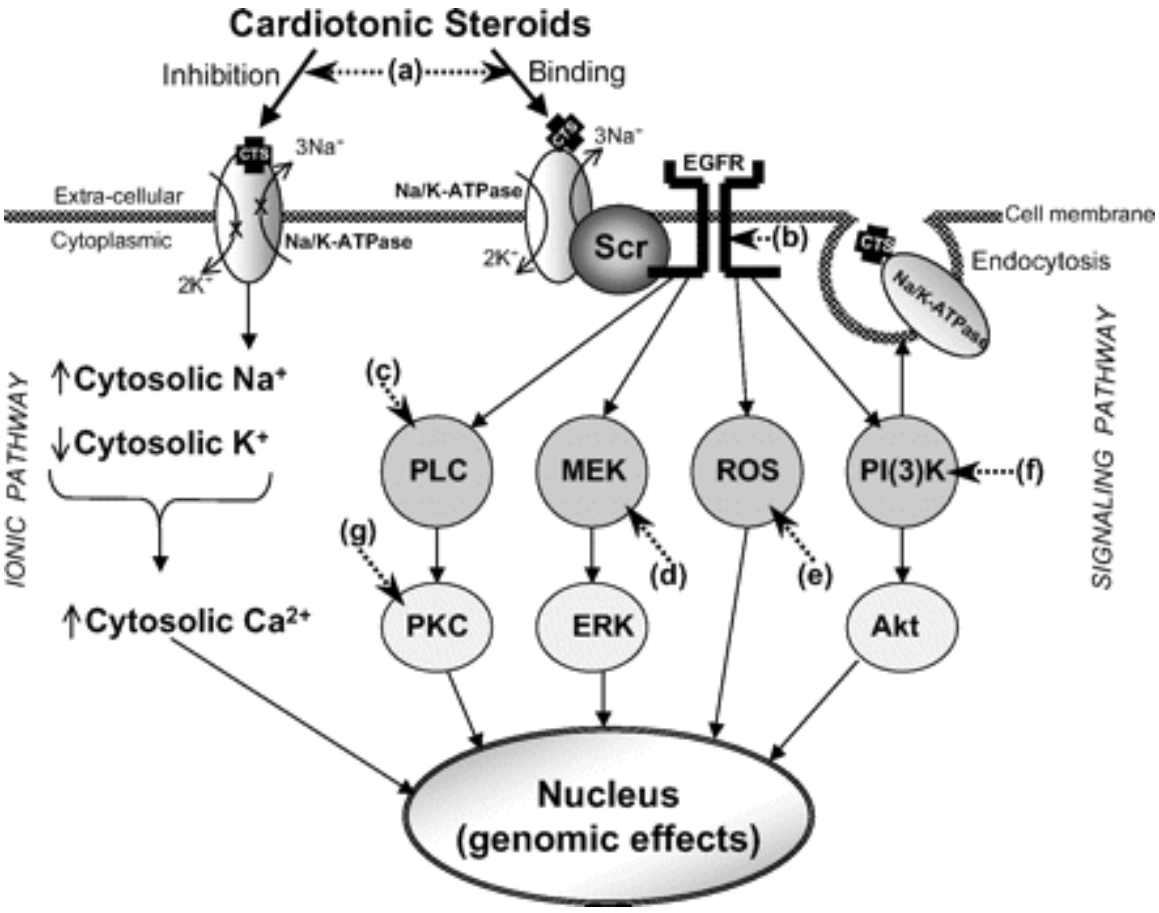

Figure 10. Schematic diagram showing "classic" ("ionic") along with "signaling" pathways for cardiotonic steroids (CTS) effects. In the classic pathway, any signaling through the Na,K-ATPase requires inhibition of the Na,K-ATPase pumping activity,

which in turn is accompanied by changes in cytosolic Na^+ and K^+. As discussed in the text, some authors feel that the caveolar Na,K-ATPase may be more sensitive to CTS in terms of enzymatic function. Na^+ uptake and K^+ loss then associated with an increase in cytosolic Ca^{2+}, which, in turn, activates a variety of pathways. In contrast, the signaling pathway involves the association of Src with the Na,K-ATPase in a caveolar domain. Binding of the CTS to the Na,K-ATPase activates Src, which, in turn, transactivates the EGFR and phospholipase C (PLC). This leads to a cascade that involves generation of ROS, activation of mitogen-activated protein kinase (ERK) through activation of its mitogen-activated protein kinase (MEK), activation of PI(3)K, stimulation of endocytosis and activation of Akt as well as activation of protein kinase C. This signaling construct proposes that these steps induce increases in cytosolic Ca^{2+} and induce the combinations of genomic and nongenomic effects. (a), binding of CTS to the Na,K-ATPase, the signaling pathway presents a number of potential targets such as (b) interference with Src activation and EGFR transactivation, (c) PLC activation, (d) MEK activation, (e) ROS generation or scavenging, or (f) PI3K activation. Modulation of the signaling pathways at the level of PKC (g), ERK, and Akt might also be possible (adopted from [53]).

In cardiac myocytes, the resulting ouabain-induced downstream events include activation of several transcription factors (activator protein-1, nuclear factor-κB and others) and the stimulation of protein synthesis and myocyte hypertrophy and apoptosis [74-76].

However the role of CTS as hormones is questioned by some researchers there are pro-and contra-arguments presented for and against the "receptor function" of the Na,K-ATPase in cardiomyocytes [77].

4. Regulation of Na,K-ATPase activity

Since the Na,K-ATPase was discovered in 1956 [78] evidence has been accumulating revealing extraordinary plasticity of this enzyme in acute responses to the changes in environmental conditions. Regulatory mechanisms engaged in acute regulation of the Na,K-ATPase activity are multiple, tissue- and species-specific. They currently remain a subject of intensive investigations. Numerous findings reported indicate that acute responses of the Na,K-ATPase are due to:

1) Alteration of V_{max} of Na,K-ATPase αβ reduced or increased;

2) Alteration of the enzyme affinity of Na,K-ATPase αβ dimer to the substrates increased or reduced;
4) De novo synthesis of the Na,K-ATPase (long-term response, that will not be elucidated in this review);
5) Internalization/externalization of pre-synthesized protein (relatively acute response).
In the following chapter a short summary on the current knowledge on the posttranslational modifications causing the changes in the enzyme activity or interaction of the Na,K-ATPase with other proteins is presented.

4.1. Inhibition of Na,K-ATPase

Substrate availability

Na,K-ATPase requires the presence of Na^+, K^+ and Mg-ATP for its function. Manipulation of the substrate availability can influence the enzyme activity. Half-maximal activation of the enzyme by Na^+ (Km for Na^+) occurs within the range of concentrations of 10–40 mM, which exceeds the steady-state Na^+ concentration in rodent cardiomyocytes (10-15 mM) [79]. This means that small changes in the cytoplasmic Na^+ concentration, or local Na^+ concentration near the enzyme compartment, will affect Na,K-ATPase activity, according to the Michaelis-Menten kinetics. Affinity of the enzyme's ion binding sites for K^+ (Km∼4 mM) is generally higher than non-lethal variations in extracellular K^+ concentrations ∼2-7mM, 3.5-4 mM under resting physiological conditions [80].
Because the Km of the Na,K-ATPase for ATP is in the range of 0.5-0.8 mM [81], the steady-state ATP concentration in cardiomyocytes (∼1-3mM) is saturating for the enzyme [82, 83]. It was shown that global reduction of ATP content in the heart to the concentration below the Km of Na,K-ATPase to ATP, may be recorded in severe anoxic (isolated adult rat cardiomyocytes, 60 min anoxia) conditions. However, during myocardial ischemia or hypoxia bulk ATP concentration in the cells often

remains above this threshold level whereas the enzyme function appears to be compromised [84-87]. However, the local concentrations and the source of ATP have to be taken in account [83].

Ca^{2+} and Ca-binding proteins inhibit Na,K-ATPase activity

Influence of Ca^{2+} ions on activity of Na,K-ATPase was addressed repeatedly. However, the concentration of Ca^{2+} reported to inhibit the Na,K-ATPase in different preparations varies: 1-5 μM for crude rabbit brain [88] to 70 μM for washed human red cell membranes [89], 500 μM for washed rat brain [90] and almost 2 mM for highly purified dog kidney [91] (the physiological values of cytoplasmic Ca^{2+} are estimated between 0.02μM and 1μM [92, 93], depending on the tissue type and cell compartment). It is hypothesized, that Ca^{2+} blocks pump-mediated ATP-ADP exchange [90], inhibits K-stimulated dephosphorylation [94], competes with Na^{+} in the presence and absence of K^{+} [90, 95, 96], and substitutes for Mg^{2+} [90, 96]. In addition, two proteins, calmodulin and calnaktin-like protein, were shown to decrease activity of Na,K-ATPase by almost half in the presence of micromolar concentrations of Ca^{2+} in erythrocytes [97]. Most of these effects were discovered in experiments in vitro, in which millimolar "intracellular" concentrations of Ca^{2+} were employed [29], These levels of free Ca^{2+} are never reached in the sarcoplasm of cardiomyocytes even upon its release from the sarcoplasmic reticulum.

Phosphorylation of the Na,K-ATPase

A. *Ca^{2+}/calmodulin-dependent protein kinase (CaMK)*

One explanation of calmodulin-dependent inhibition of Na,K-ATPase is activation of CaMK. Activation of endogenous CaMK with Ca^{2+} and calmodulin is associated with a decrease in activity of cardiac Na,K-ATPase by half [98].

B. *Phosphorylation of the α-subunit at Ser938 by cAMP-dependent protein kinase A (PKA).*

Phosphorylation of the catalytic α-subunit of the Na,K-ATPase by membrane-anchored PKA in the presence of AKAP protein (A-kinase anchoring protein [99]) occurs at Ser-938. In rat parotid gland acinar cells PKA-induced phosphorylation results in 20% decrease in the activity of the enzyme [100]. This inhibitory effect was observed only for the α1 and α2 isoforms of the enzyme. Phosphorylation of the α3 isoform has an opposite activating effect [101]. At present PKA-induced phosphorylation was not reported for the myocardial Na,K-ATPase .

C. *Phosphorylation of the α-subunit by cGMP-dependent protein kinase G (PKG).*

Direct activation of PKG inhibits Na,K-ATPase activity by up to 50% in the epithelial cells, however there were no phosphorylation sites reported. Inhibition by PKG causes reactivation of the Na,K-ATPase after treatment with protein the phosphatase 1 (PP1) [102, 103]. In isolated cardiac myocytes, introduction of recombinant PKG together with cGMP analogue (for activation of protein kinase) is associated with 100% increase in Na,K-ATPase transport activity. Whether activation of PKG results in phosphorylation of the ATPase subunits or the enzyme response is secondary to phosphorylation of some other protein remains unknown [104].

Protein thiol modifications

There are 23 cysteine residues in the α1-subunit of Na,K-ATPase, and 7 in β1-subunit [105]. Importance of these thiols in control of the Na,K-ATPase activity was first shown in 1978. Modification of Cys residues of Na,K-ATPase by treatment with thiol-targeting compound h 5,5'-dithiobis-(2-nitrobenzoic acid) or N-ethylmaleimide was shown to cause inhibition of enzyme activity due to the stabilization of the enzyme in E2K2 conformation (see Figure 2). This inhibitory effects were reversed by dithiothreitol (DTT) and was not observed in the presence

of ATP in the incubation medium [106]. The following studies have indicated that cysteine residues may be involved in ouabain binding (Cys 104 and Cys 113) [107-109], ATP hydrolysis (Cys 577) [110, 111], and αβ association (Cys 908) [112]. Several sulfhydryl-reactive reagents have been shown to inactivate the Na,K-ATPase [113-115]. However, the localization of cysteine residues involved in regulatory responses remained unknown. One of the cysteine residues modification of which was shown to alter the enzyme activity is Cys-577 of the α-subunit. Its modification by 2-(49-maleimidylanilino)naphthalene-6-sulfonic acid was shown to inactivate the Na,K-ATPase activity . Pre-incubation with ATP could prevent the enzyme from inhibition by this thiol-targeting agent [111]. On the other hand, sheep renal Na,K-ATPase α1-subunit in which all 23 cysteine residues were replaced by alanine residues has retained its activity [116].

Cysteine residues in proteins can potentially be involved in redox reactions

Redox reactions are characterized by electron transfer from an electron donor (reductant) to a recipient compound (oxidant). Thiol groups of proteins are often playing a role of reductants getting oxidized under conditions of oxidative stress losing one or more electrons and turning from -SH to -S-S-(dithiol) , -SOH (sulfenic acid), -SO_2H (sulfinic acid) or SO_3H (sulfonic acid) depending on the redox state of microenvironment. Most of free cysteines are protonated at physiological pH and therefore not susceptible to oxidation. Because it is the thiolate ion (S^-) that is reactive, low pKa of the sulfhydryl group facilitates oxidation [117]. Positive charges from nearby basic amino acids, in most cases lysine or arginine, lower the pKa of a sulfhydryl group and facilitate its susceptibility to oxidation [118].
The strength of a given oxidant or reductant is usually compared with the hydrogen ion reduction reaction ($H^+ + e^- \rightarrow H$) and is expressed as a standard redox potential (given that the corresponding potential for the hydrogen half-reaction is 0 Volts). The more positive the potential becomes, the greater is a species affinity for electrons and its power as an oxidant. Oxidation is not thermodynamically possible unless the redox potential of the oxidant is more positive than that of its target in

biological microenvironment [119, 120]. Within a cell these reactions are usually strictly controlled and compartmentalized due a relatively short half-life (10^{-9} sec to seconds) of the participating oxygen (O_2) and nitric oxide (NO) derivatives known as reactive oxygen species (ROS) and reactive nitrogen species (RNS). Sources of ROS include the mitochondrial electron transport chain, xanthine oxidases, and cytochrome p450 etc. [121]. For instance, NADPH oxidase catalyzes electron transfer from cytosolic NADPH to molecular O_2 to generate O_2^- (superoxide) as its primary product. Catalyzed reduction of O_2 results in production of conjugate reductant $O_2^-$with a half-life of 10^{-6} sec. However, further reduction of O_2^- results in spontaneous (e.g. in reaction with NO) or catalyzed (e.g. by superoxide dismutase) results in production of highly reactive oxidative species (peroxynitrite (ONOO-) and hydrogen peroxide (H_2O_2) respectively). Therefore, an increase in O_2^- production promotes development of oxidative stress. Superoxide anion generated by NADPH oxidase in the extracellular space is charged and requires a transporter to pass through the membrane. It is rapidly (k= 10^5 $M^{-1}s^{-1}$) dismutated to H_2O_2 in a process that is catalyzed both inside and outside cells by superoxide dismutases (SOD) [122]. H_2O_2 is membrane-permeable, and is further converted to O_2 and water by catalase or glutathione peroxidase (GPx) [123, 124]. In the presence of NO in the microenvironment O_2^- is converted to ONOO- much faster than to H_2O_2 (k= $7x10^9$ $M^{-1}s^{-}1$). Thus, peroxynitrite production prevails over SOD-catalyzed dismutation to hydrogen peroxide. Peroxynitrite is a highly pro-oxidant species which is readily formed at the membrane surface (as nitric oxide is lipophilic) that may diffuse through the biological membranes [125]. Schematically interaction between ROS and RNS are presented Figure 11.

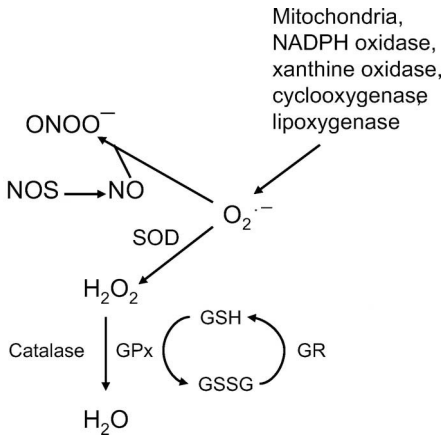

Figure 11. Sources and metabolism of reactive oxygen species. GPx, glutathione peroxidase; GR, glutathione reductase; GSH, reduced glutathione; GSSG, oxidized glutathione; H_2O_2, hydrogen peroxide; NO, nitric oxide; NOS, NO synthase; $O_2^{\bullet-}$, superoxide; $ONOO^-$, peroxynitrite; SOD, superoxide dismutase. (adapted from [123])

Interaction of reactive cysteine residues with biological oxidants (ROS or RNS) results in formation of numerous oxidized thiol intermediates: sulfenic form (Prot-SOH), the sulfenic form is unstable and can undergo further oxidation to a sulfinic (Prot-SO_2H) species. If oxidative stress persists, the sulphonic (Prot-SO_3H) species can be generated [121].

One more cysteine modification known is S-nitrosylation (Prot-SNO) [126]. Finally, oxidation may result in formation of an inter- or intramolecular disulfide bond (Prot-SS-Prot) [127].

Formation of a disulfide bond between a proteins' thiols and glutathione has received much attention as a mechanism of acute redox-sensitive modulation of the enzymes activity. Reduced glutathione (GSH) is a tripeptide (Glu-Cys-Gly) present in the cytosol of all cells in millimolar concentrations (~1-3 mM in the rat heart [87]). It is regarded as a strong antioxidant and undergoes oxidation to glutathione disulfide (GSSG) under conditions of oxidative stress. Glutathione may also form a disulfide bridge with sulfhydryl residues of protein cysteines forming “mixed disulfides” [128]. The cytosolic GSH ↔ GSSG balance is usually maintained by a cascade of cellular reducing mechanisms [129]. The sulfenic acid modification is considered to be intermediate in the formation of Prot-SSG, and the mixed disulfide may serve to protect protein sulfhydryl groups from further irreversible modifications [130]. Glutathionylation is a stable modification that is reversible in a

process specifically mediated by glutaredoxin 1 [129]. Figure 12 shows schematic protein thiol oxidation product connection.

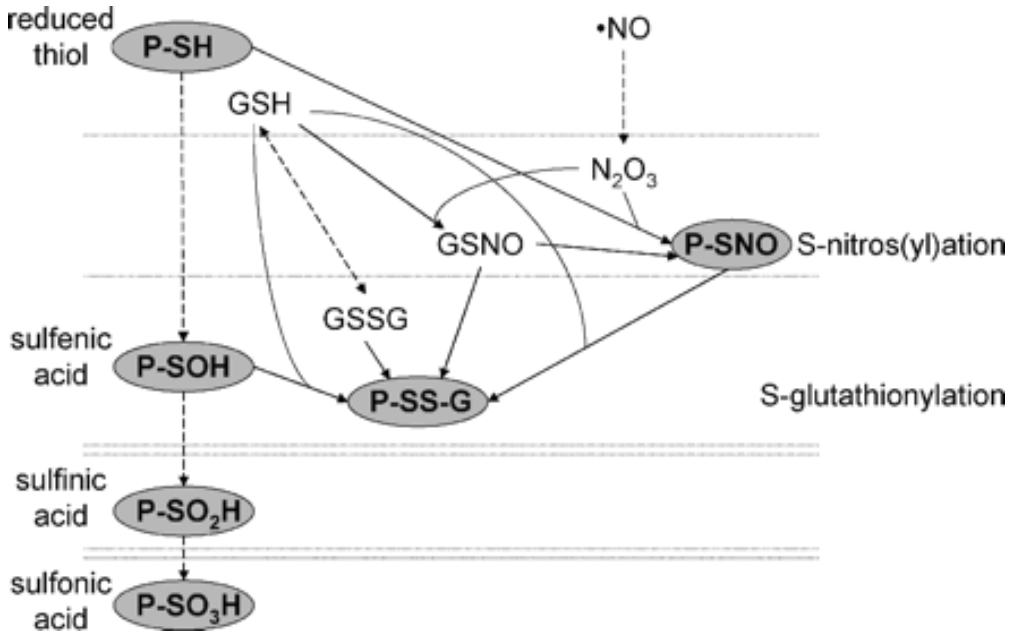

Figure 12. Schematic representation of signaling pathways leading to the formation of protein S-nitrosylation and S-glutathionylation. Horizontal dotted lines separate one-electron oxidative states. Dashed lines represent oxidations by oxidative species not depicted, including molecular oxygen (O_2). For the sake of simplicity, lines representing reaction of P-SH with GSSG or GSNO to yield P-SS-G have been omitted. GSH: reduced glutathione; GSNO; S-nitrosoglutathione; GSSG: oxidized glutathione [131].

Na,K-ATPase was shown to be redox-sensitive in many cell-types and tissues (see table 3)

Table 3. Effect of ROS on Na,K-ATPase (adapted from [132]).

Membrane and Tissue Types and Species	ROS Type and Concentration or $K_{0.5}$	Pump Parameters	Nature of ROS-Induced Mode of Action	Effective Form of ROS and its Inhibition and Mechanism of Action	Reference
Red blood cells	200 μ M $FeCl_2$/EDTA	Na,K-ATPase activity	Inhibited Na,K-ATPase	Protein cross-linking and lipid peroxidation were prevented by	[133]

Membrane and Tissue Types and Species	ROS Type and Concentration or $K_{0.5}$	Pump Parameters	Nature of ROS-Induced Mode of Action	Effective Form of ROS and its Inhibition and Mechanism of Action	Reference
				antioxidant U-89843D	
Brain microsomes from mouse	UV-C-generated · OH and ROO ·	Ouabain-sensitive Na,K-ATPase activity	Inhibited Na,K-ATPase activity	· OH thiourea and DTT have protective effects; lipid peroxidation-induced disruption of membrane integrity and membrane fluidity	[134]
Plasma membrane from smooth muscle of pig coronary artery	H_2O_2 (IC_{50}9.85) or XO (IC_{50} 5 mU/ml)	K^+-activated ouabain-sensitive hydrolysis of*p*-nitrophenyl phosphate monitored as hydrolytic activity of Na-pump	Inhibited at high H_2O_2 or XO	H_2O_2 and O_2^-	[135]
	2.5 mM $H_2O_2$and 0.5 mU/ml XO	Na^+-dependent acylphosphate levels	Reduced by 41 and 30%, respectively, with 2.5 H_2O_2 and XO		
	H_2O_2 (IC_{50}0.56 mM); O_2^- (IC_{50} 0.08 mU/ml)	Rb^+ uptake by coronary artery ring in lieu of K^+ transport	H_2O_2(IC_{50} 0.56 mM) and O_2^- (IC_{50} 0.08 mU/ml) uncoupled hydrolytic and Na^+ transport reactions	Not reversed with SOD or catalase	
Sarcolemmal vesicles from canine cardiac tissue	Irradiated rose bengal	Na,K-ATPase activity	86% Inhibition of Na,K-ATPase activity	$^1O_2$, SOD, catalase, and mannitol (· OH scavenger) are not effective; reversed with 25–100 mM histidine	[136]
Cardiac tissue	X/XO 80 mU/ml	Na^+ pumping, Na,K-ATPase	75% Inhibition of Na^+ pumping, 35–40% inhibition of Na,K-ATPase		[137]
Cardiac plasma vesicles	100 mU/ml X/XO, H_2O_2(IC_{50} 1	Na,K-ATPase	Inactivation of Na,K-ATPase	X/XO not effective; H_2O_2, $HClO_4$, and NH_2Cl effective	[138]

Membrane and Tissue Types and Species	ROS Type and Concentration or $K_{0.5}$	Pump Parameters	Nature of ROS-Induced Mode of Action	Effective Form of ROS and its Inhibition and Mechanism of Action	Reference
	mM), $HClO_3$(IC_{50} 0.1 mM), NH_2Cl (IC_{50} 0.05 mM)				
Brain cell membrane fractions	100 μM ascorbate and 25 μM $FeCl_2$	Na,K-ATPase	Ascorbate-$FeCl_2$-induced inactivation of cerebral Na,K-ATPase	Lipid peroxidation-induced reduction in the affinity for Na^+ and K^+ and increase in ATP and ouabain affinities	[139]
Partially purified outer medulla of porcine kidney	0.1 mM $FeCl_2$, 0.1–100 mM H_2O_2, or UV irradiation (254 nm; producing mainly O_2^-)	Na,K-ATPase activity deduced from ouabain-sensitive ATPase	Reduced activity and turnover rates of Na,K-ATPase by 80%; reduced SH contents Reduced Na,K-ATPase activity, E glycerophospholipids, and formation of malondialdehyde and conjugated dienes	Effective ROS unknown; effects on enzyme proteins and membrane lipids 10 mM DTT alleviated all the previous effects	[140]
Guinea pig sarcolemma	Scavengers (100 U/ml SOD, 150 U/ml catalase, 50 mM DMSO, 10 mM histidine, 50 μg/ml vitamin E or XO, and 1 mM allopurinol inhibitor) of O_2^- free	Na,K-ATPase activity deduced from ouabain-sensitive ATPase and estimated from ouabain-sensitive $^{86}Rb^+$uptake	These scavengers inhibited ischemia-reperfusion-induced reduction in Na,K-ATPase activity and specific [^{3}H]ouabain binding	Various ROS	[141]

Membrane and Tissue Types and Species	ROS Type and Concentration or $K_{0.5}$	Pump Parameters	Nature of ROS-Induced Mode of Action	Effective Form of ROS and its Inhibition and Mechanism of Action	Reference
	radicals				
Dog myocardial tissue	DHF ± FeADP	Lipid peroxidation Na,K-ATPase	Inhibition of Na,K-ATPase	Lipid peroxidation	[142]

Recent findings indicate that modification of the Cys-46 of the β1-subunit with glutathione was associated with a 25% reduction in Na,K-ATPase the activity. Exposure of isolated rabbit ventricular myocytes to angiotensin II (Ang II) caused inhibition of the sarcolemmal Na,K-ATPase, mediated by PKC-induced activation of NADPH oxidase followed by glutathionylation of the β1-subunit of the Na,K-ATPase. Glutathionylation was reversible, and de-glutathionylation was catalyzed by glutaredoxin 1 as mentioned above [16]. However, Cys-46 in the β1-subunit is located in the transmembrane segment and not expected to be accessible to the strictly cytosolic GSH [16].

Endogenous inhibitors of Na,K-ATPase

Several molecules, different to cardiac glycosides, some of which are extracellular, some intracellular and some are membrane-bound which may act as inhibitors of the Na,K-ATPase. Amongst them are fibrinogen degradation products [143], calpain [144] or octanoic acid [145] which were shown observed to reduce activity of the enzyme. The mechanism of their action remains largely unclear.

4.2. Increase in turnover of Na,K-ATPase

Increase in turnover of Na,K-ATPase can be achieved by direct phosphorylation of the α-subunit or by the association of the enzyme with other molecules.

Phosphorylation of alpha-subunit

The α-subunit has well described Tyr-10 phosphorylation site, (however potentially there can be more). Phosphorylation of the α-subunit at Tyr-10 increases the activity of the enzyme by ~50% [146]. This phosphorylation site is available for the tyrosine kinases p44/42 mitogen-activated protein kinases (MAPKs) in kidney [147] and Src kinase in neurons [148]. However there is no information regarding this regulation in heart tissue.

Phosphorylation of the regulatory FXYD1 subunit

Phospholemman, a member of FXYD family, joins the αβ heterodimer in the myocardium and regulates activity of the Na,K-ATPase. Phosphorylation of this subunit of Na,K-ATPase at Ser-68, Ser-63 or Thr-69 is catalyzed by either PKC or PKA. When phosphorylated, phospholemman dissociates from the αβ dimer and the enzyme activity is increased [149-151].

Activation of Na,K-ATPase by interaction with other proteins

Enzyme activation upon its association with other proteins has been reported. For instance, presynaptically secreted protein, follistatin-like 1 (FSTL1) serves as a direct activator of Na,K-ATPase [152].

4.3. Changes of the Na,K-ATPase affinity to its substrates

Affinity of the enzyme to substrates depends on the subunit speciation of the functional unit. Different isoforms of the α- and β-subunits vary in their affinity to Na^+, K^+, and ATP [153] (see Table 4).

Table 4. Kinetic characteristics of the rat Na,K-ATPase isozymes expressed in Sf-9 insect cells

Isozyme	**Na^+ Activation $K_{0.5}$, mM**	**K^+ Activation $K_{0.5}$, mM**	**ATP Activation K_m, mM**
α1 β1	16.4 ± 0.7	1.9 ± 0.2	0.46 ± 0.10
α2 β1	12.4 ± 0.5	3.6 ± 0.3	0.11 ± 0.01
α2 β2	8.8 ± 1.0	4.8 ± 0.4	0.11 ± 0.02
α3 β1	27.9 ± 1.3	5.3 ± 0.3	0.09 ± 0.01
α3 β2	17.1 ± 1.0	6.2 ± 0.4	0.07 ± 0.02

Values are means ± SE. Apparent affinities ($K_{0.5}$), K_m, and inhibition constant (K_i) parameters were calculated from Na,K-ATPase activity dose-response curves for the indicated effectors. For comparison, the native $\alpha 1\ \beta 1$ isozyme from the kidney has been included [29].

However, the affinity of the functional unit of the enzyme to the Na^+ and K^+ may be altered by phosphorylation of the α-subunit or by association of the αβ dimer with FXYD subunit. Some observations show that phosphorylation of the rat α1-isoform at Ser-23 leads to a decreased apparent affinity for K^+ [154]. In COS-7 cells the PKC-dependent phosphorylation of the pump at Ser-16 results in an increase in the affinity of the enzyme for Na^+ [155].

Information on the role of regulatory FXYD proteins in control of the enzyme activity is currently accumulating. In particular, association of this proteins with the αβ unit alter the enzyme affinity to Na^+, K^+, and ATP (Table 5) [24].

Table 5. Functional features of FXYD proteins

FXYD protein		FXYD1 phospholemman	FXYD2 γ-subunit	FXYD3 Mat-8	FXYD4 CHIF	FXYD5 RIC	FXYD6	FXYD7
Na,K-ATPase affinity for	Na^+	↓↓	↓	n.d.	↑↑	n.d.	n.d.	-
	K^+	↓	-	n.d.	↓↓	n.d.	n.d.	êê
	ATP	n.d.	↑	n.d.	n.d.	n.d.	n.d.	n.d.

↓, decrease in the apparent affinity; ↑, increase in the apparent affinity; –, no change in the apparent affinity; n.d. = not determined

Investigation of the role of FXYD proteins in regulation of the enzyme kinetics is currently intensively ongoing in several labs.

4.4. Acute regulation of the Na,K-ATPase activity by internalization/externalization

Dynamic regulation of the Na,K-ATPase presence at the plasmalemma is possible because of the direct interaction of the protein with caveolin, within caveoli. The resulting endo- and exocytosis follows the interaction of caveolin with N-terminal caveolin-binding motif of the α-subunit [156]. This interaction is controlled by phosphorylation of the α-subunit of the enzyme.

Several sites of phosphorylation and several protein kinases are found to maintain protein regulatory trafficking. Amongst them Ser-18 phosphorylation of which by PKC-ζ results in endocytosis of the enzyme [157]. Phosphorylation of both Ser-18 and Ser-11 by PKC-β results in incorporation of the Na,K-ATPase in the membrane [158].

As well, threonine (possibly Thr-58) phosphorylation of α-subunit by ERK½ was shown to cause endocytosis of the Na,K-ATPase in skeletal muscle cells [159].

These are the mechanisms of acute regulation of Na,K-ATPase activity. They are involved in response of the enzyme to physiological and pathological stimuli in different cell types. We were able to show that the enzyme responds to the changes in microenvironment such as reduction in oxygenation, with not a single alteration in its state, but with several modifications so that response of its activity could be easily graded or quickly reversed upon disappearance of the triggering stimulus. Certain hierarchy and timing of these regulatory modifications provides additional stability to the system accounting for most optimal preservation of ATP levels and ion gradients at the same time.

5. Myocardial responses to the changes in environmental conditions in the heart

5.1 Ion balance preservation during contractile cycle

Shown in Figure 13 are the main players in the excitation-contraction coupling in the heart. These are (1) sarcolemmal potential, that serves for electrical activity of the cell and ion transport for cell excitation, (2) Ca2+ content in SR stores, (3) contractile machinery, and (4) ATP supply to fuel active ion transport and myosin ATPases [160]. In Figure 13 the interaction of these main players is schematically presented.

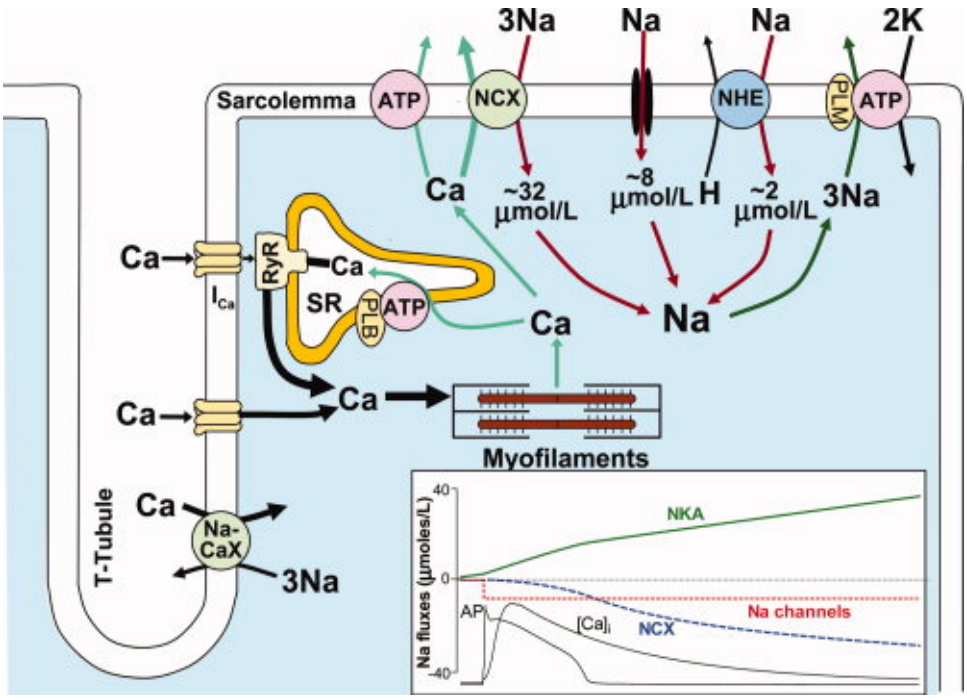

Figure 13. Na^+ and Ca^{2+} transport during cardiac cycle in ventricular myocytes. Inset shows the integrated Na^+ flux through Na^+/Ca^{2+} exchanger, voltage-gated Na^+ channels, and Na,K-ATPase during an action potential (AP). The corresponding Ca^{2+} transient is also shown. NCX-Na^+/Ca^{2+} exchanger; ATP-ATPase; PLB-phospholamban; PLM–phospholemman; SR-sarcoplasmic reticulum; NHE–Na/H exchanger (adopted from [79]).

During electrical excitation of the myocardium, Na^+ flux through voltage-dependent Na^+ channels triggers the upstroke of the action potential. Na^+ channels inactivate rapidly (within a few milliseconds) at positive potentials, which limits the gain in intracellular Na^+ ($[Na^+]_i$) to 6–15 µmol/L [79]. During the action potential, Ca^{2+} enters the myocytes via L-type Ca^{2+} channels initiating Ca^{2+}-induced Ca^{2+} release from the sarcoplasmic reticulum. When released to the sarcoplasm, Ca^{2+} binds to the TnC releasing the block preventing actin-myosin interaction, and contraction occurs. For relaxation to occur, Ca^{2+} is taken up into the sarcoplasmic reticulum by Ca-ATPase (SERCA).

Apart of that Na^+/Ca^{2+} exchanger transports one Ca^{2+} ion out of the cell in exchange for three Na^+ ions. Thus Ca^{2+} extrusion leads to an increase in $[Na^+]_i$ by approximately 32 µmol/L during each action potential. This is required to extrude the approximately 10 µmol/L Ca^{2+} that enters via L-type Ca^{2+} channels. The Na^+/H^+ exchanger brings in approximately 2 µmol/L Na^+ at physiological

intracellular pH and approximately 16 μmol/L during intracellular acidosis. Other transporters, including the Na^+/HCO_3^- cotransporter, the $Na^+/K^+/2Cl^-$ cotransporter and the Na^+/Mg^{2+} exchanger bring in smaller amounts of Na^+. At steady-state, the excess Na^+ (approximately 40–45 μmol/L) is then extruded by Na,K-ATPase to keep $[Na^+]_i$ constant. Resting $[Na^+]_i$ in cardiac myocytes is in the range of 4–8 mM for most mammalian species, including human, and higher (10–15 mM) in rat and mouse [79].

5.2 Reduction of coronary blood flow during heart ischemia and hypoxia

Performance of the heart in hypoxic conditions at least in part may be associated with performance of the Na,K-ATPase (Figure 13).

Reduction of coronary blood flow (CBF) causes rapid (within 3 minutes) decline in heart rate and contractile force (stable myocardial dysfunction). This matching of contractile function to CBF, known as myocardial hibernation, is an adaptive response preventing acute irreversible myocardial damage. It has been graded according to the duration of the stress from short-term (minutes) to long-term (days and months) [161-166].

The lower limit for the CBF reduction causing the hibernation response is 25%. Hibernation occurs within 5 min and is associated with development of stable depression of myocardial function calculated as work index (WI), by half. Work index reflects left ventricular pressure and wall thickness changes over the cardiac cycle. Hibernation state is reversible within 90 min of low-flow ischemia. The upper limits of the CBF reduction, to cause short-term myocardial hibernation were never studied. However, a 50% reduction of CBF for 3 min, causes the same stable depression of myocardial function (WI decrease by 50%) [166, 167].

Reversibility of the myocardial hibernation was reported in many studies. After the restoration of blood supply, heart performance may remain low (myocardial stunning), but recovery is observed, time required for recovery depends on the severity of cardiac ischemia [168].

Observations of the short-term myocardial hibernation on in situ and ex vivo model indicate, that initial changes in the heart performance are independent of the central

regulation and may be monitored in denervated organ. Hibernation precludes development of irreversible myocardial damage [169].
At present, the phenomenon of short-term myocardial hibernation is regarded as an autonomous regulatory event that serves to avoid an irreversible energetic deficit and to maintain myocardial integrity and viability [170].

Is there a room for Na,K-ATPase in myocardial hibernation

Mechanisms in control of activity of the main players of the excitation-contraction cycle (see Figure 13) during hibernation are currently investigated. These mechanisms should be shared by several ion transporters and elements of contractile machinery at once so that alteration in their function occurs in an orchestered fashion. Experiments using ex vivo perfused heart exposed to 30 min of global ischemia revealed a 150% elevation of $[Na^+]_I$, that could be attributed at least in part to the inhibition of Na,K-ATPase activity in the ischemic heart [171, 172]. Reduction (down to 30% of initial values) of the turnover of the enzyme was directly confirmed in the homogenate of ex vivo perfused heart subjected to 30 min global ischemia [173].

Recently developed by our research group, a model of ex vivo autologous blood-perfused rat heart allow us to study the impact of hypoxia into the development of myocardial hibernation and link autonomous heart response to hypoxia to the inhibition of Na,K-ATPase. Results obtained using this model show, that inhibition of Na,K-ATPase down to 20% of initial and depression of myocardial performance occur simultaneously in response to a graded reduction of hemoglobin oxygen saturation . These findings suggest that condition similar to a short-term myocardial hibernation response can be achieved without reduction of the CBF, but with the reduction of blood oxygen saturation (blood pO_2 5 kPa) already within 5 min [174]. Decrease in oxygen supply causes imbalance in tissue oxygen demand and consumption (hypoxia). According to the Fick's law [175], myocardial oxygen consumption (MVO_2 in ml O_2/(min *100g)) is proportional to the myocardial oxygen

extraction (difference between arterial CaO_2 and venous CvO_2 oxygen concentration, in ml O_2/ml of blood or %) and coronary blood flow (CBF in ml blood/min).

$MVO_2 = CBF \times (CaO_2 - CvO_2)$

Converting the oxygen concentration in blood to the hemoglobin oxygen saturation (CaO_2=Hb x 13,8 x SaO_2 and CvO_2=Hb x 13,8 x SvO_2, Hb – hemoglobin concentration), the equation can be transformed as follows:

MVO_2=CBF x (Hb x 13,8 x SaO_2 - Hb x 13,8 x SvO_2)

or

$MVO_2 = CBF \times Hb \times 13,8 \times (SaO_2 - SvO_2)$

From this equation one can conclude that misbalance between oxygen demand and oxygen supply may happen under conditions of compromised (i) coronary blood flow (ischemia); (ii) hemoglobin concentration (anemia); (iii) hemoglobin oxygen saturation (systemic hypoxia); (iv) mechanism of O_2 extraction (sepsis [176]). Numerous observations of myocardial oxygenation in healthy and pathological conditions show, that myocardial oxygen consumption is 1-2 ml O_2/(min*100g) for arrested heart, ~8 ml O_2/(min*100g) for resting heart and ~70 ml O_2/(min*100g) at heavy exercise [65, 177, 178].

Oxygen gradients within the myocardial tissue, are formed depending on the distance from the capillary, which have a density of ~2500 capillaries per mm^3 [179] with the partial pressure (pO_2) on average 6-7 kPa in adult heart [180-182] and going under 4 kPa in hypertrophic hearts [183]. In vivo observations of myoglobin oxygen saturation in cardiomyocytes show, that the possible pO_2 around the cell is ~3 kPa [184, 185].

Further distribution of oxygen inside cardiomyocytes shows heterogeneity and is the lowest within the mitochondrial compartment (Figure 14) [186, 187].

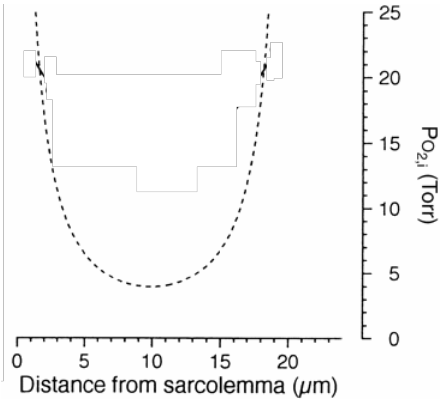

Figure 14. Intracellular pO_2 (1 Torr = 0.133 kPa) in the single isolated cardiomyocyte (extracellular pO_2 3 kPa), adapted from [188].

6. Oxygen sensing by the Na,K-ATPase

Na,K-ATPase does not possess oxygen binding sites (heme or non-heme iron or copper). Thus, mechanism of hypoxia-induced inhibition of the Na,K-ATPase turnover is probably triggered not by O2 directly, but by the secondary messengers responding to the changes in oxygenation.

Signaling messengers in control of Na,K-ATPase in hibernating myocardium are discussed below.

6.1 Changes in substrate availability

Most of the Na,K-ATPase activity measurements in ischemic heart were carried out under conditions optimal for the enzyme function, including saturating levels of substrates and ligands, temperature and pH. As mentioned earlier in the section “Inhibition of Na,K-ATPase: protein thiol modifications”, ATP protects Na,K-ATPase from the inhibitory action of oxidative stress and hypoxia. One may expect that ATP depletion may have an opposite effect allowing inhibition of the enzyme to occur.

A variety of metabolic fuels including fatty acids, glucose, lactate, and amino acids are used in the heart to produce and regenerate ATP [189, 190]. In the normal

conditions fatty acids, catabolized by β-oxidation, account for ~90% of the total energy production [191]. Oxidation of pyruvate, that comes from glycolysis of glucose and lactate oxidation, accounts for ~10% of the total energy production [192]. Fatty acids require ~10-15% more oxygen to generate an equivalent amount of ATP when compared to glucose [193]. One more important player in myocardial energy metabolism is creatine/phosphocreatine pool. Mitochondrial creatine kinase catalyzes the transfer of the high energy phosphate bond in ATP to creatine to form phosphocreatine and ADP. Phosphocreatine is a small molecule with a high diffusion rate and may therefore be quickly transferred to the compartments within cardiomyocyte, in which ATP consumption exceeds its delivery as illustrated in Figure 15 [194].

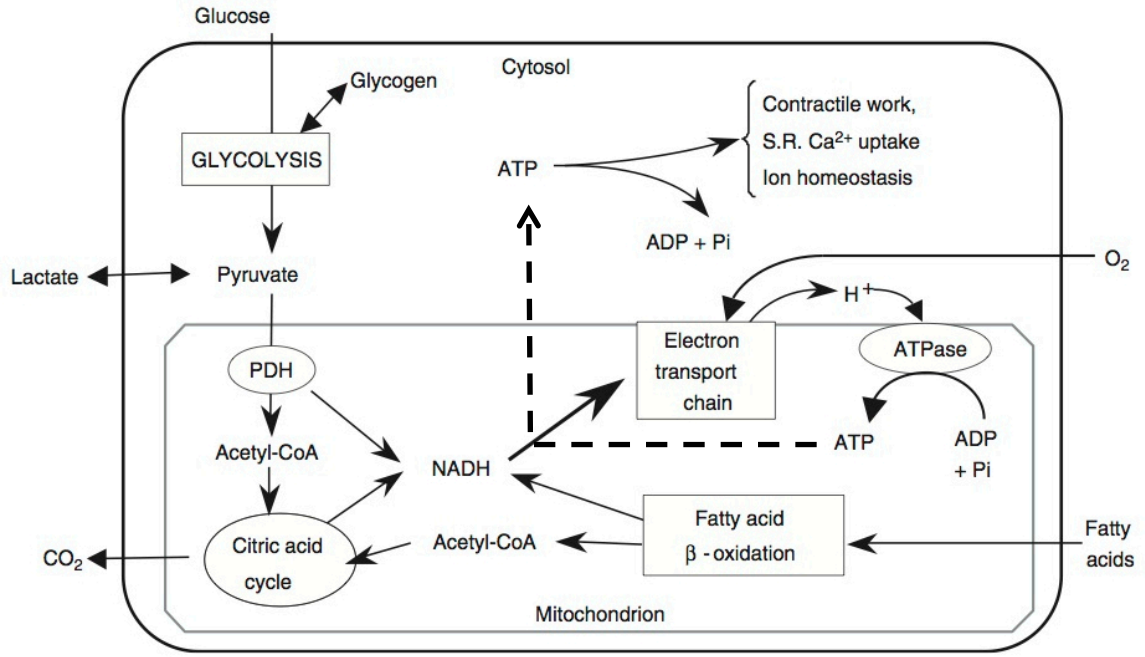

Figure 15 (adapted from [195]). Schematic representation of energy metabolism in cardiomyocytes. Dashed line – transfer of high energy phosphate from mitochondria to cytosol with help of creatine/phosphocreatine system.

Estimated ATP production rate in myocardium under normoxic conditions (O_2 consumption 80 mmol/(g_{dry} weight*min) and phosphate/oxygen ratio ~2,5) is 33 mmol/(g_{dry} weight*min), and the myocardial content is estimated 20 μmol/g_{dry} weight [196] or 4-6 μmol/g_{wet} weight [87], without continues reproduction of ATP cardiomyocytes will be exhausted by ATP within a minute. However, ATP level is

preserved in the tissue after exposure of the heart for 1,5 hour of low-flow ischemia (45% of initial CBF) [166] or 1 hour to hypoxia (S_aO_2 decrease from 98% to 3%) [87] at the level of 80% of initial, and declines (up to 30-50% of initial) under conditions of severe ischemia (10% of normal CBF [197, 198]) or after prolonged exposure of the hearts to the ischemic conditions (50-60% CBF, ~3 hours) [199].
In conclusion, analysis of kinetics of ATP depletion after the onset of ischemia shows, that within 10 min of ischemic exposure ATP concentration is decreased by 20% of initial and is preserved at this level for at least 1,5 hour. Probably, decline in subcellular ATP content within cardiomyocyte is not homogeneous, occurring first at the subsarcolemmal area and then in myofibrillar microcompartments [83, 200].

In several experimental setups, reduction of coronary blood flow by 30-60% below normal resting values results in an increase the oxygen extraction from the blood by up 22% [201]. Under these conditions relative contribution of fatty acids and carbohydrate to mitochondrial substrate oxidation remained unaltered for 1 hour did, despite accelerated anaerobic glycolysis and lactate production [193, 202].
Interestingly, phosphocreatine concentration in short-term hibernating myocardium was reduced within 5 min of hypoperfusion (from 8 to 4 $\mu mol/g_{wet}$ weight), and was then replenished to the initial levels within 60 min. [166, 167, 170, 203]
No changes in affinity of the Na,K-ATPase to ATP and ions were observed in -hearts, subjected to the global ischemia, during 45min [204].

6.2 Ca^{2+} and Ca^{2+}-binding proteins

Elevation of Ca^{2+} concentration in ischemic heart was reported repeatedly. Global myocardial ischemia resulted in an increase of intracellular systolic and diastolic Ca^{2+} concentrations from ~900nM to 1350 nM and 315 nM to 550 nM respectively within 1.5 - 7 minutes [205, 206]. However, the resulting low micromolar to submicromolar concentrations are most likely not sufficient to cause direct inhibition of Na,K-ATPase e.g. by interfering with Mg^{2+} binding(for details see the section "Ca^{2+} and Ca^{2+}-binding proteins").

Whereas direct modification of the Na,K-ATPase function by $Ca^{2+}$is rather unlikely, the enzyme may respond to the Ca^{2+}-induced activation of CaMK. In the hearts, subjected to 15 min of global ischemia, translocation of CaMK (about 40% of total CaMK) from the sarcoplasm to the sarcolemmal membrane was reported [207]. Presence of calmodulin and the elevation of the sarcoplasmic Ca^{2+} can cause activation CaMK, that are capable of phosphorylation of the catalytic subunit leading to the Na,K-ATPase inhibition [98].

6.3 Ouabain-like factors

Exposure of isolated perfused hearts to global ischemia for 15 min was followed by an increase in tissue levels of ouabain-like factors from ~4.6 (control) to ~8.6 (ischemia)(pmol/g wet weight) [208]. Taking into consideration tissue water content of 70-80% of wet weight, the concentration of released ouabain-like factors in myocardium under ischemic conditions can be estimated to be ~ 12.9 pM. Constant of half-inhibition K_i for different isoforms of Na,K-ATPase ranges between μM-nM concentrations (see section "3. Cardiac glycosides and cardiac Na,K-ATPase."). Thus, the observed release of ouabain-like factors is most likely not sufficient to cause a dramatic decrease in activity of the enzyme, however local increase of the substance can do. Furthermore, in vivo major release of ouabain-like factors into the circulation was shown to occur from the midbrain and adrenal gland [209].

6.4 Oxidative stress and its course in hypoxic/ischemic cardiac tissue

Measurements of free radical content with EPR spectroscopy and spin trapping method in the ischemic myocardium show, that 10 min of global ischemia in ex vivo perfused heart results in the 50% elevation of O_2^- and superoxide anion derived radicals (alkyl-peroxyl radicals) [210-212]. To reveal the hypoxia-induced production of O_2^- and its products in myocardial tissue, their generation and degradation/scavenging were studied. Mitochondrial respiratory system was shown to be a common source of O_2^-, its generation depending on the oxygen availability

within the respiratory chain. Many observations show, that oxygen content, required for the half-maximal production of O_2^- by the respiratory system of mitochondria (P_{50}) are in the range of ~0.1-1 kPa O_2 [213-215]. As described previously, partial pressure of oxygen in cardiomyocyte in normoxic conditions ~3-1.5 kPa (equivalent to 8.4-4.2 μM O_2) and can decrease to 0.4 kPa (equivalent to ~1.2 μM O_2) in ischemic conditions (local ischemia, ligation of left-anterior-descending coronary artery) [216]. Moreover, O_2^- production by mitochondrial respiratory chain could be inhibited by uncoupling proteins (UCP) in ischemic myocardium [217-219].

Other potential sources of O_2^- with their estimated O_2 dissociation constants K_d (data collected on different cell types) are:

NADPH oxidase family (5-15 μM),

xanthine oxidase (12-50 μM),

monoamine oxidase (140-335 μM),

cytochrome c oxidase (0.0112 μM) [3, 220-223]. (pO_2 of 1kPa for dissolved O_2 at barometric pressure of 760 mmHg, T=37^{0}C corresponds to oxygen concentration in aqueous phase of 2.8 μM O_2).

Nitric oxide production in the cells by NOS family (eNOS, nNOS/mtNOS - constitutively present enzymes in the myocardium and iNOS) is as well dependent on the oxygen availability: apparent affinity for eNOS, nNOS/mtNOS and iNOS is 0.078kPa, 7.8kPa/13kPa and 5.9kPa respectively [224-226]. NOSes produce nitric oxide, a ROS scavenger when all substrates are available but generate ROS (O_2^-) when uncoupled when substrates supply is compromised. Production of NO is supported by the presence of O_2, L-arginine and tetrahydrobiopterin (BH_4). In the absence of L-arginine or under conditions of oxidative stress and concomitant BH4 depletion NOSes get uncoupled and generate substantial amounts of O_2^- In presence of sufficient amount of oxygen NO can undergo autooxidation, forming N_2O_3, that is either rapidly oxidized to nitrite and nitrate with oxymyoglobin in the cardiomyocytes [227] or interacts with thiol residues of proteins and glutathione, forming S-nitrosothiols [228]. Oxidation of NO to nitrite catalyzed by myoglobin may be reversed in the presence of deoxymyoglobin and nitrite amount over 10 μM

(basal normoxic level of nitrite in the rodent myocardial tissue does not exceed 3 μM and Kd of myoglobin to oxygen is ~0.3kPa) [229].

If not autooxidized NO readily interacts with superoxide anion (rate constant for the reaction of NO with O_2^- was determined to be ~10^9-10^{10} $M^{-1} \times s^{-1}$ [230, 231]), forming peroxynitrite $ONOO^-$, a highly oxidant species [232], that can directly cause nitration of protein tyrosine residues [233, 234].

In conclusion, production of superoxide anion in the myocardium under mild hypoxic conditions (1.5-0.4kPa O_2) may be reduced, because the enzyme systems, responsible for production of O_2^-, are less supplied with oxygen. However, even modest reduction of oxygen availability decreases NO production by nNOS and iNOS whereas the eNOS-derived NO forms peroxynitrite due to a shift in O_2^-/NO balance towards higher superoxide abundance.

NO is an important factor providing efficient cardioprotection against ischemia and ischemia/reperfusion injury [235].

Detoxification of reactive oxygen and nitrogen species is possible in cells with enzymatic and non-enzymatic antioxidative defense systems.

Enzymatic systems of superoxide anion scavenging include family of superoxide dismutase family: (SOD), mitochondrial Mn-SOD and cytosolic CuZn-SOD convert superoxide to the hydrogen peroxide with the rate constant about $2 \times 10^9 M^{-1} \times s^{-1}$ [236]:

$$O_2^- + O_2^- + 2H^+ \rightarrow 2H_2O_2 + O_2$$

The resulting hydrogen peroxide can be further detoxified by catalases, in the mitochondria and peroxisomes (rate constant ~10^6 - $10^7 M^{-1} \times s^{-1}$):

$$2H_2O_2 \rightarrow H_2O + O_2$$

or peroxidases, by peroxidases in a following reaction:

$$RH_2 + H_2O_2 \rightarrow R + 2H_2O,$$

where R represents alkyl group.

One of the well-known peroxidase is glutathione peroxidase (GPx), located all over the cell, which requires glutathione (rate constant ~10^4 - $10^6 M^{-1} \times s^{-1}$):

$$2GSH + H_2O_2 \rightarrow GSSG + 2H_2O$$

See [237-239]

Other enzymes that may be presented in the heart and scavenge hydrogen peroxide, include peroxiredoxin and thioredoxin [240, 241].
The excess of peroxynitrite can inhibit Mn-SOD and interact with mitochondrial respiratory chain, causing increased production of superoxide [242].

Non-enzymatical utilization of ROS and RNS is conducted by interaction of oxidants with low molecular weight-reductants such as ascorbic acid, α- and β-carotene, cysteine, ubiquinone, glutathione etc.
Ascorbate and glutathione are the main contributors to the reducing equivalent's' pool. Regeneration of ascorbate from dehydroascorbate with dehydroascorbate reductase, however, relies on GSH availability [243].
Therefore, it has been suggested that half cell redox potential for the GSH:GSSG couple is a reliable marker of redox state in biological systems [244]
Reduced glutathione interacts with superoxide (rate constant $\sim 10^2$-$10^3 M^{-1} \times s^{-1}$) and with peroxynitrite (rate constant $\sim 6 \times 10^2 M^{-1} \times s^{-1}$) directly reducing them to water and nitrite respectively [245, 246].
The accumulating GSSG is regenerated to the GSH with glutathione reductase in presence of NADPH[247].
Monitoring of glutathione oxidation and regeneration in ischemic and hypoxic myocardium revealed that reduction of tissue GSH levels along with the inhibition of glutathione reductase activity [248].

In conclusion, redox state, which can be mirrored in GSH:GSSG ratio, may represent the trigger and a messenger in control of Na,K-ATPase function in hypoxic myocardium.

6.5 Downstream targets of the changes in redox state: kinases and phosphatases

The resulting oxidation of the tissue may activate redox sensitive signaling mechanisms, that can influence Na,K-ATPase activity:

Oxidative stress, converts the PKC ζ to catalytically competent form in the rat ischemic myocardium [249]. Observation in other cell types report about activation of both PKC ζ and β after exposure to H_2O_2 [250]. As it was described previously, these isoforms of PKC may phosphorylate Na,K-ATPase α-subunit and regulate the presence of the enzyme at the sarcolemma, however this two isoforms of PKC (ζ and β) have opposing effects (see section "4. Acute regulation of the Na,K-ATPase activity by internalization/externalization").
Furthermore, activation of PKC may result in phosphorylation of the FXYD subunit phospholemman which in turn will cause stimulation of the Na,K-ATPase activity. Indeed, up-regulation in phospholemman phosphorylation was reported in the ischemic heart. However, it was not associated with an increase in Na,K-ATPase in tissue homogenate, but could be demonstrated in cytosol-free sarcolemmal fraction [173, 251]

6.6 Cysteines as targets

As mentioned above, cysteines of Na,K-ATPase β-subunit can undergo S-glutathionylation in presence of GSH and peroxynitrite. Beta-subunit S-glutathionylation was associated with a decrease in activity of Na,K-ATPase by 25% [16].

7. Cardiac performance and Na,K-ATPase in hypoxia-tolerant species

Relatively few vertebrate species can survive without oxygen for hours, days and even months. Among them, the
freshwater turtle (genera *Chrysemys, Trachemys* and *Chelydra*), the crucian carp (*Carassius carassius*) and goldfish (*Carassius auratus*), blind subterranean mole rat (*Spalax*), sperm whales (*Physeter catodon*), southern elephant seals (*Mirounga leonina*), which normally dive to 300–600 m, may dive to more than 1000 m and occasionally remain submerged for 2 h. Hooded seals (*Cystophora cristata*) also normally dive to 300–600 m, with dive durations of 5–25 min, but some individuals

specialize in repetitive deep diving to more than 1000 m, with durations of up to 1 h. Even birds like the emperor penguin (*Aptenodytes forsteri*) dive to depths of 500 m, with durations of more than 15 min.

Under hypoxic (and anoxic) conditions, the hearts of these animals do not hibernate, but retain their function [252-256]. Hypoxic adaptation strategies utilized by myocardial tissue in ectothermal and endothermal animals vary among species. Two most common ones employed includes down regulation of the heart contractility to match reduction in ATP production or metabolic switch allowing to sustain metabolism and maintain cardiac output [257-259].

At the molecular level reduction in ATP consumption is achieved by reduction of Na,K-ATPase activity in liver, heart and brain tissue of hypoxia-tolerant species in response to short-term (under 100 hours)hypoxia along with deactivation of ion channels (channel arrest) to avoid irreversible depolarization of excitable tissues as in hibernating turtles and mammals. Maintenance of brain and heart function in crucian carp, in mole rat, and diving mammals and birds during short-term hypoxic insults is associated with maintenance of active ion transport by ATPases along with lack of suppression of ion channels [255, 260-262]. Prolonged in vivo exposure (over 100 hours) to anoxia leads to the depression (by half) of the enzyme activity in the heart of crucian carp [263].

Little is known about the regulation of redox state in tissues of hypoxia-tolerant animals under hypoxic conditions. Nitrosothiol levels in blood plasma, erythrocytes, myocardium and brain tissue in anoxic crucian carp were shown to be increased by 4 fold, compared to control. These changes were associated with the elevation of blood plasma nitrite levels to 10μM [264]. In the myocardium of goldfish, nitrite levels were decreased upon hypoxic exposure from 0.8 μM to 0.5 μM, but amount of nitrosothiols increased ~5 times [265]. These observations indicate that nitrite is an important pool, which may be used to produce NO in myocardial tissue in deoxymyoglobin-catalyzed reaction. Maintenance of NO production under hypoxic conditions is one of the key strategies allowing survival of anoxia-tolerant species in hypoxic environment.

Conclusions

In cardiomyocytes Na,K-ATPase is present as a heterotrimer, composed of the catalytic α-, regulatory β-subunits and phospholemman. Three isoforms of catalytic α-subunit with specific subcellular distribution and functional properties maintain Na^+/ K^+ gradient and participate in signaling processes in cardiac tissue. Multiple regulatory pathways adjust the presence of the enzyme in sarcolemma and its activity coordinating it with the heart's performance.

Adaptation of the cardiac function to the hypoxic environment includes reversible acute down-regulation of the Na,K-ATPase activity. Extensive studies did not give a clue to what is the mechanism of the Na,K-ATPase response to deoxygenation. They have revealed that inhibition of the enzyme in ischemic/hypoxic heart are most likely caused by a decline in subsarcolemmal ATP content, elevation in intracellular Ca^{2+}, decrease of NO levels and shift in the redox state of the tissue towards more oxidized. These events may result in the changes in phosphorylation of the enzyme as well as in oxidation of thiol residues of the protein. This motivated us to design a study looking at the possible involvement of reversible oxidative thiol modifications in hypoxic responses of the Na,K-ATPase.

Experimental part

Rationale, aim, tasks of the study and experimental design

Rationale

Autonomous adaptation of myocardial tissue to the short-term reduction in oxygen supply includes reversible inhibition of hydrolytic activity of Na,K-ATPase. Although this adaptive response may be beneficial for the myocardium as it results in reduction of ATP consumption, it can cause Ca^{2+} overload, myocardial injury and compromise blood supply of peripheral tissues in disease like anemia, sepsis and CBF disturbance. Decrease in production of the nitric oxide and oxidative stress

observed in hypoxic myocardium are most likely involved in acute and rapidly reversible hypoxic responses of the Na,K-ATPase. Recent studies revealed that redox sensitive inhibition of Na,K-ATPase may be induced by S-glutathionylation of Cys-46 residue of β1-subunit of Na,K-ATPase. Binding of glutathione to this thiol results in reduction of the enzyme activity by 25%, which is associated with dissociation of β-subunit from α-subunit [16]. Implication of this mechanism in inhibition of the enzyme was shown in infarcted sheep myocardium. The accessibility of thiol groups of the catalytic α-subunit (23 cysteine residues in total) to S-glutathionylation was not tested so far.

Aim of the study

This study was designed to characterize redox-dependent regulation of hydrolytic activity of Na,K-ATPase in response to the deoxygenation of the heart tissue in details. We aimed particularly to identify the role of reversible thiol modifications of the α-subunit in these responses. Special attention was paid to the effects of nitric oxide availability on tissue redox status, thiol modifications of the α-subunit and the concomitant changes in activity of the Na,K-ATPase. Furthermore the role of thiol modifications in adaptation of the heart to hypoxia were compared between hypoxia tolerant (Blind subterranean mole rat Spalax) and hypoxia sensitive (Norwegian rat) animals.

Tasks

To achieve the above-mentioned aim of the study the following tasks were carried out:

1. Investigation of oxygen-dependent modulation of the enzyme activity and the changes in redox state and NO production in the heart tissue associated with it.
2. Assessment of the post-translational amino acid modifications of the Na,K-ATPase α-subunit. Those included serine phosphorylation, tyrosine nitration, and cysteine S-nitrosylation and S-glutathionylation

3. Assessment of the actual effect of the observed reversible oxidative thiol modifications on the hydrolytic activity of Na,K-ATPase in vitro and in silico.
4. Comparison of the hypoxia induced alternations in redox status of the myocardial tissue in hypoxia sensitive rat, hypoxia tolerant Spalax and rainbow trout in vivo and ex vivo and the ability of the Na,K-ATPase to respond to thiol modifications in vitro.

Experimental design

Experimental models:

1. In vivo hypoxia model (in collaboration with Laboratory of Molecular Evolution of Animals Institute of Evolution, University of Haifa)
2. Ex vivo heart hypoxia model (autologous blood perfused heart)
3. Isolated sarcolemmal fraction and purified Na,K-ATPase

Experimental techniques:

1. Hydrolytic activity of Na,K-ATPase assay
   Isothermal titration calorimetry of ATP binding to Na,K-ATPase (in collaboration with Engelhardt Institute of Molecular Biology, Russian Academy of Sciences, Moscow, Russia; Faculty of Biology, M.V. Lomonosov Moscow State University, Moscow, Russia; and Shemyakin-Ovchinnikov Institute of Bioorganic Chemistry, Russian Academy of Sciences, Moscow, Russia)
2. Western blot, immunoprecipitation, biotin-switch for identification and quantification of Na,K-ATPase thiol modifications, serine phosphorylation and tyrosine nitration.
3. Mass-spectrometry for localization of thiol modifications of Na,K-ATPase (in collaboration with Engelhardt Institute of Molecular Biology, Russian Academy of Sciences, Moscow, Russia; Faculty of Biology, M.V. Lomonosov Moscow State University, Moscow, Russia; and Shemyakin-Ovchinnikov

Institute of Bioorganic Chemistry, Russian Academy of Sciences, Moscow, Russia)

4. Cloning and sequencing of α1-subunit of Na,K-ATPase from Spalax (in collaboration with Functional Genomics Unit, Roy J. Carver Biotechnology Center, University of Illinois at Urban-Champaign, USA)
5. Sequence alignment

Results

1. Heart function under hypoxic conditions and in the presence of NOS inhibitors

Perfusion of isolated rat hearts with autologous blood equilibrated with 20, 15 or 10% of oxygen in gas phase for 45 min didn't affect autonomous heart rate. As pO_2 in gas phase was further reduced 5 or 3 kPa heart rate was decreased to 42±4% of initial value of 254±50 beats/min, N=16 (Table 6 and Figure 16). Furthermore, decrease in oxygen supply to 5 kPa pO_2 in gas phase was associated with the changes in the form of PQRST complex on the ECG, one of which was inversion of T wave (Figure 17). Similar ECG alterations were reported earlier on in ischemic heart in vivo [266]. Hypoxia-induced bradycardia was associated with arrhythmia in some of the hearts. These responses developed within 1-20 minutes after reduction of hemoglobin oxygen saturation (Table 6 and Figure 16).

Table 6. Heart electrical and mechanical parameters as a function of O_2 concentration in blood and treatment with 300 μM L-NAME. Time from the onset of perfusion (end of restitution period) to the beginning of the bradycardia, arrhythmia and T-wave inversion was calculated from ECG recordings using LabChart 7.0 software with ECG analysis module (ADInstruments).

	O_2 concentration, %						
	20	15	10	5	3	5 + L-NAME	20 + L-NAME

total amount of analyzed hearts	15	5	5	15	5	10	10
number of hearts with bradycardia	0	0	0	12	5	10	0
begin of bradycardia, min	-	-	-	between 10 and 13 min	between 5 and 13 min	Between 1 and 5 min	-
number of hearts with T-wave inversion	-	1	1	15	5	10	0
begin of T-wave inversion, min	-	35	32	between 20 and 25 min	between 20 and 23 min	between 5 and 20 min	-
number of arrhythmic hearts	0	0	0	7	5	10	2
begin of arrhythmia, min	-	-	-	between 25 and 30 min	between 19 and 28 min	between 15 and 30 min	32

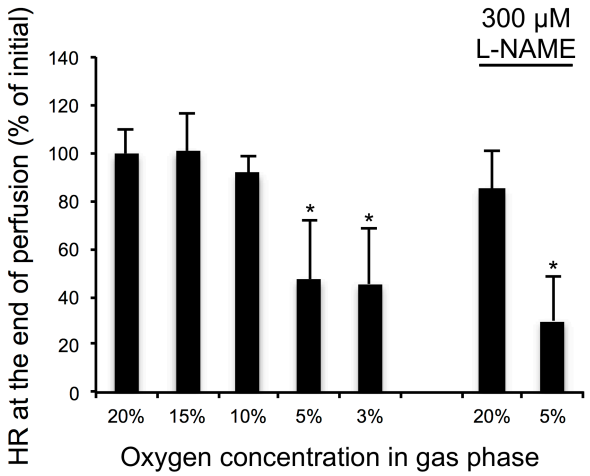

Figure 16. Oxygen-sensitivity of rat heart rate. Changes in autonomous heart rate of rat hearts after 40 min of perfusion with blood equilibrated with 20-3% O_2 in gas phase in the presence or absence of 300 µM L-NAME. Values were normalized to those at the end of 20 min of restitution during which the hearts were perfused with fully oxygenated blood (20% O_2). Values are means ± SD for 5-15 independent experiments. * denotes $p<0.05$ when compared with 20% O_2.

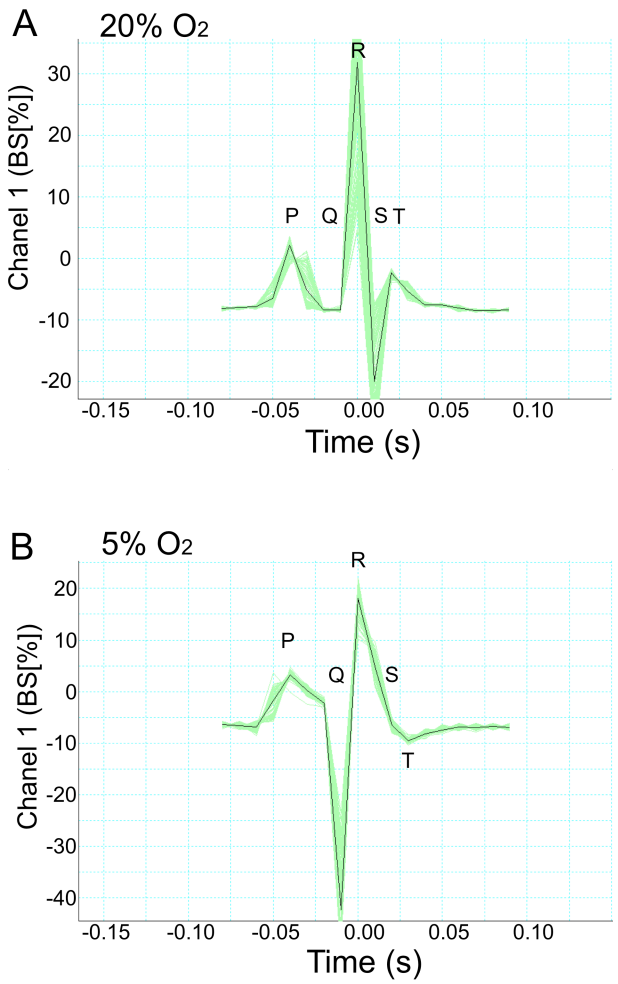

Figure 17. Example of the T-wave inversion. Changes in T-wave amplitude in the ECG recordings (with LabChart 7.0 software with ECG analysis module, ADInstruments) of rat hearts after 30 min of perfusion with blood equilibrated with 20% (A) and 5% (B) O_2 in gas phase. Figure represents the shape of the PQRST complex, made as average of 100 recorded PQRST complexes of single heart starting from the 40th minute of perfusion with blood equilibrated with 20 and 5% O_2 in gas phase.

Based on the obtained findings perfusion with blood equilibrated with 5 % O_2 in gas phase (SO_2=35%) was chosen as representing hypoxic conditions for further experiments. Hypoxia-induced changes were related to normoxic baseline, namely to the values obtained in myocardium perfused with oxygen-saturated (20% O_2, SO_2=95.8%) blood.

Suppression in NO production could be one of the factors compromising and further aggravating oxygen delivery.

To investigate the effects of nitric oxide availability on heart performance and activity of Na,K-ATPase, inhibitor of NO production L-NAME was administrated to the blood during perfusions. L-NAME had a slight pro-arrhythmogenic effect in normoxic hearts and doubled arrhythmia events in hypoxic myocardium (see Table 6 and Figure16).

2. Redox state, NO production and function of Na,K-ATPase in hypoxic rat myocardium

Hypoxia-induced changes in redox state and NO production were assessed in isolated blood-perfused rat heart. Perfusion of hearts with hypoxic blood for 40 min resulted in a shift in half-cell redox potential for GSH/GSSG couple towards more oxidized along with a decrease in NO_2^- levels reflecting NO production (Figure 18). Reduction in nitric oxide synthases (NOSes) activity was to a large extent the cause of oxidative stress. Perfusion of hearts with normoxic blood containing 300 μM L-NAME induced oxidation of GSH, and no further pro-oxidative effect of hypoxia was observed in L-NAME-treated myocardium (Figure 18). Treatment of the isolated hearts with L-NAME speeded up the onset of bradycardia (Table 6), but had no effect on the end-levels of heart rate (Figure 16). Arrhythmia induction was observed in some of the hearts exposed to L-NAME even under normoxic conditions (Table 6).

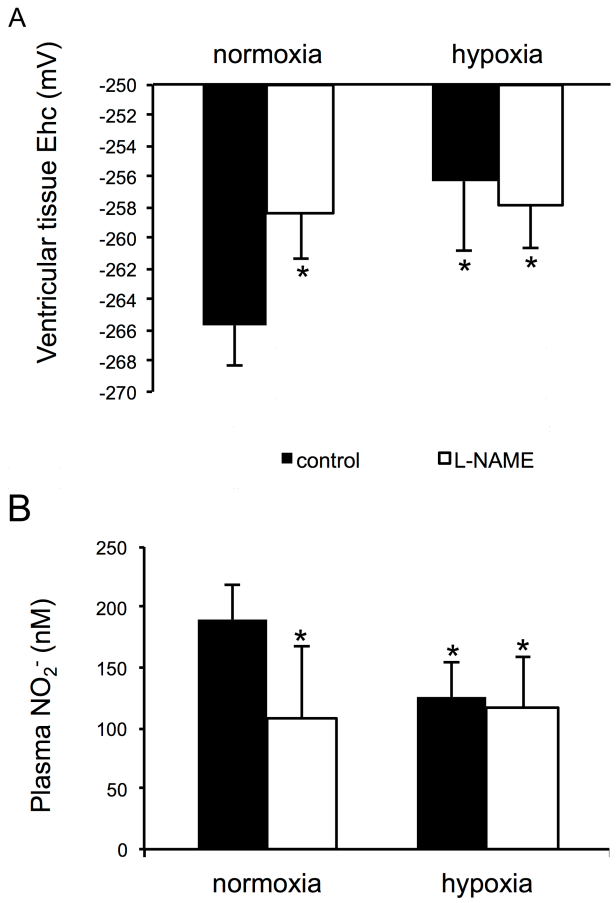

Figure 18. Oxygen-sensitivity of ventricular tissue redox state and plasma NO_2^-. A: The effect of hypoxia (5% O_2) and introduction of 300mM L-NAME into blood perfusate on ventricular half-cell redox potential Ehc for the GSH/GSSG couple that was calculated from the following equation:

$$E_{hc}(GSH:GSSG) = -240 - \frac{59.55}{2}\log\frac{[GSH]^2}{[GSSG]}$$

Decrease in oxygen supply as well as treatment with 300 µM L-NAME resulted in the shift of the redox state towards more oxidized state. The effect of combined action of hypoxia and L-NAME was equal to the effect of both separately. Bars represent means ± SD; n=4 animals. *P<0.05 vs. 20% oxygen homogenate (one-way ANOVA); #P<0.05 vs. 20% oxygen homogenate (one-way ANOVA) B: The effect of hypoxia (5% O_2) and introduction of 300mM L-NAME in to perfusion blood on content of nitrite in perfusion blood plasma. Blood samples were collected 30 min after the onset of perfusion. Bars represent means ± SD; n=4 animals. *P<0.05 vs. normoxic (20% O_2) homogenate (one-way ANOVA); # P<0.05 vs. normoxic (20% O_2) homogenate (one-way ANOVA).

These changes in myocardial function and redox state occurred along with a dose-dependent decrease in activity of Na,K-ATPase in ventricular tissue homogenates from 6.4±3.3 µmol Pi/(mg_{prot} * h) in normoxic myocardium to 1.25±0.18 µmol

Pi/(mg_{prot} * h) in tissue exposed to 3% O_2 (hemoglobin oxygen saturation SO_2 of 16%) (Figure 19A). Reduction in blood oxygenation from arterial (pO_2 20 kPa, SO_2 95.8%) to venous (pO_2 10%, SO_2 85%) hemoglobin oxygen saturation values caused a 2-fold decrease in activity of Na,K-ATPase.

Similar profound inactivation of the Na,K-ATPase was earlier on reported to occur in ventricular tissue homogenates prepared from rat heart exposed to no-flow ischemia [173]. Inhibition of the enzyme in ischemic tissue homogenate was associated with an increase in Na,K-ATPase activity in sarcolemmal membranes. Stimulatory effect of ischemia at the sarcolemmal membrane level was shown to be caused by phosphorylation of the regulatory FXYD1 subunit of the Na,K-ATPase phospholemman at Ser-68 [251]. Similar to that, in ischemic myocardium, in which hypoxia occurred along with acidosis and aglycemia, exposure of rat heart to hypoxia alone was also associated with phosphorylation of phospholemman (Figure 19B) and with a dose-dependent increase in Na,K-ATPase activity in sarcolemmal membranes from 16.5±2.7 μmol Pi/(mg_{prot} * h) to 25.0±2.2 μmol Pi/(mg_{prot} * h) (Figure 19A). Mechanisms of activation of the enzyme in sarcolemmal fraction of ischemic heart and the role of phospholemman have been addressed earlier [251]. We have therefore concentrated on characterization of the molecular mechanisms behind the inhibitory action of hypoxia on the Na,K-ATPase in ventricular homogenate. Exposure of isolated blood-perfused rat heart to hypoxia for 40 min was associated with a 6-fold reduction in activity of Na,K-ATPase in ventricular tissue homogenate (Figure 19A).

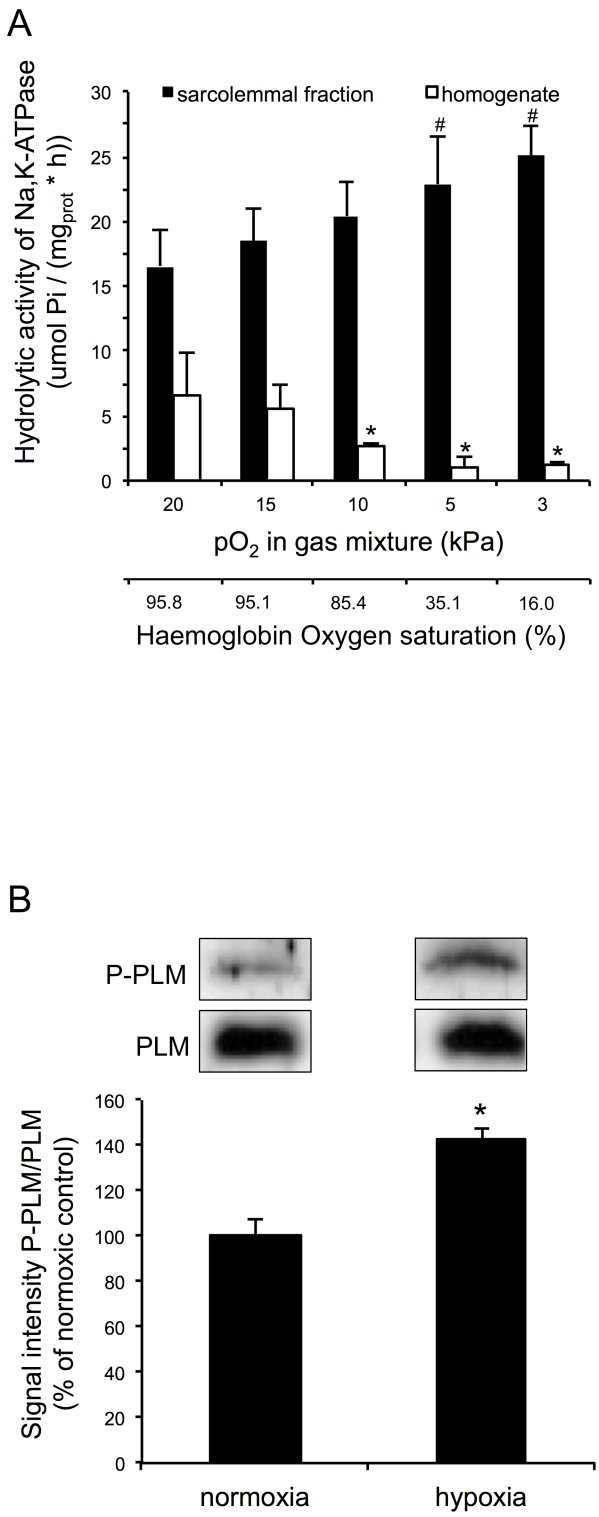

Figure 19. The effect of different concentrations of oxygen (3-20%) in gas mixture equilibrated with blood perfusate on hydrolytic activity of Na,K-ATPase in ventricular tissue homogenate (open bars) and ventricular tissue sarcolemmal fraction (filled bars) of isolated blood perfused hearts. Rat hearts were subjected to 40 min perfusion with autologous blood of various hemoglobin oxygen saturation (indicated on the lower X axes). Decrease in oxygen supply resulted in gradual inhibition of Na,K-ATPase hydrolytic activity in ventricular homogenate and gradual

increase in hydrolytic activity in sarcolemmal fraction. Bars represent means ± SD; n=10 animals. *P<0.05 vs. 20% O_2 homogenate (one-way ANOVA); **P<0.01 vs. 20% O_2 homogenate (one-way ANOVA); #P<0.05 vs. 20% oxygen sarcolemmal fraction (one-way ANOVA). B. Changes in phosphorylation of phospholemman at Ser-68 induced by reduction in oxygenation in gas phase from 20 to 5 kPa. Data are means of 5 experiments ± SD * denotes p<0.05 in Students unpaired t-Test.

Oxygen-sensitivity of Na,K-ATPase was lost in the hearts perfused with blood containing 300 μM L-NAME, in which the enzyme retained its function under hypoxic conditions (Figure 20). Taken together these data indicated that hypoxia-induced responses of the Na,K-ATPase were closely associated with the changes in GSSG and NO levels.

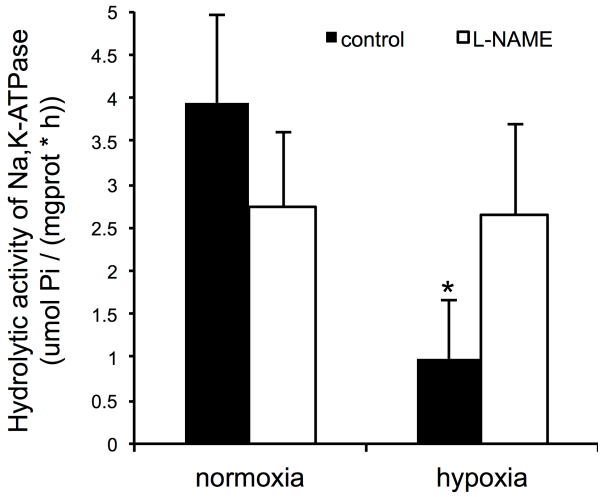

Figure 20. The effect of hypoxia (5% O_2) and introduction of 300mM L-NAME in to blood perfusate on hydrolytic activity of Na,K-ATPase in ventricular tissue homogenate. Inhibition of NO production under hypoxic conditions results in significant increase of hydrolytic activity of Na,K-ATPase. Bars represent means ± SD; n=4 animals . *P<0.01 vs. normoxic (20% O_2) homogenate (1-way ANOVA); # P<0.01 vs. hypoxic (5% O_2) homogenate (one-way ANOVA).

3. Serine phosphorylation of Na,K-ATPase α-subunit is dependent on hypoxic stress and NO production

Total serine phosphorylation in the α-subunit of Na,K-ATPase was assessed in homogenates of control and hypoxic hearts using Western blotting with antibodies against phosphoserine.

Basal serine phosphorylation was detected in normoxic control tissue samples (Figure 21). The number of phosphorylated serines in the α1-subunit didn't change in response to L-NAME treatment under normoxic conditions. Serine phosphorylation occurred in response to hypoxia. A combination of hypoxic conditions and L-NAME exposure was not associated with an increase in serine phosphorylation of the α1-subunit compared to normoxic control. This indicates that redox sensitive protein kinases in the heart (AMP-dependent proteinkinase, PKC, MAPK) [249, 267, 268] can be involved in phosphorylation of α-subunit of Na,K-ATPase.

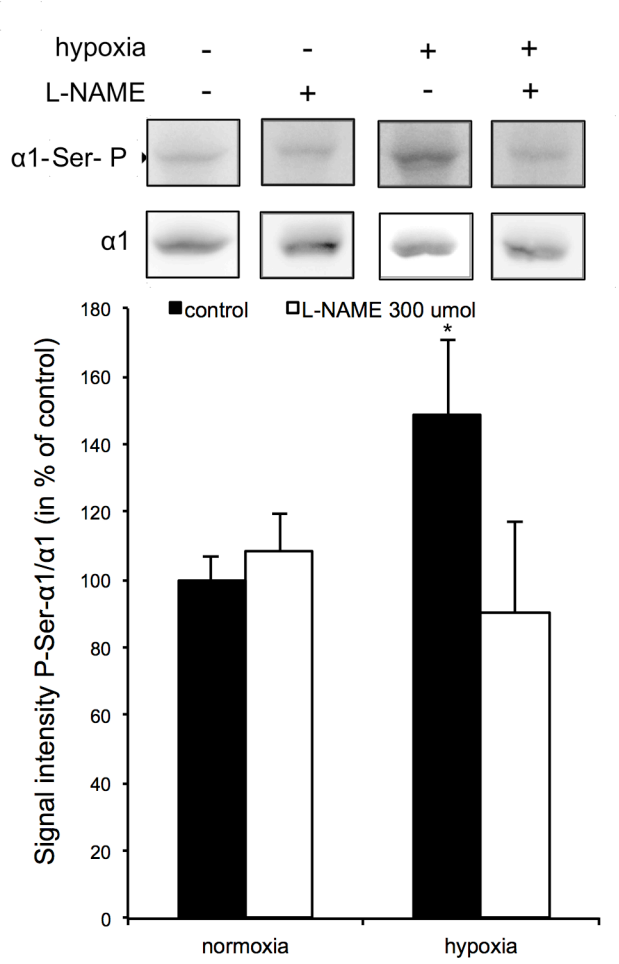

Figure 21. Phosphorylation of serine residues in the α1-subunit assessed using phosphoserine antibodies. Original recordings of phosphoserine-containing α1-subunit in tissue homogenates of the heart exposed to hypoxia and or L-NAME are presented at the top panel whereas quantification of the S-nitrosylation state of the α1-subunit normalized to the abundance of α1-subunit in homogenate is presented at the bottom panel. Data are means of 8 independent experiments ± SD. * denotes $p<0.05$ when compared to the normoxic non-treated control determined using one-way ANOVA.

4. Thiol modifications of Na,K-ATPase α-subunit are dependent on hypoxic stress and NO production

S-nitrosylation of cysteines of the catalytic α-subunit of the Na,K-ATPase was assessed in normoxic and hypoxic myocardium using Western blotting and Biotin-Switch techniques.

S-nitrosylation of the α1-subunit was high in normoxic control samples and reduced in response to hypoxia and/or L-NAME treatment (Figure 22A). Reduction in number of S-nitrosylated cysteines in the α1-subunit in hypoxic heart was associated with a pronounced increase in nitrated tyrosine residues in it. Exposure to L-NAME suppressed hypoxia-induced nitrotyrosine formation (Figure 22B).

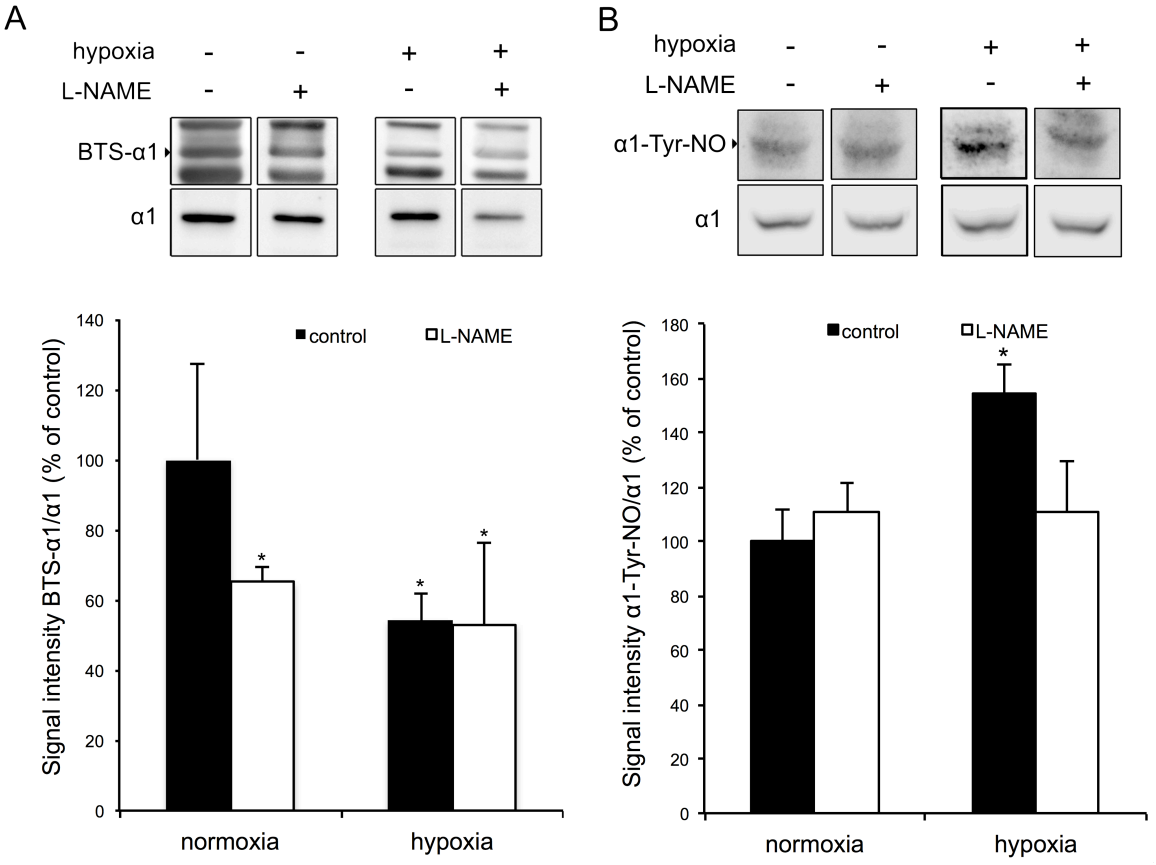

Figure 22. A. S-nitrosylation of thiols in the α1-subunit assessed using biotin switch technique. Original recordings of S-nitrosylated (biotinylated) cysteines in the α1-subunit in heart tissue homogenates exposed to hypoxia and or L-NAME are presented at the top panel whereas quantification of the S-nitrosylation state of the α1-subunit normalized to the abundance of α1-subunit in homogenate is presented at the bottom panel. B. Tyrosine nitration of the α1-subunit of the Na,K-ATPase. Normalization has been performed as in A. Data are means of 8 independent

experiments ± SD. * denotes $p<0.05$ when compared to the normoxic non-treated control determined using one-way ANOVA with the Bonferroni post-test.

To asses S-glutathionylation of cysteines of the catalytic α-subunit of the Na,K-ATPase immunoprecipitation was carried on using anti-GSH antibodies with the following immunoblotting against α1 and α2 isoforms of the catalytic subunit. The presence of S-glutathionylated thiols in the α1-subunit in crude homogenate prepared from ventricular tissue was confirmed using immunoblotting. Basal S-glutathionylation of the active enzyme was observed already in normoxic control tissue samples (Figure 23). The number of S-glutathionylated cysteines in the α1-subunit increased in response to L-NAME treatment under normoxic conditions as well as response to hypoxia. A combination of hypoxic conditions and L-NAME exposure was not associated with an increase in S-glutathionylation of the α1-subunit compared to normoxic control.

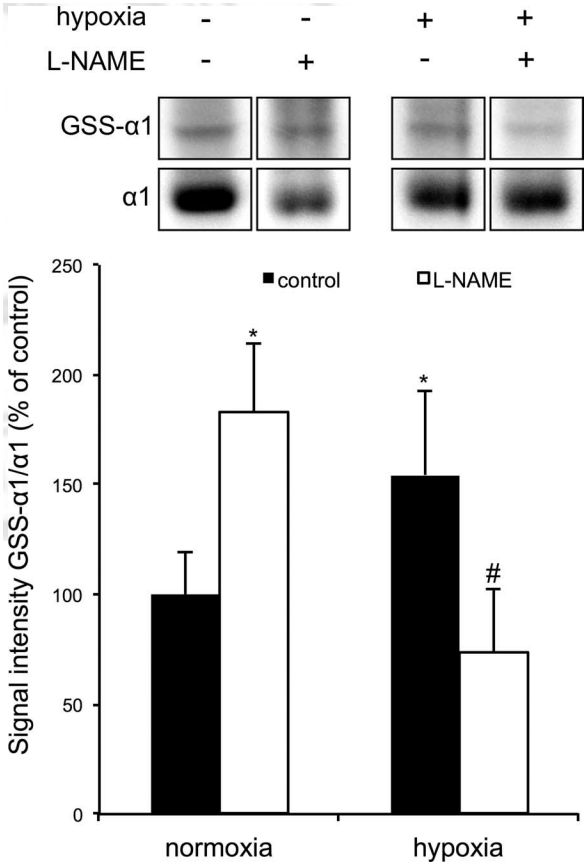

Figure 23. S-glutathionylation of thiols in the Na,K-ATPase α1-subunit in rat heart exposed to hypoxia (5% O_2) or normoxia (20% O_2) with (open bars) an without (filled bars) 300 μM L-NAME. The signal intensity for the S-glutathionylated thiols in the α1-subunit in homogenate was normalized to that of α1 abundance (see the original immunoblotting readouts above the quantification bar chart). Data are means of 8 independent experiments ±SD. * denotes $p<0.05$ when compared with normoxic control and # indicates $p<0.05$ when compared with the corresponding hypoxic control in the absence of L-NAME (one-way ANOVA).

5. S-glutathionylation of α1-subunit of Na,K-ATPase in vitro inhibits activity of the enzyme. Reversibility of S-glutathionylation

Cysteine localisation and number as well as conformation of the catalytic subunit differs between its isoforms. As the α1- and α2-subunits are most abundant in the heart playing there distinct roles in control of Na^+/K^+ gradient and Ca^{2+} levels (see paragraph 2.2 and 2.3), we have therefore set up experiments comparing their sensitivities to inhibition by GSSG. IC_{50} was assessed for the GSSG-induced inhibition of the α1β1 and α2β1 isozymes in rat sarcolemmal membranes. We have used a

profound difference in ouabain-sensitivity of the rat α1 and α2 isozymes of Na,K-ATPase to discriminate between responses of these isoforms of the enzyme catalytic subunit to GSSG. Na,K-ATPase function was assessed in two sets of samples, one of which contained 10 μM ouabain. At this concentration ouabain was earlier shown to cause complete inhibition of the α2β isozyme, whereas the α1β isozyme remained unaffected. Both sets of samples were incubated with various concentrations of GSSG for 10 min at 37˚C and then the Na,K-ATPase activity was determined in both sets using 1 mM ouabain to block both isozymes. As shown in Figure 24, two isoforms of the catalytic subunit showed different sensitivity to GSSG. "Ouabain-resistant" α1 isoform was 5-fold less sensitive to the inhibitory action of GSSG than the "ouabain-sensitive" α2 isozyme. The calculated IC_{50} values were 43.6±9.2 and 265±13 μM for the α2 and α1 isoforms respectively. Inhibition of the α1-containing isozyme with GSSG correlated with an increase in S-glutathionylation levels (grey bars and a lower panel in Figure 24).

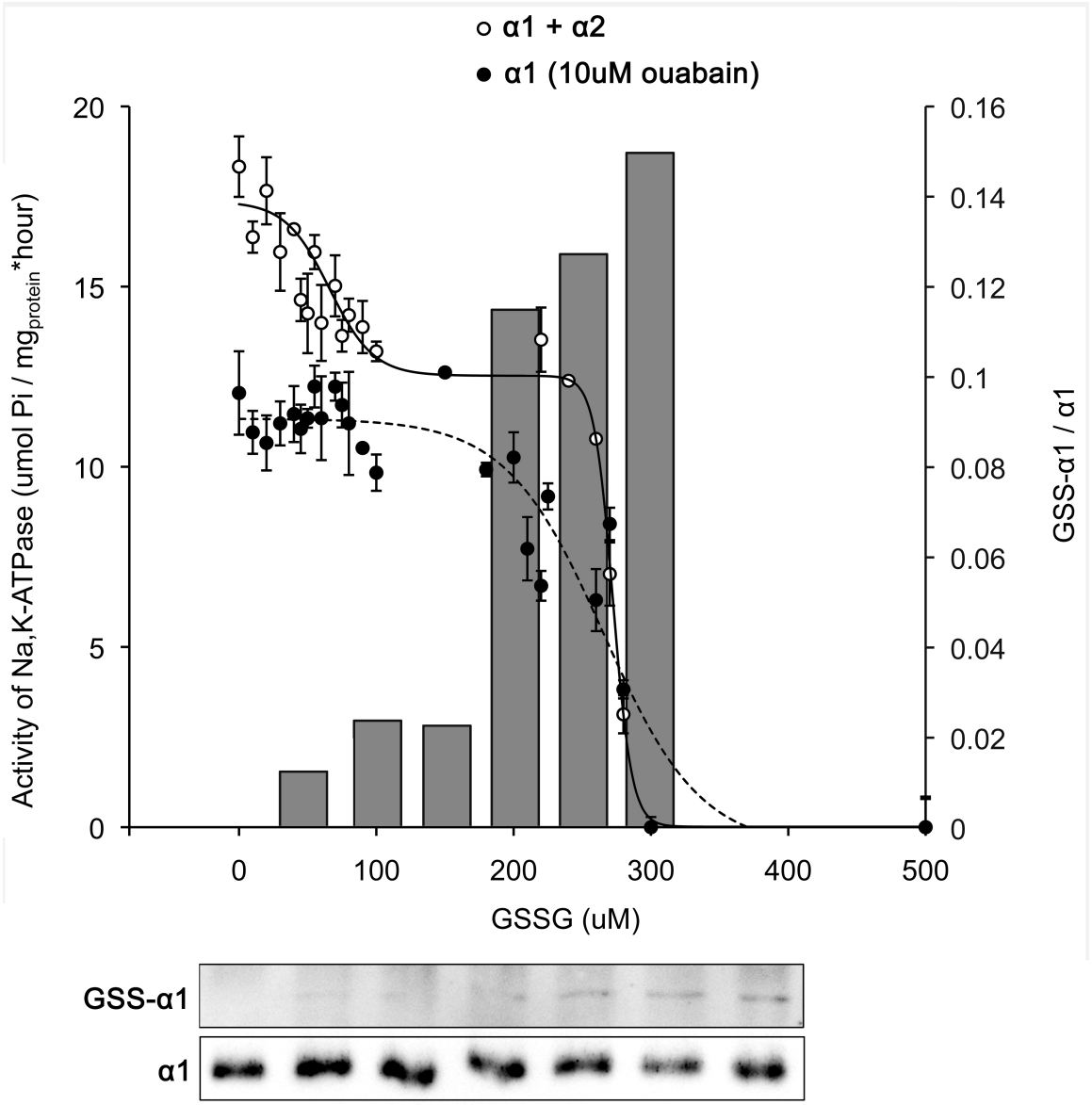

Figure 24. Differential sensitivity of the α1 and α2 isozymes to the inhibitory action of GSSG. Activity of the Na,K-ATPase (α1+α2) or α1 isozyme alone was assessed in sarcolemmal membranes prepared from normoxic heart treated with various GSSG concentrations. α2 isozyme activity was calculated by subtraction of the activity of α1 isoform from the total Na,K-ATPase activity. Fitting of the plots with double (α1+α2) or single (α1 or α2 alone) logistic sigmoidal functions was performed giving apparent IC50 for α1 is 271.1±1.7 μM and for α2 is 43.6±9.2 μM. Grey bars and the lower panel show the changes in S-glutathionylation of the α1-subunit followed by the corresponding to the changes in enzyme activity. N=5 per group. All plotted data represent mean values ± s.d.

Inhibition of the Na,K-ATPase in sarcolemmal preparation by GSSG can be prevented if NOS substrates and co-activators were present in the incubation medium along with 250 μM GSSG, inhibition of the Na,K-ATPase and glutathionylation of α1 does not occur (Figure 25).

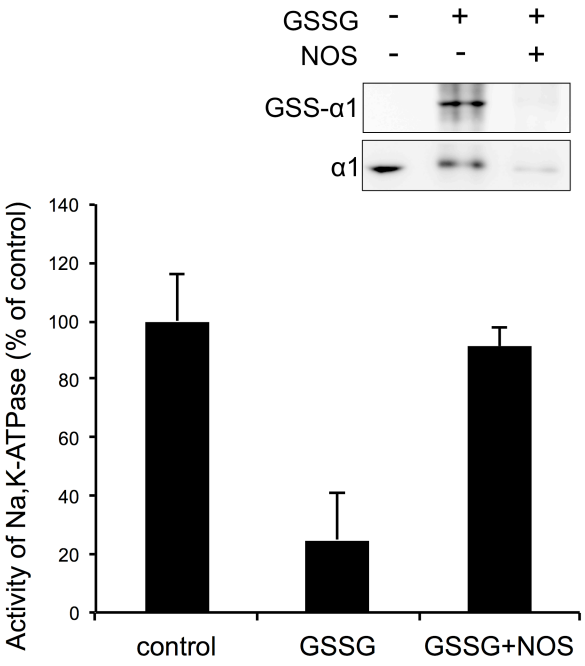

Figure 25. Induction of S-glutathionylation by treatment of sarcolemmal vesicles isolated from normoxic heart homogenate. Sarcolemmal membranes were exposed to 250 μM GSSG (GSSG) for 10 min at 37^0C in the absence or presence of substrates and co-factors of NO syntases (L-arginine, NADPH, FMN, H_2-FAD, BH_4, Ca-calmodulin, GSSG +NOS). S-glutathionylation of the α1-subunit of the Na,K-ATPase and hydrolytic activity of the enzyme were tested after exposure to GSSG. Data are means of 3 experiments ± SD. * denotes $p<0.05$ when compared to the non-treated control.

In addition, oxidation of the protein by exposure of sarcolemmal preparation to 90% O_2 for 1 hour can prevent inhibition of the Na,K-ATPase by GSSG in sarcolemmal preparation (Figure 26)

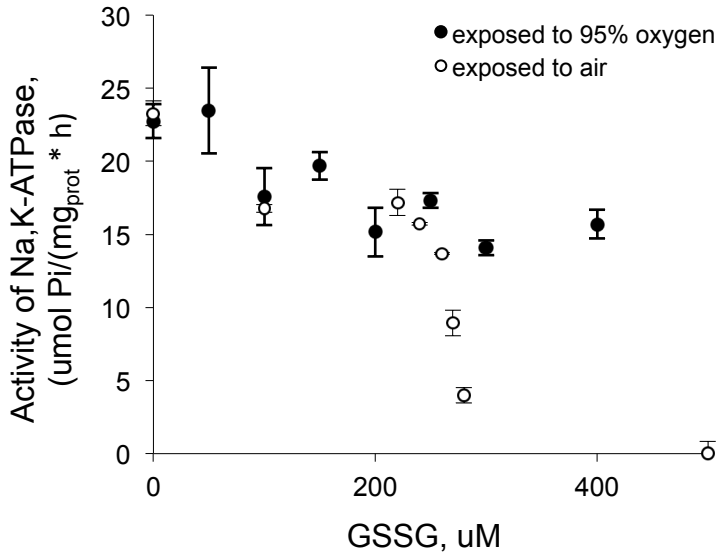

Figure 26. Absence of inhibition of Na,K-ATPase in sarcolemmal fraction by GSSG after exposure of oxygen. Sarcolemmal membranes were exposed (filled circles) or not exposed (empty circles) to 90% O_2 for 1 h and afterwards incubated with different concentration of GSSG for 10 min at 37^0C. Data are means of 3 experiments ± SD.

Furthermore, we could induce de-glutathionylation and restore the function of S-glutathionylated inactive enzyme by exposing it to a Glutaredoxin 1 (GRX1) and GSH. As shown in Figure 27, exposure of sarcolemmal membranes isolated from normoxic rat heart to 250 μM GSSG induced S-glutathionylation of the α1-subunit associated with a marked suppression of the enzyme hydrolytic activity. Both S-glutathionylation and inhibition of the enzyme by GSSG in sarcolemmal preparations could be reversed in presence of 250 μM GSH and 0.6U GRX1

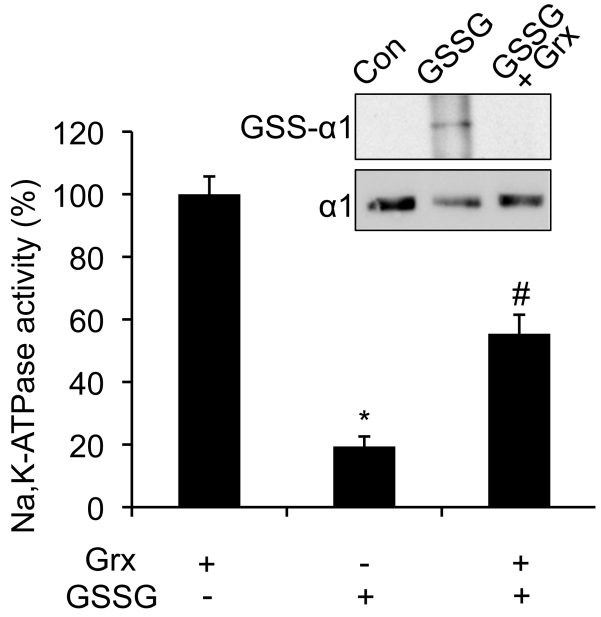

Figure 27. Induction of S-glutathionylation by treatment of sarcolemmal vesicles isolated from normoxic heart homogenate. Sarcolemmal membranes were exposed to 250 μM GSSG (GSSG) for 10 min at 37^{0}C and treated afterwards with mixture of 250 μM GSH and 0.6U Glutaredoxin 1 (GRX) for 1 h at 37^{0}C. S-glutathionylation of the α1-subunit of the Na,K-ATPase and hydrolytic activity of the enzyme were tested after the induction of S-glutathionylation. Data are means of 3 experiments ± SD. * denotes $p<0.05$ when compared to the non-treated control.

6. GRX1 reverse mode cause S-glutathionylation of Na,K-ATPase

In the myocardium GRX1 may catalyze de-glutathionylation (Figure 27) as well as promote binding of GSH to the protein thiols in the presence of a GS-radical-generating system [129, 269, 270].

$O_2^{\cdot-} + GSH + H^+ \leftrightarrow H_2O_2 + GS^{\cdot}$

$2GRX\text{-}S^- + 2\ GS^{\cdot} \rightarrow 2GRX\text{-}SSG^{\cdot-}$

$GRX\text{-}SG^{\cdot-} + Protein\text{-}SH \rightarrow Protein\text{-}S^{\cdot} + GRX\text{-}S^{\cdot} + GSH$

$GRX\text{-}SSG^{\cdot-} + Protein\text{-}S^{\cdot} \rightarrow Protein\text{-}SSG + GRX\text{-}S^-$

We explored if this can happen in homogenate of normoxic heart. Therefore we introduced 0.6 U glutaredoxin 1, 0.2mM NADPH (to activate NADPH oxidase in homogenate) as well as different amount of glutathione reductase (to keep the GSH

level high) to the heart homogenate under normoxic conditions. We were able to see, that this treatment resulted in the increased S-glutathionylation of Na,K-ATPase and reduction of its activity, proportional to amount of introduced glutathione reductase (Figure 28)

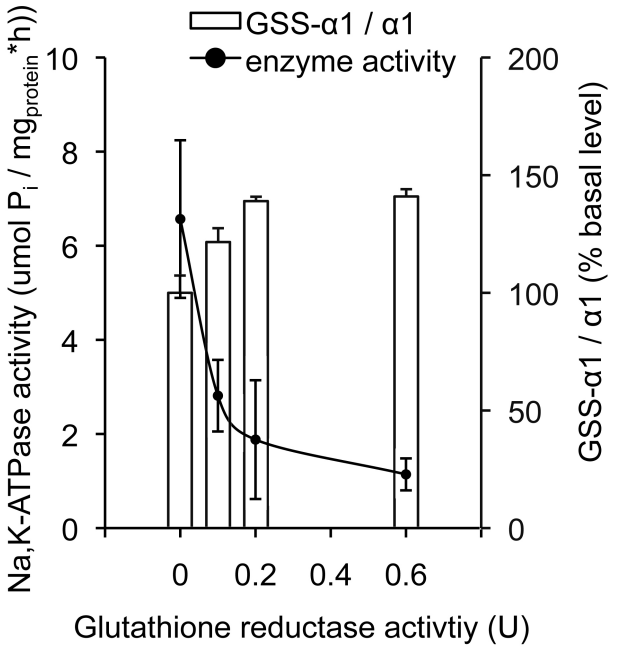

Figure 28. Dose-dependent GSH-induced S-glutathionylation (grey bars) and the corresponding changes in activity of the enzyme (line) in crude homogenate treated with glutathione reductase and glutaredoxin1/NADPH. Data are means of 4 experiments ± SD

7. Kinetics of GSSG-induced inhibition of rabbit kidney Na,K-ATPase. ATP and ADP binding to the S-glutathionylated and native enzyme. Identification of the S-glutathionylated cysteines in ATP binding pocket with mass-spectrometry as well as in silico modeling of glutathione binding

(This part of the study was preformed in collaboration with Dr. I. Petrushanko, Prof. A. Makarov from Engelhardt Institute of Molecular Biology and Prof. O. Lopina from Moscow State University. Data obtained in collaboration are presented in detail in the manuscript 1. Shown below is a brief summary of the data obtained by our

collaborators which is of pivotal importance for understanding of the molecular mechanism of the observed phenomena)

Alpha-subunit of the purified Na,K-ATPase preparations is S-glutathionylated

S-glutathionylation of the catalytic subunit was monitored in the Na,K-ATPase preparation purified from duck salt glands and rabbit kidneys exclusively expressing the α1β1 form of the enzyme. The α1- and β1-subunit of the Na,K-ATPase isolated from the duck salt gland **(manuscript 2, Fig. 1a,b)** and rabbit kidney **(manuscript 2, Fig. 1c)** were S-glutathionylated. Basal S-glutathionylation of the α1-subunit was further enhanced after exposure of the enzyme to 1 mM GSSG **(manuscript 2, Fig. 1a,c).** The glutathionylation state of the β-subunit was not affected by GSSG treatment (**manuscript 2, Fig. 1b**). Basal S-glutathionylation level of the α1-subunit was reduced in Na,K-ATPase preparations in the presence of 100 μM DTT **(manuscript 2, Fig. 1c)**.

GSSG treatment causes inhibition of the Na,K-ATPase

Exposure of Na,K-ATPase purified from rabbit kidneys to increasing concentrations of GSSG resulted in the time- and dose-dependent inhibition of Na,K-ATPase **(manuscript 2, Fig. 2a)**. The inhibitory action of GSSG was biphasic. Fast interaction of GSSG with the enzyme accounted for ~80% inhibition of the Na,K-ATPase activity whereas the complete inhibition was delayed **(manuscript 2, Fig. 2b)**. Plotting of the data in semi-logarithmic coordinates allowed estimation of the rate constants of the fast (1655 M^{-1} min^{-1}) and slow (163 M^{-1} min^{-1}) phases from the slope of the linear parts of the curves **(manuscript 2, Fig 2b)**. The biphasic nature of the inhibitory action of GSSG strongly suggested the existence of two classes of GSSG binding sites on the catalytic subunit or, alternatively, two conformational states of the enzyme in which the same thiol groups show either fast or slow S-glutathionylation kinetics.

Dose-dependence of GSSG-induced inhibition of Na,K-ATPase was assessed in purified enzyme preparations. Enzyme activity was measured after 30 min of exposure to 10-100 μM GSSG. GSSG concentration at half maximal inhibition (IC_{50})

was similar for the duck and rabbit α1β1 isozymes (59±2 and 66±3 μM, respectively) (**manuscript 2, Fig. 3a,b**). Sensitivity of the purified duck Na,K-ATPase to GSSG was lost after 4 h exposure of the enzyme preparation to air at 4°C (**manuscript 2, Fig. 3b**).

S-Glutathionylation prevents adenine nucleotides' binding to Na,K-ATPase

The experiments presented above were performed in the absence of ATP since GSSG treatment of the Na,K-ATPase precluded enzyme activity measurements. Pre-treatment of rabbit Na,K-ATPase with GSSG prior to exposing the enzyme to ATP completely inhibited the enzyme (**manuscript 2, Fig. 5a**). However, when GSSG was added to the enzyme, in the presence of ATP at concentration exceeding 0.5 mM, the inhibitory effect of GSSG was completely averted (**manuscript 2, Fig. 5b**). Thus, the inhibitory action of GSSG on the Na,K-ATPase was caused by its interaction with the free enzyme and not with the enzyme-substrate complex.

Isothermal titration calorimetry (ITC) was used for direct assessment of the thermodynamic parameters for nucleotide binding to rabbit Na,K-ATPase in non-glutathionylated and glutathionylated forms. Heat production associated with the interaction of ADP with the rabbit enzyme was measured in the presence of DTT or GSSG. A set of original data obtained in such experiments is shown in **manuscript 2, Fig. 5c**. The ADP binding to Na,K-ATPase was enthalpy-driven (ΔH= – 8.2 ± 0.3 kcal mole^{-1}, $T\Delta S$=1.1 kcal mole^{-1}) with a binding constant K_a of 6.8 ± 1.4 × 10^6 M^{-1}. The stoichiometry of ADP binding to Na,K-ATPase was ~0.8. S-glutathionylation of the enzyme by GSSG completely abolished ADP binding to the Na,K-ATPase (**manuscript 2, Fig. 5c**).

Glutathionylated SH-groups are localised in the large and small cytosolic loops of the α-subunit

Identification of the cysteine residues of the duck Na,K-ATPase that are S-glutathionylated in the native active enzyme, and cysteines undergoing S-glutathionylation upon exposure to GSSG was performed using mass-spectrometry. Duck Na,K-ATPase was exposed to a mixture of 1.7 mM GSH and 170 μM GSSG which was earlier on shown to be present in hypoxic heart and effectively inhibit the

enzyme function. Enzyme activity measurements were performed in control and GSH/GSSG-treated protein samples. Thereafter two enzyme samples were collected from either control or treated enzyme and proteolyzed by either trypsin or chymotrypsin and MALDI TOF MS was used to detect cysteine thiol modifications in proteolytic fragments obtained thereby. The α1 sequence coverage reached 70-80% for chymotrypsin-digested fragments and was 50-60% for tryptic fragments. The state of all cysteine residues of the α1-subunit in control and treated enzyme is summarized in **manuscript 2, suppl. Table 1**. Listed there are the m/z ratios for each fragment and relative peak intensities. Localisation of cysteines within the sequence is schematically shown in **manuscript 2, Fig. 6**. As follows from the **manuscript 2, suppl. Table 1**, treatment of the enzyme with GSH/GSSG was associated with an increase in S-glutathionylation of the Cys454, 458, 459 of the big cytosolic loop and the Cys244 localized within the small cytosolic loop of the α1-subunit. Only the treated protein contained all three cysteines (454, 458 and 459) in S-glutathionylated state. Cysteine residues 369 and 423 have never been found S-glutathionylated.

When bound to the α-subunit glutathione can interact with amino acids of the ATP binding site

The structural alignment of the model containing three glutathionyl residues bound to the Cys 452^{p}, 456^{p}, 457^{p} residues (corresponding to the Cys 454, 458 and 459 residues in the duck, rabbit and rat sequences), and the model with the ATP docked to the protein, has been done by the MOE software (**manuscript 2, supp. Fig. 2**). According to the model, the distance between the terminal negatively charged phosphate of ATP molecule and carboxyl group of glutathione bound to the Cys 452^{p} carrying the same negative charge is less than 8 Å (**manuscript 2, supp. Fig. 3**). Electrostatic retraction forces between these two negative charges are sufficient to hinder attachment of the ATP to the S-glutathionylated binding site moiety. The same is true for glutathione binding to the Cys452^{p} in the presence of ATP in docked position. This electrostatic retraction will become even more pronounced as further two cysteines

in the vicinity of ATP binding site, Cys456^{p} and 457^{p} (**manuscript 2, Fig. 7**), will get S-glutathionylated. These results of modeling comply with the experimental data on mutually exclusive integration of ATP or glutathione with the regulatory S-glutathionylation sites of the catalytic subunit (**manuscript 2, Fig.5a, b**). Modeling based on the crystal structure of the enzyme in E2P conformation did not show any significant interaction of Cys246^{p} with the ATP binding site. However, this may not hold true for the enzyme in E1 conformation [8].

7. Lack of oxygen-sensitivity of Na,K-ATPase in mole rat and rainbow trout heart

The impact of hypoxic exposure on the Na,K-ATPase activity in the heart was explored in hypoxia-tolerant *S. galili* and *S. judaei*. Whereas normoxic animal groups were exposed to ambient air, hypoxic groups were exposed to hypoxic atmosphere containing 6% O_2/94% N_2 for 6 h. Activity of Na,K-ATPase was then assessed in ventricular tissue homogenate. The absolute values of enzyme activity as well as the α1 abundance in normoxic Spalax heart were reduced by ~3-fold compared to that in Wistar rat heart (Figures 29 and 30). In contrast to that in rat heart, Na,K-ATPase in myocardium of both Spalax species was not suppressed in response to hypoxic exposure (Figure 29).

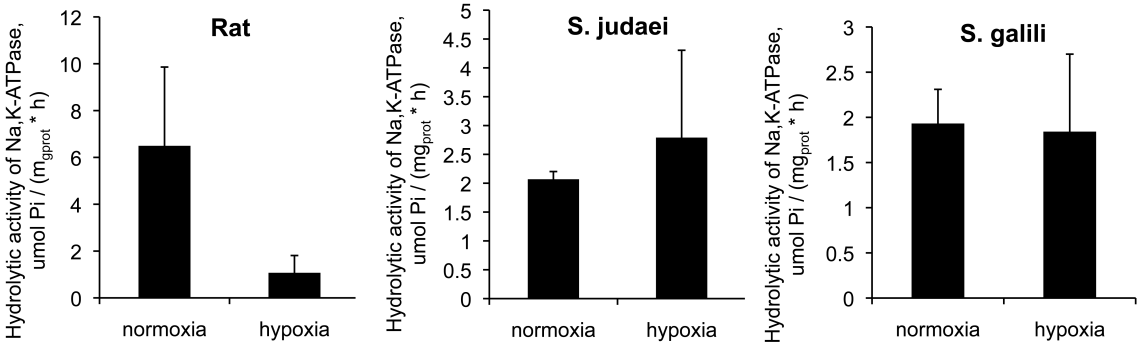

Figure 29. The effect of oxygen deprivation on activity of Na,K-ATPase in ventricular homogenate of Rat (*Rattus Norvegicus*) and two specious of Spalax: most hypoxia tolerant *Spalax Galili* and less hypoxia tolerant *Spalax judaei*. *Ex vivo* hypoxia model was used in experiments with rat heart tissue and in vivo hypoxia model was used in experiments with Spalax. Activity of Na,K-ATPase was reduced significantly only

in rat ventricle tissue homogenate. In Spalax ventricular homogenate activity of Na,K-ATPase was not sensitive to hypoxia. Bars represent means ± SD; n=4. *P<0.01 vs. normoxic homogenate (1-way ANOVA).

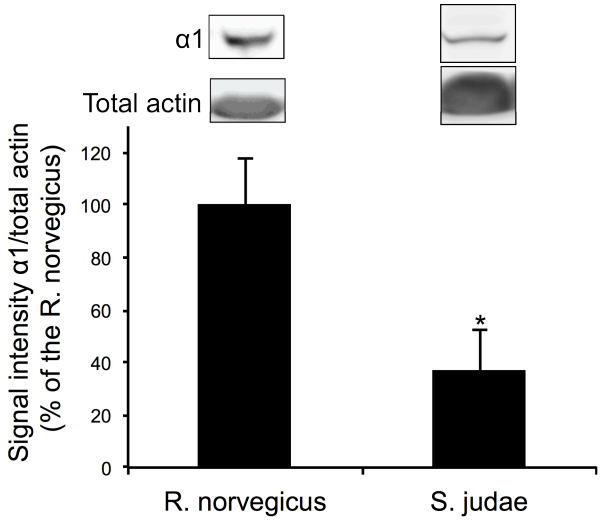

Figure 30. Content of Na,K-ATPase α1-subunit in the ventricular tissue homogenates of rat (*R. norvegicus*) and blind subterranean mole rat (*S. judae*). The signal intensity for the α1-subunit was normalized to that of total-actin abundance (see the original immunoblotting readouts above the quantification bar chart). Data are means of 4-6 independent experiments ±SD. * denotes p<0.05 when compared with rat.

Rainbow trout is a hypoxia-sensitive fish responding to acute reduction in oxygen levels in water with a short bout of escape response. The latter is supported by maintenance of cardiac output as hypoxia-induced bradycardia is associated with a 3-fold increase in stroke volume [271]. Maintenance of myocardial function implies that the Na,K-ATPase activity is preserved. Is it indeed preserved?

At present no trout-specific antibodies for the catalytic subunit isoforms are commercially available. Using the antibodies against the α1- and α2-subunit isoforms we were able to detect the α2, but not the α1 isoform of the Na, K-ATPase in trout (*O. mykiss*) heart by Western-blotting (Figure 31, insertion). Activity of the enzyme in trout heart was significantly reduced compared to that in rat and Spalax myocardium. Exposure of the animal to gradual hypoxia for 1 hour didn't change the hydrolytic activity of the Na,K-ATPase, measured at 13°C and 37°C (Figure 31).

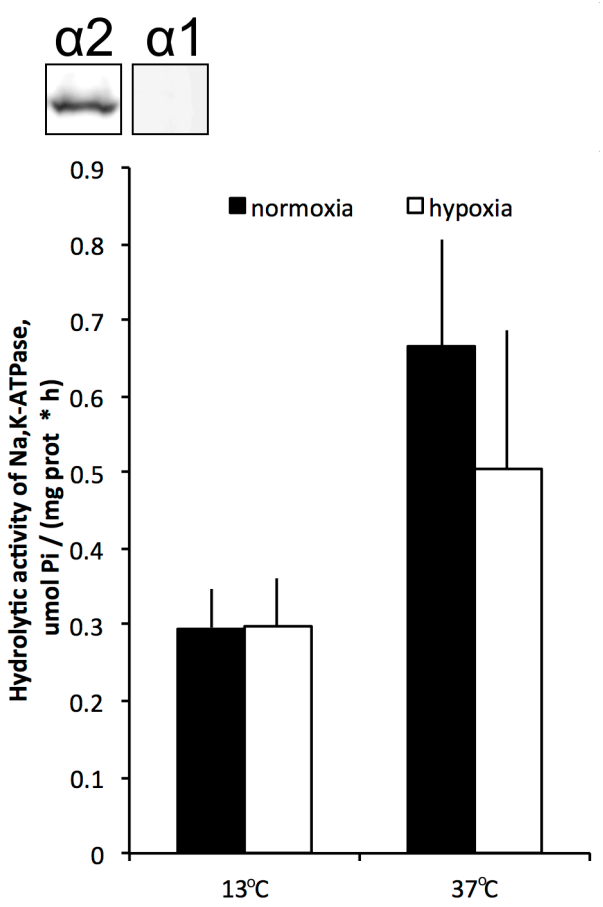

Figure 31. Fishes were exposed to a gradual hypoxia for one hour and hydrolytic activity was assessed in crude homogenate at 13oC and 37oC. Data are means of 4 independent heart samples ±SD. Insertion above are original readouts of immunoblotting with antibodies against α1- and α2-subunits of Na,K-ATPase.

8. Is Spalax and Trout Na,K-ATPase redox-sensitive?

We have further tested if apparent insensitivity of Na,K-ATPase Spalax and trout hearts to hypoxia were stemming from the lack of regulatory cysteine residues, which were present in rat enzyme.

To do so, α1-subunit of Na,K-ATPase of *S. ehrenbergi* was sequenced **(in collaboration with Dr. A. Avivi Laboratory of Molecular Evolution of Animals Institute of Evolution, University of Haifa and Dr. M. Band Functional Genomics Unit, Roy J. Carver Biotechnology Center, University of Illinois at Urban-Champaign, Urbana)** and localization of cysteine residues within the sequence was compared with that of *Rattus Norvegicus*. Sequence alignment

presented in Table 7 showed strong similarity of both proteins and conserved localization of all cysteine residues within the sequences.

Table 7. Sequence comparison of α1-subunit of Na,K-ATPase of *Rattus Norvegicus* (R) and *Spalax judae* (Sp). BLASTP was performed for the sequence alignment.

Sp	MGKGVGRDKYEPAAVSEPTDKKGKKAKKERDMDELKKEVSMDDHKLSLDELHRKYGTDLS	60
R	MGKGVGRDKYEPAAVSEHGDKKSKKAKKERDMDELKKEVSMDDHKLSLDELHRKYGTDLS	60
Sp	RGLTPARAAEILARDGPNALTPPPTTPEWVKF**C**RQLFGGFSMLLWIGAIL**C**FLAYGIRSA	120
R	RGLTPARAAEILARDGPNALTPPPTTPEWVKF**C**RQLFGGFSMLLWIGAIL**C**FLAYGIRSA	120
Sp	TEEEPPNDDLYLGVVLSAVVIITG**C**FSYYQEAKSSKIMESFKNMVPQQALVIRNGEKMSI	180
R	TEEEPPNDDLYLGVVLSAVVIITG**C**FSYYQEAKSSKIMESFKNMVPQQALVIRNGEKMSI	180
Sp	NAEDVVVGDLVEVKGGDRIPADLRIISANG**C**KVDNSSLTGESEPQTRSPDFTNENPLETR	240
R	NAEDVVVGDLVEVKGGDRIPADLRIISANG**C**KVDNSSLTGESEPQTRSPDFTNENPLETR	240
Sp	NIAFFSTN**C**VEGTARGIVVYTGDRTVMGRIATLASGLEGGQTPIAEEIEHFIHLITGVAV	300
R	NIAFFSTN**C**VEGTARGIVVYTGDRTVMGRIATLASGLEGGQTPIAEEIEHFIHLITGVAV	300
Sp	FLGVSFFILSLILEYTWLEAVIFLIGIIVANVPEGLLATVTV**C**LTLTAKRMARKN**C**LVKN	360
R	FLGVSFFILSLILEYTWLEAVIFLIGIIVANVPEGLLATVTV**C**LTLTAKRMARKN**C**LVKN	360
Sp	LEAVETLGSTSTI**C**SDKTGTLTQNRMTVAHMWFDNQIHEADTTENQSGVSFDKTSATWFA	420
R	LEAVETLGSTSTI**C**SDKTGTLTQNRMTVAHMWFDNQIHEADTTENQSGVSFDKTSATWFA	420
Sp	LSRIAGL**C**NRAVFQANQENLPILKRSVAGDASESALLK**C**IEL**CC**GSVSEMREKYAKIVEI	480
R	LSRIAGL**C**NRAVFQANQENLPILKRAVAGDASESALLK**C**IEV**CC**GSVMEMREKYTKIVEI	480
Sp	PFNSTNKYQLSIHKNPNPSEPKHLLVMKGAPERILDR**C**SSILLHGKEQPLDEELKDAFQN	540
R	PFNSTNKYQLSIHKNPNASEPKHLLVMKGAPERILDR**C**SSILLHGKEQPLDEELKDAFQN	540
Sp	AYLELGGLGERVLGF**C**HLLLPDEQFPEGFQFDTDEVNFPVDNL**C**FVGLISMIDPPRAAVP	600
R	AYLELGGLGERVLGF**C**HLLLPDEQFPEGFQFDTDEVNFPVDNL**C**FVGLISMIDPPRAAVP	600
Sp	DAVGK**C**RSAGIKVIMVTGDHPITAKAIAKGVGIISEGNETVEDIAARLNIPVNQVNPRDA	660
R	DAVGK**C**RSAGIKVIMVTGDHPITAKAIAKGVGIISEGNETVEDIAARLNIPVNQVNPRDA	660
Sp	KA**C**VVHGSDLKDMTSEELDDILRYHTEIVFARTSPQQKLIIVEG**C**QRQGAIVAVTGDGVN	720
R	KA**C**VVHGSDLKDMTSEELDDILRYHTEIVFARTSPQQKLIIVEG**C**QRQGAIVAVTGDGVN	720

```
Sp      DSPALKKADIGVAMGIVGSDVSKQAADMILLDDNFASIVTGVEEGRLIFDNLKKSIAYTL  780
R       DSPALKKADIGVAMGIVGSDVSKQAADMILLDDNFASIVTGVEEGRLIFDNLKKSIAYTL  780

Sp      TSNIPEITPFLIFIIANIPLPLGTVTILCIDLGTDMVPAISLAYEQAESDIMKRQPRNPK  840
R       TSNIPEITPFLIFIIANIPLPLGTVTILCIDLGTDMVPAISLAYEQAESDIMKRQPRNPK  840

Sp      TDKLVNERLISMAYGQIGMIQALGGFFTYFVILAENGFLPFHLLGIRETWDDRWINDVED  900
R       TDKLVNERLISMAYGQIGMIQALGGFFTYFVILAENGFLPFHLLGIRETWDDRWINDVED  900

Sp      SYGQQWTYEQRKIVEFTCHTAFFVSIVVVQWADLVICKTRRNSVFQQGMKNKILIFGLFE  960
R       SYGQQWTYEQRKIVEFTCHTAFFVSIVVVQWADLVICKTRRNSVFQQGMKNKILIFGLFE  960

Sp      ETALAAFPSYCPGMGAALRMYPLKPTWWFCAFPYSLLIFVYDEVRKLIIRRRPGGWVEKE  1020
R       ETALAAFLSYCPGMGAALRMYPLKPTWWFCAFPYSLLIFVYDEVRKLIIRRRPGGWVEKE  1020


Sp      TYY  1023
R       TYY  1023
```

Sequence alignment of rat α1-subunit of Na,K-ATPase with α1a, α1b, α1c, α2 and α3 of rainbow trout presented in the Table 8 showed similarity of these proteins with small difference in localization of cysteine residues within the sequences: all isoforms of the fish enzyme contain additional cysteine residue at position corresponding threonine-573 in rat enzyme. In addition to that, α2 isoform, which was found in the myocardial tissue, contains the switch of serine and cysteine in position 463 and 456, corresponding rat enzyme.

Table 8. Sequence comparison of α1-subunit of Na,K-ATPase of *Rattus Norvegicus* (Rat) and α1a (1A), α1b (1B), α1c (1C), α2 (2) and α3 (3) of rainbow trout. BLASTP was performed for the sequence alignment.

```
RAT     1     MGKGVGRDKYEPAAVSEHGDKK--SKKAKKER---DMDELKKEVSMDDHKLSLDELHRKYGTDLSRGLTPARAAEILARD  75
1A      1     MGLVKGKDDYKLAATSEDDGKKKSEKQVKKAKEKMDKDDLKKEVDLDDHKLTLDELNRKYGTDLARGLSSVRAKEILLRD  80
1B      1     MGLGKGKDDYKLVATSEDNGNRKSKKEVKKAREKKDMDDLKKEVDLDDHKLTLDELHRKYGTDLARGLTSARAKEILLRD  80
1C      1     MGRGEGREQYELAATSEQGGKKKNAKAMKKER---DMDELKKEVDLDDHKLTLDELNRKYGTDLSKGLSSAKAAENLARD  77
3       1     MG---------------DKDGKSSPSKKNKKGK---DMDELKKEVPITEHKMSIEECCRKFNTDIVQGLTNAKAAEFLIRD  63
2       1     MGKGSG----------AEYGDGK--KKK-KKEQ---ELDELKKEVSMDDHKISLDDLGRRYGVDLARGLTNAKALEVLARE  65

RAT     76    GPNALTPPPTTPEWVKFCRQLFGGFSMLLWIGAILCFLAYGIRSATEEEPPNDDLYLGVVLSAVVIITGCFSYYQEAKSS  155
1A      81    GPNTLTPPRTTPEWVKFCKQLFGGFCMLLWIGAVLCFIAHIIQVTSEEEPTNANLYLGLVLAVVVIITGCFSYYQEAKSS  160
1B      81    GPNTLTPPPTTPEWVKFCRQLFGGFSMLLWIGAMLCFLAYGIQAASEDEPANDNLYLGVVLSVVVIVTGCFSYYQEAKSS  160
1C      78    GPNSLTPPPTTPEWVKFCKQMFGGFSMLLWTGALLCFLAYGIQAAMEDEPANDNLYLGVVLSAGVIVTGCFSYYQEAKSS  157
3       64    GPNCLTPPPTTPEWIKFCRQLFGGFSILLWTGAILCFLAYAIQAATEDEPAGDNLYLGIVLSVVVVVTGCFSYFQEAKSS  143
2       66    GPNVLTPPPTTPEWVKFCRQLFGGFSLLLWIGAILCFLAYSIQVATEDEPANDNLYLGVVLSAVVIITGCFSYYQEAKSS  145
```

```
RAT     156   KIMESFKNMVPQQALVIRNGEKMSINAEDVVVGDLVEVKGGDRIPADLRIISANGCKVDNSSLTGESEPQTRSPDFTNEN  235
1A      161   KIMDSFKNLVPQQALVVRDGEKKNINTEEVVVGDIVEVKGGDRIPADLRIVSASGCKVDNSSLTGESEPQTRSPDFSNDN  240
1B      161   KIMDSFKNLVPQQALVVRDGEKKNINAEEVVVGDLVEVKGGDRIPADLRIVSASGCKVDNSSLTGESEPQTRTPDFSNDN  240
1C      158   KIMDSFKNLVPQQALVVRDGEKMNINAQQVVVGDLVEVKGGDRIPADLRIISASGCKVDNSSLTGESEPQTRTPDYSNDN  237
3       144   KIMESFKNMVPQQALVIREGEKMTINAEEVVAGDLVEVKGGDRIPADLRVVSAHGCKVDNSSLTGESEPQSRSPDCTHDN  223
2       146   RIMDSFKNMVPQQALVIREGEKMTINAELVVRGDLVEIKGGDRIPADLRVVSAAGCKVDNSSLTGESEPQTRTPEFTHEN  225

RAT     236   PLETRNIAFFSTNCVEGTARGIVVYTGDRTVMGRIATLASGLEGGQTPIAEEIEHFIHLITGVAVFLGVSFFILSLILEY  315
1A      241   PLETRNIAFFSTNCVEGTARGIVINTGDHTIMGRIAALAMSLESGQTPLGIEIDHFIEIITGVSVFFGVTFLILSVILGY  320
1B      241   PLETRNIAFFSTNCVEGTARGIVINTGDHTVMGRIATLATSLEGGKTPIAKEIEHFIHIITGVAVFLGVSFFVLSLILGY  320
1C      238   PLETRNIAFFSTNCVEGTARGIVINTGDRTVMGRIATLASGLEVGRTPISIEIEHFIHIITGVAVFLGMSFFVLSLILGY  317
3       224   PLETRNVAFFSTNCVEGTARGIVVCTGDRTVMGRIATLTSGLESGKTPIAKEIEHFIHLITGVAVFLGITFFILAVCLGY  303
2       226   PLETRNIAFFSTNCVEGTAHGVVVGTGDHTVMGRIATLASGLETGQTPINMEIEHFIQLITAVAVFLGVSFFILAIILGY  305

RAT     316   TWLEAVIFLIGIIVANVPEGLLATVTVCLTLTAKRMARKNCLVKNLEAVETLGSTSTICSDKTGTLTQNRMTVAHMWFDN  395
1A      321   GWLPSIIFLIGIIVANVPEGLLATVTVCLTLTAKRMAKKNCLVKNLEAVETLGSTSTICSDKTGTLTQNRMTVAHMWFDN  400
1B      321   GWLEAVIFLIGIIVANVPEGLLATVTVCLTLTAKRMAKKNCLVKNLEAVETLGSTSTICSDKTGTLTQNRMTVAHMWFDN  400
1C      318   SWLEAVIFLIGIIVANVPEGLLATVTVCLTLTAKRMAKKNCLVKNLEAVETLGSTSTICSDKTGTLTQNRMTVAHMWFDN  397
3       304   TWLEAVIFLIGIIVANVPEGLLATVTVCLTLTAKRMAKKNCLVKNLEAVETLGSTSTICSDKTGTLTQNRMTVAHMWFDN  383
2       306   TWLEAVIFLIGIIVANVPEGLLATVTVCLTLTAKRMAKKNCLVKNLEAVETLGSTSTICSDKTGTLTQNRMTVAHMWFDN  385

RAT     396   QIHEADTTENQSGVSFDKTSATWFALSRIAGLCNRAVFQANQENLPILKRAVAGDASESALLKCIEVCCGSVMEMREKYT  475
1A      401   QIHDADTTENQSGTSFDKSSATWAALARVAGLCNRAVFLAEQNNVPILKRDVSGDASETALLKCIELCCGSVKDMREKYS  480
1B      401   QIHEADTTENQSGTCFDKSSATWASLARVAGLCNRAVFLAEQNNVPILKRDVAGDASESALLKCIELCCGSVKDMREKYS  480
1C      398   QIHEADTTENQSGTSFDRSSATWAALARVAGLCNRAVFLAEQNGIPILKRDVAGDASESALLKCIELCCGSVQGMRDQYT  477
3       384   QIHEADTTEDQSGASFDKTSASWAALARVAALCNRAVFKAGQDQLPILKRDTAGDASESALLKCIELSCGSVKQIREKNK  463
2       386   MIHEADTTEDQSGATFDKSSATWHALSRVAGLCNRAEFKAGQETLPILKRDTAGDASESALLKCIQLSCGCVRSMRERNA  465

RAT     476   KIVEIPFNSTNKYQLSIHKNPNASEPKHLLVMKGAPERILDRCSSILLHGKEQPLDEELKDAFQNAYLELGGLGERVLGF  555
1A      481   KVVEIPFNSTNKYQLSIHENNMAGESNHLLVMKGAPERILDSCSTILLQGKEHPLDDEIKESFQKAYEALGGLGERVLGF  560
1B      481   KIAEIPFNSTNKYQLSIHKNIVAGESNHLLVMKGAPERILDRCSTILIQGKEQTLNDELKEAFQNAYEELGGLGERVLGF  560
1C      478   KVAEIPFNSTNKYQLSVHLNKNEGESKHLLVMKGAPERILDRCSTILIQGKEQPLDDEMKDSFQNAYMELGGLGERVLGF  557
3       464   KVAEIPFNSTNKYQLSVHETEDPNDNRYLLVMKGAPERILDRCTTIIIQGKEQPMDEEMKESFQNAYMELGGLGERVLGF  543
2       466   KVGEIPFNSTNKYQLSIHEQED-NENGHLLVMKGAPERILDRCSTILIHGQEVPMDANWNEAFQSAYMELGGLGERVLGF  544

RAT     556   CHLLLPDEQFPEGFQFDTDEVNFPVDNLCFVGLISMIDPPRAAVPDAVGKCRSAGIKVIMVTGDHPITAKAIAKGVGIIS  635
1A      561   CHFQLPDDQFPEGFDFDCEDVNFPTENLCFVGLMSMIDPPRAAVPDAVGKCRCAGIKVIMVTGDHPITAKAIAKGVGIIS  640
1B      561   CHFQLPDDQFAEGFQFDCEEVNFPTENLCFVGLMSMIDPPRAAVPDAVGKCRSAGIKVIMVTGDHPITAKAIAKGVGIIS  640
1C      558   CHFQLPDDQFAEGFQFDCEEVNFPTENLCFVGLMSMIDPPRAAVPDAVGKCRSAGIKVIMVTGDHPITAKAIAKGVGIIS  637
3       544   CHLLMPEDQYPKGFAFDCDDVNFTTESLCFVGLMSMIDPPRAAVPDAVGKCRSAGIKVIMVTGDHPITAKAIAKGVGIIS  623
2       545   CHLPLSPAQFPRGFSFDCEEVNFPIKGLCFVGLMSMIDPPRAAVPDAVGKCRSAGIKVIMVTGDHPITAKAIAKGVGIIS  624

RAT     636   EGNETVEDIAARLNIPVNQVNPRDAKACVVHGSDLKDMTSEELDDILRYHTEIVFARTSPQQKLIIVEGCQRQGAIVAVT  715
1A      641   EGNETVEEIAARLKIPVSEVNPRDAKACVVHGGELKDMTPEELDDILKHHTEIVFARTSPQQKLIIVEGCQRQGAIVAVT  720
1B      641   EGNETVEDIAARLKIPVSEVNPRDAKACVVHGGELKDLSAEQLDDILAHHTEIVFARTSPQQKLIIVEGCQRQGAIVAVT  720
1C      638   EGNETVEDIAARLNIPVNEVDPRDAKACVVHGGDLKDLSAEQLDDILKYHTEIVFARTSPQQKLIIVEGCQRQGAIVAVT  717
3       624   EGNETVEDIASRLNIPVSRSNPRDAKACVIHGTDLKELSQDQMDDILRNHTEIVFARTSPQQKLIIVEGCQRLGAIVAVT  703
2       625   EGNETVEDIAERLNIPLSQVNPRDAKACVVHGGDLKDMSAEYLDDLLRNHTEIVFARTSPQQKLIIVEGCQRTGAIVAVT  704

RAT     716   GDGVNDSPALKKADIGVAMGIVGSDVSKQAADMILLDDNFASIVTGVEEGRLIFDNLKKSIAYTLTSNIPEITPFLIFII  795
1A      721   GDGVNDSPALRKADIGVAMGIAGSDVSKQAADMILLDDNFASIVTGVEEGRLIFDNLKKSITYTLSSKIPEMTPFLFLLL  800
1B      721   GDGVNDSPALKKADIGVAMGISGSDVSKQAADMILLDDNFASIVTGVEEGRLIFDNLKKSIAYTLTSNIPEISPFLLFII  800
1C      718   GDGVNDSPALKKADIGVAMGISGSDVSKQAADMILLDDNFASIVTGVEEGRLIFDNLKKSIAYTLTSNIPEITPFLFFII  797
3       704   GDGVNDSPALKKADIGVAMGISGSDVSKQAADMILLDDNFASIVTGVEEGRLIFDNLKKSIAYTLTSNIPEITPFLLFII  783
2       705   GDGVNDSPALKKADIGVAMGIAGSDVSKQAADMILLDDNFASIVTGVEEGRLIFDNLKKSIAYTLTSNIPEISPFLLFII  784

RAT     796   ANIPLPLGTVTILCIDLGTDMVPAISLAYEQAESDIMKRQPRNPKTDKLVNERLISMAYGQIGMIQALGGFFTYFVILAE  875
1A      801   ANIPLALGTVTILCIDLGTDMIPAISLAYEQAENDIMKRQPRNPKTDRLVNERLISVAYGQFGVMLAAAGFFTYFVIMAE  880
```

```
1B      801   ANIPLPLGTVTILCIDLGTDMVPAISLAYEEAENDIMKRQPRNPKTDKLVNERLISIAYGQIGMMQATAGFFTYFVILAE  880
1C      798   ANIPLPLGTVTILCIDLGTDMVPAISLAYEAAESDIMKRQPRNSKTDKLVNERLISIAYGQIGMIQALAGFFTYFVILAE  877
3       784   VNIPLPLGTITILCIDLGTDMVPAISLAYEAAESDIMKRQPRNPTRDKLVNERLISIAYGQIGMIQALGGFFSYFVILAE  863
2       785   ASIPLPLGTVTILCIDLGTDMVPAISLAYETAESDIMKRQPRCPKTDKLVNDRLISMAYGQIGMIQALAGFFTYFVILAE  864

RAT     876   NGFLPFHLLGIRETWDDRWINDVEDSYGQQWTYEQRKIVEFTCHTAFFVSIVVVQWADLVICKTRRNSVFQQG-MKNKIL  954
1A      881   NGFYPMDLLGIRLDWENQYINDLEDSYGQQWTYESRKIIEFSCHTAYFAAVVIAQWAVLIVCKTRKNSFFQQGLMKNRVL  960
1B      881   NGFLPMDLLGMRVDWDNKIMNDMEDSYGQQWTYEHRKIVEFTCHTAFFASIVVVQWADLIICKTRRNSILQQG-MKNRIL  959
1C      878   NGFLPSRLLGIRVDWDNKFCNDLEDSYGQQWTYEQRKIVEFTCHTAFFASIVVVQWADLIICKTRRNSVFQQG-MRNKIL  956
3       864   NGFLPSILVGIRLNWDDRACNDLEDSYGQQWTYEQRKIVEFTCHTAFFVSIVVVQWADVIVCKTRRNSVFQQG-MKNKIL  942
2       865   NGFWPETLLGIRLNWDDRANNEVEDSYGQQWTYEQRKIIEFTCHTSFFVSIVVVQWADVIICKTRRNSVFQQG-MKNRIL  943

RAT     955   IFGLFEETALAAFLSYCPGMGAALRMYPLKPTWWFCAFPYSLLIFVYDEVRKLIIRRRPGGWVEKETYY  1023
1A      961   IFGLCSESALALFLSYCPGMDIAIRMDPLKPFWWVCAFPYTLLIFIYDEVRKYIMRRNSGGWVYQETYY  1029
1B      960   IFGLFEETALAVFLSYCPGMDVALRMYPLKPCWWFCALPYSLLIFLYDEGRRYILRRNPGGWVEQETYY  1028
1C      957   IFGLFEETALAAFLSYCPGMGIALRMYPLKPSWWFCAFPYSLLIFIYDEIRKLIIRRSPGGWVERETYY  1025
3       943   IFGLFEETALAAFLSYTPGMDVALRMFPLKPSWWFCAVPYSVLIFVYDEIRKLLIRRNPGGWVERETYY  1011
2       944   IFGLFAETALAAFLSYCPGMDIALRMYPLKVSWWFCALPYSLLIFIYDEVRKLIIRRYPGGWVELETYY  1012
```

The ability of the enzyme to respond to GSSG-induced S-glutathionylation has been confirmed for *O. mykiss*, *S. galili* and *S. judaei*. Treatment of crude ventricular tissue homogenates with 300 µM of GSSG for 10 min caused a complete inhibition of the enzyme in both Spalax species, in Wistar rat and in rainbow trout (Figure 32).

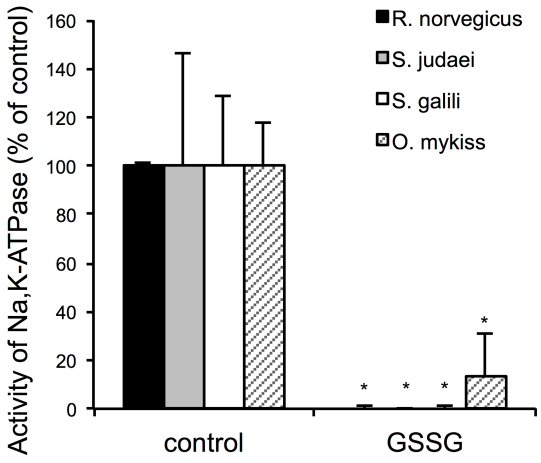

Figure 32. The effect of 300 µM GSSG on activity of Na,K-ATPase in ventricular tissue homogenate of S. judaei and S. galili. Activity of Na,K-ATPase in ventricular tissue homogenate was inhibited with 300 µM GSSG in all species. Bars represent means ± SD; n=3. *P<0.01 vs. control (1-way ANOVA).

Thus, both rodents and fish possessed the redox-sensitive Na,K-ATPase in the heart. However, amongst them only *R. Norvegicus* responded to systemic hypoxia or deoxygenation of isolated blood-perfused heart with glutathione oxidation. Neither

of mole rat super-species tested did show any signs of oxidative stress in the heart in response to hypoxia (Figure 33). Moreover, E_{hc} (GSH:GSSG) in normoxic myocardium of *S. galili* and *S. judaei* was significantly more reduced than that in the heart of *R. norvegicus.* Similar to that, in hypoxic rainbow trout myocardium both GSH and GSSG levels were maintained (see **abstract 1, table 2**).

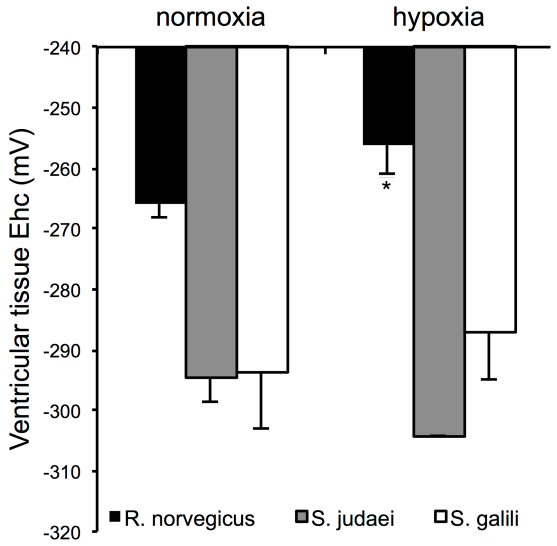

Figure 33. The effect of hypoxia on rat and Spalax ventricular half-cell redox potential Ehc for the GSH/GSSG couple that was calculated from the following equation: Ehc(mV) = −240 − 59.55/2 *log ([GSH]^2/[GSSG]) Decrease in oxygen supply resulted in the shift of the redox state towards more oxidized state in rat ventricular tissue. The ventricular tissue redox state of Spalax was not changed significantly. Bars represent means ± SD; n=4 animals. *P<0.01 vs. 20% oxygen homogenate (1-way ANOVA).

Discussion

Acute response of the heart to hypoxia and inhibition of Na,K-ATPase.

In vivo rat heart responds to hypoxia with acute bout of centrally-driven tachycardia followed autonomous bradycardia along with induction of arrhythmia in vivo [272, 273] and ex vivo (Table 6 and Figure 16), as it was shown in this study. Na,K-ATPase is an active player in control of heart rhythm, excitation propagation, and contractile force [274]. Hypoxia-induced inactivation of the Na,K-ATPase in rat

heart contributes to an increase in RR interval and scooping of the ST interval which has earlier on been reported in digitalis-treated hearts [275]. Some of these changes in ECG are observed in ischemic myocardium along with dose-dependent suppression of Na,K-ATPase triggered by reduction in oxygenation [276].

Sensitivity of Na,K-ATPase to the changes in tissue redox state and NO production

Our findings indicate that Na,K-ATPase in the heart is extremely sensitive to the changes in GSSG/GSH ratio (that reflects tissue redox state) and NO levels. Progressive development of oxidative stress in hypoxic myocardium was suggested to reflect uncoupling in electron transduction in the mitochondria [277]. Our data suggest that oxidation is largely (but not exclusively) caused by reduction in NO production in hypoxic heart. Indeed, oxygen affinities of inducible and neuronal NO synthases (K_d of 7.8 kPa and 5.9 kPa respectively) are significantly lower than those of superoxide generating enzymes including K_d of ~ 2 kPa NOX2 and 4 and even higher affinities of mitochondrial cytochromes [1, 278]. Nitric oxide interacts with superoxide anion four orders of magnitude faster than superoxide dismutase (rate constants being $7x10^9$ vs. 10^5 $M^{-1}s^{-1}$ respectively) [234]. The imbalance between O_2^- and NO production towards superoxide will result in an increased $ONOO^-$ production and accumulation of H_2O_2 generated in SOD-catalyzed reaction [234]. An increase in nitrotyrosine levels along with reduction in NO_2^- was observed in hypoxic rat myocardium (Figure 18B and 22B). Thus, accumulation of GSSG following hypoxic exposure (Figure 18A) mirrors an increase in H_2O_2 and $ONOO^-$ (Figure 34).

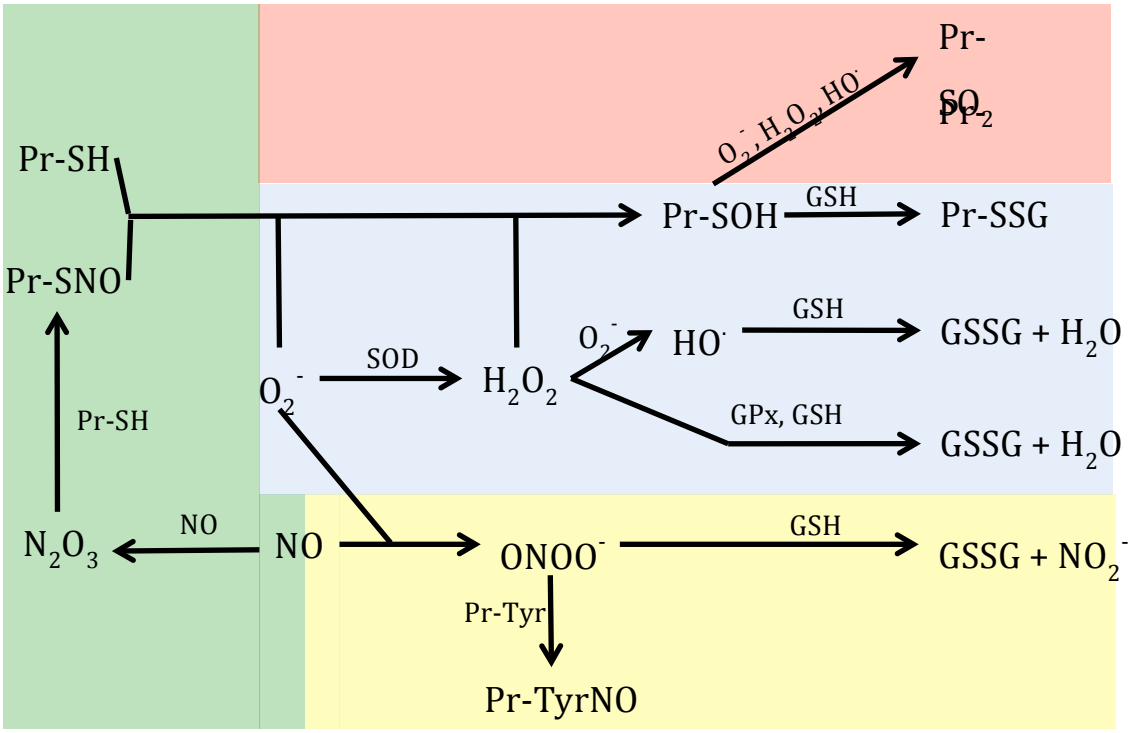

Figure 34. Concluding scheme of redox reactions. Although all presented reactions take place in the living cells simultaneously with different rates competing with each other, in normoxic conditions the reactions marked blue and green mostly occur. In hypoxic conditions reactions marked in blue and yellow are dominating, and in the absence of NO reactions marked blue and red prevail.

Mechanisms of Na,K-ATPase inhibition: fine tuning and "on-off"regulatory modalities

Multiple processes are known to mediate the changes in activity of Na,K-ATPase in response to hypoxia. Among them are phosphorylation of serine and tyrosine residues of α-subunit, internalization of the enzyme (triggered by phosphorylation), phosphorylation of FXYD subunit and S-glutathionylation of β-subunit and FXYD subunit [1, 16, 279]. Some of these regulatory mechanisms function as "on-off" switches, the other mediate fine-tuning of the enzyme partially suppressing or activating it.

Fine-tuning of the enzyme activity in hypoxic tissue is achieved by S-glutathionylation of the β-subunit and FXYD subunit [16, 279] as well as by phosphorylation of phospholemman at Ser-68 ([173, 251, 280]) resulting in modest suppression or stimulation of Na,K-ATPase in the heart.

Internalization of the enzyme in clathrin-coated vesicles [281] represents the "on-off" mechanisms, which dominate over the fine-tuning regulatory mechanisms. However internalization of the Na,K-ATPase was shown in cultured neonatal rat cardiac myocytes, but not in beating heart [282].

In this study we have described yet one more "on-off" mechanism of Na,K-ATPase inhibition in hypoxic heart mediated by S-glutathionylation of the α-subunit. This effect was substantially more sound than a minor (20%) inhibition reduction in the enzyme activity associated with binding of glutathione to β-subunit [16].

Mechanism of Na,K-ATPase inhibition caused by S-glutathionylation of the α-subunit.

In vitro studies have shown that complete inactivation of the Na,K-ATPase is caused by binding of glutathione to a cysteine residue within adenine nucleotide binding site making it inaccessible to ATP.

We have observed endogenous α1-subunit S-glutathionylation in Na,K-ATPase preparation from rabbit kidneys and in crude homogenates of rat heart. This basal S-glutathionylation is an intrinsic feature of Na,K-ATPase catalytic subunit supported by the enzyme microenvironment under physiological conditions. Basal S-glutathionylation did not affect the enzyme function directly since deglutathionylation by treatment of the enzyme with reducing agents (DTT) or during the sarcolemmal membrane isolation procedure was not followed by alteration of the Na,K-ATPase activity. These data are in agreement with results on the effect of point mutagenesis on the Na,K-ATPase function reported earlier. Replacement of all 23 cysteine residues of the catalytic α1-subunit by alanine or serine did not result in substantial alterations of the enzyme hydrolytic function [283]. The lack of direct effect of basal S-glutathionylation on the Na,K-ATPase activity does not necessarily imply that it is irrelevant for the enzyme stability and performance. It may protect the SH-groups from irreversible oxidation to sulfinic and sulfonic acid states. Oxidation was previously shown to cause a progressive loss of the Na,K-ATPase activity [284, 285]. Furthermore, binding of glutathione to cysteine residues may alter accessibility of the catalytic α-subunit to regulatory factors such as kinases or cardiac glycosides. Basal S-glutathionylation has been

reported for one more member of P-ATPases, SERCA-2A [286] as well as for ryanodine receptors [287]. Although the physiological relevance of basal S-glutathionylation remains unclear its high abundance suggests that it is required for the maintenance of optimal protein function.

In contrast to that for basal S-glutathionylation sites, interaction of glutathione with cysteine residues localised in close proximity to the nucleotide binding pocket resulted in complete blockage of the enzyme function. S-glutathionylation of the catalytic subunit associated with the changes in enzyme activity fulfilled all conditions formulated for regulatory protein glutathionylation [129]. Namely, binding of glutathione to regulatory cysteine residues (sites of regulatory S-glutathionylation) (1) results in complete inhibition of the enzyme function; (2) occurring under physiological conditions, e.g. in hypoxic rat myocardium; (3) is induced within physiological GSH and GSSG levels and (4) may be rapidly induced in purified protein and in heart tissue homogenate spontaneously or in reactions catalyzed by glutaredoxin and reversed by glutaredoxin or DTT.

Binding of ATP or GSSG to their respective binding sites appeared to be mutually exclusive. This implies that the sites of regulatory S-glutathionylation are localized in close proximity to or within the nucleotide binding pocket. The ability of ATP (but not ADP or AMP) to protect the Na,K-ATPase from oxidation-induced inhibition has been shown previously [288]. In our study inhibition caused by regulatory S-glutathionylation could be attenuated by ATP and *vice versa* binding of glutathione to the regulatory sites may prevent interaction of ATP with its binding site. Consequently, hypoxia-induced reduction of ATP levels in rat heart was associated with an increase in regulatory S-glutathionylation and enzyme inhibition. These data suggest that regulatory thiol groups are localized within the ATP binding pocket or in close juxtaposition. All fifteen cytosolic cysteines are localized within the small (MM3) and large (M4M5) cytosolic loops of the catalytic α1-subunit. Using mass spectrometry, modelling and structure-function analysis of the data available in the literature we have assessed the potential localisation of regulatory S-glutathionylation sites. Based on the findings obtained using mass spectrometry on the proteolytic fragments of the α1-subunit of the Na,K-ATPase in its active (control) and inhibited (GSSG-treated) forms, we can conclude that inhibition of the

Na,K-ATPase activity may be induced by S-glutahtionylation of at least 3 regulatory cysteine residues localized within the big cytosolic loop of its α-subunit, Cys 454, 458, and 459 and one localized within the small cytosolic loop, Cys 244.
In silico modelling was recruited to assess the possible involvement of identified cysteine residues of large cytosolic loop in regulatory glutathionylation. The inability of the enzyme to bind ATP in S-glutathionylated form results from an increase in negative charge within the ATP binding pocket. The effect is thereby cumulative, and increased proportionally to the amount of S-glutathionylated thiols within this area.
The role of S-glutathionylation of the Cys 244 remains to be clarified. Along with the data of mass spectrometry, clear differences in sensitivity to the inhibitory action of GSSG on the α1β and α2β isozymes (Figure 24) suggests that this cysteine residue may play a regulatory role as well. The more sensitive α2 isoform of the catalytic subunit possesses one additional cysteine in position 236, which may be a target for S-glutathionylation along with Cys 244. It is tempting to suggest that this difference in sequence of α2 and α1 isoforms is a cause of amplification of the inhibitory effect of GSSG observed for the α2β isozyme in rat heart.

Conditions promoting regulatory S-glutathionylation

Among the characteristic features of Na,K-ATPase regulation by S-glutathionylation are high rates and complete reversibility of the inhibitory effect. GSSG-induced inhibition of the Na,K-ATPase is a fast process. Eighty per cents of enzyme activity were lost within 10 min of incubation with GSSG at room temperature. The inhibitory action of GSSG on Na,K-ATPase activity of purified enzyme from rabbit kidney followed biphasic kinetics with a 10-fold difference in constants of fast and slow inhibition phases (1655 vs. 163 M^{-1} min^{-1}). These biphasic kinetics may reflect the existence of two distinct classes of thiol groups, as shown before for the glycogen debranching enzyme in rabbit skeletal muscle [289], or two conformational states (E1 and E2) of the Na,K-ATPase in which the same thiol groups become more or less accessible for interaction with GSSG.
S-glutathionylation is differentially regulating activity of two isozymes of the catalytic α-subunit of the Na,K-ATPase in rat heart. The α2 isoform in rat heart

showed a 6-fold higher sensitivity to the inhibitory action of GSSG compared with the α1 isoform. It has been suggested that α1 and α2 isoforms of the Na,K-ATPase catalytic subunits fulfill different functions in the myocardium and are differentially distributed within the sarcolemma. Alpha1 isoform maintains the transmembrane Na^+ and K^+ gradient and is less abundant in the T-tubular zones, which are enriched with the α2 isoform associated with the Na^+/Ca^+ exchanger [43]. Thus, the α2 isoform of the catalytic subunit is believed to be actively involved in control of intracellular Ca^{2+} handling in cardiomyocytes [43, 290, 291]. Taken together these findings indicate that S-glutathionylation will selectively alter activity of the α2 isozyme in the heart targeting Ca^{2+} homeostasis. This hypothesis is supported by the earlier reports on the high sensitivity of the α2 isoform of the catalytic subunit to oxidation by hydrogen peroxide [292]. So the α2 isoform of the catalytic subunit is known to be more sensitive to oxidation than the α1 isozyme. We have shown here that the α2 isozyme is also more sensitive to GSSG-induced inhibition. Among possible reasons for high GSSG-sensitivity of the α2 isoform are differences in cysteine localisation (presence of $Cys236^d$ and absence of $Cys458^d$, which is located near ATP binding site, in the α2 isozyme), a shift in E1/E2 conformation ratio towards E1 in α2 compared to α1 isoform [293] and differences in polarity/charge of the amino acids proximal to the cytosolic cysteine residues.

Physiological concentrations of GSH and GSSG reported for different tissues lie within 1-10 millimolar (for GSH) and 50-500 micromolar (for GSSG) [244], whereas ATP levels vary within millimolar range. Our data indicate that inhibition of the purified duck and rabbit enzyme as well as that it the sarcolemmal fraction of rat heart caused by its regulatory S-glutathionylation may occur in the presence of as little as 100 μM GSSG in the absence of ATP. This concentration of GSSG is sufficient to block the α2 isozyme in ATP-depleted (local concentrations below 500 μM) rat heart whereas inhibition of the α1 isoform requires higher doses of GSSG (250-300 μM), which may be reached under conditions of oxidative stress developing in hypoxic rat myocardium. Regulatory S-glutathionylation could thus be mediated by an increase in GSSG level. In addition, elevated GSH concentration in the heart could also promote regulatory S-glutathionylation in a reaction catalysed by GRX.

Taken together these observations reveal how sensitive the Na,K-ATPase may be to the changes in redox state under conditions of ATP deprivation. Sensitivity of enzyme function to shifts in intracellular GSH/GSSG levels was demonstrated earlier on in freshly isolated cerebellar granule cells and mouse erythrocytes [2, 294].
The present study revealed that the regulatory S-glutathionylation may only occur under conditions of oxidative stress coupled to local ATP deprivation. The enzyme is thereby resistant to GSSG-induced inactivation during acute reversible changes in redox state that may compromise cellular viability especially in excitable tissues. Regulatory S-glutathionylation on the other hand protects cells from the irreversible ATP depletion under conditions of limited energy supply such as oxygen deprivation.
These requirements put Na,K-ATPase into a group of proteins that may undergo S-glutathionylation under physiological conditions by simple thiol-disulfide exchange mechanism without any catalysts or intermediate activation states required. For most proteins, GSSG levels required for 50% conversion of R-SH to R-SSG by thiol-disulfide exchange are too high (up to ~50% of total glutathione content) to be physiologically relevant [129]. This suggests that formation of S-glutathionylated thiol adducts occurs by alternative mechanisms involving oxidized sulfhydryl derivatives (sulfenic acid, thiyl radical, nitrosothiol). In contrast to the vast majority of proteins studied so far, transcriptional activator c-Jun may be inhibited by 50% when interacting with GSSG directly already at physiological GSSG levels, corresponding to the [GSH]:2[GSSG]=13, whereas complete inhibition is reached at the ratio being 0.1 [295]. Similar to that, complete inhibition of Na,K-ATPase is reached at [GSH]:2[GSSG] ratio required of 5, which is well within physiological concentration range for the GSH/GSSG couple in living cells. Thus, Na,K-ATPase may be inhibited by GSSG *in vivo*.
Glutaredoxin 1, an efficient and specialised enzyme catalysing de-glutathionylation in the presence of sufficient amounts of NADPH [296], turned the inactive S-glutathionylated form of Na,K-ATPase back to the active de-glutathionylated state.
Incubation of the Na,K-ATPase at 20% (in pure enzyme preparations) or 100% (sarcolemmal fraction) O_2 makes the enzyme insensitive to GSSG, but has no profound effect on its hydrolytic function. Of note, physiologic normoxia

corresponds to an oxygen partial pressure of ~3-5 kPa in adult brain and 6-8 kPa in the heart [1]. Similar effect may be reached during prolong myocardial tissue storage at -80˚C in contact with air. Insensitivity of the enzyme to GSH and GSSG during hyperoxia suggests that regulatory cysteines undergo irreversible oxidation under these experimental conditions.

Triggers of S-glutathionylation of Na,K-ATPase in rat heart

S-glutathionylation of the α1-subunit thiols in hypoxic myocardium occurred in parallel to reduction of the number of S-nitrosylated cysteine residues and increase in nitrated tyrosines. S-glutathionylation of thiols by thiol/disulfide exchange with GSSG requires dissociation of the target thiol. Alternative pathways include binding of GSH to the protein thiol groups that have undergone S-nitrosylation or oxidation to sulfenic anion ($-SO^-$) [297, 298]. For many but not all proteins including the β-subunit of Na,K-ATPase [16] and SERCA2A [299] S-nitrosylation of a thiol is a necessary intermediate step precluding S-glutathionylation. Nitrosothiols are formed in reaction with N_2O_3, an adduct of NO and O_2 [131, 234]. Hypoxic conditions in the heart do not support S-nitrosylation as NO is converted to $ONOO^-$ instead of N_2O_3. Accumulation of the peroxynitrite, but not other intermediates of NO metabolism, causes nitration of tyrosine residues, which were observed in our studies. The resulting $ONOO^-$ - and H_2O_2-induced oxidation of thiols to thiyl radicals and sulfenic anions generation as well as GSSG accumulation promotes thiol S-glutathionylation [129, 131].

Accumulation of GSSG and reduction of NO production occur in hypoxic rat myocardium making the enzyme particularly sensitive to deoxygenation.

Plasticity of the enzyme function appears to be tightly related to the reversible transition for SH groups to S-nitrosylated to S-glutathionylated forms. The present study revealed that Na,K-ATPase is one more element contributing to the complex responses of cardiomyocytes to the changes in redox state [223]. Whether or not the enzyme will respond to the changes in oxygen supply entirely depends on the shifts in redox state and NO production in the heart.

Integration in Ca^{2+} handling

Na,K-ATPase is not only a mediator of transmembrane Na^+/K^+ gradients, but also actively participates in Ca^{2+} handling in the heart [300]. Recently S-glutathionylation was proposed as a universal mechanism regulating all Ca^{2+} handling systems in cardiomyocytes including ryanodine receptors, SERCAs, L-type Ca^{2+} channels, and Na^+/Ca^+ exchange [223, 301]. Inhibition of the Na,K-ATPase occurs in parallel with activation of ryanodine receptors and SERCA in the heart as these ion transporters also possess sites of regulatory S-glutathionylation [286, 302, 303]. Thus, S-glutathionylation allows coordinated regulation of several ion transport systems with the following increase in intracellular calcium stores in cardiomyocytes. Hypoxia-induced S-glutathionylation promotes fast Ca^{2+} release and pumping back into the sarcoplasmic reticulum as well as facilitation of intracellular Ca^{2+} accumulation. Taken together these alterations result in an increase in contractile force. However, extensive calcium accumulation increases the danger of necrotic tissue damage resulting from calcium overload [304].
Reduction of Na,K-ATPase activity in hypoxic myocardium is mediated by S-glutathionylation of the catalytic α-subunit of the enzyme. S-glutathionylation coordinates the activity of a number of ion transport systems in control of contractile function of the heart in response to the changes in redox state and NO production.

Hypoxia-sensitive vs. hypoxia-tolerant animals

Wistar rats are very sensitive to hypoxia and have a threshold of acute hypoxia-tolerance above 8 % of atmospheric O_2. Compared to *Rattus norvegicus*, *Spalax* survives at lower O_2 and higher CO_2 levels for longer periods of time [252, 305]. *Spalax* is a fossorial animal which remains in the borrow all its life. Oxygen availability in this habitat is reduced from 20 % at the surface to 6-3% being particularly low during rainy seasons [306]. *Spalax* can conduct aerobic work under low O_2 partial pressures due to numerous adaptations in the structural design of skeletal muscles and the cardiorespiratory system allowing better oxygenation and more efficient perfusion of tissues with blood in the course of hypoxic exposure [252, 307]. These animals respond to hypoxia with tachycardia and maintained

stroke volume increasing thereby cardiac output under hypoxic conditions [308, 309]. Arrhythmia reported in mole rats under normoxic conditions was diminished during the hypoxia-induced increase in heart rate [309].

Rainbow trout is not a hypoxia-tolerant species. Exposure of the fish to the environmental hypoxia in vivo causes intense heart bradycardia (reduction of heart rate down to 50%), however, due to elevation of the stroke volume, the cardiac output is maintained high during the first 20 min of hypoxic insult. Interestingly, bradycardic response is central and, and anatomical or chemical denervation of the heart results in insensitivity of the heart to deoxygenation [310]. This allows concluding, that autonomous trout heart function is oxygen-insensitive.

Comparison of hypoxic responses of the Na,K-ATPase in myocardial tissue of mole rats, rainbow trout and Wistar rats reveals the importance of redox state and nitric oxide in control of the enzyme function. Lack of oxidative stress in *Spalax* and trout hearts exposed to acute hypoxia is associated with insensitivity of Na,K-ATPase to hypoxia. Maintenance of redox state is associated with the maintenance of NO production in trout (according to the plasma NO_2^- readouts [311]). Addition of GSSG to ventricular tissue homogenates of all species studied induced complete inhibition of the enzyme. This finding suggests that reduction of Na,K-ATPase activity by S-glutathionylation of its catalytic α-subunit is a highly conserved early response of the

Na,K-ATPase to a combination of oxidative stress and ATP deprivation which may be observed under multiple occasions: hypoxia, hypertrophy, sepsis, etc.

Our findings do not allow any speculations on the molecular mechanisms of resistance of Spalax and trout myocardium to hypoxia-driven oxidation. Among the possible contributors are maintenance of NO production (NO_2^- reduction [312], high activity of eNOS), lower O_2^- production rates (particularly by the mitochondria), and more efficient H_2O_2 processing enzymes.

Conclusion

The present study demonstrates the power of the redox state and nitric oxide availability in control the activity of Na,K-ATPase via S-glutathionylation of cysteines in its catalytic α-subunit. This regulatory S-glutathionylation is precisely

controlled by ATP availability, thereby representing a powerful adaptive mechanism by which terminal ATP depletion and irreversible oxidation may be prevented under conditions of oxidative stress. Our data contribute to the accumulating information on the profound role of S-glutathionylation in regulation of protein structure and activity. We demonstrated that S-glutathionylation of multiple cysteines is a distinctive feature of the catalytic α-subunit of the Na,K-ATPase in four different species. Binding of glutathione to some cysteines causes complete inhibition of the enzyme function that may be restored by shifting the balance from an oxidative toward a reduced state.

Outlook

Thiol modifications of the proteins were known since a very long time: formation of intra- and interprotein disulfide bonds, oxidation of the cysteine residues, cysteine nitrosylation and formation of the mixed disulfides were described for a large number of the intracellular and extracellular proteins. These modifications, especially S-glutathionylation, were considered as a hallmark for pathological conditions of intoxication or misbalance in production and scavenge of oxidizing molecules. Currently, S-glutathionylation is being rediscovered as a mechanism of redox- and NO-sensitive signaling and as an adaptive response of the proteins to the oxidative and nitrosative stimuli.

This feature was described for different groups of proteins: transcriptional factors, ion transporters, kinases, phosphatases etc. in vitro and less in vivo models.

Among described proteins there is a clear difference between precise adjustment of the protein activity and mechanism of “on-off” switches in response to redox stimuli. The “on-off” switch presented in this study is probably universal for many nucleotide-binding proteins – targets of the redox stimuli, it was already described for transcriptional factors (AP-1, NF-kappaB, p53, PAX), creatine kinase, actomyosin ATPase and others.

It is tempting to conclude, that S-glutathionylation of the proteins, mastered by the redox stimuli, conducts the adaptation response on the metabolic, transport and gene-expression levels. Therefor further investigation of the network of redox

sensitive proteins, their possibility to undergo S-glutathionylation (and other thiol modifications) and character of the changes in their functioning will be very helpful for understanding of cellular mechanism of adaptation to the changing environment, cell cycle control, genome replication and energy metabolism.

Special attention has to be paid to the specific physiological, environmental and evolutionary properties of the investigated subject. As it was shown in this study, implication of the molecular mechanism of S-glutathionylation is species-specific and is strongly physiologically relevant. Therefor investigation of the triggers and conditions of implication of the S-glutathionylation (and other thiol modifications) is important to understand the origin and mechanism of adaptation of different species to unusual environment.

References

1. Bogdanova, A., Petrushanko, I., Boldyrev, A., Gassmann, M., *Oxygen- and redox-induced regulation of the Na/K ATPase.* Current Enzyme Inhibition, 2006. **2**(1): p. 37-59.
2. Bogdanova, A.Y., et al., *Pivotal role of reduced glutathione in oxygen-induced regulation of the Na(+)/K(+) pump in mouse erythrocyte membranes.* J.Membr.Biol., 2003. **195**(1): p. 33-42.
3. Petrushanko, I.Y., et al., *Oxygen-induced Regulation of Na/K ATPase in cerebellar granule cells.* J Gen Physiol, 2007. **130**(4): p. 389-98.
4. Bublitz, M., et al., *In and out of the cation pumps: P-type ATPase structure revisited.* Curr Opin Struct Biol, 2010. **20**(4): p. 431-9.
5. Taniguchi, K., et al., *The oligomeric nature of Na/K-transport ATPase.* J Biochem, 2001. **129**(3): p. 335-42.
6. Geering, K., *FXYD proteins: new regulators of Na-K-ATPase.* Am J Physiol Renal Physiol, 2006. **290**(2): p. F241-50.
7. Hilge, M., et al., *ATP-induced conformational changes of the nucleotide-binding domain of Na,K-ATPase.* Nat Struct Biol, 2003. **10**(6): p. 468-74.
8. Morth, J.P., et al., *Crystal structure of the sodium-potassium pump.* Nature, 2007. **450**(7172): p. 1043-9.
9. Morth, J.P., et al., *A structural overview of the plasma membrane Na+,K+-ATPase and H+-ATPase ion pumps.* Nat Rev Mol Cell Biol, 2011. **12**(1): p. 60-70.
10. Jorgensen, P.L., K.O. Hakansson, and S.J. Karlish, *Structure and mechanism of Na,K-ATPase: functional sites and their interactions.* Annu Rev Physiol, 2003. **65**: p. 817-49.
11. Post, R.L., C. Hegyvary, and S. Kume, *Activation by adenosine triphosphate in the phosphorylation kinetics of sodium and potassium ion transport adenosine triphosphatase.* J Biol Chem, 1972. **247**(20): p. 6530-40.
12. Martin, D.W. and J.R. Sachs, *Preparation of Na+,K+-ATPase with near maximal specific activity and phosphorylation capacity: evidence that the reaction mechanism involves all of the sites.* Biochemistry, 1999. **38**(23): p. 7485-97.
13. Lupfert, C., et al., *Rate limitation of the Na(+),K(+)-ATPase pump cycle.* Biophys J, 2001. **81**(4): p. 2069-81.
14. Ding, Y. and R.F. Rakowski, *The effect of holding potential on charge translocation by the Na+/K +-ATPase in the absence of potassium.* J Membr Biol, 2010. **236**(2): p. 203-14.
15. Colonna, T., et al., *Subunit interactions in the sodium pump.* Ann N Y Acad Sci, 1997. **834**: p. 498-513.
16. Figtree, G.A., et al., *Reversible oxidative modification: a key mechanism of Na+-K+ pump regulation.* Circ Res, 2009. **105**(2): p. 185-93.
17. DeTomaso, A.W., et al., *Expression, targeting, and assembly of functional Na,K-ATPase polypeptides in baculovirus-infected insect cells.* J Biol Chem, 1993. **268**(2): p. 1470-8.

18. Xie, Z., et al., *Similarities and differences between the properties of native and recombinant Na+/K+-ATPases.* Arch Biochem Biophys, 1996. **330**(1): p. 153-62.
19. Gatto, C., S.M. McLoud, and J.H. Kaplan, *Heterologous expression of Na(+)-K(+)-ATPase in insect cells: intracellular distribution of pump subunits.* Am J Physiol Cell Physiol, 2001. **281**(3): p. C982-92.
20. Noguchi, S., et al., *Expression of functional (Na+ + K+)-ATPase from cloned cDNAs.* FEBS Lett, 1987. **225**(1-2): p. 27-32.
21. Horowitz, B., et al., *Synthesis and assembly of functional mammalian Na,K-ATPase in yeast.* J Biol Chem, 1990. **265**(8): p. 4189-92.
22. Hasler, U., et al., *Role of beta-subunit domains in the assembly, stable expression, intracellular routing, and functional properties of Na,K-ATPase.* J Biol Chem, 1998. **273**(46): p. 30826-35.
23. Ivanov, A.V., N.N. Modyanov, and A. Askari, *Role of the self-association of beta subunits in the oligomeric structure of Na+/K+-ATPase.* Biochem J, 2002. **364**(Pt 1): p. 293-9.
24. Crambert, G. and K. Geering, *FXYD proteins: new tissue-specific regulators of the ubiquitous Na,K-ATPase.* Sci STKE, 2003. **2003**(166): p. RE1.
25. Geering, K., *Functional roles of Na,K-ATPase subunits.* Curr Opin Nephrol Hypertens, 2008. **17**(5): p. 526-32.
26. Rajarao, S.J., et al., *The repertoire of Na,K-ATPase alpha and beta subunit genes expressed in the zebrafish, Danio rerio.* Genome Res, 2001. **11**(7): p. 1211-20.
27. Segall, L., et al., *Structural basis for alpha1 versus alpha2 isoform-distinct behavior of the Na,K-ATPase.* J Biol Chem, 2003. **278**(11): p. 9027-34.
28. Segall, L., S.E. Daly, and R. Blostein, *Mechanistic basis for kinetic differences between the rat alpha 1, alpha 2, and alpha 3 isoforms of the Na,K-ATPase.* J Biol Chem, 2001. **276**(34): p. 31535-41.
29. Blanco, G. and R.W. Mercer, *Isozymes of the Na-K-ATPase: heterogeneity in structure, diversity in function.* Am J Physiol, 1998. **275**(5 Pt 2): p. F633-50.
30. Gibbs, C.L. and W.R. Gibson, *Effect of ouabain on the energy output of rabbit cardiac muscle.* Circ Res, 1969. **24**(6): p. 951-67.
31. Hoerter, J.A., et al., *A phosphorus-31 nuclear magnetic resonance study of the metabolic, contractile, and ionic consequences of induced calcium alterations in the isovolumic rat heart.* Circ Res, 1986. **58**(4): p. 539-51.
32. Rolfe, D.F. and G.C. Brown, *Cellular energy utilization and molecular origin of standard metabolic rate in mammals.* Physiol Rev, 1997. **77**(3): p. 731-58.
33. Dos Santos, P., et al., *Metabolic control of contractile performance in isolated perfused rat heart. Analysis of experimental data by reaction:diffusion mathematical model.* J Mol Cell Cardiol, 2000. **32**(9): p. 1703-34.
34. Matsuoka, S., et al., *Simulation of ATP metabolism in cardiac excitation-contraction coupling.* Prog Biophys Mol Biol, 2004. **85**(2-3): p. 279-99.
35. Clausen, T., C. Van Hardeveld, and M.E. Everts, *Significance of cation transport in control of energy metabolism and thermogenesis.* Physiol Rev, 1991. **71**(3): p. 733-74.
36. Kabakov, A., *The resting potential equations incorporating ionic pumps and osmotic concentration.* J Theor Biol, 1994. **169**(1): p. 51-64.
37. Shank, B.B. and N.E. Smith, *Regulation of cellular growth by sodium pump activity.* J Cell Physiol, 1976. **87**(3): p. 377-87.

38. Banerjee, I., et al., *Determination of cell types and numbers during cardiac development in the neonatal and adult rat and mouse.* Am J Physiol Heart Circ Physiol, 2007. **293**(3): p. H1883-91.
39. Lederer, W.J., E. Niggli, and R.W. Hadley, *Sodium-calcium exchange in excitable cells: fuzzy space.* Science, 1990. **248**(4953): p. 283.
40. Norgaard, A., K. Kjeldsen, and O. Hansen, *K+-dependent 3-O-methylfluorescein phosphatase activity in crude homogenate of rodent heart ventricle: effect of K+ depletion and changes in thyroid status.* Eur J Pharmacol, 1985. **113**(3): p. 373-82.
41. Larsen, J.S. and K. Kjeldsen, *Quantification in crude homogenates of rat myocardial Na+, K(+)- and Ca(2+)-ATPase by K+ and Ca(2+)-dependent pNPPase. Age-dependent changes.* Basic Res Cardiol, 1995. **90**(4): p. 323-31.
42. McDonough, A.A., et al., *Subcellular distribution of sodium pump isoform subunits in mammalian cardiac myocytes.* Am J Physiol, 1996. **270**(4 Pt 1): p. C1221-7.
43. Despa, S. and D.M. Bers, *Functional analysis of Na+/K+-ATPase isoform distribution in rat ventricular myocytes.* Am J Physiol Cell Physiol, 2007. **293**(1): p. C321-7.
44. Swift, F., et al., *The Na+/K+-ATPase alpha2-isoform regulates cardiac contractility in rat cardiomyocytes.* Cardiovasc Res, 2007. **75**(1): p. 109-17.
45. Ziegelhoffer, A., et al., *Na,K-ATPase in the myocardium: molecular principles, functional and clinical aspects.* Gen Physiol Biophys, 2000. **19**(1): p. 9-47.
46. Despa, S., et al., *Na/Ca exchange and Na/K-ATPase function are equally concentrated in transverse tubules of rat ventricular myocytes.* Biophys J, 2003. **85**(5): p. 3388-96.
47. Mohler, P.J., J.Q. Davis, and V. Bennett, *Ankyrin-B coordinates the Na/K ATPase, Na/Ca exchanger, and InsP3 receptor in a cardiac T-tubule/SR microdomain.* PLoS Biol, 2005. **3**(12): p. e423.
48. Wang, J., et al., *Regulation of in vivo cardiac contractility by phospholemman: role of Na+/Ca2+ exchange.* Am J Physiol Heart Circ Physiol, 2011. **300**(3): p. H859-68.
49. Brette, F. and C. Orchard, *Resurgence of cardiac t-tubule research.* Physiology (Bethesda), 2007. **22**: p. 167-73.
50. Larbig, R., et al., *Activation of reverse Na+-Ca2+ exchange by the Na+ current augments the cardiac Ca2+ transient: evidence from NCX knockout mice.* J Physiol, 2010. **588**(Pt 17): p. 3267-76.
51. Yamamoto, T., et al., *Relative abundance of alpha2 Na(+) pump isoform influences Na(+)-Ca(2+) exchanger currents and Ca(2+) transients in mouse ventricular myocytes.* J Mol Cell Cardiol, 2005. **39**(1): p. 113-20.
52. O'Brien, W.J., J.B. Lingrel, and E.T. Wallick, *Ouabain binding kinetics of the rat alpha two and alpha three isoforms of the sodium-potassium adenosine triphosphate.* Arch Biochem Biophys, 1994. **310**(1): p. 32-9.
53. Bagrov, A.Y., J.I. Shapiro, and O.V. Fedorova, *Endogenous cardiotonic steroids: physiology, pharmacology, and novel therapeutic targets.* Pharmacol Rev, 2009. **61**(1): p. 9-38.
54. Dostanic, I., et al., *The alpha2 isoform of Na,K-ATPase mediates ouabain-induced cardiac inotropy in mice.* J Biol Chem, 2003. **278**(52): p. 53026-34.

55. Schatzmann, H.J., *[Cardiac glycosides as inhibitors of active potassium and sodium transport by erythrocyte membrane].* Helv Physiol Pharmacol Acta, 1953. **11**(4): p. 346-54.
56. Hansen, O., *Interaction of cardiac glycosides with (Na+ + K+)-activated ATPase. A biochemical link to digitalis-induced inotropy.* Pharmacol Rev, 1984. **36**(3): p. 143-63.
57. Bagrov, A.Y. and J.I. Shapiro, *Endogenous digitalis: pathophysiologic roles and therapeutic applications.* Nat Clin Pract Nephrol, 2008. **4**(7): p. 378-92.
58. Sandtner, W., et al., *Ouabain binding site in a functioning Na+/K+ ATPase.* J Biol Chem, 2011.
59. Erdmann, E., K. Werdan, and L. Brown, *Evidence for two kinetically and functionally different types of cardiac glycoside receptors in the heart.* Eur Heart J, 1984. **5 Suppl F**: p. 297-302.
60. Hansen, O., *Heterogeneity of Na,K-ATPase from kidney.* Acta Physiol Scand Suppl, 1992. **607**: p. 229-34.
61. Harashima, H., et al., *Kinetic analysis of the positive inotropic action (PIA) of ouabain in isolated perfused rabbit heart. Slow onset of PIA and slow binding to Na+, K+-adenosine triphosphatase.* J Pharmacobiodyn, 1988. **11**(8): p. 533-40.
62. Jensen, J., *Heterogeneity of pig kidney Na,K-ATPase as indicated by ADP- and ouabain-binding stoichiometry.* Biochim Biophys Acta, 1992. **1110**(1): p. 81-7.
63. McDonough, A.A., J. Wang, and R.A. Farley, *Significance of sodium pump isoforms in digitalis therapy.* J Mol Cell Cardiol, 1995. **27**(4): p. 1001-9.
64. Vassalle, M. and C.I. Lin, *Calcium overload and cardiac function.* J Biomed Sci, 2004. **11**(5): p. 542-65.
65. Klabunde, R.E., *Cardiovascular physiology concepts*2005, Philadelphia, Penn. London: Lippincott Williams & Wilkins. ix, 235 p.
66. Delk, C., C.P. Holstege, and W.J. Brady, *Electrocardiographic abnormalities associated with poisoning.* Am J Emerg Med, 2007. **25**(6): p. 672-87.
67. Goodman, L.S., A. Gilman, and A.G. Gilman, *Goodman and Gilman's The pharmacological basis of therapeutics*. 8th ed1990, New York ; Oxford: Pergamon. xvi, 1811 p., [1] folded leaf of plates.
68. Goodman, L.S., et al., *Goodman & Gilman's The pharmacological basis of therapeutics*. 9th ed1996, New York ; London: McGraw Hill. xxi, 1905 p.
69. Liu, J. and J.I. Shapiro, *Regulation of sodium pump endocytosis by cardiotonic steroids: Molecular mechanisms and physiological implications.* Pathophysiology, 2007. **14**(3-4): p. 171-81.
70. Xie, Z. and A. Askari, *Na(+)/K(+)-ATPase as a signal transducer.* Eur J Biochem, 2002. **269**(10): p. 2434-9.
71. Tian, J. and Z.J. Xie, *The Na-K-ATPase and calcium-signaling microdomains.* Physiology (Bethesda), 2008. **23**: p. 205-11.
72. Tian, J., et al., *Binding of Src to Na+/K+-ATPase forms a functional signaling complex.* Mol Biol Cell, 2006. **17**(1): p. 317-26.
73. Yudowski, G.A., et al., *Phosphoinositide-3 kinase binds to a proline-rich motif in the Na+, K+-ATPase alpha subunit and regulates its trafficking.* Proc Natl Acad Sci U S A, 2000. **97**(12): p. 6556-61.
74. Zhang, L., et al., *Na+/K+-ATPase-mediated signal transduction and Na+/K+-ATPase regulation.* Fundam Clin Pharmacol, 2008. **22**(6): p. 615-21.

75. Xie, Z., et al., *Intracellular reactive oxygen species mediate the linkage of Na+/K+-ATPase to hypertrophy and its marker genes in cardiac myocytes.* J Biol Chem, 1999. **274**(27): p. 19323-8.
76. Liu, J., et al., *Ouabain interaction with cardiac Na+/K+-ATPase initiates signal cascades independent of changes in intracellular Na+ and Ca2+ concentrations.* J Biol Chem, 2000. **275**(36): p. 27838-44.
77. Hansen, O., *No evidence for a role in signal-transduction of Na+/K+-ATPase interaction with putative endogenous ouabain.* Eur J Biochem, 2003. **270**(9): p. 1916-9.
78. Skou, J.C., *The influence of some cations on an adenosine triphosphatase from peripheral nerves.* Biochim Biophys Acta, 1957. **23**(2): p. 394-401.
79. Bers, D.M., W.H. Barry, and S. Despa, *Intracellular Na+ regulation in cardiac myocytes.* Cardiovasc Res, 2003. **57**(4): p. 897-912.
80. Clausen, T., *Hormonal and pharmacological modification of plasma potassium homeostasis.* Fundam Clin Pharmacol, 2010. **24**(5): p. 595-605.
81. Vrbjar, N., I. Bernatova, and O. Pechanova, *Changes of sodium and ATP affinities of the cardiac (Na,K)-ATPase during and after nitric oxide deficient hypertension.* Mol Cell Biochem, 1999. **202**(1-2): p. 141-7.
82. Haworth, R.A. and A.B. Goknur, *Regulation of sodium-calcium exchange in intact myocytes by ATP and calcium.* Ann N Y Acad Sci, 1996. **779**: p. 464-79.
83. Guzun, R., et al., *Systems bioenergetics of creatine kinase networks: physiological roles of creatine and phosphocreatine in regulation of cardiac cell function.* Amino Acids, 2011. **40**(5): p. 1333-48.
84. Arai, A.E., et al., *Energy metabolism and contractile function after 15 beats of moderate myocardial ischemia.* Circ Res, 1992. **70**(6): p. 1137-45.
85. Vogt, A.M. and W. Kubler, *Heart failure: is there an energy deficit contributing to contractile dysfunction?* Basic Res Cardiol, 1998. **93**(1): p. 1-10.
86. Piper, H.M., et al., *Energy metabolism and enzyme release of cultured adult rat heart muscle cells during anoxia.* J Mol Cell Cardiol, 1984. **16**(11): p. 995-1007.
87. Komniski, M.S., et al., *Interventricular heterogeneity in rat heart responses to hypoxia: the tuning of glucose metabolism, ion gradients, and function.* Am J Physiol Heart Circ Physiol, 2011. **300**(5): p. H1645-52.
88. Whittam, R. and D.M. Blond, *Respiratory control by an adenosine triphosphatase involved in active transport in brain cortex.* Biochem J, 1964. **92**(1): p. 147-58.
89. Dunham, E.T. and I.M. Glynn, *Adenosinetriphosphatase activity and the active movements of alkali metal ions.* J Physiol, 1961. **156**: p. 274-93.
90. Tobin, T., et al., *Calcium ion and sodium- and potassium-dependent adenosine triphosphatase: its mechanism of inhibition and identification of the E 1 -P intermediate.* Mol Pharmacol, 1973. **9**(3): p. 336-49.
91. Huang, W.H. and A. Askari, *Ca2+-Dependent activities of (Na+ + K+)-ATPase.* Arch Biochem Biophys, 1982. **216**(2): p. 741-50.
92. Rossi, J.P., P.J. Garrahan, and A.F. Rega, *The activation of phosphatase activity of the Ca2+-ATPase from human red cell membranes by calmodulin, ATP and partial proteolysis.* Biochim Biophys Acta, 1986. **858**(1): p. 21-30.
93. Tsien, R.Y., *Intracellular measurements of ion activities.* Annu Rev Biophys Bioeng, 1983. **12**: p. 91-116.

94. Knauf, P.A., F. Proverbio, and J.F. Hoffman, *Electrophoretic separation of different phophosproteins associated with Ca-ATPase and Na, K-ATPase in human red cell ghosts.* J Gen Physiol, 1974. **63**(3): p. 324-36.
95. Blostein, R. and V.K. Burt, *Interaction of N-ethylmaleimide and Ca 2+ with human erythrocyte membrane ATPase.* Biochim Biophys Acta, 1971. **241**(1): p. 68-74.
96. Fukushima, Y. and R.L. Post, *Binding of divalent cation to phosphoenzyme of sodium- and potassium-transport adenosine triphosphatase.* J Biol Chem, 1978. **253**(19): p. 6853-62.
97. Yingst, D.R., *Modulation of the Na,K-ATPase by Ca and intracellular proteins.* Annu Rev Physiol, 1988. **50**: p. 291-303.
98. Netticadan, T., et al., *Phosphorylation of cardiac Na+-K+ ATPase by Ca2+/calmodulin dependent protein kinase.* Biochem Biophys Res Commun, 1997. **238**(2): p. 544-8.
99. Kurihara, K., et al., *Specific expression of an A-kinase anchoring protein subtype, AKAP-150, and specific regulatory mechanism for Na(+),K(+)-ATPase via protein kinase A in the parotid gland among the three major salivary glands of the rat.* Biochem Pharmacol, 2003. **66**(2): p. 239-50.
100. Kurihara, K., N. Nakanishi, and T. Ueha, *Regulation of Na(+)-K(+)-ATPase by cAMP-dependent protein kinase anchored on membrane via its anchoring protein.* Am J Physiol Cell Physiol, 2000. **279**(5): p. C1516-27.
101. Blanco, G., G. Sanchez, and R.W. Mercer, *Differential regulation of Na,K-ATPase isozymes by protein kinases and arachidonic acid.* Arch Biochem Biophys, 1998. **359**(2): p. 139-50.
102. Pontiggia, L., K. Winterhalter, and S.M. Gloor, *Inhibition of Na,K-ATPase activity by cGMP is isoform-specific in brain endothelial cells.* FEBS Lett, 1998. **436**(3): p. 466-70.
103. Kawamoto, E.M., et al., *Age-related changes in cerebellar phosphatase-1 reduce Na,K-ATPase activity.* Neurobiol Aging, 2008. **29**(11): p. 1712-20.
104. William, M., et al., *The nitric oxide donor sodium nitroprusside stimulates the Na+-K+ pump in isolated rabbit cardiac myocytes.* J Physiol, 2005. **565**(Pt 3): p. 815-25.
105. Portal, S.B.R. *SIB Bioinformatics Resource Portal*. SIB Bioinformatics Resource Portal]. Available from: http://www.expasy.org.
106. Schoot, B.M., J.J. De Pont, and S.L. Bonting, *Studies on (Na+ + K+)-activated ATPase. XLII. Evidence for two classes of essential sulfhydryl groups.* Biochim Biophys Acta, 1978. **522**(2): p. 602-13.
107. Schultheis, P.J., E.T. Wallick, and J.B. Lingrel, *Kinetic analysis of ouabain binding to native and mutated forms of Na,K-ATPase and identification of a new region involved in cardiac glycoside interactions.* J Biol Chem, 1993. **268**(30): p. 22686-94.
108. Schultheis, P.J. and J.B. Lingrel, *Substitution of transmembrane residues with hydrogen-bonding potential in the alpha subunit of Na,K-ATPase reveals alterations in ouabain sensitivity.* Biochemistry, 1993. **32**(2): p. 544-50.
109. Canessa, C.M., et al., *Mutation of a cysteine in the first transmembrane segment of Na,K-ATPase alpha subunit confers ouabain resistance.* EMBO J, 1992. **11**(5): p. 1681-7.

110. Pedemonte, C.H. and J.H. Kaplan, *Chemical modification as an approach to elucidation of sodium pump structure-function relations.* Am J Physiol, 1990. **258**(1 Pt 1): p. C1-23.
111. Gatto, C., et al., *Cys(577) is a conformationally mobile residue in the ATP-binding domain of the Na,K-ATPase alpha-subunit.* J Biol Chem, 1999. **274**(35): p. 24995-5003.
112. Wang, S.G. and R.A. Farley, *Valine 904, tyrosine 898, and cysteine 908 in Na,K-ATPase alpha subunits are important for assembly with beta subunits.* J Biol Chem, 1998. **273**(45): p. 29400-5.
113. Esmann, M., *Sulphydryl groups of (Na+ + K+)-ATPase from rectal glands of Squalus acanthias. Detection of ligand-induced conformational changes.* Biochim Biophys Acta, 1982. **688**(1): p. 260-70.
114. Kaplan, J.H. and M.D. Mone, *Modified cation activation of the (Na+K)-ATPase following treatment with thimerosal.* Arch Biochem Biophys, 1985. **237**(2): p. 386-95.
115. Anner, B.M., M. Moosmayer, and E. Imesch, *Chelation of mercury by ouabain-sensitive and ouabain-resistant renal Na,K-ATPase.* Biochem Biophys Res Commun, 1990. **167**(3): p. 1115-21.
116. Hu, Y.K., J.F. Eisses, and J.H. Kaplan, *Expression of an active Na,K-ATPase with an alpha-subunit lacking all twenty-three native cysteine residues.* J Biol Chem, 2000. **275**(39): p. 30734-9.
117. Benesch, R.E., H.A. Lardy, and R. Benesch, *The sulfhydryl groups of crystalline proteins. I. Some albumins, enzymes, and hemoglobins.* J Biol Chem, 1955. **216**(2): p. 663-76.
118. Copley, S.D., W.R. Novak, and P.C. Babbitt, *Divergence of function in the thioredoxin fold suprafamily: evidence for evolution of peroxiredoxins from a thioredoxin-like ancestor.* Biochemistry, 2004. **43**(44): p. 13981-95.
119. Halliwell, B. and J.M.C. Gutteridge, *Free radicals in biology and medicine*. 4th ed2007, Oxford: Oxford University Press. xxxvi, 851 p.
120. Winterbourn, C.C., *Reconciling the chemistry and biology of reactive oxygen species.* Nat Chem Biol, 2008. **4**(5): p. 278-86.
121. Finkel, T., *Signal transduction by reactive oxygen species.* J Cell Biol, 2011. **194**(1): p. 7-15.
122. Afonso, V., et al., *Reactive oxygen species and superoxide dismutases: role in joint diseases.* Joint Bone Spine, 2007. **74**(4): p. 324-9.
123. Shen, G.X., *Oxidative stress and diabetic cardiovascular disorders: roles of mitochondria and NADPH oxidase.* Can J Physiol Pharmacol, 2010. **88**(3): p. 241-8.
124. Rasmussen, H.H., et al., *Reversible oxidative modification: implications for cardiovascular physiology and pathophysiology.* Trends Cardiovasc Med, 2010. **20**(3): p. 85-90.
125. Marla, S.S., J. Lee, and J.T. Groves, *Peroxynitrite rapidly permeates phospholipid membranes.* Proc Natl Acad Sci U S A, 1997. **94**(26): p. 14243-8.
126. Stamler, J.S., D.J. Singel, and J. Loscalzo, *Biochemistry of nitric oxide and its redox-activated forms.* Science, 1992. **258**(5090): p. 1898-902.
127. Bardwell, J.C., *Building bridges: disulphide bond formation in the cell.* Mol Microbiol, 1994. **14**(2): p. 199-205.

128. Cooper, A.J., J.T. Pinto, and P.S. Callery, *Reversible and irreversible protein glutathionylation: biological and clinical aspects.* Expert Opin Drug Metab Toxicol, 2011. **7**(7): p. 891-910.
129. Gallogly, M.M. and J.J. Mieyal, *Mechanisms of reversible protein glutathionylation in redox signaling and oxidative stress.* Curr Opin Pharmacol, 2007. **7**(4): p. 381-91.
130. Janssen-Heininger, Y.M., et al., *Redox-based regulation of signal transduction: principles, pitfalls, and promises.* Free Radic Biol Med, 2008. **45**(1): p. 1-17.
131. Martinez-Ruiz, A. and S. Lamas, *Signalling by NO-induced protein S-nitrosylation and S-glutathionylation: convergences and divergences.* Cardiovasc Res, 2007. **75**(2): p. 220-8.
132. Kourie, J.I., *Interaction of reactive oxygen species with ion transport mechanisms.* Am J Physiol, 1998. **275**(1 Pt 1): p. C1-24.
133. Rohn, T.T., T.R. Hinds, and F.F. Vincenzi, *Inhibition of the Ca pump of intact red blood cells by t-butyl hydroperoxide: importance of glutathione peroxidase.* Biochim Biophys Acta, 1993. **1153**(1): p. 67-76.
134. Jamme, I., et al., *Modulation of mouse cerebral Na+,K(+)-ATPase activity by oxygen free radicals.* Neuroreport, 1995. **7**(1): p. 333-7.
135. Elmoselhi, A.B., et al., *Free radicals uncouple the sodium pump in pig coronary artery.* Am J Physiol, 1994. **266**(3 Pt 1): p. C720-8.
136. Vinnikova, A.K., R.C. Kukreja, and M.L. Hess, *Singlet oxygen-induced inhibition of cardiac sarcolemmal Na+K(+)-ATPase.* J Mol Cell Cardiol, 1992. **24**(5): p. 465-70.
137. Vlessis, A.A., et al., *Mechanism of peroxide-induced cellular injury in cultured adult cardiac myocytes.* Faseb J, 1991. **5**(11): p. 2600-5.
138. Kukreja, R.C., A.B. Weaver, and M.L. Hess, *Sarcolemmal Na(+)-K(+)-ATPase: inactivation by neutrophil-derived free radicals and oxidants.* Am J Physiol, 1990. **259**(5 Pt 2): p. H1330-6.
139. Mishra, O.P., et al., *Lipid peroxidation as the mechanism of modification of the affinity of the Na+, K+-ATPase active sites for ATP, K+, Na+, and strophanthidin in vitro.* Neurochem Res, 1989. **14**(9): p. 845-51.
140. Kako, K., et al., *Depression of membrane-bound Na+-K+-ATPase activity induced by free radicals and by ischemia of kidney.* Am J Physiol, 1988. **254**(2 Pt 1): p. C330-7.
141. Kim, M.S. and T. Akera, *O2 free radicals: cause of ischemia-reperfusion injury to cardiac Na+-K+-ATPase.* Am J Physiol, 1987. **252**(2 Pt 2): p. H252-7.
142. Kramer, J.H., I.T. Mak, and W.B. Weglicki, *Differential sensitivity of canine cardiac sarcolemmal and microsomal enzymes to inhibition by free radical-induced lipid peroxidation.* Circ Res, 1984. **55**(1): p. 120-4.
143. Buczko, W., *Influence of fibrinogen degradation products (FDP) on the ATPase activity in the rat heart.* Acta Physiol Pol, 1978. **29**(2): p. 185-7.
144. Singh, R.B. and N.S. Dhalla, *Ischemia-reperfusion-induced changes in sarcolemmal Na+/K+-ATPase are due to the activation of calpain in the heart.* Can J Physiol Pharmacol, 2010. **88**(3): p. 388-97.
145. de Assis, D.R., et al., *Evidence that antioxidants prevent the inhibition of Na+,K(+)-ATPase activity induced by octanoic acid in rat cerebral cortex in vitro.* Neurochem Res, 2003. **28**(8): p. 1255-63.

146. Feraille, E., et al., *Insulin-induced stimulation of Na+,K(+)-ATPase activity in kidney proximal tubule cells depends on phosphorylation of the alpha-subunit at Tyr-10.* Mol Biol Cell, 1999. **10**(9): p. 2847-59.
147. Narkar, V., T. Hussain, and M. Lokhandwala, *Role of tyrosine kinase and p44/42 MAPK in D(2)-like receptor-mediated stimulation of Na(+), K(+)-ATPase in kidney.* Am J Physiol Renal Physiol, 2002. **282**(4): p. F697-702.
148. Wang, X.Q. and S.P. Yu, *Novel regulation of Na, K-ATPase by Src tyrosine kinases in cortical neurons.* J Neurochem, 2005. **93**(6): p. 1515-23.
149. Fuller, W., et al., *FXYD1 phosphorylation in vitro and in adult rat cardiac myocytes: threonine 69 is a novel substrate for protein kinase C.* Am J Physiol Cell Physiol, 2009. **296**(6): p. C1346-55.
150. Han, F., et al., *Phospholemman phosphorylation mediates the protein kinase C-dependent effects on Na+/K+ pump function in cardiac myocytes.* Circ Res, 2006. **99**(12): p. 1376-83.
151. Han, F., et al., *Role of phospholemman phosphorylation sites in mediating kinase-dependent regulation of the Na+-K+-ATPase.* Am J Physiol Cell Physiol, 2010. **299**(6): p. C1363-9.
152. Li, K.C., et al., *Follistatin-like 1 suppresses sensory afferent transmission by activating Na+,K+-ATPase.* Neuron, 2011. **69**(5): p. 974-87.
153. Zahler, R., et al., *Sodium kinetics of Na,K-ATPase alpha isoforms in intact transfected HeLa cells.* J Gen Physiol, 1997. **110**(2): p. 201-13.
154. Logvinenko, N.S., et al., *Phosphorylation by protein kinase C of serine-23 of the alpha-1 subunit of rat Na+,K(+)-ATPase affects its conformational equilibrium.* Proc Natl Acad Sci U S A, 1996. **93**(17): p. 9132-7.
155. Feraille, E., et al., *Is phosphorylation of the alpha1 subunit at Ser-16 involved in the control of Na,K-ATPase activity by phorbol ester-activated protein kinase C?* Mol Biol Cell, 2000. **11**(1): p. 39-50.
156. Cai, T., et al., *Regulation of caveolin-1 membrane trafficking by the Na/K-ATPase.* J Cell Biol, 2008. **182**(6): p. 1153-69.
157. Dada, L.A., et al., *Phosphorylation and ubiquitination are necessary for Na,K-ATPase endocytosis during hypoxia.* Cell Signal, 2007. **19**(9): p. 1893-8.
158. Efendiev, R., et al., *Simultaneous phosphorylation of Ser11 and Ser18 in the alpha-subunit promotes the recruitment of Na(+),K(+)-ATPase molecules to the plasma membrane.* Biochemistry, 2000. **39**(32): p. 9884-92.
159. Al-Khalili, L., et al., *ERK1/2 mediates insulin stimulation of Na(+),K(+)-ATPase by phosphorylation of the alpha-subunit in human skeletal muscle cells.* J Biol Chem, 2004. **279**(24): p. 25211-8.
160. Bers, D.M. and S. Despa, *Na+ transport in cardiac myocytes; Implications for excitation-contraction coupling.* IUBMB Life, 2009. **61**(3): p. 215-21.
161. Camici, P.G., S.K. Prasad, and O.E. Rimoldi, *Stunning, hibernation, and assessment of myocardial viability.* Circulation, 2008. **117**(1): p. 103-14.
162. Wiggers, C.J., *The functional consequences of acute coronary occlusion.* J Ark Med Soc, 1946. **43**: p. 48.
163. Camici, P.G. and O.E. Rimoldi, *Myocardial blood flow in patients with hibernating myocardium.* Cardiovasc Res, 2003. **57**(2): p. 302-11.
164. Underwood, S.R., et al., *Imaging techniques for the assessment of myocardial hibernation. Report of a Study Group of the European Society of Cardiology.* Eur Heart J, 2004. **25**(10): p. 815-36.

165. Redwood, S.R., R. Ferrari, and M.S. Marber, *Myocardial hibernation and stunning: from physiological principles to clinical practice.* Heart, 1998. **80**(3): p. 218-22.
166. Schulz, R., et al., *Regional short-term myocardial hibernation in swine does not involve endogenous adenosine or KATP channels.* Am J Physiol, 1995. **268**(6 Pt 2): p. H2294-301.
167. Schulz, R., et al., *Recruitment of an inotropic reserve in moderately ischemic myocardium at the expense of metabolic recovery. A model of short-term hibernation.* Circ Res, 1992. **70**(6): p. 1282-95.
168. Braunwald, E. and R.A. Kloner, *The stunned myocardium: prolonged, postischemic ventricular dysfunction.* Circulation, 1982. **66**(6): p. 1146-9.
169. Heusch, G., *Hibernating myocardium.* Physiol Rev, 1998. **78**(4): p. 1055-85.
170. Heusch, G., R. Schulz, and S.H. Rahimtoola, *Myocardial hibernation: a delicate balance.* Am J Physiol Heart Circ Physiol, 2005. **288**(3): p. H984-99.
171. van Echteld, C.J., et al., *Intracellular sodium during ischemia and calcium-free perfusion: a 23Na NMR study.* J Mol Cell Cardiol, 1991. **23**(3): p. 297-307.
172. Tani, M. and J.R. Neely, *Role of intracellular Na+ in Ca2+ overload and depressed recovery of ventricular function of reperfused ischemic rat hearts. Possible involvement of H+-Na+ and Na+-Ca2+ exchange.* Circ Res, 1989. **65**(4): p. 1045-56.
173. Fuller, W., et al., *Cardiac ischemia causes inhibition of the Na/K ATPase by a labile cytosolic compound whose production is linked to oxidant stress.* Cardiovasc.Res., 2003. **57**(4): p. 1044-1051.
174. Bogdanova, A. and J. Vogel, *Isolated, autologous blood-perfused heart: replacement of heterotopic heart transplantation.* ALTEX, 2007. **24 Spec No**: p. 75-6.
175. McMichael, J. and E.P. Sharpey-Schafer, *CARDIAC OUTPUT IN MAN BY A DIRECT FICK METHOD: Effects of Posture, Venous Pressure Change, Atropine, And Adrenaline.* Br Heart J, 1944. **6**(1): p. 33-40.
176. Lorigados, C.B., F.G. Soriano, and C. Szabo, *Pathomechanisms of myocardial dysfunction in sepsis.* Endocr Metab Immune Disord Drug Targets, 2010. **10**(3): p. 274-84.
177. Tune, J.D., M.W. Gorman, and E.O. Feigl, *Matching coronary blood flow to myocardial oxygen consumption.* J Appl Physiol, 2004. **97**(1): p. 404-15.
178. Zong, P., J.D. Tune, and H.F. Downey, *Mechanisms of oxygen demand/supply balance in the right ventricle.* Exp Biol Med (Maywood), 2005. **230**(8): p. 507-19.
179. Chilian, W.M., *Coronary microcirculation in health and disease. Summary of an NHLBI workshop.* Circulation, 1997. **95**(2): p. 522-8.
180. Hiebl, B., et al., *Influence of polymeric microspheres on the myocardial oxygen partial pressure in the beating heart of pigs.* Microvasc Res, 2011. **82**(1): p. 52-7.
181. Heineman, F.W. and R.S. Balaban, *Control of mitochondrial respiration in the heart in vivo.* Annu Rev Physiol, 1990. **52**: p. 523-42.
182. Lopez-Barneo, J., et al., *First aid kit for hypoxic survival: sensors and strategies.* Physiol Biochem Zool, 2010. **83**(5): p. 753-63.
183. Zuurbier, C.J., M. van Iterson, and C. Ince, *Functional heterogeneity of oxygen supply-consumption ratio in the heart.* Cardiovasc Res, 1999. **44**(3): p. 488-97.

184. Takahashi, E., et al., *Direct observation of radial intracellular PO2 gradients in a single cardiomyocyte of the rat.* Am J Physiol, 1998. **275**(1 Pt 2): p. H225-33.
185. Gayeski, T.E. and C.R. Honig, *Intracellular PO2 in individual cardiac myocytes in dogs, cats, rabbits, ferrets, and rats.* Am J Physiol, 1991. **260**(2 Pt 2): p. H522-31.
186. Lin, P.C., U. Kreutzer, and T. Jue, *Myoglobin translational diffusion in rat myocardium and its implication on intracellular oxygen transport.* J Physiol, 2007. **578**(Pt 2): p. 595-603.
187. Takahashi, E., et al., *In vivo oxygen imaging using green fluorescent protein.* Am J Physiol Cell Physiol, 2006. **291**(4): p. C781-7.
188. Takahashi, E., H. Endoh, and K. Doi, *Intracellular gradients of O2 supply to mitochondria in actively respiring single cardiomyocyte of rats.* Am J Physiol, 1999. **276**(2 Pt 2): p. H718-24.
189. Bing, R.J., et al., *Metabolic studies on the human heart in vivo. I. Studies on carbohydrate metabolism of the human heart.* Am J Med, 1953. **15**(3): p. 284-96.
190. Bing, R.J., et al., *Metabolism of the human heart. II. Studies on fat, ketone and amino acid metabolism.* Am J Med, 1954. **16**(4): p. 504-15.
191. van der Vusse, G.J., et al., *Fatty acid homeostasis in the normoxic and ischemic heart.* Physiol Rev, 1992. **72**(4): p. 881-940.
192. Gertz, E.W., et al., *Myocardial substrate utilization during exercise in humans. Dual carbon-labeled carbohydrate isotope experiments.* J Clin Invest, 1988. **82**(6): p. 2017-25.
193. Liedtke, A.J., *Alterations of carbohydrate and lipid metabolism in the acutely ischemic heart.* Prog Cardiovasc Dis, 1981. **23**(5): p. 321-36.
194. Chagas, A.C., P.M. Dourado, and F. Galvao Tde, *Modulation of cardiac metabolism during myocardial ischemia.* Curr Pharm Des, 2008. **14**(25): p. 2563-71.
195. Stanley, W.C., *Partial fatty acid oxidation inhibitors for stable angina.* Expert Opin Investig Drugs, 2002. **11**(5): p. 615-29.
196. Rosano, G.M., et al., *Cardiac metabolism in myocardial ischemia.* Curr Pharm Des, 2008. **14**(25): p. 2551-62.
197. Neill, W.A. and J.S. Ingwall, *Stabilization of a derangement in adenosine triphosphate metabolism during sustained, partial ischemia in the dog heart.* J Am Coll Cardiol, 1986. **8**(4): p. 894-900.
198. Kroll, K., D.J. Kinzie, and L.A. Gustafson, *Open-system kinetics of myocardial phosphoenergetics during coronary underperfusion.* Am J Physiol, 1997. **272**(6 Pt 2): p. H2563-76.
199. Schaefer, S., et al., *Myocardial adaptation during acute hibernation: mechanisms of phosphocreatine recovery.* Cardiovasc Res, 1993. **27**(11): p. 2044-51.
200. Saks, V.A., *Molecular system bioenergetics : energy for life*2007, Weinheim: Wiley-VCH. xxviii, 604 p.
201. Cason, B.A., et al., *Effects of high arterial oxygen tension on function, blood flow distribution, and metabolism in ischemic myocardium.* Circulation, 1992. **85**(2): p. 828-38.

202. McNulty, P.H., et al., *Glucose metabolism distal to a critical coronary stenosis in a canine model of low-flow myocardial ischemia.* J Clin Invest, 1996. **98**(1): p. 62-9.
203. Schulz, R., et al., *Consequences of regional inotropic stimulation of ischemic myocardium on regional myocardial blood flow and function in anesthetized swine.* Circ Res, 1989. **64**(6): p. 1116-26.
204. Vrbjar, N., A. Dzurba, and A. Ziegelhoffer, *Enzyme kinetics and the activation energy of (Na,K)-ATPase in ischaemic hearts: influence of the duration of ischaemia.* Gen Physiol Biophys, 1994. **13**(5): p. 405-11.
205. Mohabir, R., et al., *Effects of ischemia and hypercarbic acidosis on myocyte calcium transients, contraction, and pHi in perfused rabbit hearts.* Circ Res, 1991. **69**(6): p. 1525-37.
206. Steenbergen, C., et al., *Correlation between cytosolic free calcium, contracture, ATP, and irreversible ischemic injury in perfused rat heart.* Circ Res, 1990. **66**(1): p. 135-46.
207. Uemura, A., Y. Naito, and T. Matsubara, *Dynamics of Ca(2+)/calmodulin-dependent protein kinase II following acute myocardial ischemia-translocation and autophosphorylation.* Biochem Biophys Res Commun, 2002. **297**(4): p. 997-1002.
208. D'Urso, G., et al., *Production of ouabain-like factor in normal and ischemic rat heart.* J Cardiovasc Pharmacol, 2004. **43**(5): p. 657-62.
209. De Angelis, C. and G.T. Haupert, Jr., *Hypoxia triggers release of an endogenous inhibitor of Na(+)-K(+)-ATPase from midbrain and adrenal.* Am J Physiol, 1998. **274**(1 Pt 2): p. F182-8.
210. Nakazawa, H., et al., *Is superoxide demonstration by electron-spin resonance spectroscopy really superoxide?* Am J Physiol, 1988. **255**(1 Pt 2): p. H213-5.
211. Maupoil, V. and L. Rochette, *Evaluation of free radical and lipid peroxide formation during global ischemia and reperfusion in isolated perfused rat heart.* Cardiovasc Drugs Ther, 1988. **2**(5): p. 615-21.
212. Zweier, J.L., J.T. Flaherty, and M.L. Weisfeldt, *Direct measurement of free radical generation following reperfusion of ischemic myocardium.* Proc Natl Acad Sci U S A, 1987. **84**(5): p. 1404-7.
213. Hoffman, D.L., J.D. Salter, and P.S. Brookes, *Response of mitochondrial reactive oxygen species generation to steady-state oxygen tension: implications for hypoxic cell signaling.* Am J Physiol Heart Circ Physiol, 2007. **292**(1): p. H101-8.
214. Scandurra, F.M. and E. Gnaiger, *Cell respiration under hypoxia: facts and artefacts in mitochondrial oxygen kinetics.* Adv Exp Med Biol, 2010. **662**: p. 7-25.
215. Poyton, R.O., K.A. Ball, and P.R. Castello, *Mitochondrial generation of free radicals and hypoxic signaling.* Trends Endocrinol Metab, 2009. **20**(7): p. 332-40.
216. Khan, M., et al., *Oxygen and oxygenation in stem-cell therapy for myocardial infarction.* Life Sci, 2010. **87**(9-10): p. 269-74.
217. Mailloux, R.J. and M.E. Harper, *Uncoupling proteins and the control of mitochondrial reactive oxygen species production.* Free Radic Biol Med, 2011. **51**(6): p. 1106-15.

218. Borutaite, V., et al., *Kinetic analysis of changes in activity of heart mitochondrial oxidative phosphorylation system induced by ischemia.* J Mol Cell Cardiol, 1996. **28**(10): p. 2195-201.
219. Nadtochiy, S.M., A.J. Tompkins, and P.S. Brookes, *Different mechanisms of mitochondrial proton leak in ischaemia/reperfusion injury and preconditioning: implications for pathology and cardioprotection.* Biochem J, 2006. **395**(3): p. 611-8.
220. Ward, J.P., *Oxygen sensors in context.* Biochim Biophys Acta, 2008. **1777**(1): p. 1-14.
221. Porwol, T., et al., *Tissue oxygen sensor function of NADPH oxidase isoforms, an unusual cytochrome aa3 and reactive oxygen species.* Respir Physiol, 2001. **128**(3): p. 331-48.
222. Sies, H., *Oxidative stress*1985, London: Orlando : Academic Press. xv, 507 p.
223. Santos, C.X., et al., *Redox signaling in cardiac myocytes.* Free Radic Biol Med, 2011. **50**(7): p. 777-93.
224. Umar, S. and A. van der Laarse, *Nitric oxide and nitric oxide synthase isoforms in the normal, hypertrophic, and failing heart.* Mol Cell Biochem, 2010. **333**(1-2): p. 191-201.
225. Hein, T.W., et al., *Ischemia-reperfusion selectively impairs nitric oxide-mediated dilation in coronary arterioles: counteracting role of arginase.* Faseb J, 2003. **17**(15): p. 2328-30.
226. Alvarez, S., et al., *Oxygen dependence of mitochondrial nitric oxide synthase activity.* Biochem Biophys Res Commun, 2003. **305**(3): p. 771-5.
227. Fukuto, J.M., A.J. Hobbs, and L.J. Ignarro, *Conversion of nitroxyl (HNO) to nitric oxide (NO) in biological systems: the role of physiological oxidants and relevance to the biological activity of HNO.* Biochem Biophys Res Commun, 1993. **196**(2): p. 707-13.
228. Sun, J., C. Steenbergen, and E. Murphy, *S-nitrosylation: NO-related redox signaling to protect against oxidative stress.* Antioxid Redox Signal, 2006. **8**(9-10): p. 1693-705.
229. Rassaf, T., et al., *Nitrite reductase function of deoxymyoglobin: oxygen sensor and regulator of cardiac energetics and function.* Circ Res, 2007. **100**(12): p. 1749-54.
230. Huie, R.E. and S. Padmaja, *The reaction of no with superoxide.* Free Radic Res Commun, 1993. **18**(4): p. 195-9.
231. Peluffo, G. and R. Radi, *Biochemistry of protein tyrosine nitration in cardiovascular pathology.* Cardiovasc Res, 2007. **75**(2): p. 291-302.
232. Hughes, M.N., *Chemistry of nitric oxide and related species.* Methods Enzymol, 2008. **436**: p. 3-19.
233. Martinez-Ruiz, A., S. Cadenas, and S. Lamas, *Nitric oxide signaling: classical, less classical, and nonclassical mechanisms.* Free Radic Biol Med, 2011. **51**(1): p. 17-29.
234. Pacher, P., J.S. Beckman, and L. Liaudet, *Nitric oxide and peroxynitrite in health and disease.* Physiol Rev, 2007. **87**(1): p. 315-424.
235. Weerateerangkul, P., S. Chattipakorn, and N. Chattipakorn, *Roles of the nitric oxide signaling pathway in cardiac ischemic preconditioning against myocardial ischemia-reperfusion injury.* Med Sci Monit, 2011. **17**(2): p. RA44-52.

236. Fridovich, I., *Superoxide anion radical (O2-.), superoxide dismutases, and related matters.* J Biol Chem, 1997. **272**(30): p. 18515-7.
237. D'Autreaux, B. and M.B. Toledano, *ROS as signalling molecules: mechanisms that generate specificity in ROS homeostasis.* Nat Rev Mol Cell Biol, 2007. **8**(10): p. 813-24.
238. Ng, C.F., et al., *The rate of cellular hydrogen peroxide removal shows dependency on GSH: mathematical insight into in vivo H2O2 and GPx concentrations.* Free Radic Res, 2007. **41**(11): p. 1201-11.
239. Antunes, F., D. Han, and E. Cadenas, *Relative contributions of heart mitochondria glutathione peroxidase and catalase to H(2)O(2) detoxification in in vivo conditions.* Free Radic Biol Med, 2002. **33**(9): p. 1260-7.
240. Arteel, G.E., K. Briviba, and H. Sies, *Function of thioredoxin reductase as a peroxynitrite reductase using selenocystine or ebselen.* Chem Res Toxicol, 1999. **12**(3): p. 264-9.
241. Hattori, F., et al., *Mitochondrial peroxiredoxin-3 protects hippocampal neurons from excitotoxic injury in vivo.* J Neurochem, 2003. **86**(4): p. 860-8.
242. Brown, G.C. and V. Borutaite, *Nitric oxide and mitochondrial respiration in the heart.* Cardiovasc Res, 2007. **75**(2): p. 283-90.
243. Apel, K. and H. Hirt, *Reactive oxygen species: metabolism, oxidative stress, and signal transduction.* Annu Rev Plant Biol, 2004. **55**: p. 373-99.
244. Schafer, F.Q. and G.R. Buettner, *Redox environment of the cell as viewed through the redox state of the glutathione disulfide/glutathione couple.* Free Radic Biol Med, 2001. **30**(11): p. 1191-212.
245. Briviba, K., et al., *Kinetic study of the reaction of glutathione peroxidase with peroxynitrite.* Chem Res Toxicol, 1998. **11**(12): p. 1398-401.
246. Winterbourn, C.C. and D. Metodiewa, *The reaction of superoxide with reduced glutathione.* Arch Biochem Biophys, 1994. **314**(2): p. 284-90.
247. Aceto, A., et al., *Effect of ischaemia-reperfusion on glutathione peroxidase, glutathione reductase and glutathione transferase activities in human heart protected by hypothermic cardioplegia.* Free Radic Res Commun, 1990. **8**(2): p. 85-91.
248. Guarnieri, C., F. Flamigni, and C.M. Caldarera, *Role of oxygen in the cellular damage induced by re-oxygenation of hypoxic heart.* J Mol Cell Cardiol, 1980. **12**(8): p. 797-808.
249. Korichneva, I., *Redox regulation of cardiac protein kinase C.* Exp Clin Cardiol, 2005. **10**(4): p. 256-61.
250. Rimessi, A., R. Rizzuto, and P. Pinton, *Differential recruitment of PKC isoforms in HeLa cells during redox stress.* Cell Stress Chaperones, 2007. **12**(4): p. 291-8.
251. Fuller, W., et al., *Ischemia-induced phosphorylation of phospholemman directly activates rat cardiac Na/K-ATPase.* Faseb J, 2004. **18**(1): p. 197-9.
252. Avivi, A., et al., *Adaptive hypoxic tolerance in the subterranean mole rat Spalax ehrenbergi: the role of vascular endothelial growth factor.* FEBS Lett, 1999. **452**(3): p. 133-40.
253. Stecyk, J.A., et al., *Maintained cardiac pumping in anoxic crucian carp.* Science, 2004. **306**(5693): p. 77.

254. Farrell, A.P. and J.A. Stecyk, *The heart as a working model to explore themes and strategies for anoxic survival in ectothermic vertebrates.* Comp Biochem Physiol A Mol Integr Physiol, 2007. **147**(2): p. 300-12.
255. Stecyk, J.A., B.C. Larsen, and G.E. Nilsson, *Intrinsic contractile properties of the crucian carp (Carassius carassius) heart during anoxic and acidotic stress.* Am J Physiol Regul Integr Comp Physiol, 2011. **301**(4): p. R1132-42.
256. Stecyk, J.A., et al., *Cardiac survival in anoxia-tolerant vertebrates: An electrophysiological perspective.* Comp Biochem Physiol C Toxicol Pharmacol, 2008. **148**(4): p. 339-54.
257. Ramirez, J.M., L.P. Folkow, and A.S. Blix, *Hypoxia tolerance in mammals and birds: from the wilderness to the clinic.* Annu Rev Physiol, 2007. **69**: p. 113-43.
258. Tota, B., et al., *Hypoxia and anoxia tolerance of vertebrate hearts: an evolutionary perspective.* Antioxid Redox Signal, 2011. **14**(5): p. 851-62.
259. Ostadal, B., I. Ostadalova, and N.S. Dhalla, *Development of cardiac sensitivity to oxygen deficiency: comparative and ontogenetic aspects.* Physiol Rev, 1999. **79**(3): p. 635-59.
260. Schwarzbaum, P., et al., *Effect of chemical anoxia on protein kinase C and Na+, K+-ATPase in hepatocytes of goldfish (Carassius auratus) and rainbow trout (Oncorhynchus mykiss).* J Exp Biol, 1996. **199**(Pt 7): p. 1515-21.
261. Iftikar, F.I., V. Matey, and C.M. Wood, *The ionoregulatory responses to hypoxia in the freshwater rainbow trout Oncorhynchus mykiss.* Physiol Biochem Zool, 2010. **83**(2): p. 343-55.
262. Hylland, P., et al., *Brain Na+/K+-ATPase activity in two anoxia tolerant vertebrates: crucian carp and freshwater turtle.* Neurosci Lett, 1997. **235**(1-2): p. 89-92.
263. Aho, E. and M. Vornamen, *Seasonality of ATPase activities in crucian carp (Carassius carassius L.) heart.* Fish Physiology and Biochemistry, 1997. **16**(5): p. 355-364.
264. Sandvik, G.K., G.E. Nilsson, and F.B. Jensen, *Dramatic increase of nitrite levels in hearts of anoxia-exposed crucian carp supporting a role in cardioprotection.* Am J Physiol Regul Integr Comp Physiol, 2011.
265. Hansen, M.N. and F.B. Jensen, *Nitric oxide metabolites in goldfish under normoxic and hypoxic conditions.* J Exp Biol, 2010. **213**(Pt 21): p. 3593-602.
266. Hanna, E.B. and D.L. Glancy, *ST-segment depression and T-wave inversion: classification, differential diagnosis, and caveats.* Cleve Clin J Med, 2011. **78**(6): p. 404-14.
267. Seko, Y., et al., *Hypoxia and hypoxia/reoxygenation activate Raf-1, mitogen-activated protein kinase kinase, mitogen-activated protein kinases, and S6 kinase in cultured rat cardiac myocytes.* Circ Res, 1996. **78**(1): p. 82-90.
268. Han, Y., et al., *Redox regulation of the AMP-activated protein kinase.* PLoS One, 2010. **5**(11): p. e15420.
269. Xiao, R., et al., *Catalysis of thiol/disulfide exchange. Glutaredoxin 1 and protein-disulfide isomerase use different mechanisms to enhance oxidase and reductase activities.* J Biol Chem, 2005. **280**(22): p. 21099-106.
270. Starke, D.W., P.B. Chock, and J.J. Mieyal, *Glutathione-thiyl radical scavenging and transferase properties of human glutaredoxin (thioltransferase). Potential role in redox signal transduction.* J Biol Chem, 2003. **278**(17): p. 14607-13.

271. Sandblom, E. and M. Axelsson, *Effects of hypoxia on the venous circulation in rainbow trout (Oncorhynchus mykiss).* Comp Biochem Physiol A Mol Integr Physiol, 2005. **140**(2): p. 233-9.
272. Marshall, J.M. and J.D. Metcalfe, *Analysis of the cardiovascular changes induced in the rat by graded levels of systemic hypoxia.* J Physiol, 1988. **407**: p. 385-403.
273. Rosen, K.G. and I. Kjellmer, *Changes in the fetal heart rate and ECG during hypoxia.* Acta Physiol Scand, 1975. **93**(1): p. 59-66.
274. Ziegelhoffer, A., et al., *Na,K-ATPase in the myocardium: molecular principles, functional and clinical aspects.* Gen.Physiol Biophys., 2000. **19**(1): p. 9-47.
275. Hornestam, B., P. Held, and N. Edvardsson, *Effects of digoxin on electrocardiogram in patients with acute atrial fibrillation--a randomized, placebo-controlled study. Digitalis in Acute Atrial Fibrillation (DAAF) Trial Group.* Clin Cardiol, 1999. **22**(2): p. 96-102.
276. Kudenchuk, P.J., et al., *Utility of the prehospital electrocardiogram in diagnosing acute coronary syndromes: the Myocardial Infarction Triage and Intervention (MITI) Project.* J Am Coll Cardiol, 1998. **32**(1): p. 17-27.
277. Loor, G., et al., *Mitochondrial oxidant stress triggers cell death in simulated ischemia-reperfusion.* Biochim Biophys Acta, 2011. **1813**(7): p. 1382-94.
278. Dweik, R.A., *Nitric oxide, hypoxia, and superoxide: the good, the bad, and the ugly!* Thorax, 2005. **60**(4): p. 265-7.
279. Bibert, S., et al., *FXYD proteins reverse inhibition of the Na-K pump mediated by glutathionylation of its {beta}1 subunit.* J Biol Chem, 2011.
280. Silverman, B.Z., et al., *Serine 68 phosphorylation of phospholemman: acute isoform-specific activation of cardiac Na/K ATPase.* Cardiovasc Res, 2005. **65**(1): p. 93-103.
281. Dada, L.A., et al., *Hypoxia-induced endocytosis of Na,K-ATPase in alveolar epithelial cells is mediated by mitochondrial reactive oxygen species and PKC-zeta.* J Clin Invest, 2003. **111**(7): p. 1057-64.
282. Liu, L., et al., *Involvement of Na+/K+-ATPase in hydrogen peroxide-induced hypertrophy in cardiac myocytes.* Free Radic Biol Med, 2006. **41**(10): p. 1548-56.
283. Shi, H.G., et al., *Functional role of cysteine residues in the (Na,K)-ATPase alpha subunit.* Biochim.Biophys.Acta, 2000. **1464**(2): p. 177-187.
284. Kurella, E.G., O.V. Tyulina, and A.A. Boldyrev, *Oxidative resistance of Na/K-ATPase.* Cell Mol.Neurobiol., 1999. **19**(1): p. 133-140.
285. Dobrota, D., et al., *Na/K-ATPase under oxidative stress: molecular mechanisms of injury.* Cell Mol.Neurobiol., 1999. **19**(1): p. 141-149.
286. Lancel, S., et al., *Nitroxyl activates SERCA in cardiac myocytes via glutathiolation of cysteine 674.* Circ Res, 2009. **104**(6): p. 720-3.
287. Aracena-Parks, P., et al., *Identification of cysteines involved in S-nitrosylation, S-glutathionylation, and oxidation to disulfides in ryanodine receptor type 1.* J Biol Chem, 2006. **281**(52): p. 40354-68.
288. Xu, K.Y., J.L. Zweier, and L.C. Becker, *Oxygen-free radicals directly attack the ATP binding site of the cardiac Na+,K(+)-ATPase.* Ann N Y Acad Sci, 1997. **834**: p. 680-3.
289. Cappel, R.E., et al., *Thiol/disulfide redox equilibrium between glutathione and glycogen debranching enzyme (amylo-1,6-glucosidase/4-alpha-*

glucanotransferase) from rabbit muscle. J Biol Chem, 1986. **261**(33): p. 15385-9.
290. Swift, F., et al., *Altered Na+/Ca2+-exchanger activity due to downregulation of Na+/K+-ATPase alpha2-isoform in heart failure.* Cardiovasc Res, 2008. **78**(1): p. 71-8.
291. Bers, D.M. and S. Despa, *Cardiac Myocytes Ca(2+) and Na(+) Regulation in Normal and Failing Hearts.* J Pharmacol Sci, 2006.
292. Xie, Z., et al., *Different oxidant sensitivities of the alpha 1 and alpha 2 isoforms of Na+/K(+)-ATPase expressed in baculovirus-infected insect cells.* Biochem.Biophys.Res.Commun., 1995. **207**(1): p. 155-159.
293. Segall, L., L.K. Lane, and R. Blostein, *Insights into the structural basis for modulation of E1<-->E2 transitions by cytoplasmic domains of the Na,K-ATPase alpha subunit.* Ann N Y Acad Sci, 2003. **986**: p. 58-62.
294. Petrushanko, I., et al., *Na-K-ATPase in rat cerebellar granule cells is redox sensitive.* Am J Physiol Regul Integr Comp Physiol, 2006. **290**(4): p. R916-25.
295. Klatt, P. and S. Lamas, *Regulation of protein function by S-glutathiolation in response to oxidative and nitrosative stress.* Eur J Biochem, 2000. **267**(16): p. 4928-44.
296. Shelton, M.D., P.B. Chock, and J.J. Mieyal, *Glutaredoxin: role in reversible protein s-glutathionylation and regulation of redox signal transduction and protein translocation.* Antioxid Redox Signal, 2005. **7**(3-4): p. 348-66.
297. Dalle-Donne, I., et al., *Protein S-glutathionylation: a regulatory device from bacteria to humans.* Trends Biochem Sci, 2009. **34**(2): p. 85-96.
298. Mieyal, J.J., et al., *Molecular mechanisms and clinical implications of reversible protein S-glutathionylation.* Antioxid Redox Signal, 2008. **10**(11): p. 1941-88.
299. Adachi, T., et al., *S-Glutathiolation by peroxynitrite activates SERCA during arterial relaxation by nitric oxide.* Nat Med, 2004. **10**(11): p. 1200-7.
300. Bers, D.M. and S. Despa, *Na/K-ATPase--an integral player in the adrenergic fight-or-flight response.* Trends Cardiovasc Med, 2009. **19**(4): p. 111-8.
301. Zima, A.V. and L.A. Blatter, *Redox regulation of cardiac calcium channels and transporters.* Cardiovasc Res, 2006. **71**(2): p. 310-21.
302. Lancel, S., et al., *Oxidative posttranslational modifications mediate decreased SERCA activity and myocyte dysfunction in Galphaq-overexpressing mice.* Circ Res, 2010. **107**(2): p. 228-32.
303. Donoso, P., et al., *Modulation of cardiac ryanodine receptor activity by ROS and RNS.* Front Biosci. **16**: p. 553-67.
304. Dong, Z., et al., *Calcium in cell injury and death.* Annu Rev Pathol, 2006. **1**: p. 405-34.
305. Arieli, R. and E. Nevo, *Hypoxic survival differs between two mole rat species (Spalax ehrenbergi) of humid and arid habitats.* Comp Biochem Physiol A Comp Physiol, 1991. **100**(3): p. 543-5.
306. Nevo, E., *Mosaic evolution of subterranean mammals : regression, progression, and global convergence*1999, Oxford: Oxford University Press. xxvi, 413 p., [14] p. of plates.
307. Widmer, H.R., et al., *Working underground: respiratory adaptations in the blind mole rat.* Proc Natl Acad Sci U S A, 1997. **94**(5): p. 2062-7.

308. Edoute, Y., R. Arieli, and E. Nevo, *Evidence for improved myocardial oxygen delivery and function during hypoxia in the mole rat.* J Comp Physiol B, 1988. **158**(5): p. 575-82.
309. Arieli, R. and A. Ar, *Heart rate response of the mole rat (Spalax Ehrenbergi) in hypercapnic, hypoxc, and cold conditions.* Physiol Zool, 1981. **54**(1): p. 14-21.
310. Farrell, A.P., *Tribute to P. L. Lutz: a message from the heart--why hypoxic bradycardia in fishes?* J Exp Biol, 2007. **210**(Pt 10): p. 1715-25.
311. McNeill, B. and S.F. Perry, *The interactive effects of hypoxia and nitric oxide on catecholamine secretion in rainbow trout (Oncorhynchus mykiss).* J Exp Biol, 2006. **209**(Pt 21): p. 4214-23.
312. Flogel, U., A. Fago, and T. Rassaf, *Keeping the heart in balance: the functional interactions of myoglobin with nitrogen oxides.* J Exp Biol, 2010. **213**(Pt 16): p. 2726-33.

Manuscripts & Abstracts

Manuscript 1:
S. Yakushev, M. Band, M. Tissot van Patot, M. Gassmann, A. Avivi, A. Bogdanova
"Cross-talk between S-nitrosylation and S-glutathionylation in control of the Na,K-ATPase regulation in hypoxic heart", Am J Physiol Heart Circ Physiol. 2012 Sep 14. [Epub ahead of print], Submitted 22 February 2012; accepted in final form 29 August 2012

Manuscript 2:
Petrushanko I., Yakushev S., Mitkevich V., Kamanina Y., Ziganshin R., Meng Xian Yu, Anashkina A., Makhro A., Lopina O., Gassmann M, Makarov A., Bogdanova A.
"Catalytic subunit S-glutathionylation of the Na,K-ATPase as a determinant of the enzyme oxygen-sensitivity", J Biol Chem. 2012 Sep 14;287(38):32195-205. Epub 2012 Jul 13.

Manuscript 3:
Komniski M., Yakushev S., Bogdanov N., Gassmann M., Bogdanova A.
"Interventricular heterogeneity in rat heart responses to hypoxia: the tuning of glucose metabolism, ion gradients, and function", Am J Physiol Heart Circ Physiol. 2011, 300(5):H1645-52

Abstract 1:
Bogdanova A., Vogel J., Yakushev S., Segato Komniski M., Makhro A., Bogdanov N., Gassmann M.
"Hypoxic heart: be a trout, not a rat", 4th CBP Meeting in Africa: MARA 2008, Molecules to Migration: The Pressures of Life

Manuscript 1

S. Yakushev, M. Band, M. Tissot van Patot, M. Gassmann, A. Avivi, A. Bogdanova
"Cross-talk between S-nitrosylation and S-glutathionylation in control of the Na,K-ATPase regulation in hypoxic heart", Am J Physiol Heart Circ Physiol. 2012 Sep 14. [Epub ahead of print], Submitted 22 February 2012; accepted in final form 29 August 2012

Am J Physiol Heart Circ Physiol 303: H000–H000, 2012.
First published September 14, 2012; doi:10.1152/ajpheart.00145.2012.

Cross-talk between S-nitrosylation and S-glutathionylation in control of the Na,K-ATPase regulation in hypoxic heart

Sergej Yakushev,[1] Mark Band,[3] Martha Tissot van Patot,[1] Max Gassmann,[1] Aaron Avivi,[2]* and Anna Bogdanova[1]*

[1]*Institute of Veterinary Physiology, Vetsuisse Department and Zurich Center for Integrative Human Physiology (ZIHP), University of Zurich, Zurich, Switzerland;* [2]*Laboratory of Molecular Evolution of Animals Institute of Evolution, University of Haifa, Haifa, Israel; and* [3]*Functional Genomics Unit, Roy J. Carver Biotechnology Center, University of Illinois at Urban-Champaign, Urbana, Illinois*

Submitted 22 February 2012; accepted in final form 29 August 2012

Yakushev S, Band M, van Patot MT, Gassmann M, Avivi A, Bogdanova A. Cross-talk between S-nitrosylation and S-glutathionylation in control of the Na,K-ATPase regulation in hypoxic heart. *Am J Physiol Heart Circ Physiol* 303: H000–H000, 2012. First published September 14, 2012; doi:10.1152/ajpheart.00145.2012.—Oxygen-induced regulation of Na,K-ATPase was studied in rat myocardium. In rat heart, Na,K-ATPase responded to hypoxia with a dose-dependent inhibition in hydrolytic activity. Inhibition of Na,K-ATPase in hypoxic rat heart was associated with decrease in nitric oxide (NO) production and progressive oxidative stress. Accumulation of oxidized glutathione (GSSG) and decrease in NO availability in hypoxic rat heart were followed by a decrease in S-nitrosylation and upregulation of S-glutathionylation of the catalytic α-subunit of the Na,K-ATPase. Induction of S-glutathionylation of the α-subunit by treatment of tissue homogenate with GSSG resulted in complete inhibition of the enzyme in rat a myocardial tissue homogenate. Inhibitory effect of GSSG in rat sarcolemma could be significantly decreased upon activation of NO synthases. We have further tested whether oxidative stress and suppression of the Na,K-ATPase activity are observed in hypoxic heart of two subterranean hypoxia-tolerant blind mole species (*Spalax galili* and *Spalax judaei*). In both hypoxia-tolerant Spalax species activity of the enzyme and tissue redox state were maintained under hypoxic conditions. However, localization of cysteines within the catalytic subunit of the Na,K-ATPase was preserved and induction of S-glutathionylation by GSSG in tissue homogenate inhibited the Spalax ATPase as efficiently as in rat heart. The obtained data indicate that oxygen-induced regulation of the Na,K-ATPase in the heart is mediated by a switch between S-glutathionylation and S-nitrosylation of the regulatory thiol groups localized at the catalytic subunit of the enzyme.

Na,K-ATPase; heart; hypoxia; S-nitrosylation; S-glutathionylation; redox stat; adaptation

LOCAL OR GLOBAL, HYPOXIA CAUSES acute changes in the myocardial function. Hypoxic responses include adjustments of cardiac output mediated by vagal control, humoral factors, and by autonomous heart oxygen sensors. At the cellular level, these responses are mirrored by coordinated regulation of electric, mechanical, and metabolic processes. Thereby decrease in energy demand is achieved to match the changes in ATP supply (19).

Oxygen-induced regulation of the Na,K-ATPase activity in cardiomyocytes is of particular importance for successful adaptation to hypoxia. Responsible for about 20% of total ATP expenditure in the heart (51), this enzyme sustains the transmembrane Na^+/K^+ gradients that are used for action potential generation. Furthermore, Na,K-ATPase actively participates in regulation of contractile force as it is functionally coupled to the Na^+/Ca^{2+} exchanger (57, 62). Inhibitors of Na,K-ATPase, known as cardiac glycosides, have been used to treat congestive heart failure for over 200 years (50). Suppression of the Na,K-ATPase activity reported in hypoxic mammalian heart is a result of several converging processes at systemic, organ, and cellular levels. Systemic hypoxia stimulates release of endogenous inhibitors of Na,K-ATPase, ouabain-like factors, into the circulation (14). Hypoxia-induced ATP depletion may also contribute to enzyme inactivation at later stages. However, induction of hypoxic response of Na,K-ATPase occurs long before intracellular ATP drops to the submillimolar levels, which may result in shortage of substrate supply (23, 29, 64). Indirect evidence suggests that the enzyme responds not to the changes in O_2 availability but to resulting shifts in the tissue redox state and nitric oxide (NO) production (10, 11, 47). Labile cytosolic inhibitory factor causing the enzyme inactivation in ischemic rat heart was reported to be redox sensitive (23). Apart from hypoxia or ischemia, loading of cells with reduced glutathione or using glutahtione depleting agents was shown to cause alterations in Na,K-ATPase activity (45). Accumulating evidence links hypoxia-induced changes in Na,K-ATPase function to the changes in NO production (9, 20, 44). In ischemic myocardium Na,K-ATPase activity could be rescued by NO donors (61). Na,K-ATPase in the hearts of transgenic mice lacking NO synthases ($eNOS^{-/-}$, nNOS, and a double eNOS-nNOS knockout animals) is suppressed (63).

These single observations do not provide a molecular mechanism of redox- or oxygen-induced regulation of the enzyme until more recently. Oxidative thiol modifications (S-nitrosylation and S-glutathionylation) of Cys46 in the β-subunit of Na,K-ATPase were recently reported to cause a 20% decrease in the enzyme activity upon exposure of isolated cardiomyocytes to hypoxia (8, 20). S-nitrosylation was shown to be necessary as an intermediate step in the induction of regulatory S-glutathionylation of the regulatory β-subunit of the enzyme. However, inhibition of the Na,K-ATPase in ischemic heart was much more extensive than that shown in cardiomyocytes exposed to low oxygen in which S-glutathionylation of the β-subunit was shown (23, 61).

At present there are no reports in the literature on hypoxia-induced reversible thiol modifications in the catalytic α-subunit. The rodent Na,K-ATPase α-subunit contains over 20 cysteine

* A. Avivi and A. Bogdanova contributed equally to this article.
Address for reprint requests and other correspondence: A. Bogdanova, Institute of Veterinary Physiology, Vetsuisse Faculty, Univ. of Zurich, Winterthurerstrasse 260 CH-8057 Zurich, Switzerland (e-mail: annab@access.uzh.ch).

residues, most of which are localized in cytosolic loops forming nucleotide- and ion-binding sites (10). Localization of cysteine residues within the protein sequence is largely conserved, suggesting that they play an important role in enzyme function. Our recent findings indicated that S-glutathionylation of the cysteine residues of large and small cytosolic loops of the Na,K-ATPase α-subunit occurs when the isolated enzyme is incubated with oxidized glutathione (46). Interaction of glutathione with several cysteine residues of the large cytosolic loop occurs only under conditions of mild ATP deprivation. Upon S-glutathionylation of these few cysteines, the ATP binding site of the enzyme becomes inaccessible for ATP and the enzyme is completely inhibited (46). Deglutathionylation occurring in the presence of glutaredoxin and NADPH is associated with restoration of the enzyme activity (46).

The present study was designed to explore the possible interplay between S-nitrosylation and S-glutathionylation in control of function of Na,K-ATPase in hypoxic myocardium and its role in the adaptation success of rodents to oxygen deprivation. We have monitored the changes in enzyme activity in rat heart as a function of oxygen availability and related alterations in phospholemman phosphorylation state, and S-nitrosylation and S-glutathionylation of cysteine residues in the Na,K-ATPase catalytic subunit. The shifts in tissue reduced and oxidized glutathione and nitrite production associated with reversible thiol modifications were assessed. Furthermore, we have compared oxygen-sensitivity of Na,K-ATPase in the myocardium of hypoxia-sensitive Wistar rats (*Rattus norvegicus*) with that of two species of the blind subterranean mole rat (*Spalax ehrenbergi*): *Spalax galili* and *Spalax judaei*. These subterranean rodents share suborder (Myomorpha) with rats, but show profound hypoxia-tolerance (41, 42).

Our results revealed that Na,K-ATPase in Wistar rat myocardium shows a profound sensitivity to oxygen availability. A switch from S-nitrosylation to S-glutathonylation of cysteine residues within the catalytic α-subunit plays a key role in oxygen-induced regulation of the Na,K-ATPase in Wistar rat heart. In parallel, hypoxia induces a shift in phosphorylation of phospholemman. Na,K-ATPase function in *Spalax* myocardium is preserved during hypoxic exposure. Lack of inhibitory response of Na,K-ATPase to hypoxia in *Spalax* heart was associated with the absence of hypoxia-induced changes is redox state.

MATERIALS AND METHODS

Rat myocardial tissue isolation and handling. Animal handling and experimentation was approved by the Swiss Federal Veterinary Office and performed in accordance with Swiss animal protection laws and institutional guidelines that comply with those of the Institute for Laboratory Animal Research.

Heparin (100 μl of 10,000 units/ml heparin; Braun, Grenchen, Switzerland) was injected into the caudal vena cava of anesthetized (3% isoflurane in a 1:1 mixture of O_2 and N_2O) Wistar male rats (300–400 g) purchased from Janvier (Le Genest, St. Isle, France) via abdominal incision, and 8–10 ml of blood were collected. The heart was excised and cooled down in heparin-containing isotonic phosphate buffer (in mM) containing 120 NaCl, 25 $NaHCO_3$, 1 $CaCl_2$, 0.15 $MgCl_2$, 10 glucose, 0.1 L-arginine, 10 Tris·HCl (pH 7.4).

A perfusion circuit including a hollow fiber mini-oxygenator was filled with the collected heparinized blood, and the heart was mounted on a cannulae and perfused via aorta with autologous blood equilibrated with humidified gas phase (20% O_2, 5% CO_2, and 75% N_2 PanGas; Basel, Switzerland; 37°C) for 20 min (29). After the restitution period, oxygen concentration in gas phase was retained at 20% (normoxia) or readjusted to 15%, 10%, 5%, and 3% depending on scientific protocol and perfused for 40 min. Glucose consumption by erythrocytes and water loss from the organ chamber were compensated for by supplementation of 1.1 mmol/l glucose every 20 min.

Aqueous solution of L-NAME (to a final concentration 300 μM) was administrated to blood in the perfusion circuit after the restitution period, according to protocol.

Heart rate and ECG (aVL projection) were continuously recorded with a Heart Rate Module (Hugo Sachs Elektronik-Harvard Apparatus, March-Hugstetten, Germany) connected to an analog-digital transducer (Power Lab; ADInstruments, Oxfordshire, UK) and LabChart 7 software (ADInstruments, Oxfordshire, UK). ECG recordings were then analyzed using LabChart Pro software (ADInstruments, Oxfordshire, UK).

Aliquots of blood (100 μl) were collected at the end of the perfusion for plasma nitrite and nitrate analysis.

At the end of the blood perfusion protocol, the heart was chilled and perfused with ice-cold sucrose-buffer solution containing 300 mM sucrose in 20 mM of a HEPES·Tris buffer (pH 7.4 at 0°C) to remove blood from coronary vessels. Ventricular tissue was frozen in liquid nitrogen and later analyzed for reduced (GSH) and oxidized (GSSG) glutathione content, Na,K-ATPase activity, and used for preparation of sarcolemmal fraction, immunoblotting and biotin-switch.

Spalax myocardial tissue isolation and handling. Superspecies *Spalax ehrenbergi* includes four distinct biological species and is located in Israel (42). The most extreme differences in ecological conditions exist between regions inhabited by *Spalax galili* in the northern cool-humid Upper Galilee Mountains, and *Spalax judaei* in the southern warm-dry xeric regions of Israel. Differences in environment are reflected in differential adaptations to hypoxia. An improved hypoxic adaptation of *S. galili* has been established with higher hematocrit and hemoglobin levels as compared with *S. judaei* (3, 4). In laboratory experiments the lowest levels of oxygen concentrations tolerated by *S. galili* (2.6 ± 0.4%) were significantly lower than *S. judaei* (3.7 ± 0.9%) (5). Using field measurements, we recorded 6% O_2 and 7% CO_2 in *S. ehrenbergi* burrows in flooded heavy soils during the Mediterranean rainy season (55).

All animal handling protocols were approved by the Haifa University Committee for Ethics on Animal Subject Research, permit No. 193/10, and approved by the Israel Ministry of Health. Six animals of *S. galili* and six further animals of *S. judaei* of both sexes 2–4 years old were captured in the field and housed under ambient conditions in individual cages. Three out of six animals of each *Spalax* species were randomly assigned into the hypoxic group. These animals were placed in a 70 × 70 × 50 cm chamber divided into separate cells flushed with gas mixture at 5 l/min. Oxygen concentration in the gas mixture was gradually decreased for 45–60 min and finally adjusted at 6% O_2. This oxygen concentration was chosen as the lowest oxygen levels recorded in *S. ehrenbergi* tunnels after rainstorms (55). Animals were exposed to hypoxia for 6 h. Animals in normoxic groups were exposed to ambient air. After hypoxic exposure the animals were administered Ketaset CIII at 5 mg/kg of body weight and heart muscle tissue was harvested and immediately frozen in liquid nitrogen.

Nitrite assessment in blood plasma. One of the widely used markers for NO production in biological systems is nitrite (NO_2^-) concentration because its accumulation is proportional to the NO production (28). Blood aliquots collected during perfusion were pelleted by centrifugation (16,000 *g*), and the supernatant (blood plasma) was collected. Nitrate was reduced to nitrite using Cd coated with Cu and (NO_2^- + NO_3^-) assessed by a chemiluminiscence detector CLD 88 (Eco Medics AG, Switzerland) as described elsewhere (39). Briefly, a sample aliquot was deproteinized by addition of methanol (100%) and centrifuged (13,200 *g*, 10 min). Supernatant (50 μl) was injected into the preheated (65°C) reaction chamber containing acidic triiodide (I_3^-) reagent. The reagent was prepared fresh before the

tapraid4/zh4-ahea/zh4-ahea/zh402212/zh40572d12z | xppws | S=5 | 10/13/12 | 16:43 | MS: H-00145-2012 | Ini: 11/BYF/

EQ:1 Table 1. *Heart performance as a function of O_2 concentration and treatment with 300 μM L-NAME*

	O_2 Concentration, %						
	20	15	10	5	3	5 + L-NAME	20 + L-NAME
Total amount of analyzed hearts	15	5	5	15	5	10	10
Number of hearts with bradycardia	0	0	0	12	5	10	0
Beginning of bradycardia, min	—	—	—	Between 10 and 13 min	Between 5 and 13 min	Between 1 and 5 min	—
Number of hearts with T-wave inversion	—	1	1	15	5	10	0
Beginning of T-wave inversion, min	—	35	32	Between 20 and 25 min	Between 20 and 23 min	Between 5 and 20 min	—
Number of arrhythmic hearts	0	0	0	7	5	10	2
Beginning of arrhythmia, min	—	—	—	Between 25 and 30 min	Between 19 and 28 min	Between 15 and 30 min	32

Data are means of 5-10 independent recordings ± SD. Time after restitution period until beginning of the bradycardia, arrhythmia, and T-wave inversion was calculated from ECG recordings with LabChart 7.0 software with ECG analysis module (ADInstruments). l-NAME, N^G-nitro-L-arginine methyl ester. Data not sufficient for statistical analysis.

measurements (1.65 g KI, 0.57 g I_2, 15 ml H_2O, 200 ml glacial CH_3COOH). The reaction chamber was purged with helium and released NO was detected using CLD-88 analyzer (ECO MEDICS, Durnten, Switzerland). The signal was processed using PowerChrom 280 system (eDAQ Pty; Spechbach, Germany).

GSH and GSSG levels in myocardium. Tissue GSH and GSSG were assessed in blood-free ventricular tissue preparations. Frozen ventricular fragments (0.1 g) were homogenized on ice in KCl-MOPS buffer (100 mM KCl and 10 mM MOPS, pH 7.4) and deproteinized with 5% trichloracetic acid. GSH and GSSG were assessed in the protein-free supernatant using Ellmann's reagent and normalized to sample wet weight (58). Briefly, GSH concentration was determined in deproteinized samples using 5,5′-dithiobis (2-nitrobenzoic acid) (Ellman's reagent). Optical density of the colored complex was measured photometrically at 412 nm. Simultaneously, aliquots from the same samples were incubated in the presence of glutathione reductase and NADPH for reduction of GSSG to GSH, and total glutathione levels (GSH + GSSG) were determined. The half-cell reduction potential (E_{hc}) was then calculated for GSH/GSSG couple (54).

Isolation of sarcolemmal fraction from rat myocardium. Sarcolemmal fraction of rat myocardium was performed as described elsewhere (27). Briefly, the ventricle tissue samples were washed, minced, and homogenized in 0.6 M sucrose and 10 mM imidazole-HCl (pH 7.0, 3.5 ml/g tissue) with a Polytron PT-3000 (9,000 rpm). The resulting homogenate was centrifuged at 12,000 *g* for 30 min, and the pellet was discarded. After dilution (5 ml/g tissue) with 140 mM KCl-MOPS buffer containing 140 mM KCl and 10 mM MOPS (pH 7.4), the supernatant was centrifuged (95,000 *g*, 60 min). The resulting pellet was resuspended in the KCl-MOPS buffer and layered over a 30% sucrose solution, 0.3 M KCl with 50 mM $Na_4P_20_7$ in 0.1 M Tris·HCl (pH 8.3). After centrifugation (95,000 *g*, 90 min), the band at the sucrose-buffer interface was taken and diluted with 3 vol of KCl-MOPS solution. A final centrifugation (95,000 *g*, 30 min) resulted in a pellet rich in sarcolemma. The pellet was resuspended in KCl-MOPS buffer.

Protein concentration was assayed in all experiments by the Lowry method (34).

Na,K-ATPase activity. Ouabain-sensitive (1 mM) inorganic phosphate production (49) was used to assess Na,K-ATPase hydrolytic activity. Activity of the enzyme was measured in the presence of saturating concentrations of ligands and substrate of (mM) 130 NaCl, 20 KCl, 3 $MgCl_2$, 3 ATP, and 30 imidazole (pH 7.30 at 37°C) as described elsewhere (45). Briefly, protein samples were mixed with media containing (in mM) 130 NaCl, 20 KCl, 3 $MgCl_2$, and 30 ATP with or without 1 ouabain according to the experimental protocol at 37°C for 10 min. The reaction was then stopped by ice-cold 4% formaldehyde in 1.3 M sodium acetate buffer (pH 4.3). Accumulated inorganic phosphate was determined using the Rathbun-Betlach method (49).

In vitro treatment of isolated sarcolemmal fraction with oxidized glutathione. The inhibitory action of GSSG on the Na,K-ATPase activity was assessed on sarcolemal fraction and ventricular homogenates of all species used in this study. The sarcolemmal membrane fraction and ventricular tissue homogenate were exposed to 300 μM GSSG for 10 min (37°C). Na,K-ATPase activity was then assessed as described above.

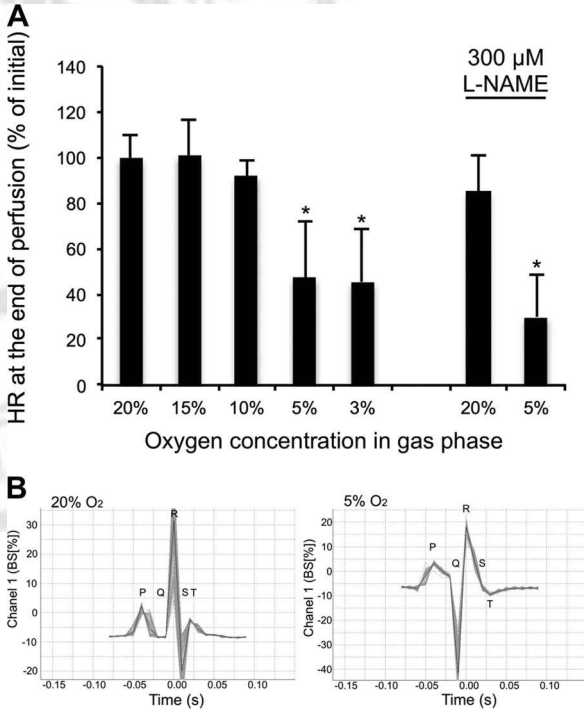

Fig. 1. A Oxygen-sensitivity of rat heart rate. Changes in autonomous heart rate of rat hearts after 40 min of perfusion with blood equilibrated with 20–3% O2 in gas phase in the presence or absence of 300 μM L-NAME. Values were normalized to those at the end of 20 min of restitution during which the hearts were perfused with fully oxygenated blood (20% O2). Calculated from ECG recordings with LabChart 7.0 software with ECG analysis module (ADInstruments). Values are means ± SD for 6–15 independent experiments. * denotes $P < 0.05$ when compared with 20% O2. *B* Example of the T-wave inversion. Changes in T-wave amplitude in the ECG recordings (with LabChart 7.0 software with ECG analysis module, ADInstruments) of rat hearts after 30 min of perfusion with blood equilibrated with 20% (*A*) and 5% (*B*) O2 in gas phase. Figure represents the shape of the PQRST complex, made as average of 100 recorded PQRST complexes of single heart starting from the 40th minute of perfusion with blood equilibrated with 20 and 5% O2 in gas phase.

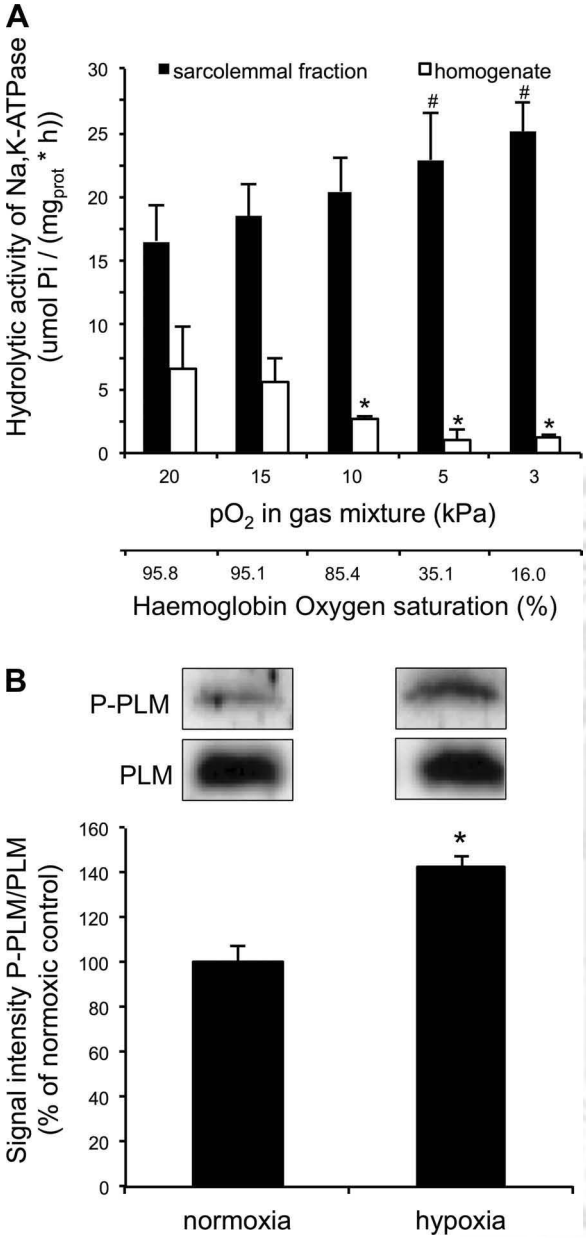

Fig. 2. The effect of different concentrations of oxygen (3–20%) in gas mixture at perfusion on hydrolytic activity of Na,K-ATPase in ventricular tissue homogenate (open bars) and ventricular tissue sarcolemmal fraction (black bars) of isolated blood perfused hearts. Rat hearts were subjected to 40 min perfusion with autologous blood, corresponding haemoglobin oxygen saturation is indicated on the axes below the plot. Decrease in oxygen supply results in gradual inhibition of Na,K-ATPase hydrolytic activity in ventricular homogenate and gradual increase in hydrolytic activity in sarcolemmal fraction. Bars represent means ± SD; $n = 10$ animals. $^{*}P < 0.05$ vs. 20% O_2 homogenate (one-way ANOVA); $^{**}P < 0.01$ vs. 20% O_2 homogenate (one-way ANOVA); $\#P < 0.05$ vs. 20% oxygen sarcolemmal fraction (one-way ANOVA). *B*: Changes in phosphorylation of phospholemman at Ser68 induced by decrease in oxygenation in gas phase from 20 to 5 kPa. Data are means of 5 experiments ± SD * denotes $P < 0.05$ in Students unpaired t-Test.

In vitro activation of nitric oxide synthase. Substrates and cofactors for NOS were administrated to rat sarcolemmal fractions to a final concentration of 0.1 mM L-Arginine, 0.5 mM $CaCl_2$, 10 μg/ml calmoduline, 0.2 mM NADPH, 10 μM biopterin, 5 μM FMN, and 5 μM FAD, and the samples were incubated for 10 min at room temperature. After incubation the sample was used in the Na,K-ATPase activity assay with or without treatment with GSSG as described above. Nitrite accumulation in the incubation medium was used as a marker of NO generation.

Western blot analysis. Tissue homogenates and isolated sarcolemmal fraction from the in vitro studies were separated by 7.5%, 10%, and 12.5% SDS-PAGE with Tris-Glycine (for resolution of high molecular weight proteins) or Tris-Tricine (for resolution of low molecular weight proteins) buffer systems and transferred to Protean BA83 nitrocellulose membranes (Schleicher and Schuell, Dassel, Germany). Protein transfer was controlled by Ponceau red staining. Membranes were blocked for 1 h at room temperature and incubated overnight at 4°C with the appropriate primary antibodies.

Primary antibodies kindly provided by M. J. Shattok and W. Fuller (35) were used to assess Ser68 phosphorylation of the FXYD1 subunit of Na,K-ATPase (phospholemman) and determine total and phosphorylated forms. The S-glutathionylation state of the α_1-subunits of Na,K-ATPase in sarcolemmal preparations, as well as in crude ventricular homogenates, was assessed using monoclonal anti-glutathione antibody (Chemicon Millipore, MAB5310). The membranes were

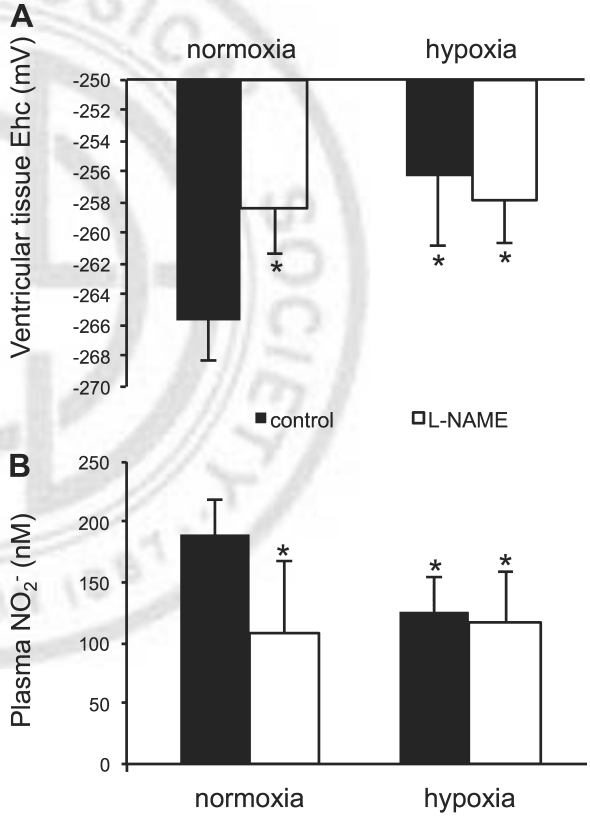

Fig. 3. Oxygen-sensitivity of ventricular tissue redox state and plasma NO_2^-. *A*: The effect of hypoxia (5% O_2) and introduction of 300mM L-NAME in to perfusion blood on ventricular half-cell redox potential Ehc for the GSH/GSSG couple that was calculated from the following equation: $E_{hc}(GSH{:}GSSG) = -240 - \frac{59.55}{2}\log\frac{[GSH]^2}{[GSSG]}$ Decrease in oxygen supply as well as treatment with 300 μM L-NAME resulted in the shift of the redox state towards more oxidized state. The effect of combined action of hypoxia and L-NAME was equal to the effect of both separately. Bars represent means ± SD; $n = 4$ animals. $^{*}P < 0.05$ vs. 20% oxygen homogenate (one-way ANOVA); $\#P < 0.05$ vs. 20% oxygen homogenate (one-way ANOVA) *B*: The effect of hypoxia (5% O_2) and introduction of 300mM L-NAME in to perfusion blood on content of nitrite in perfusion blood plasma. Blood samples were collected 30 min after the onset of perfusion. Bars represent means ± SD; $n = 4$ animals. $^{*}P < 0.05$ vs. normoxic (20% O_2) homogenate (one-way ANOVA); $\#P < 0.05$ vs. normoxic (20% O_2) homogenate (one-way ANOVA).

Table 2. *Absolute values of GSH and GSSG content in ventricular homogenates of rat and Spalax heart*

Species, Condition	GSH, μmol/mg	GSSG μmol/mg
Rat, *Rattus norvegicus*		
Normoxia	1.382 ± 0.005	0.263 ± 0.049
Normoxia L-NAME	1.221 ± 0.053*	0.358 ± 0.075
Hypoxia	1.144 ± 0.103*	0.321 ± 0.052
Hypoxia L-NAME	1.196 ± 0.083*	0.358 ± 0.044
Mole rat *Spalax judaei*		
Normoxia	1.412 ± 0.109	0.028 ± 0.014*
Hypoxia	1.294 ± 0.143	0.011 ± 0.096*
Mole rat, *Spalax galili*		
Normoxia	1.232 ± 0.109	0.023 ± 0.038*
Hypoxia	1.263 ± 0.147	0.040 ± 0.074*

Values are means ± SD. *$P < 0.05$ in unpaired *t*-test compared to the levels in normoxic rat heart.

then stripped and mouse monoclonal anti-Na,K-ATPase α_1-antibody clone C464–6 (Upstate Millipore) were applied for detection of the total amount of α1 subunit. Appropriate horseradish peroxidase-conjugated secondary antibodies were applied and enhanced chemiluminescent detection system (Fujifilm LAS-3000 System; Fujifilm Life Science) was used for detection. Antinitotyrosine antobodies (Antinitrotyrosine, clone 1A6, HRP conjugate from Upstate; cat No. 16-207; 1:1,000 dilution) were used to assess tyrosine nitration. As a negative control for the staining nitrocellulose membrane after the transfer was incubated for 1 min (room temperature) in 100 mM $Na_2S_2O_4$ (in 100mM $Na_2B_4O_7$, pH 9). Afterward it was washed and probed with antinitrotyrosine antibody according to the protocol. No staining was detected after $Na_2S_2O_4$ pretreatment indicating that the signal from the antibodies was specific for nitro-tyrosine. ImageJ software was used for quantification of the recorded signals. Total-actin (Sigma; A2066) was used as a loading control.

Biotin-switch. S-nitrosylation of the α_1-subunit of Na,K-ATPase in the rat ventricular homogenate was assessed using the S-Nitrosylated Protein Detection Kit (Cayman Chemical Ann Arbor, MI). Briefly, in the first step free thiols are blocked by incubation with the thiol-specific methylthiolating agent methyl methanethiosulfonate (MMTS). After block of free thiols, nitrosothiol bonds are selectively decomposed with ascorbate, which results in the reduction of nitrosothiols to thiols. In the last step, the newly formed thiols are reacted with N-[6-(biotinamido)hexyl]-3′-(2′-pyridyldithio)propionamide (biotin-HPDP), a sulfhydryl-specific biotinylating reagent. Labeled proteins can were detected by immunoblotting with antibiotin antibodies, after SDS-PAGE (26). In parallel, we have used anti-S-nitrosocysteine antibody [S-nitroso-Cys (SNO-Cys), Alpha Diagnostic, cat No. NISC11-A, dilution 1:1,000] and were able to reproduce the findings obtained using biotin switch assay.

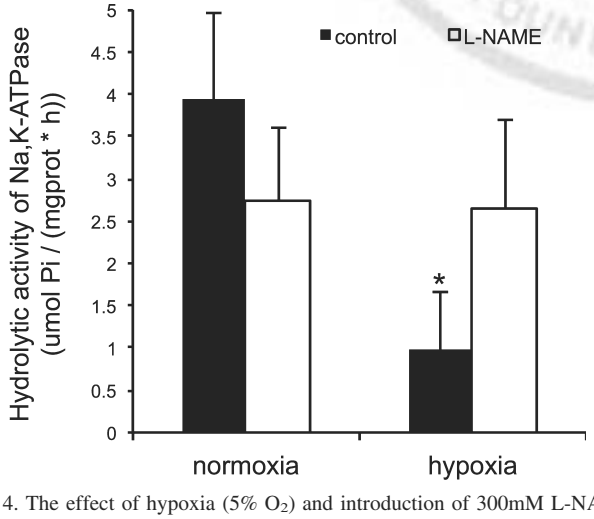

Fig. 4. The effect of hypoxia (5% O_2) and introduction of 300mM L-NAME in to perfusion blood on hydrolytic activity of Na,K-ATPase in ventricular tissue homogenate. Inhibition of NO production under hypoxic conditions results in significant increase of hydrolytic activity of Na,K-ATPase. Bars represent means ± SD; n = 4 animals. *$P < 0.01$ vs. normoxic (20% O_2) homogenate (1-way ANOVA); #$P < 0.01$ vs. hypoxic (5% O_2) homogenate (one-way ANOVA).

RESULTS

Oxygen-dependence of Na,K-ATPase function. Perfusion of isolated rat heart with autologous blood equilibrated with 20%, 15%, 10%, 5%, or 3% oxygen in gas phase for 45 min resulted in decrease of autonomous heart rate to 42 ± 4% of the normoxic value of 254 ± 50 beats/min (n = 16). The time course of the response is reflected by a decrease in heart rate when pO_2 in the gas phase was decreased from 20% to 5% or 3% (Table 1 and Fig. 1*A*). Furthermore, the ECG showed inversion of the T wave (Fig. 1*B*) characteristic of ischemic myocardium in hearts perfused with blood equilibrated to 5% or 3% O_2 (30). Hypoxia-induced bradycardia was associated

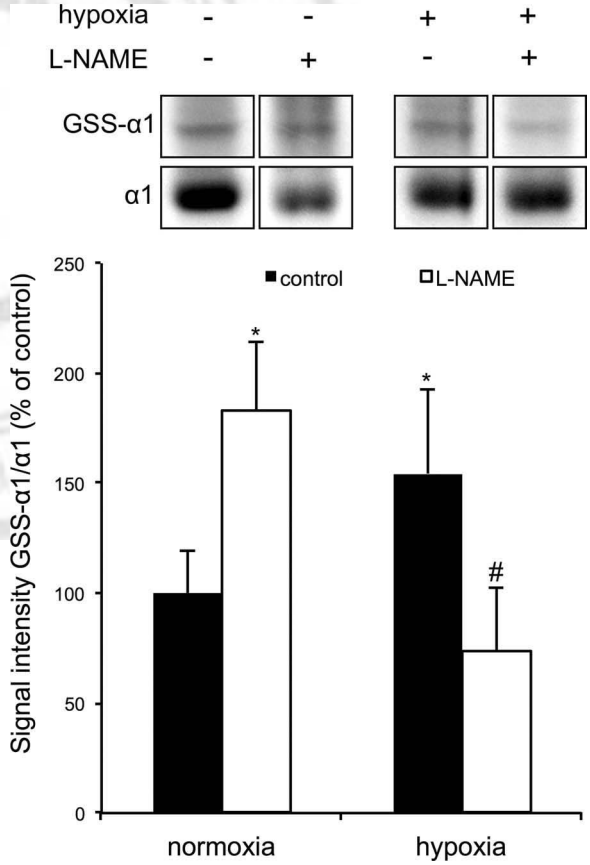

Fig. 5. S-glutathionylation of thiols in the Na,K-ATPase α1 subunit in rat heart exposed to hypoxia (5% O_2) or normoxia (20% O_2) with (open bars) an without (filled bars) 300 μM L-NAME. The signal intensity for the S-glutathionylated thiols in the α1 subunit in homogenate was normalized to that of α1 abundance (see the original immunoblotting readouts above the quantification bar chart). Data are means of 8 independent experiments ±SD. * denotes $P < 0.05$ when compared with normoxic control and # indicates $P < 0.05$ when compared with the corresponding hypoxic control in the absence of L-NAME (one-way ANOVA).

tapraid4/zh4-ahea/zh4-ahea/zh402212/zh40572d12z | xppws | S=5 | 10/13/12 | 16:43 | MS: H-00145-2012 | Ini: 11/BYF/

with arrhythmia in some of the hearts. These responses developed within 1–20 min after decrease of hemoglobin oxygen saturation.

These changes in myocardial function occurred along with a dose-dependent decrease in activity of Na,K-ATPase in ventricular tissue homogenates from 6.4 ± 3.3 umol Pi/(mg_{prot}·h) in normoxic myocardium to 1.25 ± 0.18 umol Pi/(mg_{prot}·h) in tissue exposed to 3% O_2 (hemoglobin oxygen saturation SO_2 of 16%; Fig. 2*A*).

Decrease in oxygen levels in gas phase to which the blood was equilibrated from 20% to 10%, and the resulting decrease in hemoglobin oxygen saturation SO_2 from 95.8% to 85% was associated with a twofold decrease in the activity of Na,K-ATPase.

Similar profound inactivation of the Na,K-ATPase was previously reported to occur in ventricular tissue homogenates prepared from rat heart exposed to no-flow ischemia (22). Inhibition of the enzyme in ischemic tissue homogenate was associated with an increase in Na,K-ATPase activity in sarcolemmal membranes. The stimulatory effect of ischemia at the sarcolemmal membrane level was caused by phosphorylation of the regulatory FXYD1 subunit of the Na,K-ATPase, phospholemman at Ser68 (22). Similar to that in ischemic myocardium, in which hypoxia occurred along with acidosis and aglycemia, exposure of rat heart to hypoxia alone was also associated with phosphorylation of phospholemman (Fig. 2*B*) and with a dose-dependent increase in Na,K-ATPase activity in sarcolemmal membranes from 16.5 ± 2.7 μmol Pi/(mg_{prot}·h) to 25.0 ± 2.2 μmol Pi/(mg_{prot}·h) (Fig. 2*A*). Mechanisms of activation of the enzyme in sarcolemmal fraction of ischemic heart and the role of phospholemman have been addressed earlier (22). We have therefore concentrated on characterization of the molecular mechanisms behind the inhibitory action of hypoxia on the Na,K-ATPase in ventricular homogenate. Hypoxic conditions for further experiments were defined as perfusion with blood equilibrated with 5% O_2 in gas phase (SO_2 = 35%). Hypoxia-induced changes were related to the values obtained in hearts perfused with oxygen-saturated blood (blood equilibrated with gas phase containing 20% O_2, SO_2 = 95.8%). Exposure of isolated blood-perfused rat heart to hypoxia for 40 min was associated with a sixfold suppression in activity of Na,K-ATPase in ventricular tissue homogenate (Fig. 2*A*).

Redox state, NO production, and function of Na,K-ATPase in hypoxic rat myocardium. We have assessed hypoxia-induced changes in redox state and NO production in isolated

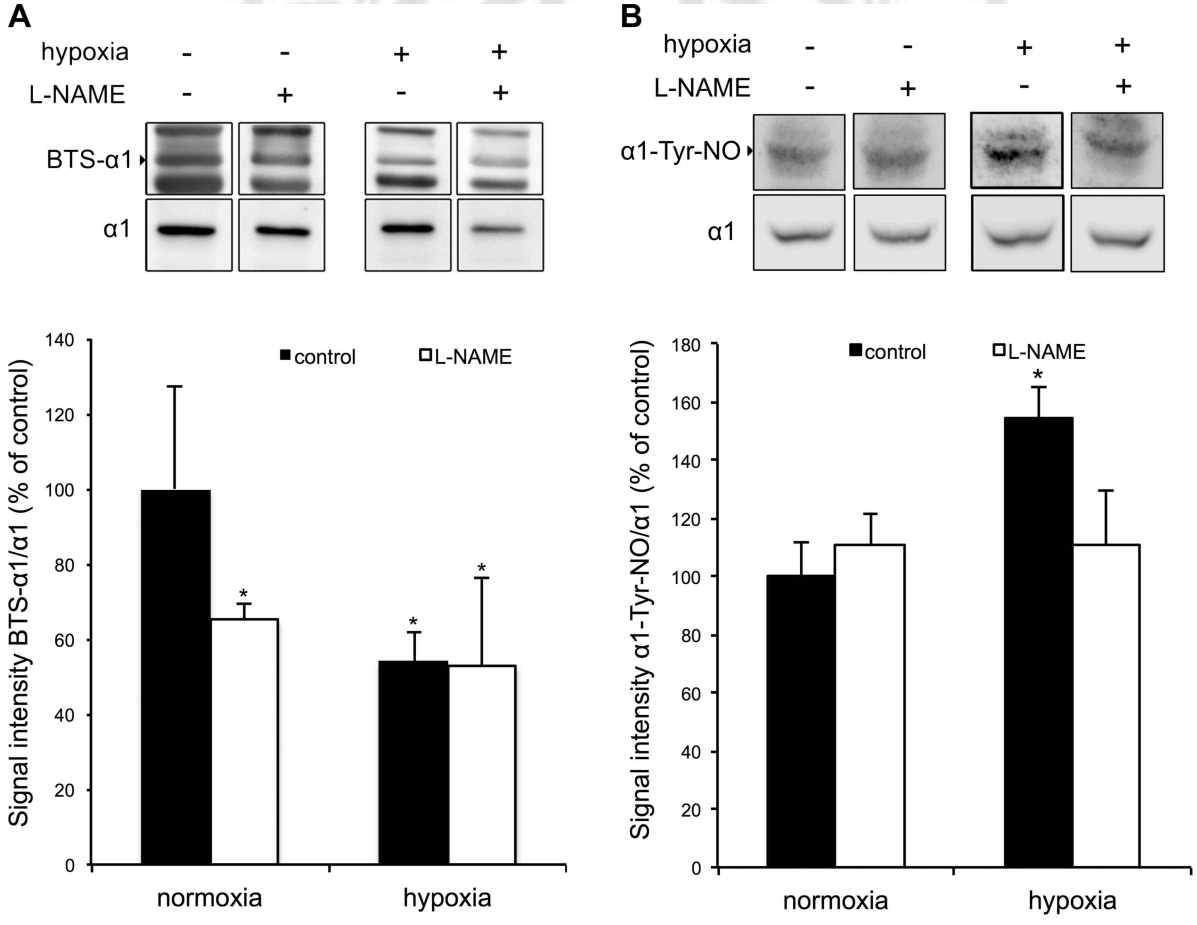

Fig. 6. *A*: S-nitrosylation of thiols in the α1 subunit assessed using biotin switch technique. Original recordings of S-nitrosylated (biotinylated) α1 subunit in heart tissue homogenates exposed to hypoxia and or L-NAME are presented at the top panel whereas quantification of the S-nitrosylation state of the α1 subunit normalized to the abundance of α1 subunit in homogenate is presented at the bottom panel. *B*: Tyrosine nitration of the α1 subunit of the Na,K-ATPase. Normalization has been performed as in A. Data are means of 8 independent experiments ± SD. * denotes $P < 0.05$ when compared to the normoxic non-treated control determined using one-way ANOVA with the Bonferroni post-test.

blood-perfused rat heart. Perfusion of hearts with hypoxic blood for 40 min resulted in a shift in half-cell redox potential for GSH/GSSG couple oxidation and in a decrease in NO_2^- levels reflecting NO production (Fig. 3). Inhibition in nitric oxide synthase (NOS) activity was, to a large extent, the cause of oxidative stress. Perfusion of hearts with normoxic blood containing 300 μM L-NAME induced oxidation of GSH (expressed as E_{hc}, a measure of GSH:GSSG), and no further pro-oxidative effect of hypoxia was observed in L-NAME-treated myocardium (Fig. 3). The changes in actual tissue GSH and GSSG concentrations are presented in Table 2. It appears the onset of bradycardia was elevated in the hypoxic hearts treated with L-NAME, whereas L-NAME had little effect on heart rate in the normoxic hearts (Table 1 and Fig. 1). Exposure to L-NAME induced arrhythmia in some of the hearts even under normoxic conditions (Table 1). Oxygen sensitivity of Na,K-ATPase was lost in hearts perfused with blood containing 300 μM L-NAME, in which the enzyme was preserved under hypoxic conditions (Fig. 4). Taken together these data indicated that, apart of gradual ATP deprivation, hypoxia-induced responses of the Na,K-ATPase were closely associated with the changes in GSSG and NO levels.

Thiol modifications of Na,K-ATPase α-subunit are dependent on hypoxic stress and NO production. We have assessed S-glutathionylation and S-nitrosylation of cysteines in the catalytic α-subunit of the Na,K-ATPase in normoxic and hypoxic myocardium using immunoprecipitation, Western blotting, and Biotin-Switch techniques. Immunoprecipitation was carried out using anti-GSH antibodies and was then followed by Western blotting against α_1 and α_2 isoforms of the catalytic subunit, revealing the presence of both in immunoprecipitate (data not shown).

The presence of S-glutathionylated thiols in the α_1-subunit in crude homogenate prepared from ventricular tissue was confirmed using immunoblotting. Basal S-glutathionylation was detected in normoxic tissue samples (Fig. 5). The number of S-glutathionylated cysteines in the α_1-subunit increased in response to L-NAME treatment under normoxic conditions as well as in response to hypoxia without L-NAME. A combination of hypoxic conditions and L-NAME exposure was not associated with an increase in S-glutathionylation of the α_1-subunit compared with normoxic control.

S-nitrosylation of the α_1-subunit was high in normoxic samples and decreased in response to hypoxia and L-NAME treatment (Fig. 6*A*). Decrease in the number of S-nitrosylated cysteines in the α_1-subunit in the hypoxic heart was accompanied by pronounced increase in nitrated tyrosine residues. Exposure to L-NAME suppressed hypoxia-induced nitrotyrosine formation (Fig. 6*B*).

We have further explored the effect of S-glutathionylation on Na,K-ATPase activity. Exposure of sarcolemmal membranes isolated from normoxic rat heart to 250 μM GSSG-induced S-glutathionylation of the α_1-subunit was associated with a marked suppression of the enzyme hydrolytic activity (Fig. 7). Activation of NO production was observed in suspension of sarcoplasmic reticulum microsomes was induced by supplementation of NOS substrates and coactivators. NO production was monitored as NO_2^- accumulation in the incubation medium. Nitrite accumulation was found to be 0.7 nmol/(μg protein·30 min). Calculations based on the assumption of the 2.5% of cysteine occurrence frequency in mammalian protein

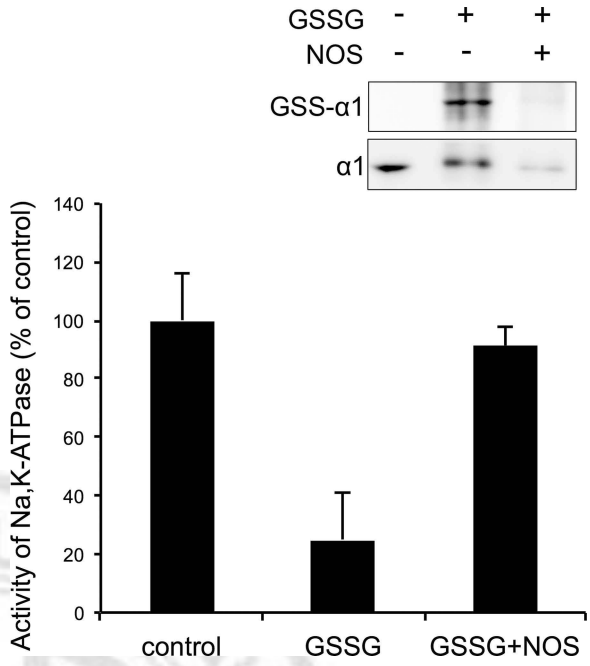

Fig. 7. Induction of S-glutathionylation by treatment of sarcolemmal vesicles isolated from normoxic heart homogenate. Sarcolemmal membranes were exposed to 250 μM GSSG (GSSG) for 10 min at 37°C in the absence or presence of substrates and co-factors of NO syntases (L-arginine, NADPH, FMN, H_2-FAD, BH_4, Ca-calmoduline, GSSG +NOS). S-glutathionylation of the α1 subunit of the Na,K-ATPase and hydrolytic activity of the enzyme were tested after the induction of S-glutathionylation. Data are means of 3 experiments ± SD. * denotes $P < 0.05$ when compared to the non-treated control.

sequences reported earlier (40) and an average molecular weight of an amino acid of 110 g/mol give an estimation of 11 nmol of cysteines in our samples containing 50 μg of protein. The amount of NO transferred to NO_2^- and not bound to protein thiols in a sample containing 50 μg protein is 35 nmol. This amount exceeds the number of potential binding sites by 3.5-fold and suggests that NO produced by microvesicles upon activation of NOSes was sufficient to cause S-nitrosylation of at least some thiol groups. Both S-glutathionylation and inhibition of the enzyme by GSSG was prevented if NOSes were activated at the moment of administration of 250 μM GSSG (Fig. 7).

Lack of oxygen-sensitivity of Na,K-ATPase in spalax heart. The impact of hypoxic exposure on Na,K-ATPase activity in the heart was explored in hypoxia-tolerant *Spalax* genus, *S. galili* and *S. judaei*, blind fossorial mole rats. Whereas normoxic animals were exposed to ambient air, hypoxic individuals were exposed to hypoxic atmosphere containing 6% O_2-94% N_2 for 6 h. Activity of Na,K-ATPase was then assessed in ventricular tissue homogenate. The absolute values of enzyme activity as well as the α_1 abundance in normoxic *Spalax* hearts were decreased by approximately threefold compared with that in Wistar rat (*R. norvegicus*) hearts (Fig. 8). In contrast with that in *R. norvegicus* hearts, Na,K-ATPase in the myocardium of both *Spalax* species was not suppressed in response to hypoxic exposure (Fig. 8).

Is spalax Na,K-ATPase redox-sensitive? We have further tested if the apparent insensitivity of *Spalax* myocardial Na,K-ATPase to hypoxia was stemming from the lack of regulatory cysteine residues, which were present in rat enzyme. To do so,

tapraid4/zh4-ahea/zh4-ahea/zh402212/zh40572d12z | xppws | S=5 | 10/13/12 | 16:43 | MS: H-00145-2012 | Ini: 11/BYF/

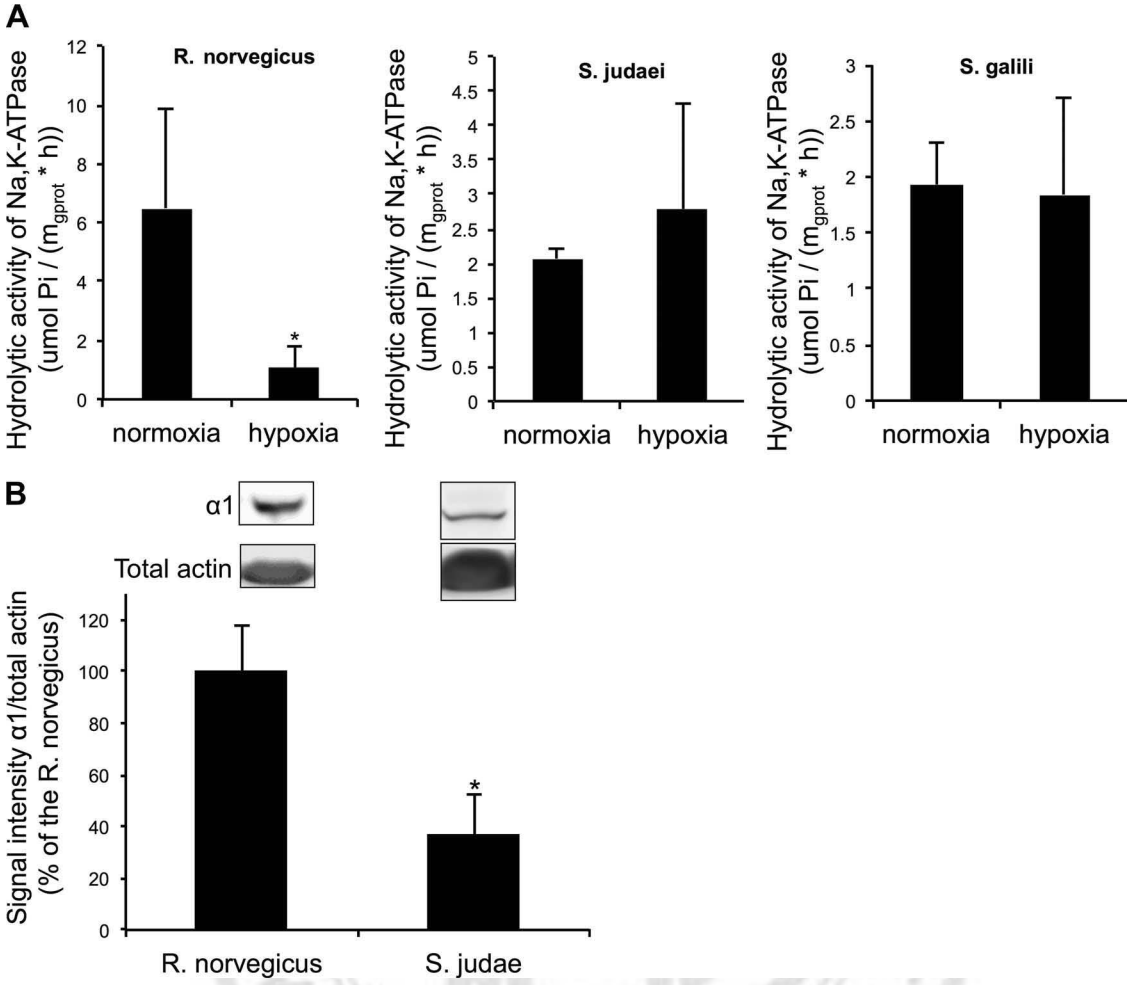

Fig. 8. Na,K-TPase abundance and activity in normoxic and hypoxic rat and *Spalax* hearts. *A*: Hydrolytic activity of the Na,K-ATPase in hypoxic and normoxic heart homogenates of *Rattus norvegicus*, *S. judaei* and *S. galili*. Data are means of 3 independent experiments ±SD. * denotes $P < 0.05$ when compared to normoxic control value as tested by unpaired Student's t-Test. *B*: Na,K-ATPase α1 subunit protein levels in the ventricular tissue homogenates of rat (*R. norvegicus*) and blind subterranean mole rat (*S. judae*). The signal intensity for the α1 subunit was normalized to that of total-actin abundance (see the original immunoblotting readouts above the quantification bar chart). Data are means of 4–6 independent experiments ±SD. * denotes $P < 0.05$ when compared with rat.

the α_1-subunit of Na,K-ATPase of *Spalax* was cloned and sequenced and localization of cysteine residues within the sequence was compared with that of *R. norvegicus*. Sequence alignment presented as supplementary data set showed strong similarity of both proteins and particularly conserved localization of all cysteine residues within the sequences. The ability of the enzyme to respond to GSSG-induced S-glutathionylation has been confirmed for *S. galili* and *S. judaei*. Treatment of crude ventricular tissue homogenates with 300 μM of GSSG for 10 min caused complete inhibition of the enzyme in both *Spalax* and *R. norvegicus* species (Fig. 9). Thus all rodents possess redox-sensitive Na,K-ATPase in the heart. However, only *R. norvegicus* responded to systemic hypoxia (29) or deoxygenation of isolated blood-perfused heart with glutathione oxidation. Neither of the mole rat species tested showed any signs of oxidative stress in the heart in response to hypoxia (Fig. 10, actual tissue GSH and GSSG levels in Table 2). Moreover, E_{ch} (GSH:GSSG) in normoxic myocardium of *S. galili* and *S. judaei* was significantly more reduced than that in *R. norvegicus* hearts.

DISCUSSION

Our findings indicate that the changes of Na,K-ATPase activity in the heart is very tightly controlled by reversible thiol modifications in the catalytic α-subunit, which occur to even slight changes in oxygen availability. NO availability as well as maintenance of local ATP levels in premembrane space protect regulatory cysteines from inhibition, which follows their S-glutathionylation (46). Accumulation of GSSG and decrease in NO production occur in hypoxic rat myocardium (Figs. 2 and 3) along with gradual ATP deprivation (29) making the enzyme oxygen sensitive. At the molecular level changes in activity of Na,K-ATPase are associated with modifications of protein cysteine residues. Plasticity of the enzyme function appears to be tightly coupled to the reversible transition for SH groups to switch between S-nitrosylated to S-glutathionylated forms. The present study revealed that Na,K-ATPase is one more element contributing to the complex responses of cardiomyocytes to changes in redox state (53). Whether the enzyme will respond to the changes in oxygen

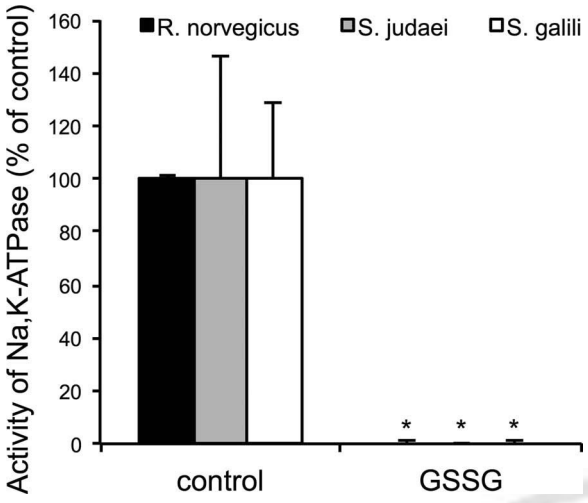

Fig. 9. Changes in Na,K-ATPase activity in ventricular tissue homogenates prepared from normoxic hearts of *R. norvegicus*, *S. judaei* and *S. galili* caused by 10 min incubation with 300 μM GSSG. Data are means of 3 experiments (*5 for R. norvegicus*) ± SD. * indicates $P < 0.05$ as determined using one-way ANOVA test.

supply depends entirely on shifts in redox state and NO production in the heart and ATP availability.

Progressive development of oxidative stress in hypoxic myocardium was suggested to reflect uncoupling in electron transduction in the mitochondria (33). Our data suggest that suppression in NO production in hypoxic heart contributes to this process as well (Figs. 3 and 4). Indeed, oxygen affinities of inducible and neuronal NO sythases (K_d of 7.8 kPa and 5.9 kPa, respectively) are significantly lower than those of superoxide generating enzymes including K_d of ~2 kPa NOX2 and 4 and even higher affinities of mitochondrial cytochromes (10, 17). NO interacts with superoxide anion four orders of magnitude faster than superoxide dismutase (rate constants being $7 \cdot 10^9$ vs. 10^5 $M^{-1}s^{-1}$, respectively) (43). The imbalance between $O_2^{\cdot -}$ and NO production towards superoxide will result in an increased $ONOO^-$ production and accumulation of H_2O_2 generated in the SOD-catalysed reaction (43). An increase in nitrotyrosine levels along with decrease in NO_2^- levels in hypoxic rat myocardium indicate that this shift indeed occurs in hypoxic heart (Fig. 6, *A* and *B*). Accumulation of GSSG following hypoxic exposure mirrors an increase in H_2O_2 and $ONOO^-$ (Fig. 3*A*). These processes do not occur in *Spalax* heart exposed to hypoxia as follows from the lack of changes in E_{hc} for the GSH/GSSG couple (Fig. 10). Our findings do not allow any speculations on the molecular mechanisms of resistance of Spalax myocardium to hypoxia-driven oxidation. Among the possible contributors are maintenance of NO production (downregulation of NO_2^- levels (21), high activity of eNOS), lower $O_2^{\cdot -}$ production rates, and/or more efficient H_2O_2 processing enzymes.

Determinants of oxygen sensitivity of Na,K-ATPase. Multiple processes are known to mediate the changes in activity of Na,K-ATPase in response to hypoxia. Among them are phosphorylation, internalization of the enzyme, and S-glutathionylation of β- and FXYD subunits of the enzyme (8, 10, 20). Some of these regulatory mechanisms function as on-off switches; others mediate fine-tuning of the enzyme resulting in partial suppression or activation. Internalization of the enzyme in clathrin-coated vesicles (12) and complete inhibition of the enzyme caused by S-glutathionylation of the α-subunit (Fig. 9) (46) represent the on-off mechanisms, which dominate over the fine-tuning regulatory mechanisms. In a separate study we have shown that complete inactivation of the Na,K-ATPase is caused by binding of glutathione to a cysteine residue within an adenine nucleotide binding site, making it inaccessible to ATP (46).

Fine-tuning of the enzyme activity in hypoxic tissue is achieved by S-glutathionylation of the β- and FXYD1 (phospholemman) subunits (8, 20) as well as by phosphorylation of phospholemman at Ser68 (Fig. 2) (22, 23, 56), resulting in modest suppression or stimulation of Na,K-ATPase in the heart.

NO and S-glutathionylation of the catalytic α-subunit. Over the last few years the number of reports on reversible thiol modifications as potent regulators of the protein function has increased exponentially (13, 37, 48, 59).

S-glutathionylation of thiols by thiol/disulfide exchange with GSSG requires dissociation of the target thiol. Alternative pathways include binding of GSH to the protein thiol groups that have undergone S-nitrosylation or oxidation to sulfenic anion ($-SO^-$) (13, 38). For many, but not all proteins including the β-subunit of Na,K-ATPase (20) and SERCA2A (1), S-nitrosylation of a thiol is a necessary intermediate step precluding S-glutathionylation. Nitrosothiols are formed in reaction with N_2O_3, an adduct of NO and O_2 (37, 43). Hypoxic conditions in the heart do not support S-nitrosylation as NO is converted to $ONOO^-$ instead of N_2O_3 (Fig. 3). The resulting $ONOO^-$- and H_2O_2-induced oxidation of thiols to thiyl radicals and sulfenic anions generation as well as GSSG accumulation promotes thiol S-glutathionylation (24, 37).

S-glutathionylation of the α_1-subunit thiols in hypoxic myocardium occurred in parallel to the decrease of the number of S-nitrosylated cysteine residues (Figs. 5 and 6). However, due to the fact that hypoxic conditions were associated with glutathione oxidation, S-glutathionylation most likely was not mediated by

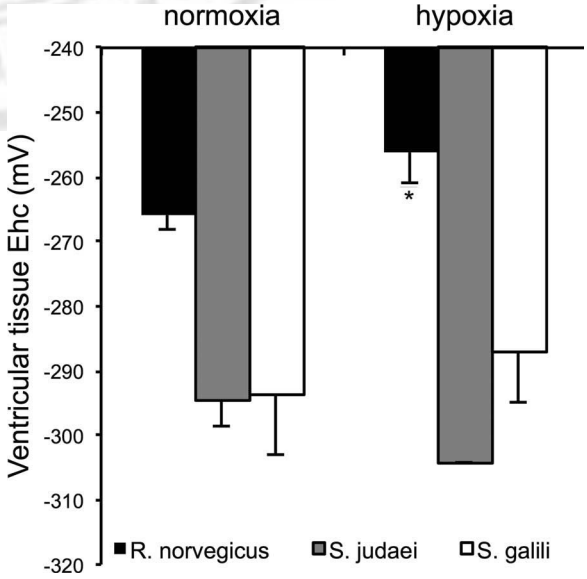

Fig. 10. Changes in ventricular tissue redox state in the myocardium of *Rattus norvegicus*, *Spalax judaei* and *Spalax galili* caused by hypoxic exposure Data are means of 3–5 independent experiments ± SD. * indicates $P < 0.05$ as determined using one-way ANOVA test.

interaction of GSH with nitrosylated thiols of the α-subunit, but via formation of thiyl and sulfenic derivatives (37).

Acute response of the heart to hypoxia: the role of S-glutathionylation. Rat heart responds to hypoxia with an acute bout of centrally driven tachycardia followed by autonomous bradycardia along with induction of arrhythmias, in vivo (36, 52) and ex vivo (Fig. 1 and Table 1). Wistar rats are very sensitive to hypoxia and acute decrease in the atmospheric O_2 levels below 10% renders them unconscious. When compared with *R. norvegicus*, *Spalax* survive at lower O_2 and higher CO_2 levels for longer periods of time (5, 6). *Spalax* live predominately in underground tunnels in which the oxygen tension is often very low (41). *Spalax* can conduct aerobic work under low O_2 pressures due to adaptations in the structural design of skeletal muscles and the cardiorespiratory system, allowing better oxygenation and more efficient perfusion of tissues in the course of hypoxic exposure (6, 60). These animals respond to hypoxia with tachycardia and maintained stroke volume, which altogether results in increased in cardiac output under hypoxic conditions (2, 18). Arrhythmias reported in mole rats under normoxic conditions were diminished during hypoxia-induced increase in heart rate (2).

Comparison of hypoxic responses of the Na,K-ATPase in myocardial tissue of mole rats and Wistar rats provided further support for the importance of the redox state in control of enzyme function. Lack of oxidative stress in *Spalax* hearts exposed to hypoxia is associated with insensitivity of Na,K-ATPase to hypoxia. However, complete inhibition of the enzyme may be induced by adding of GSSG to ventricular tissue homogenates in all species studied. Of note, mole rats survive hypoxic periods with their hearts-on. This is in marked contrast with the majority of hibernating and hypoxia-sensitive species (19).

Na,K-ATPase is an active player in control of heart rhythm, excitation propagation, and contractile force (64). Hypoxia-induced inactivation of the Na,K-ATPase in rat heart contributes to an decrease in heart rate and scooping of the ST interval (Fig. 1), which has previously been reported in digitalis-treated hearts (25). Some of these changes in ECG are observed in ischemic myocardium along with dose-dependent suppression of Na,K-ATPase triggered by oxygen deprivation (30). Na,K-ATPase is not only a mediator of transmembrane Na/K gradients but also actively participates in Ca^{2+} handling in the heart (7). Recently, S-glutathionylation was proposed as a universal mechanism regulating all Ca^{2+} handling systems in cardiomyocytes including ryanodine receptors, SERCAs, L-type Ca^{2+} channels, and Na/Ca exchange (53, 65). Inhibition of the Na,K-ATPase occurs in parallel with activation of ryanodine receptors and SERCA in the heart as these ion transporters also possess sites of regulatory S-glutathionylation (16, 31, 32). Thus S-glutathionylation allows coordinated regulation of several ion transport systems with the associated increase in intracellular calcium stores in cardiomyocytes. Hypoxia-induced S-glutathionylation promotes fast Ca^{2+} release and pumping back into the sarcoplasmic reticulum as well as facilitation of intracellular Ca^{2+} accumulation. Together, these alterations result in increased in contractile force. However, extensive calcium accumulation elevates the danger of necrotic tissue damage (15).

Our data reveal that hypoxia-induced inhibition of the Na,K-ATPase in rat heart shares similar mechanisms with those in ischemic myocardium. Oxygen deprivation is, hence, decisive in regulation of the enzyme, dominating over acidosis and the lack of glucose. Suppression of Na,K-ATPase activity in hypoxic myocardium is mediated by S-glutathionylation of the catalytic α-subunit of the enzyme, which occurs with gradual ATP deprivation. S-glutathionylation coordinates the activity of a number of ion transport systems in control of contractile function of the heart in response to the changes in redox state and NO production. This regulatory mechanism is conserved in Na,K-ATPase of hypoxia-sensitive and hypoxia-tolerant rodent species. Na,K-ATPase in hypoxia-tolerant *Spalax* myocardium remains active under hypoxic condition due to the preservation of redox state in heart tissue.

ACKNOWLEDGMENTS

We thank M. J. Shattok and W. Fuller for primary antibodies to total and phosphorylated forms of phospholemman.

GRANTS

This work has been supported by the Swiss National Academy of Sciences Grants SNF No. 112449 and No.310030_124970 (to A. Bogdanova), Forschungskredit UZH Candoc Grant No. 7082, and by the United States-Israel Binational Science Foundation Grant No. 2005346 (to A. Avivi and M. Band).

DISCLOSURES

No conflicts of interest, financial or otherwise, are declared by the author(s).

AUTHOR CONTRIBUTIONS

Author contributions: S.Y., M.B., and A.A. performed experiments; S.Y., M.B., A.A., and A.B. analyzed data; S.Y., M.B., M.T.v.P., M.G., A.A., and A.B. interpreted results of experiments; S.Y., M.B., and A.B. prepared figures; S.Y., M.B., M.T.v.P., M.G., A.A., and A.B. edited and revised manuscript; S.Y., M.B., M.T.v.P., M.G., A.A., and A.B. approved final version of manuscript; M.T.v.P. and A.B. drafted manuscript; A.B. conception and design of research.

REFERENCES

1. **Adachi T, Weisbrod RM, Pimentel DR, Ying J, Sharov VS, Schoneich C, Cohen RA.** *S*-glutathiolation by peroxynitrite activates SERCA during arterial relaxation by nitric oxide. *Nat Med* 10: 1200–1207, 2004.
2. **Arieli R, Ar A.** Heart rate response of the mole rat (*Spalax Ehrenbergi*) in hypercapnic, hypoxic, and cold conditions. *Physiol Zool* 54: 14–21, 1981.
3. **Arieli R, Arieli M, Heth G, Nevo E.** Adaptive respiratory variation in 4 chromosomal species of mole rats. *Experientia* 40: 512–514, 1984.
4. **Arieli R, Heth G, Nevo E, Zamir Y, Neutra O.** Adaptive heart and breathing frequencies in 4 ecologically differentiating chromosomal species of mole rats in Israel. *Cell Mol Life Sci* 42: 131–133, 1986.
5. **Arieli R, Nevo E.** Hypoxic survival differs between two mole rat species (Spalax ehrenbergi) of humid and arid habitats. *Comp Biochem Physiol A Comp Physiol* 100: 543–545, 1991.
6. **Avivi A, Resnick MB, Nevo E, Joel A, Levy AP.** Adaptive hypoxic tolerance in the subterranean mole rat Spalax ehrenbergi: the role of vascular endothelial growth factor. *FEBS Lett* 452: 133–140, 1999.
7. **Bers DM, Despa S.** Na/K-ATPase—an integral player in the adrenergic fight-or-flight response. *Trends Cardiovasc Med* 19: 111–118, 2009.
8. **Bibert S, Liu CC, Figtree GA, Garcia A, Hamilton EJ, Marassi FM, Sweadner KJ, Cornelius F, Geering K, Rasmussen HH.** FXYD proteins reverse inhibition of the Na-K pump mediated by glutathionylation of its β_1 subunit. *J Biol Chem* 286: 18562–18572. 2011.
9. **Bogdanov N, Petrushanko I, Boldyrev A, Gassmann M, Bogdanova A.** Sensitivity to Oxygen of Potassium Fluxes across Plasma Membrane in Cerebellar Granule Cells. *Biochem Moscow Suppl Ser A* 2: 26–32, 2008.
10. **Bogdanova A, Petrushanko I, Boldyrev A, Gassmann M.** Oxygen- and redox-induced regulation of the Na/K ATPase. *Curr Enzym Inhib* 2: 37–59, 2006.

11. **Bogdanova AY, Ogunshola OO, Bauer C, Gassmann M.** Pivotal role of reduced glutathione in oxygen-induced regulation of the Na^+/K^+ pump in mouse erythrocyte membranes. *J Membr Biol* 195: 33–42, 2003.
12. **Dada LA, Chandel NS, Ridge KM, Pedemonte C, Bertorello AM, Sznajder JI.** Hypoxia-induced endocytosis of Na,K-ATPase in alveolar epithelial cells is mediated by mitochondrial reactive oxygen species and PKC-zeta. *J Clin Invest* 111: 1057–1064, 2003.
13. **Dalle-Donne I, Rossi R, Colombo G, Giustarini D, Milzani A.** Protein *S*-glutathionylation: a regulatory device from bacteria to humans. *Trends Biochem Sci* 34: 85–96, 2009.
14. **De Angelis C, Haupert GT Jr.** Hypoxia triggers release of an endogenous inhibitor of Na^+-K^+-ATPase from midbrain and adrenal. *Am J Physiol Renal Physiol* 274: F182–F188, 1998.
15. **Dong Z, Saikumar P, Weinberg JM, Venkatachalam MA.** Calcium in cell injury and death. *Annu Rev Pathol* 1: 405–434, 2006.
16. **Donoso P, Sanchez G, Bull R, Hidalgo C.** Modulation of cardiac ryanodine receptor activity by ROS and RNS. *Front Biosci* 16: 553–567, 2010.
17. **Dweik RA.** Nitric oxide, hypoxia, and superoxide: the good, the bad, and the ugly! *Thorax* 60: 265–267, 2005.
18. **Edoute Y, Arieli R, Nevo E.** Evidence for improved myocardial oxygen delivery and function during hypoxia in the mole rat. *J Comp Physiol B* 158: 575–582, 1988.
19. **Farrell Tribute to PL AP.** Lutz: a message from the heart—why hypoxic bradycardia in fishes? *J Exp Biol* 210: 1715–1725, 2007.
20. **Figtree GA, Liu CC, Bibert S, Hamilton EJ, Garcia A, White CN, Chia KK, Cornelius F, Geering K, Rasmussen HH.** Reversible oxidative modification: a key mechanism of Na^+-K^+ pump regulation. *Circ Res* 105: 185–193, 2009.
21. **Flogel U, Fago A, Rassaf T.** Keeping the heart in balance: the functional interactions of myoglobin with nitrogen oxides. *J Exp Biol* 213: 2726–2733, 2010.
22. **Fuller W, Eaton P, Bell JR, Shattock MJ.** Ischemia-induced phosphorylation of phospholemman directly activates rat cardiac Na/K-ATPase. *FASEB J* 18: 197–199, 2004.
23. **Fuller W, Parmar V, Eaton P, Bell JR, Shattock MJ.** Cardiac ischemia causes inhibition of the Na/K ATPase by a labile cytosolic compound whose production is linked to oxidant stress. *Cardiovasc Res* 57: 1044–1051, 2003.
24. **Gallogly MM, Mieyal JJ.** Mechanisms of reversible protein glutathionylation in redox signaling and oxidative stress. *Curr Opin Pharmacol* 7: 381–391, 2007.
25. **Hornestam B, Held P, Edvardsson N.** Effects of digoxin on electrocardiogram in patients with acute atrial fibrillation—a randomized, placebo-controlled study. Digitalis in Acute Atrial Fibrillation (DAAF) Trial Group. *Clin Cardiol* 22: 96–102, 1999.
26. **Jaffrey SR, Snyder SH.** The biotin switch method for the detection of *S*-nitrosylated proteins. *Sci STKE* 2001: pl1, 2001.
27. **Kaneko M, Elimban V, Dhalla NS.** Mechanism for depression of heart sarcolemmal Ca^{2+} pump by oxygen free radicals. *Am J Physiol Heart Circ Physiol* 257: H804–H811, 1989.
28. **Kleinbongard P, Dejam A, Lauer T, Rassaf T, Schindler A, Picker O, Scheeren T, Godecke A, Schrader J, Schulz R, Heusch G, Schaub GA, Bryan NS, Feelisch M, Kelm M.** Plasma nitrite reflects constitutive nitric oxide synthase activity in mammals. *Free Radic Biol Med* 35: 790–796, 2003.
29. **Komniski MS, Yakushev S, Bogdanov N, Gassmann M, Bogdanova A.** Interventricular heterogeneity in rat heart responses to hypoxia: the tuning of glucose metabolism, ion gradients, and function. *Am J Physiol Heart Circ Physiol* 300: H1645–H1652, 2011.
30. **Kudenchuk PJ, Maynard C, Cobb LA, Wirkus M, Martin JS, Kennedy JW, Weaver WD.** Utility of the prehospital electrocardiogram in diagnosing acute coronary syndromes: the Myocardial Infarction Triage and Intervention (MITI) Project. *J Am Coll Cardiol* 32: 17–27, 1998.
31. **Lancel S, Qin F, Lennon SL, Zhang J, Tong X, Mazzini MJ, Kang YJ, Siwik DA, Cohen RA, Colucci WS.** Oxidative posttranslational modifications mediate decreased SERCA activity and myocyte dysfunction in Galphaq-overexpressing mice. *Circ Res* 107: 228–232, 2010.
32. **Lancel S, Zhang J, Evangelista A, Trucillo MP, Tong X, Siwik DA, Cohen RA, Colucci WS.** Nitroxyl activates SERCA in cardiac myocytes via glutathiolation of cysteine 674. *Circ Res* 104: 720–723, 2009.
33. **Loor G, Kondapalli J, Iwase H, Chandel NS, Waypa GB, Guzy RD, Vanden Hoek TL, Schumacker PT.** Mitochondrial oxidant stress triggers cell death in simulated ischemia-reperfusion. *Biochim Biophys Acta* 1813: 1382–1394, 2011.
34. **Lowry OH, Rosebrough NJ, Farr AL, Randall RJ.** Protein measurement with the Folin phenol reagent. *J Biol Chem* 193: 265–275, 1951.
35. **Madhani M, Hall AR, Cuello F, Charles RL, Burgoyne JR, Fuller W, Hobbs AJ, Shattock MJ, Eaton P.** Phospholemman Ser69 phosphorylation contributes to sildenafil-induced cardioprotection against reperfusion injury. *Am J Physiol Heart Circ Physiol* 299: H827–H836, 2010.
36. **Marshall JM, Metcalfe JD.** Analysis of the cardiovascular changes induced in the rat by graded levels of systemic hypoxia. *J Physiol* 407: 385–403, 1988.
37. **Martinez-Ruiz A, Lamas S.** Signalling by NO-induced protein S-nitrosylation and S-glutathionylation: convergences and divergences. *Cardiovasc Res* 75: 220–228, 2007.
38. **Mieyal JJ, Gallogly MM, Qanungo S, Sabens EA, Shelton MD.** Molecular mechanisms and clinical implications of reversible protein S-glutathionylation. *Antioxid Redox Signal* 10: 1941–1988, 2008.
39. **Mihov D, Vogel J, Gassmann M, Bogdanova A.** Erythropoietin activates nitric oxide synthase in murine erythrocytes. *Am J Physiol Cell Physiol* 297: C378–C388, 2009.
40. **Miseta A, Csutora P.** Relationship between the occurrence of cysteine in proteins and the complexity of organisms. *Mol Biol Evol* 17: 1232–1239, 2000.
41. **Nevo E.** *Mosaic Evolution of Subterranean Mammals: Regression, Progression, and Global Convergence*. Oxford: Oxford Univ. Press, 1999.
42. **Nevo E, Ivanita EN, Beiles A.** *Adaptive Radiation of Blind Subterranean Mole Rats: Naming and Revisiting the Four Sibling Species of the Spalax Ehrenbergi Superspecies in Israel: Spalax galili (2n=52), S. golani (2n=54), S. carmeli (2n=58) and S. judaei (2n=60).* Leiden: Backhuys Publishers, 2001.
43. **Pacher P, Beckman JS, Liaudet L.** Nitric oxide and peroxynitrite in health and disease. *Physiol Rev* 87: 315–424, 2007.
44. **Pagan RM, Prieto D, Hernandez M, Correa C, Garcia-Sacristan A, Benedito S, Martinez AC.** Regulation of NO-dependent acetylcholine relaxation by K^+ channels and the Na^+-K^+ ATPase pump in porcine internal mammary artery. *Eur J Pharmacol* 641: 61–66, 2010.
45. **Petrushanko I, Bogdanov N, Bulygina E, Grenacher B, Leinsoo T, Boldyrev A, Gassmann M, Bogdanova A.** Na-K-ATPase in rat cerebellar granule cells is redox sensitive. *Am J Physiol Regul Integr Comp Physiol* 290: R916–R925, 2006.
46. **Petrushanko I, Yakushev S, Mitkevich V, Kamanina Y, Ziganshin R, Meng X, Anashkina A, Makhro A, Lopina O, Gassmann M, Makarov AA, Bogdanova A.** S-glutathionylation of the Na,K-ATPase catalytic subunit is a determinant of the enzyme redox-sensitivity. *J Biol Chem* resubmitted after revision JBC/2012/391094, 2012.
47. **Petrushanko IY, Bogdanov NB, Lapina N, Boldyrev AA, Gassmann M, Bogdanova AY.** Oxygen-induced Regulation of Na/K ATPase in cerebellar granule cells. *J Gen Physiol* 130: 389–398, 2007.
48. **Rasmussen HH, Hamilton EJ, Liu CC, Figtree GA.** Reversible oxidative modification: implications for cardiovascular physiology and pathophysiology. *Trends Cardiovasc Med* 20: 85–90, 2010.
49. **Rathbun W, Betlach M.** Estimation of enzymically produced orthophosphate in the presence of cysteine and adenosine triphosphate. *Anal Biochem* 28: 436–445, 1969.
50. **Rathore SS, Curtis JP, Wang Y, Bristow MR, Krumholz HM.** Association of serum digoxin concentration and outcomes in patients with heart failure. *JAMA* 289: 871–878, 2003.
51. **Rolfe DF, Brown GC.** Cellular energy utilization and molecular origin of standard metabolic rate in mammals. *Physiol Rev* 77: 731–758, 1997.
52. **Rosen KG, Kjellmer I.** Changes in the fetal heart rate and ECG during hypoxia. *Acta Physiol Scand* 93: 59–66, 1975.
53. **Santos CX, Anilkumar N, Zhang M, Brewer AC, Shah AM.** Redox signaling in cardiac myocytes. *Free Radic Biol Med* 50: 777–793, 2011.
54. **Schafer FQ, Buettner GR.** Redox environment of the cell as viewed through the redox state of the glutathione disulfide/glutathione couple. *Free radical biology & medicine* 30: 1191–1212, 2001.
55. **Shams I, Avivi A, Nevo E.** Oxygen and carbon dioxide fluctuations in burrows of subterranean blind mole rats indicate tolerance to hypoxic-hypercapnic stresses. *Comparative biochemistry and physiology Part A, Molecular & integrative physiology* 142: 376–382, 2005.
56. **Silverman BZ, Fuller W, Eaton P, Deng J, Moorman JR, Cheung JY, James AF, Shattock MJ.** Serine 68 phosphorylation of phospholemman: acute isoform-specific activation of cardiac Na/K ATPase. *Cardiovasc Res* 65: 93–103, 2005.

57. **Swift F, Tovsrud N, Enger UH, Sjaastad I, Sejersted OM.** The Na+/K+-ATPase alpha2-isoform regulates cardiac contractility in rat cardiomyocytes. *Cardiovasc Res* 75: 109–117, 2007.
58. **Tietze F.** Enzymic method for quantitative determination of nanogram amounts of total and oxidized glutathione: applications to mammalian blood and other tissues. *Analytical biochemistry* 27: 502–522, 1969.
59. **Townsend DM, Manevich Y, He L, Hutchens S, Pazoles CJ, Tew KD.** Novel role for glutathione S-transferase pi. *Regulator of protein S-Glutathionylation following oxidative and nitrosative stress The Journal of biological chemistry* 284: 436–445, 2009.
60. **Widmer HR, Hoppeler H, Nevo E, Taylor CR, Weibel ER.** Working underground: respiratory adaptations in the blind mole rat. *Proc Natl Acad Sci U S A* 94: 2062–2067, 1997.
61. **Xu KY, Kuppusamy SP, Wang JQ, Li H, Cui H, Dawson TM, Huang PL, Burnett AL, Kuppusamy P, Becker LC.** Nitric oxide protects cardiac sarcolemmal membrane enzyme function and ion active transport against ischemia-induced inactivation. *The Journal of biological chemistry* 278: 41798–41803, 2003.
62. **Yamamoto T, Su Z, Moseley AE, Kadono T, Zhang J, Cougnon M, Li F, Lingrel JB, Barry WH.** Relative abundance of alpha2 Na(+) pump isoform influences Na(+)-Ca(2+) exchanger currents and Ca(2+) transients in mouse ventricular myocytes. *J Mol Cell Cardiol* 39: 113–120, 2005.
63. **Zhou L, Burnett AL, Huang PL, Becker LC, Kuppusamy P, Kass DA, Kevin Donahue J, Proud D, Sham JS, Dawson TM, Xu KY.** Lack of nitric oxide synthase depresses ion transporting enzyme function in cardiac muscle. *Biochem Biophys Res Commun* 294: 1030–1035, 2002.
64. **Ziegelhoffer A, Kjeldsen K, Bundgaard H, Breier A, Vrbjar N, Dzurba A.** Na,K-ATPase in the myocardium: molecular principles, functional and clinical aspects. *GenPhysiol Biophys* 19: 9–47, 2000.
65. **Zima AV, Blatter LA.** Redox regulation of cardiac calcium channels and transporters. *Cardiovasc Res* 71: 310–321, 2006.

Manuscript 2

Petrushanko I., Yakushev S., Mitkevich V., Kamanina Y., Ziganshin R., Meng Xian Yu, Anashkina A., Makhro A., Lopina O., Gassmann M, Makarov A., Bogdanova A.

"Catalytic subunit S-glutathionylation of the Na,K-ATPase as a determinant of the enzyme oxygen-sensitivity", J Biol Chem. 2012 Sep 14;287(38):32195-205. Epub 2012 Jul 13.

THE JOURNAL OF BIOLOGICAL CHEMISTRY VOL. 287, NO. 38, pp. 32195–32205, September 14, 2012

S-Glutathionylation of the Na,K-ATPase Catalytic α Subunit Is a Determinant of the Enzyme Redox Sensitivity*

Received for publication, June 14, 2012, and in revised form, July 11, 2012 Published, JBC Papers in Press, July 13, 2012, DOI 10.1074/jbc.M112.391094

Irina Yu. Petrushanko[‡], Sergej Yakushev[§], Vladimir A. Mitkevich[‡], Yuliya V. Kamanina[¶], Rustam H. Ziganshin[‖], Xianyu Meng[¶], Anastasiya A. Anashkina[‡], Asya Makhro[§], Olga D. Lopina[¶], Max Gassmann[§], Alexander A. Makarov[‡1,2], and Anna Bogdanova[§1,3]

From the [‡]Engelhardt Institute of Molecular Biology, Russian Academy of Sciences, 11999 Moscow, Russia, the [§]Institute of Veterinary Physiology and Zurich Center for Integrative Human Physiology, University of Zurich, CH 8057 Zurich, Switzerland, the [¶]Faculty of Biology, M. V. Lomonosov Moscow State University, 119234 Moscow, Russia, and the [‖]Shemyakin-Ovchinnikov Institute of Bioorganic Chemistry, Russian Academy of Sciences, 117997 Moscow, Russia

Background: Na,K-ATPase activity is extremely sensitive to changes in the redox state.
Results: Binding of glutathione to the regulatory cysteine residues of the catalytic subunit completely inhibits the Na,K-ATPase by blocking the ATP-binding site.
Conclusion: *S*-Glutathionylation of the catalytic subunit is revealed as a mechanism controlling the Na,K-ATPase function.
Significance: Regulatory *S*-glutathionylation adjusts Na,K-ATPase activity to the changes in intracellular redox state and ATP levels.

Na,K-ATPase is highly sensitive to changes in the redox state, and yet the mechanisms of its redox sensitivity remain unclear. We have explored the possible involvement of *S*-glutathionylation of the catalytic α subunit in redox-induced responses. For the first time, the presence of *S*-glutathionylated cysteine residues was shown in the α subunit in duck salt glands, rabbit kidneys, and rat myocardium. Exposure of the Na,K-ATPase to oxidized glutathione (GSSG) resulted in an increase in the number of *S*-glutathionylated cysteine residues. Increase in *S*-glutathionylation was associated with dose- and time-dependent suppression of the enzyme function up to its complete inhibition. The enzyme inhibition concurred with *S*-glutathionylation of the Cys-454, -458, -459, and -244. Upon binding of glutathione to these cysteines, the enzyme was unable to interact with adenine nucleotides. Inhibition of the Na,K-ATPase by GSSG did not occur in the presence of ATP at concentrations above 0.5 mM. Deglutathionylation of the α subunit catalyzed by glutaredoxin or dithiothreitol resulted in restoration of the Na,K-ATPase activity. Oxidation of regulatory cysteines made them inaccessible for glutathionylation but had no profound effect on the enzyme activity. Regulatory *S*-glutathionylation of the α subunit was induced in rat myocardium in response to hypoxia and was associated with oxidative stress and ATP depletion. *S*-Glutathionylation was followed by suppression of the Na,K-ATPase activity. The rat α2 isoform was more sensitive to GSSG than the α1 isoform. Our findings imply that regulatory *S*-glutathionylation of the catalytic subunit plays a key role in the redox-induced regulation of Na,K-ATPase activity.

Na,K-ATPase uses the energy of ATP to transport Na^+ and K^+ across the plasma membrane, thus mediating the transmembrane ion gradients responsible for the generation of the action potential in excitable tissues and for the secondary active transport of ions and metabolic substrates (1, 2). The enzyme is composed of α and β subunits. The catalytic α subunit is formed by the nucleotide binding, phosphorylation and actuator domains, and the ion transport pore. This subunit mediates ATP hydrolysis and ion transport. The β subunit is required for the enzyme translocation to the membrane and K^+ transport (1). In some tissues, the enzyme also contains a regulatory subunit belonging to the FXYD protein family. For each subunit, a number of isoforms showing tissue-specific expression patterns and functional diversity have been described (3, 4).

Na,K-ATPase is known to be redox- and oxygen-sensitive in a number of cell types (5, 6). H_2O_2 inhibits Na,K-ATPase in brain and kidneys (7). The tissue-specific α2β isozyme is more susceptible to reduction in activity by H_2O_2 than ubiquitously expressed α1β isozyme (8). Previously, the inhibitory action of oxidants on the Na,K-ATPase was attributed to irreversible oxidation of thiol groups. Whereas the α subunit possesses 23 reduced cysteine residues, the β subunit has only one of them (7). However, accumulating evidence suggests that redox-induced responses of the Na,K-ATPase cannot be explained by irreversible oxidation of –SH groups alone. Our earlier findings indicated that both loading of cerebellar granule cells with reduced glutathione (GSH) and GSH depletion were equally efficient in blocking Na,K-ATPase (9). Maximal activity of the enzyme in freshly isolated cerebellar neurons was only observed within a "physiological" range of pO_2 and redox state

* This work was supported by Swiss Academy of Sciences Grants 112449 and 310030_124970/1 (to A. B.), a Forschungskredit scholarship (to S. Y.), Russian Foundation for Basic Research Grants 07-04-01355 (to I. P.) and 08-04-01321 (to O. L.), the Molecular and Cellular Biology Program of the Russian Academy of Sciences, and by Russian Federal Program Contract 16.512.11.2280 (to A. M. and I. P.).
[1] Both authors contributed equally to this work.
[2] To whom correspondence may be addressed: Engelhardt Institute of Molecular Biology, RAS, 32 Vavilova St., Moscow 119991, Russia. Tel.: 7-499-1354095; Fax: 7-499-1351405, E-mail: aamakarov@eimb.ru.
[3] To whom correspondence may be addressed: Institute of Veterinary Physiology, Vetsuisse Faculty, University of Zurich, Winterthurerstrasse 260, CH-8057 Zurich, Switzerland. Tel.: 41-44-6358811; Fax: 41-44-6358932; E-mail: annab@access.uzh.ch.

characteristic for neonatal rat cerebellum. Hypoxic and hyperoxic conditions and oxidative and reductive stress were associated with a decrease in Na,K-ATPase activity (9, 10). Alterations of NO production in response to hypoxia or ischemia have been shown to play a decisive role in oxygen-induced inhibition of Na,K-ATPase (10–13). Taken together, these findings suggest that Na,K-ATPase, similar to numerous other redox-sensitive enzymes (14, 15), may respond to shifts in the redox state and oxygen availability by *S*-nitrosylation and *S*-glutathionylation of the regulatory thiol groups. *S*-Glutathionylation of the Na,K-ATPase β1 and F*X*YD subunits has been recently demonstrated (16, 17). Binding of glutathione to a single reduced cysteine residue in the regulatory β subunit caused a modest decrease in the Na,K-ATPase activity in cardiomyocytes (16). These minor effects of *S*-glutathionylation on the enzyme function did not explain robust redox-induced responses of the enzyme (9, 10, 12). *S*-Glutathionylation for any of the 23 evolutionarily conserved cysteine residues of the catalytic α subunit has never been reported. Fifteen of them are localized in the cytosolic loops of the subunit forming the ATP-binding site. These cysteine residues are potentially accessible for interaction with the cytosolic glutathione pool and for enzymes catalyzing deglutathionylation. Hence, we have hypothesized that *S*-glutathionylation of cysteine residues of the catalytic α subunit may be actively involved in redox-induced regulation of the Na,K-ATPase.

Using purified enzyme preparations from rabbit kidneys and duck salt glands (α1β1 isozyme), and crude homogenate from isolated blood-perfused rat hearts (α1β and α2β isozymes), we have revealed the presence of basal and regulatory *S*-glutathionylation sites in the α subunit of the Na,K-ATPase. Binding of glutathione to the Cys-454, -458, -459, and -244 was associated with complete inhibition of the enzyme. The inhibitory action of *S*-glutathionylation was caused by occlusion of the adenine nucleotide-binding site by glutathione.

EXPERIMENTAL PROCEDURES

Animal handling and experimentation was approved by the Swiss Federal Veterinary Office and the Bioethic Committee of the Faculty of Biology, M.V. Lomonosov Moscow State University. Experiments were performed in accordance with the Swiss and Russian Federation animal protection laws and institutional guidelines that comply with the guidelines of the Institute for Laboratory Animal Research.

Myocardial Tissue Isolation and Handling—Wistar male rats (300–400 g) were anesthetized and heparinized, and 8–10 ml of blood and the heart were collected. The hearts were then perfused via aorta with autologous blood equilibrated with a humidified gas phase containing 20% (normoxia, hemoglobin oxygen saturation, $SO_2 = 98\%$) or 5% O_2 (hypoxia, $SO_2 = 35\%$), 5% CO_2, and 75 or 90% N_2, 37 °C, 1 h) (13). The hearts were then chilled and perfused with an ice-cold sodium/potassium-free isotonic buffer solution. Ventricular tissue was subsequently used to assess the Na^+, K^+, water content, GSH and GSSG content, and Na,K-ATPase activity (13).

Na,K-ATPase Purification and Activity Measurements—Na,K-ATPase (α1β1 isozyme) was purified from duck salt glands and rabbit kidney medulla (for details see Refs. 18, 19) up to the purity grade of 99 and 95% of total protein, respectively, as confirmed by electrophoresis. Na,K-ATPase-specific activity of the duck enzyme reached ~2400 μmol of P_i (mg of protein × h)$^{-1}$ at 37 °C, and in rabbit preparations was 800–1200 μmol of P_i (mg of protein × h)$^{-1}$. The activity of Na,K-ATPase (α1β and α2β isozymes) from the rat heart was assessed either in the crude homogenate prepared from ventricular tissue (13) or in the sarcolemmal membrane fraction (20). Activity of the duck, rabbit, and rat Na,K-ATPase was measured as ouabain-sensitive (1 mM) ATP cleavage in the medium containing (in mM) 130 NaCl, 20 KCl, 3 $MgCl_2$, 3 ATP, and 30 imidazole, pH 7.4, 37 °C, when not stated otherwise (9, 13, 21).

Kinetics of the inhibitory action of GSSG on the rabbit Na,K-ATPase was monitored over 30 min in the presence of 25, 71.5, or 143 μM GSSG at room temperature. Samples containing 3–5 μg of Na,K-ATPase were collected every 5 min for activity measurements. An ~500-fold excess of GSSG over the number of enzyme –SH groups made the Na,K-ATPase inhibition rate essentially independent of the inhibitor concentration. The interaction of GSSG with the enzyme was described by the pseudo-first order kinetics Equation 1,

$$A_t = A_0 \cdot e^{-k[GSSG]t} \quad \text{(Eq. 1)}$$

where A_0 and A_t are the enzyme initial and current activity; k is the inhibition rate constant; [GSSG] is the inhibitor concentration; and t is the time of exposure to GSSG. The product of k and [GSSG] was then determined from the slope of the linear plot showing $\ln(A_t/A_0)$ as a function of time, and the inhibition rate constant was calculated.

Na,K-ATPase activity was assessed as a function of the GSSG concentration. The purified duck and rabbit enzyme as well as the sarcolemmal fraction isolated from the ventricular homogenate were exposed to 0.05–1 mM GSSG. Na,K-ATPase activity was then plotted against GSSG concentration and fitted using the logistic sigmoid function to obtain the values of apparent IC_{50} values (22) using Origin 7.0 (MicroCal).

Immunoblotting—*S*-Glutathionylation of the α1 and β1 subunits in purified Na,K-ATPase preparations and of the α1 subunit in the crude ventricular homogenates and sarcolemmal fraction were assessed using immunoblotting. Proteins were separated on SDS-PAGE and transferred to a nitrocellulose membrane. After the blocking procedure, mouse monoclonal anti-glutathione antibody (Chemicon Millipore, MAB5310) was added. The membranes were then stripped, and mouse monoclonal anti-Na,K-ATPase α1 antibody clone C464-6 (Upstate Millipore) and anti-Na,K-ATPase β1 antibody clone C464-8 (Upstate Millipore) were applied to detect the total amount of α1 and β1 subunits, followed by horseradish peroxidase-conjugated secondary antibodies. Densitometric analysis was performed, and the results were expressed as α1(β1)-SSG/total α1.

Isothermal Titration Calorimetry—The thermodynamic parameters of adenine nucleotide binding to rabbit Na,K-ATPase were measured using a MicroCal iTC200 instrument (MicroCal, Northampton, MA), as described elsewhere (23). Experiments with nonglutathionylated (dithiothreitol (DTT), 100 μM) and glutathionylated (GSSG, 1 mM) Na,K-ATPase were carried

out at 25 °C in imidazole buffer containing 25 mM imidazole, 1 mM EDTA, 250 mM sucrose, pH 7.5. Aliquots of the ligand (3.8 μl, 20–30 μM) were injected into the cell containing 2–3 μM Na,K-ATPase to achieve a complete binding isotherm. To obtain the effective heat of binding, the heat of dilution was subtracted from the heat of the reaction. The resulting titration curves were fitted using the MicroCal Origin software, assuming one set of binding sites. Affinity constants (K_a) and enthalpy variations (ΔH) were determined, and the Gibbs energy (ΔG) and the entropy variations (ΔS) were calculated from Equation 2,

$$\Delta G = -RT \ln K_a = \Delta H - T\Delta S \quad \text{(Eq. 2)}$$

Mass Spectrometry—Cysteine residues undergoing *S*-glutathionylation in the duck Na,K-ATPase α1 subunit were identified using MALDI-TOF MS. The enzyme was exposed to 1.7 mM GSH and 170 μM GSSG for 30 min at room temperature and then incubated with SDS (5 min, 37 °C). α and β subunits were separated by SDS-PAGE in the absence of β-mercaptoethanol, and the band corresponding to the α1 subunit was excised and subjected to an in-gel digestion by trypsin (24) or by α-chymotrypsin. For in-gel digestion, α-chymotrypsin or trypsin was dissolved in 50 mM ammonium bicarbonate buffer solution in a concentration of 30 or 13 ng/μl correspondingly just before use. MALDI-TOF MS analysis of the resulting peptide fragments was performed using Ultraflex II TOF/TOF mass spectrometer (Bruker Daltonics, Germany). Tryptic fragments in solution were transferred onto the MTP 384 target plate polished steel TF mass spectrometric target, dried on air, and then overlaid with a matrix solution consisting of 2,4-dihydroxybenzoic acid (201346, Bruker Daltonics) and α-cyano-4-hydroxycinnamic acid (201344, Bruker Daltonics) in concentrations of 2.4 and 3 mg/ml, respectively, in 50% acetonitrile in water, 0.1% TFA. Results of 4000 laser impulses (200 impulses from 20 different points of one spot) were summed up for every spectrum. The MS data were processed using Bruker Daltonics Flex Analysis 2.4 software, and the accuracy of mass determination of peptides was fixed to 100 ppm. Correlation of the MS data with the protein sequence was done using Bruker Daltonics BioTools 3.0 software.

Modeling—Comparison of the amino acid sequences of pig (P05024 in the UniProtKB database), duck (Q7ZYV1), rabbit (Q9N0Z6), and rat (P06685) indicates that the localization of cysteine residues is conserved in all species. This allowed us to use the existing crystallographic 3.5 Å structure of the porcine α1 subunit of Na,K-ATPase (Protein Data Bank code 3b8e) to model the changes appearing in the enzyme after glutathionylation. Three-dimensional models of the *S*-glutathionylated Na,K-ATPase catalytic α1 subunit were created on the basis of the previously published 3.5 Å structure of the porcine α1 subunit (25). Cartesian coordinates were obtained from the Brookhaven Protein Data Bank (Protein Data Bank code 3b8e). Corresponding cysteine residues in duck, rabbit, or rat α1 subunits are shifted upward by 2 compared with the numbering for cysteines in porcine α1 sequence (denoted as cysteines^P). For the simulation of *S*-glutathionylation, GSH molecules were inserted into the protein via disulfide bridges with cysteines. Two models have been built as follows: a model containing four glutathiones bound to the Cys-246^P, -452^P, -456^P, and -457^P residues, and a model with the ATP docked to the protein as described (26). Glutathione and ATP were inserted into protein with minimal geometric strain and no steric overlaps. Each model was subjected to energy minimization until convergence, using a combination of Steepest Descents, Conjugate Gradients, and Truncated Newton algorithms. The energy calculations were carried out under the MMFF94x force field using the MOE version 2009.10 modeling software (Molecular Operating Environment (MOE), 2011.10; Chemical Computing Group Inc., Montreal, Quebec, Canada). Then the models were superimposed using the structural alignment by MOE software.

Statistical Analysis—Values are shown as means ± S.D. Statistical analysis was performed using GraphPad InStat 3 (GraphPad Software, Inc., La Jolla, CA). Either the Student's *t* test or one-way analysis of variance with Bonferroni post-test were applied depending on the type of experiments, and the difference was considered significant at $p < 0.05$.

RESULTS

α Subunit of the Na,K-ATPase Is S-Glutathionylated—The presence of *S*-glutathionylated cysteine residues in ubiquitously expressed α1 subunit of the Na,K-ATPase was assessed using immunoblotting. Basal *S*-glutathionylation was observed in the α1 subunit of the duck (Fig. 1*A*), rabbit (Fig. 1*C*), and rat (Fig. 1*D*) enzyme. β1 subunit was also *S*-glutathionylated as shown in Fig. 1*B* for the duck enzyme preparation. *S*-Glutathionylation of the α1, but not of β1, subunit was further enhanced upon exposure of the enzyme to GSSG (1 mM) (Fig. 1, *A*–*C*). Treatment of the rabbit enzyme with 100 μM DTT reduced the basal *S*-glutathionylation level of the α1 subunit (Fig. 1*C*). Exposure of rat myocardium to hypoxia was associated with an increase in the α1 subunit *S*-glutathionylation in crude ventricular homogenates up to 1.5-fold over the values observed in normoxic heart (Fig. 1*D*). *S*-Glutathionylation of the α1 subunit of the Na,K-ATPase in hypoxic myocardium occurred concurrently with an increase of GSSG levels in tissue from 86 ± 8 to 176 ± 10 μmol/liter tissue water. Exposure of the purified duck Na,K-ATPase to a mixture of 1.7 mM GSH and 170 μM GSSG imitating conditions occurring in hypoxic heart resulted in complete inactivation of the enzyme.

GSSG Treatment Causes Inhibition of the Na,K-ATPase—Exposure of rabbit Na,K-ATPase to GSSG resulted in time- and dose-dependent suppression of Na,K-ATPase activity (Fig. 2*A*). The inhibitory action of GSSG was biphasic. Fast interaction of GSSG with the enzyme accounting for ~80% inhibition of the Na,K-ATPase was followed by a slow interaction phase leading to complete inactivation of the enzyme (Fig. 2*B*). The corresponding rate constants were 1655 M^{-1} min^{-1} for the fast and 163 M^{-1} min^{-1} for the slow interaction phases (Fig. 2*B*).

The GSSG concentration at half-maximal inhibition (IC_{50}) was similar for the rabbit and duck α1β1 isozymes (66 ± 3 and 59 ± 2 μM, respectively) (Fig. 3, *A* and *B*). Complete inhibition of the Na,K-ATPase by 100 μM GSSG was observed even at the presence of 10 mM GSH. The sensitivity of the duck Na,K-ATPase to GSSG was lost after 4 h of exposure of the enzyme to

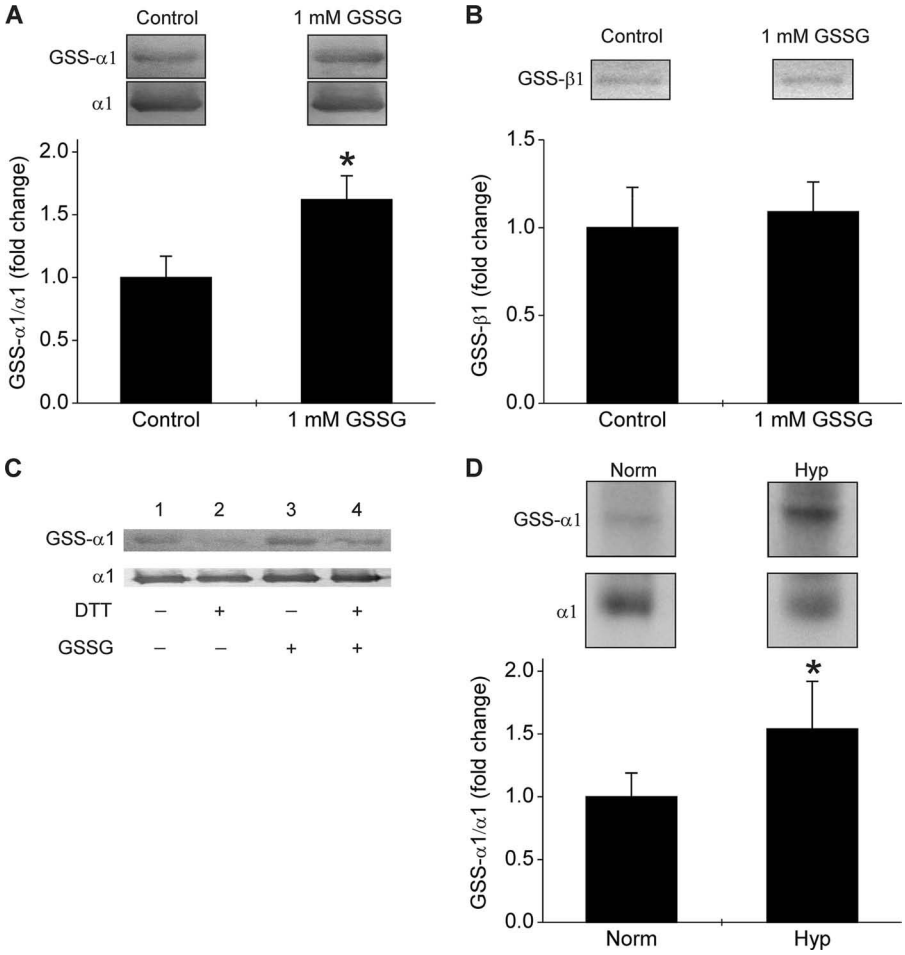

FIGURE 1. ***S*-Glutathionylation of the α and β subunits of Na,K-ATPase.** Basal *S*-glutathionylation and *S*-glutathionylation after 1 h of incubation with 1 mM GSSG for α1 (*A*) and β1 (*B*) subunits of the duck Na,K-ATPase. *Bars* represent the changes in the *S*-glutathionylated (GS*S*-α1/β) form of the protein normalized by its total amount. $n = 3$, mean ± S.D. Presented above are the original immunoblotting readouts. *Asterisk* indicates significant differences ($p = 0.014$) relative to control as determined by the two-tailed *t* test. *C,* changes in *S*-glutathionylation of the α1 subunit isolated from rabbit kidneys in the absence (*lanes 1* and *3*) or in the presence (*lanes 2* and *4*) of 100 μM dithiothreitol and thereafter exposed to 1 mM GSSG at 25 °C for 25 min (*lanes 3* and *4*). *D, S*-glutathionylation of the α1 subunit in rat hearts perfused with normoxic (*Norm, n* = 3) or hypoxic (*Hyp*, $n = 5$) blood for 1 h. *Bars* represent the *S*-glutathionylated form of the protein (GS*S*-α1) normalized to total amount of the α1 protein (mean ± S.D.). *Asterisk* indicates significant differences ($p = 0.0124$) relative to the normoxic heart sample as determined by one-way analysis of variance.

20% O_2 (air) at 4 °C prior to GSSG treatment (Fig. 3*B*). Similar desensitization to the inhibitory action of GSSG was confirmed for the rat sarcolemmal Na,K-ATPase pre-exposed to 100% O_2 for 30 min prior to GSSG treatment (Fig. 4*A*). The loss of sensitivity to GSSG was not associated with any profound effect on the Na,K-ATPase function (Fig. 4). Prolonged (6–9 months) storage of myocardial tissue at −80 °C at 20% O_2 (air) was associated with the same loss of sensitivity of the rat Na,K-ATPase to GSSG along with preservation of its hydrolytic activity. This did not occur in tissue samples stored in liquid nitrogen (Fig. 4*B*).

α Subunit S-Glutathionylation Regulates Na,K-ATPase Activity in Hypoxic Rat Heart—*S*-Glutathionylation of the Na,K-ATPase α1 subunit triggered by hypoxic exposure of rat heart (Fig. 1*D*) was associated with suppression of the enzyme function in crude ventricular tissue homogenate (Fig. 5*A*). Inhibition of the enzyme contributed to significant Na^+ accumulation in ventricular tissue (from 40.1 ± 4.3 to 55.0 ± 2.7 mmol kg^{-1} dry weight, $p = 0.043$) and K^+ loss (from 269 ± 9 to 222 ± 15 mmol kg^{-1} dry weight, $p = 0.031$) during hypoxic exposure. Some of the enzyme remained inhibited by the α subunit *S*-glutathionylation even in normoxic myocardium because deglutathionylation (DTT exposure) was associated with only a modest increase in Na,K-ATPase activity (Fig. 5*B*). Induction of *S*-glutathionylation of the α subunit by supplementation of glutaredoxin 1 (GRX)[4] and its substrates, NADPH and GSH, caused inhibition of the enzyme (Fig. 5*B*). The inhibitory effect of GRX treatment was directly proportional to the *S*-glutathionylation level (Fig. 5*C*). Depending on GSH/GSSG availability, GRX catalyzed either *S*-glutathionylation or deglutathionylation of the α subunit as described earlier for other GRX targets (27). Shifting the GSH levels by treating the tissue homogenate with glutathione reductase resulted in GRX-induced *S*-glutathionylation and the enzyme inhibition (Fig. 5*C*). GSH binding to cysteine residues affecting the Na,K-ATPase activity occurred only in the presence of GRX as a catalyst (Fig. 5, *B* and *C*). Deglutathionylation of the α subunit was catalyzed by GRX in a

[4] The abbreviation used is: GRX, glutaredoxin 1.

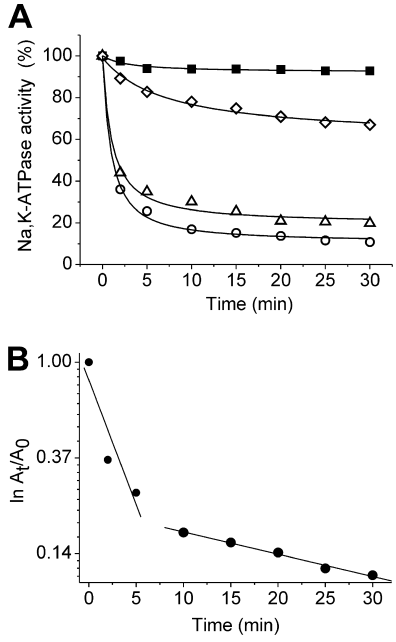

FIGURE 2. **Kinetics of GSSG-induced inhibition of rabbit kidney Na,K-ATPase.** *A,* changes in the activity of the Na,K-ATPase during the incubation in the absence (*filled squares*) or presence of 25 (*open diamonds*), 71.5 (*open triangles*), or 143 μM (*open circles*) GSSG. Data are represented as the mean of three experiments ± S.D. Errors are less than 2 (not shown). *B,* logarithm of the relative Na,K-ATPase activity A_t/A_0 was plotted against the time (*t*) of incubation with 143 μM GSSG. A_0 denotes the activity of Na,K-ATPase without GSSG, and A_t denotes the activity at time (*t*) of incubation with GSSG. The inhibition constants (*k*) for the fast and slow phases of the reaction were obtained from the slope of the linear part of the curve by dividing it by the GSSG concentration in the medium.

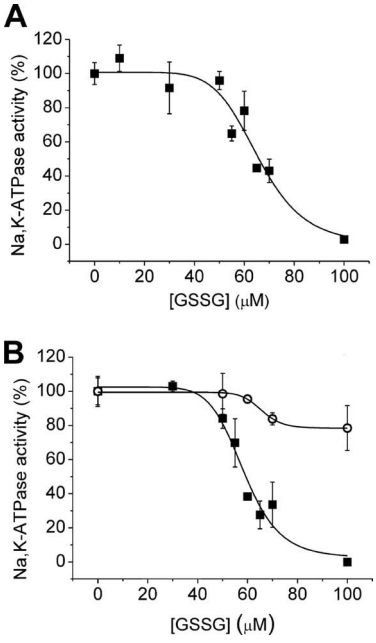

FIGURE 3. **Dose response of the inhibitory effect of GSSG on the purified Na,K-ATPase preparations.** *A,* inhibition of the Na,K-ATPase isolated from rabbit kidneys by GSSG as a function of GSSG concentration. The enzyme activity was assessed after incubation with GSSG (25 min, 25 °C) and normalized to activity of the nontreated enzyme. The apparent IC_{50}, obtained by fitting the data using the logistic sigmoid function, was 66 ± 3 μM. *B,* inhibition of the Na,K-ATPase isolated from duck salt glands by GSSG as a function of GSSG concentration (*filled squares*), as described above. The effect of exposure to air (4 h, 4 °C) prior to treatment with GSSG was also determined (*open circle*). The apparent IC_{50} for the inhibition with GSSG of the duck enzyme before exposure to air was 59 ± 2 μM. Data are represented as the mean of three experiments ± S.D.

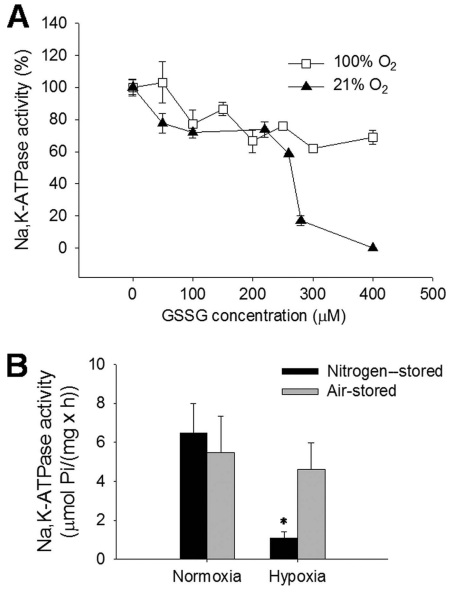

FIGURE 4. **Effect of incubation of the SL fraction in the atmosphere of pure O_2 and tissue storage at −80 °C in contact with air on the response of the Na,K-ATPase to hypoxia or GSSG treatment.** *A,* effect of various concentrations of GSSG on the Na,K-ATPase function in freshly prepared sarcolemmal membranes (*filled triangles*) or sarcolemmal membranes pre-exposed to an atmosphere of 100% O_2 for 30 min before GSSG treatment (*open squares*) $n = 4$ per condition, means ± S.D. *B,* Na,K-ATPase activity in crude ventricular tissue homogenates prepared from ventricular tissue and stored for 4–8 weeks either at −80 °C in contact with air (*gray bars*) or in an atmosphere of liquid nitrogen (*black bars*). Data are presented as a mean of five independent experiments ± S.D. *Asterisk* indicates significant differences ($p = 0.0078$) relative to the corresponding N_2-stored normoxic control as determined by the two-tailed unpaired *t* test.

sarcolemmal fraction pretreated with GSSG to induce *S*-glutathionylation (Fig. 5*D*). As mentioned above, Na,K-ATPase in the myocardium is presented by $\alpha1\beta$ and $\alpha2\beta$ isozymes. The $\alpha2\beta$ isozyme was known to be more susceptible to oxidation than the $\alpha1\beta$ isozyme and may be blocked by 10 μM ouabain, whereas the $\alpha1\beta$ isozyme in rat did not respond to this inhibitor concentration (28). We have used this difference in ouabain sensitivity to assess the responses of both isozymes in rat sarcolemmal membranes to GSSG treatment. Na,K-ATPase function was assessed in two sets of samples, one of which contained 10 μM ouabain and the other was ouabain-free. As shown in Fig. 5*E*, the $\alpha2\beta$ isozyme was blocked by GSSG at concentrations 6-fold lower than the $\alpha1\beta$ isozyme with IC_{50} at 43.6 ± 9.2 and 265 ± 13 μM for the $\alpha2$ and $\alpha1$ isoforms, respectively. Progressive inhibition of the $\alpha1\beta$ isozyme followed a dose-dependent increase in *S*-glutathionylation of the $\alpha1$ subunit shown as *bars* in Fig. 5*E*.

S-Glutathionylation Prevents the Adenine Nucleotide Binding to Na,K-ATPase—The experiments presented above were performed in the absence of ATP because GSSG treatment of the Na,K-ATPase precluded enzyme activity measurements. Pretreatment of rabbit Na,K-ATPase with GSSG prior to exposing the enzyme to ATP completely inhibited the enzyme (Fig. 6*A*). However, when GSSG was added to the enzyme, in the presence of ATP at a concentration exceeding 0.5 mM, the inhibitory effect of GSSG was completely averted (Fig. 6*B*). Thus, the inhibitory action of GSSG on the Na,K-ATPase was caused by its interaction with the free enzyme and not with the enzyme-substrate complex.

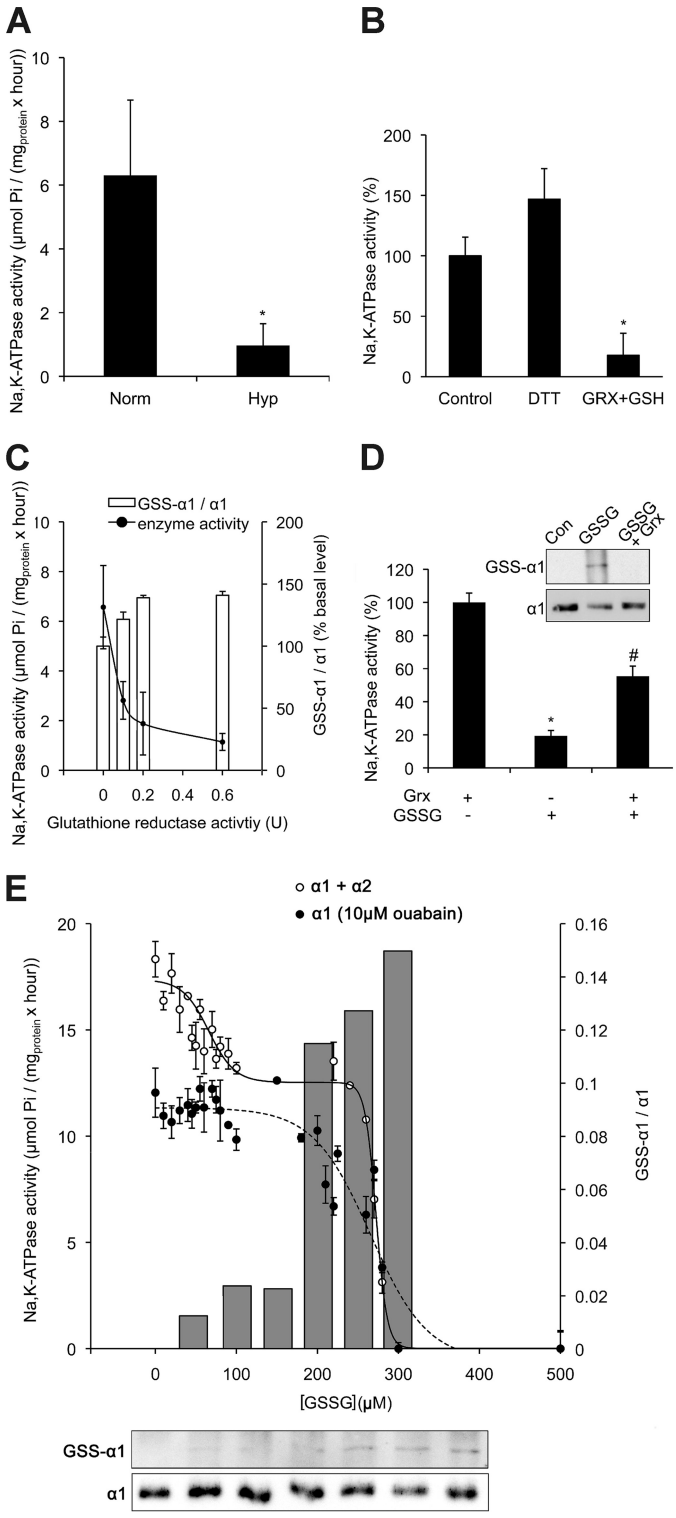

FIGURE 5. **Regulation of the Na,K-ATPase in rat heart by *S*-glutathionylation.** *A,* activity of the Na,K-ATPase in crude homogenate prepared from normoxic (*Norm*) and hypoxic (*Hyp*) hearts. $n = 5$ per condition. *Asterisk* denotes $p = 0.0039$. *B,* effects of 100 μM DTT and GRX/NADPH-catalyzed (0.6 units of GRX/200 μM NADPH) *S*-glutathionylation by 300 μM GSH on Na,K-ATPase activity in normoxic crude ventricular homogenates. $n = 4$ per group. *Asterisk* indicates $p = 0.0059$ relative to the nontreated crude homogenate sample as determined by the two-tailed paired *t* test. *C,* dose-dependent GSH-induced *S*-glutathionylation (*open bars*) and the corresponding changes in the activity of the enzyme (*line*) in crude homogenate treated with glutathione reductase and 0.6 units GRX/200 μM NADPH. $n = 4$. *D,* effect of GSSG-induced glutathionylation and GRX-catalyzed deglutathionylation on the enzyme function in sarcolemmal membranes prepared from normoxic crude homogenate. *S*-Glutathionylation was induced by treating the sarcolemmal membranes with 300 μM GSSG and reversed with 0.6 units of GRX/200 μM NADPH. Data are represented as the mean of four hearts per condition ± S.D. Shown in the *upper panel* is a representative Western blot for the total and *S*-glutathionylated α1 subunit. * denotes $p = 0.0001$ compared with the GRX-treated control (*Con*) and # stands for $p = 0.002$ compared with the sample treated with GSSG alone. *E,* differential sensitivity of the α1 and α2 isozymes to the inhibitory action of GSSG. Activity of the Na,K-ATPase (*α1 + α2*) or the α1 isozyme alone was assessed in sarcolemmal membranes prepared from the normoxic heart treated with various GSSG concentrations. Activity of the α2 isozyme was calculated by subtracting the activity of the α1 isoform from the total Na,K-ATPase activity. Fitting of the plots with double (α1 + α2) or single (α1 or α2 alone) logistic sigmoidal functions was performed giving apparent IC_{50} values for α1 as 271.1 ± 1.7 μM and for α2 as 43.6 ± 9.2 μM. *Gray bars* and the *lower panel* show the changes in *S*-glutathionylation of the α1 subunit followed by the corresponding changes in the enzyme activity. $n = 5$ per group. All plotted data are represented as mean values ± S.D.

Isothermal titration calorimetry was used for direct assessment of the thermodynamic parameters for nucleotide binding to rabbit Na,K-ATPase in nonglutathionylated and glutathionylated forms. Heat production associated with the interaction of ADP with the rabbit enzyme was measured in the presence of DTT or GSSG. A set of original data obtained in such experiments is shown in Fig. 5*C*. The ADP binding to Na,K-ATPase was enthalpy-driven ($\Delta H = -8.2 \pm 0.3$ kcal mol^{-1}, $T\Delta S = 1.1$ kcal mol^{-1}) with a binding constant K_a of $6.8 \pm 1.4 \times 10^6$ M^{-1}. The stoichiometry of ADP binding to Na,K-ATPase was ~0.8. *S*-Glutathionylation of the enzyme by GSSG completely abolished ADP binding to the Na,K-ATPase (Fig. 6*C*).

Glutathionylated SH Groups Are Localized in the Large and Small Cytosolic Loops of the α Subunit—Identification of the cysteine residues of the duck Na,K-ATPase that are *S*-glutathionylated in the native active enzyme and cysteines undergoing *S*-glutathionylation upon exposure to GSSG was performed using mass spectrometry. Duck Na,K-ATPase was exposed to a mixture of 1.7 mM GSH and 170 μM GSSG, and the concentrations were found to be present in hypoxic heart and to effectively inhibit the enzyme function. Enzyme activity measurements were performed in control and GSH/GSSG-treated protein samples. Thereafter, two enzyme samples were collected from control and treated enzyme, and each of them proteolyzed by either trypsin or chymotrypsin and MALDI-TOF MS was used to detect cysteine thiol modifications in resulting proteolytic fragments. The α1 sequence coverage reached 70–80% for chymotrypsin-digested fragments and was 50–60% for tryptic fragments. The list of cysteine residues of the α1 subunit undergoing *S*-glutathionylation in the control and treated enzyme is summarized in Table 1. Listed there are the *m*/*z* ratios for each fragment and relative peak intensities. Localization of cysteines within the sequence is schematically shown in Fig. 6*D*. As shown in Table 1, treatment of the enzyme with GSH/GSSG was associated with an increase in *S*-glutathionylation of the Cys-454, -458, and -459 of the big cytosolic loop and the Cys-244 localized within the small cytosolic loop of the α1 subunit. Cysteine residue 423 has never been found *S*-glutathionylated.

Glutathionylation of Residues Cys-452^p, -456^p, and 457^p Disrupts the ATP Binding by α1 Subunit of Na,K-ATPase—The structural alignment of the model containing three glutathionyl residues bound to the Cys-452^P, -456^P, and -457^P residues (cor-

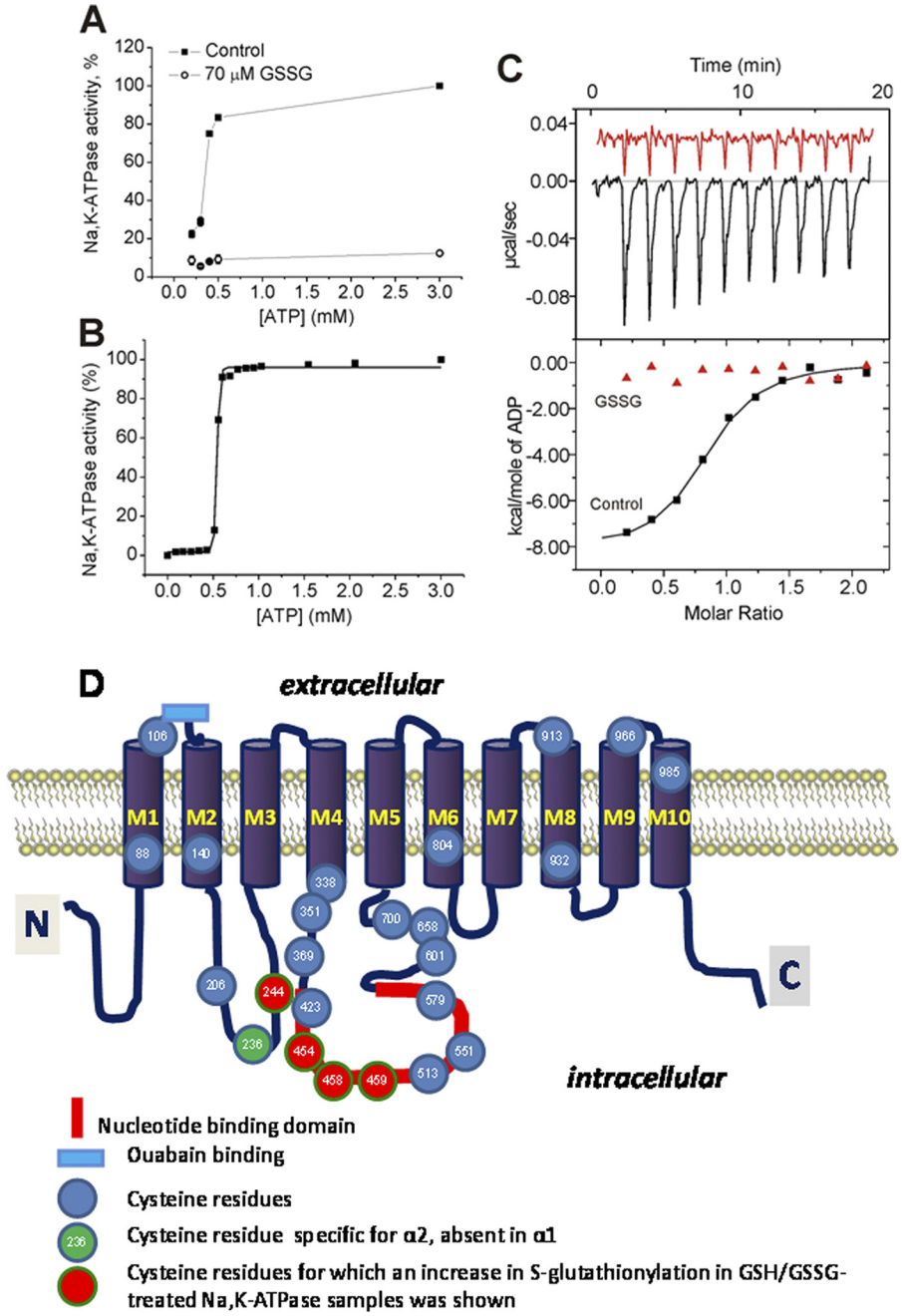

FIGURE 6. **Competition between nucleotides and GSSG for the Na,K-ATPase nucleotide-binding site.** *A,* pretreatment of the Na,K-ATPase prevents the dose-dependent activation of the Na,K-ATPase with ATP. Na,K-ATPase purified from rabbit kidney was preincubated both in the presence and absence 70 μM GSSG for 25 min and then its activity was measured as a function of ATP availability. The data are represented as mean values ± S.D. $n = 3$. *B,* ATP causes dose-dependent prevention of the inhibitory action of 1 mM GSSG when ATP and GSSG are simultaneously present in the incubation medium. The data are represented as mean values ± S.D. $n = 3$. *C,* inhibitory effect of *S*-glutathionylation on the ADP binding to Na,K-ATPase. An original isothermal titration calorimetry recording (*upper panel*) and binding isotherms (*lower panel*) of the Na,K-ATPase interaction with ADP in the presence of DTT (100 μM, *black*) or GSSG (1 mM, *red*) at 25 °C. *D,* localization of *S*-glutathionylation sites on the α1 subunit. Membrane domains of the α1 subunit are shown as *barrels* numbered as *M1–M10*. Cytosolic or extracellular domains are shown as *lines*, where the ouabain-binding site is shown in *blue* and nucleotide binding domain is in *red*. "*C*" and "*N*" indicate the C and N terminus. Cysteine residues are presented as *filled circles* with *numbers* corresponding to the duck/rabbit/rat α1 sequence. Cysteines, which undergo *S*-glutathionylation upon GSH/GSSG treatment, are shown in *red*. The Cys-236 absent in the α1 but present in the α2 isozyme is shown in *green*.

responding to the Cys-454, -458, and -459 residues in the duck, rabbit, and rat sequences), and the model with the ATP molecule docked to the protein, has been done by the MOE software (Fig. 7*A*). According to the model, the distance between the terminal negatively charged phosphate of the ATP molecule and the carboxyl group of glutathione bound to the Cys 452^P carrying the same negative charge is less than 8 Å (Fig. 7*A*). Electrostatic repulsion forces between these two negative charges are sufficient to hinder attachment of the ATP to the *S*-glutathionylated binding site moiety. The same is true for glutathione binding to the Cys-452^P in the presence of ATP in docked position. This electrostatic repulsion will become even more pronounced as an additional two cysteines in the vicinity of the ATP-binding site, Cys 456^P and 457^P (Fig. 7*A*), are *S*-glu-

TABLE 1

MALDI-TOF-MS analysis of the glutathionylated Cys-containing peptides of α1 subunit of the Na,K-ATPase

Na,K-ATPase isolated from duck salt glands was treated with a mixture of GSH (1.7 mM) and GSSG (170 μM), and the α1 subunit of the enzyme before (control, active enzyme) and after (GSH/GSSG, inactivated enzyme) treatment was subjected to either tryptic or chymotryptic digestion. The resulting fragments were analyzed by MALDI-TOF MS. Shown in the table are only the tryptic and chymotryptic fragments containing *S*-glutathionylated cysteine residues. Listed in the table are the experimental and calculated *m*/*z* ratio values (monoisotopic mass-to-charge ratio of the singly charged peptide ions) of the fragments. The calculated *m*/*z* values are for the fragments in which all cysteine residues are present in nonmodified (reduced) form. Cysteine modification was assessed by comparison of the experimental *m*/*z* values with the calculated ones. Binding of glutathione (–SG) increases mass of the fragments by 305 Da. Peaks with maximal intensity were chosen as referent ones for analysis of tryptic and chymotryptic fragments. These peaks differed for tryptic and chymotryptic fragments. The same referent peaks were used for analysis of fragments obtained from control and GSH/GSSG-treated samples. The peak intensity of the fragment normalized to intensity of the corresponding referent peak is presented in the table as relative intensity. Peak detection was made by the SNAP algorithm of the program Flex Analysis (Bruker Daltonics, Germany). Experiment has been repeated three times.

Cysteine no.	Fragment/ type of fragment	Sequence	Experimental *m*/*z*		Calculated *m*/*z* for nonmodified fragment	Calculated *m*/*z* for modified fragment	Cysteine modification	Relative intensity	
			Control	GSH/ GSSG				Control	GSH/ GSSG
206	194–207 tryptic	IPADLRIISAHGCK	1798.82	1798.89	1493.82	1798.89	SG	0.72	0.77
244	236–250 tryptic	NIAFFSTNCVEGTAR	1934.95	1934.86	1629.76	1934.84	SG	0.08	0.47
338, 351	336–353 chymotryptic	TVCLTLTAKRMARKNCLV	2326.19	2326.19	2021.14	2326.21	SG, SH	0.14	0.21
351, 369	350–372 tryptic	NCLVKNLEAVETLGSTSTICSDK	3035.49	3035.48	2425.19	3035.33	SG, SG	0.03	0.03
454, 458, 459	454–468 tryptic	CIELCCGSVKEMRER	2671.20	2671.19	1755.79	2671.01	SG, SG, SG	0.05	0.13
458, 459	456–462 chymotryptic	ELCCGSV	1015.34	1015.34	710.28	1015.35	SG, SH	0.28	0.49
513	502–516 chymotryptic	MKGAPERILDRCSSI	1981.0	1981.01	1675.86	1980.93	SG	2.98	2.62
551	549–564 chymotryptic	GFCHLALPDDQFPEGF	2097.96	2097.95	1792.79	2097.87	SG	1.88	2.13
658	640–660 chymotryptic	AARLNIPVSQVNPRDAKACVV	2526.24	2526.36	2221.22	2526.29	SG	0.19	0.13
700	694–702 tryptic	LIIVEGCQR	1335.65	1335.65	1030.56	1335.64	SG	0.58	0.78

tathionylated. The results of modeling comply with the observation that interaction of ATP with its binding site and binding of glutathione to the regulatory cysteine residues are mutually exclusive (Fig. 6, *A*–*C*). Modeling based on the crystal structure of the enzyme in E2P conformation did not show any significant interaction of Cys-246^{P} with the ATP-binding site. However, this may not hold true for the enzyme in E1 conformation (25).

DISCUSSION

The obtained data indicate that *S*-glutathionylation of the catalytic α subunit may result in complete inactivation of the enzyme by making its adenine nucleotide-binding site inaccessible for ATP. Regulatory *S*-glutathionylation does not occur spontaneously, only when ATP depletion reaches a threshold of ~500 μM (Fig. 6*B*). Therefore, inactivation of the enzyme prevents irreversible ATP deprivation under conditions of limited ATP supply. *S*-Glutathionylation of regulatory cysteines is promoted under oxidative stress when GSSG concentration increases in the cytosol. However, it may also be mediated by GSH in the presence of GRX (Fig. 5*C*) indicating that oxidative stress is not necessarily required to trigger *S*-glutathionylation. ATP depletion on the contrary is absolutely required to induce regulatory *S*-glutathionylation. The ability of ATP to protect Na,K-ATPase from HO•-induced inactivation has been shown previously (27).

Basal S-Glutathionylation of α Subunit—In contrast to regulatory *S*-glutathionylation, endogenous basal *S*-glutathionylation is an intrinsic feature of the Na,K-ATPase catalytic subunit and is independent of the ATP availability. Removal of basal glutathionylation by DTT was not followed by an alteration of the Na,K-ATPase activity. Physiological relevance of basal *S*-glutathionylation remains unclear. However, its high abundance suggests that basal *S*-glutathionylation is required for the maintenance of optimal protein function. Similar to the α subunit of Na,K-ATPase, basal *S*-glutathionylation was described for its structural homologue, SERCA-2A (28), as well as for ryanodine receptors (29).

S-Glutathionylation of α Subunit Leads to Complete Inhibition of the Na,K-ATPase—Interaction of glutathione with regulatory cysteine residues resulted in complete inhibition of the enzyme (Figs. 3 and 5). *S*-Glutathionylation of the catalytic subunit associated with the changes in enzyme activity represents typical regulatory glutathionylation as described earlier (30). Hypoxia is a physiological stimulus that induces regulatory *S*-glutathionylation in rat heart. Oxygen consumption rate in the myocardium exceeds that in the brain, and reduction of the O_2 supply of this tissue is followed by rapid reduction in ATP levels (13) along with GSSG accumulation (see above). As we have demonstrated in this study, these conditions promote regulatory *S*-glutathionylation. Na,K-ATPase may be *S*-glutathionylated in a reaction of thiol-disulfide exchange within the physiological concentration range of GSH and GSSG of 1–10 mM and 50–500 μM, respectively (Figs. 3 and 5*E*) (9, 31, 32). Thiol-disulfide exchange reaction with glutathione is comparatively rare, and the few other proteins where it is also physiologically relevant are c-Jun (33) and aldose reductase (34). For the vast majority of other proteins, including the β subunit of the Na,K-ATPase, intermediate *S*-nitrosylation step or other thiol modifications preclude the formation of *S*-glutathionylated adducts (16).

Regulation of the Na,K-ATPase function by *S*-glutathionylation is fast (Fig. 2) and completely reversible (Fig. 5*D*). GRX actively participates in deglutathionylation or induction of *S*-glutathionylation depending on the changes in GSH and NADPH levels. Therefore, GRX coordinates the activity of numerous redox-sensitive proteins adjusting to the changes in the redox microenvironment (Fig. 5, *C* and *D*) (35–37). Spontaneous deglutathionylation catalyzed by GRX and thioredoxins is most likely to be the cause of the gradual loss of the inhibitory effect of ischemia on the Na,K-ATPase in heart tissue homogenate with time, as reported by Fuller *et al.* (12).

Biphasic kinetics of the inhibitory action of GSSG on Na,K-ATPase activity may reflect the existence of two dis-

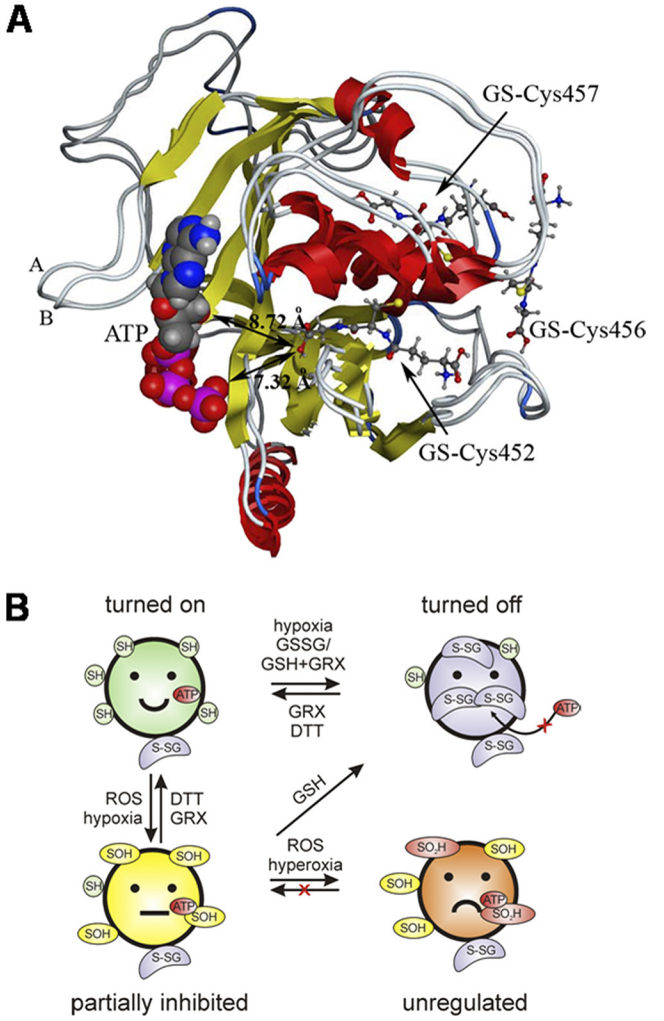

FIGURE 7. ***S*-Glutathionylation of the α subunit as a mechanism of regulation of the Na,K-ATPase.** *A,* superimposition of the three-dimensional structures of the nucleotide binding domain (Arg-378 to Arg-589) with ATP *A* or glutathione *B* bound to Cys-452^P, -456^P, and -457^P. Shown as a ribbon diagram is a model created on the basis of 3.5-Å structure of the porcine α1 subunit (Protein Data Bank code 3b8e). The structural alignment was simulated with the program MOE. Glutathione is shown as a ball-and-stick representation, and ATP is presented as a space-filling van der Waals representation with atoms in standard colors for atom type (carbon, *gray*; oxygen, *red*; nitrogen, *blue*; sulfur, *yellow*; phosphorus, *pink*). The distance between the negatively charged phosphate ATP tail and the negatively charged carboxyl group of the glutathione bound to the Cys-452^P is shown in *green* and is less than 8 Å. *B,* schematic representation of the regulatory *S*-glutathionylation of the Na,K-ATPase. The enzyme is shown in dynamic equilibrium between three distinct states as follows: "turned on" (active, regulated), "turned off" (reversibly inhibited), and "partially inhibited." Transformation to the "unregulated" state is irreversible. Maximal activity of the enzyme may be achieved under the conditions supporting the optimal redox environment. Mild oxidation (GSSG accumulation coupled to ATP depletion or –SH to –SOH transformation of the cysteine residues in the partially inhibited mode) or GSH overload in the presence of GRX transfers the Na,K-ATPase from turned-on to the turned-off state in which the regulatory cysteines are *S*-glutathionylated. Severe oxidative stress causes oxidation of the –SH groups of the regulatory cysteines to $–SO_2H$ or $–SO_3H$ and thus turns the enzyme into the unregulated state, in which it is unable to respond to the changes in redox state and remains constantly active.

tinct classes of regulatory thiol groups, as shown before for the glycogen debranching enzyme in rabbit skeletal muscle (38) or alternatively two conformational states (*e.g.* E_1 and E_2) of the Na,K-ATPase in which the same thiol groups become more or less accessible to interactions with GSSG.

Greater susceptibility of the α2β isozyme to inhibitory *S*-glutathionylation by GSSG in rat sarcolemmal membranes is of physiological importance (Fig. 5*E*). The α2 isoform of the catalytic subunit is mainly localized in the T-tubular zones, where it is associated with the Na^+/Ca^{2+} exchanger (36). Thus, *S*-glutathionylation and the following inhibition of the α2β isozyme may have a profound effect on the intracellular Ca^{2+} handling in cardiomyocytes (36, 37, 39). As the α2 isoform has been reported to be particularly prone to oxidation (8), more favorable binding of glutathione to this isoform will protect it from oxidation.

Severe oxidative stress is associated with irreversible oxidation of the regulatory thiols to sulfinic or sulfonic acid. When oxidized to $–SO_2^-$ or $–SO_3^-$, the thiol groups cannot be *S*-glutathionylated, and the Na,K-ATPase loses its redox sensitivity. In our study, oxidation has been induced by exposure of the enzyme to 20–100% O_2 (Figs. 3*B* and 4). Isolation of cardiomyocytes from adult myocardium also inevitably results in oxidative stress and most likely leads to the inaccessibility of the α subunit cysteines for regulatory glutathionylation (16). Cys-46 of the β subunit is localized almost within the lipid bilayer, which is less exposed to the cytosol and hence is more resistant to oxidation. It may still undergo *S*-glutathionylation even in isolated cardiomyocytes as reported earlier (16).

Localization of the Regulatory Cysteines—The obtained results indicate that inhibition of the Na,K-ATPase activity may be induced by *S*-glutathionylation of at least three regulatory cysteine residues localized within the big cytosolic loop of its α subunit, Cys-454, -458, and -459. The inability of the enzyme to bind ATP in *S*-glutathionylated form results from an increase in negative charge within the ATP binding pocket. The role of *S*-glutathionylation of the Cys-244 remains to be clarified. Along with the data of mass spectrometry, clear differences in sensitivity to the inhibitory action of GSSG on the α1β and α2β isozymes (Fig. 5*E*) suggest that this cysteine residue may play a regulatory role as well. The more sensitive α2 isoform of the catalytic subunit possesses one additional cysteine is at position 236, which may be a target for *S*-glutathionylation along with Cys-244. It is tempting to suggest that this alteration in the α2 sequence compared with that of α1 is a cause of amplification of the inhibitory effect of GSSG observed for the α2β isozyme in rat heart (Fig. 5*E*).

Ca^{2+}-transporting ATPase SERCA2A, a homologue of the Na,K-ATPase, has also been reported to possess a site of regulatory *S*-glutathionylation (28). But in contrast to Na,K-ATPase, SERCA2A is activated upon *S*-glutathionylation of a single cysteine residue, Cys-674. This cysteine is absent in all α subunit isoforms of the Na,K-ATPase. The conserved localization of cysteine residues within the sequence of SERCA2A and the α subunit of the Na,K-ATPase is necessitated by the regulatory function of these amino acids. Although mutations of the Cys residues to Ser or Ala in the α subunit were not associated with significant changes in the enzyme activity (40), reversible thiol modifications of some of them may have a striking effect on the Na,K-ATPase function. Our data indicate that the resulting mutants will render the enzyme largely redox-insensitive due to the lack of sites of regulatory *S*-glutathionylation.

Schematic representation of the role of regulatory *S*-glutathionylation in the control of Na,K-ATPase is shown in Fig. 7*B*. Induction of regulatory *S*-glutathionylation allows us to quickly inactivate the enzyme under conditions of limited ATP supply. Mild oxidative stress (*e.g.* associated with hypoxic exposure) results in an increase in GSSG and oxidation of regulatory thiols to sulfenic acid (–SOH). Taken together, these changes promote *S*-glutathionylation of cysteine residues thereby inhibiting the Na,K-ATPase and protecting thiols from irreversible oxidation. When not protected, the regulatory thiols get further oxidized to sulfinic and sulfonic acid making the enzyme insensitive to the changes in ATP levels and the redox state.

Our findings reveal the importance of *S*-glutathionylation of cysteine residues of the Na,K-ATPase catalytic subunit in redox-induced responses of the enzyme. *S*-Glutathionylation of the regulatory cysteine(s) acts as a switch turning off the Na,K-ATPase at the low ATP level to prevent irreversible ATP depletion.

REFERENCES

1. Blanco, G., and Mercer, R. W. (1998) Isozymes of the Na-K-ATPase. Heterogeneity in structure, diversity in function. *Am. J. Physiol.* **275,** F633–F650
2. Glitsch, H. G. (2001) Electrophysiology of the sodium-potassium-ATPase in cardiac cells. *Physiol. Rev.* **81,** 1791–1826
3. Geering, K. (2008) Functional roles of Na,K-ATPase subunits. *Curr. Opin. Nephrol. Hypertens.* **17,** 526–532
4. Kaplan, J. H. (2002) Biochemistry of Na,K-ATPase. *Annu. Rev. Biochem.* **71,** 511–535
5. Bogdanova, A., Petrushanko, I., Boldyrev, A., Gassmann, M. (2006) Oxygen- and redox-induced regulation of the Na/K-ATPase. *Curr. Enzyme Inhibition* **2,** 37–59
6. Rasmussen, H. H., Hamilton, E. J., Liu, C. C., and Figtree, G. A. (2010) Reversible oxidative modification. Implications for cardiovascular physiology and pathophysiology. *Trends Cardiovasc. Med.* **20,** 85–90
7. Kurella, E. G., Tyulina, O. V., and Boldyrev, A. A. (1999) Oxidative resistance of Na/K-ATPase. *Cell. Mol. Neurobiol.* **19,** 133–140
8. Xie, Z., Jack-Hays, M., Wang, Y., Periyasamy, S. M., Blanco, G., Huang, W. H., and Askari, A. (1995) Different oxidant sensitivities of the α1 and α2 isoforms of Na^+/K^+-ATPase expressed in baculovirus-infected insect cells. *Biochem. Biophys. Res. Commun.* **207,** 155–159
9. Petrushanko, I., Bogdanov, N., Bulygina, E., Grenacher, B., Leinsoo, T., Boldyrev, A., Gassmann, M., and Bogdanova, A. (2006) Na-K-ATPase in rat cerebellar granule cells is redox sensitive. *Am. J. Physiol. Regul. Integr. Comp. Physiol* **290,** R916–R925
10. Petrushanko, I. Y., Bogdanov, N. B., Lapina, N., Boldyrev, A. A., Gassmann, M., and Bogdanova, A. Y. (2007) Oxygen-induced Regulation of Na/K-ATPase in cerebellar granule cells. *J. Gen. Physiol.* **130,** 389–398
11. Duranteau, J., Chandel, N. S., Kulisz, A., Shao, Z., and Schumacker, P. T. (1998) Intracellular signaling by reactive oxygen species during hypoxia in cardiomyocytes. *J. Biol. Chem.* **273,** 11619–11624
12. Fuller, W., Parmar, V., Eaton, P., Bell, J. R., and Shattock, M. J. (2003) Cardiac ischemia causes inhibition of the Na/K-ATPase by a labile cytosolic compound whose production is linked to oxidant stress. *Cardiovasc. Res.* **57,** 1044–1051
13. Komniski, M. S., Yakushev, S., Bogdanov, N., Gassmann, M., and Bogdanova, A. (2011) Interventricular heterogeneity in rat heart responses to hypoxia. The tuning of glucose metabolism, ion gradients, and function. *Am. J. Physiol. Heart Circ. Physiol.* **300,** H1645–H1652
14. Martínez-Ruiz, A., and Lamas, S. (2007) Signaling by NO-induced protein *S*-nitrosylation and *S*-glutathionylation. Convergences and divergences. *Cardiovasc. Res.* **75,** 220–228
15. Mieyal, J. J., Gallogly, M. M., Qanungo, S., Sabens, E. A., and Shelton, M. D. (2008) Molecular mechanisms and clinical implications of reversible protein *S*-glutathionylation. *Antioxid. Redox. Signal.* **10,** 1941–1988
16. Figtree, G. A., Liu, C. C., Bibert, S., Hamilton, E. J., Garcia, A., White, C. N., Chia, K. K., Cornelius, F., Geering, K., and Rasmussen, H. H. (2009) Reversible oxidative modification. A key mechanism of Na^+-K^+ pump regulation. *Circ. Res.* **105,** 185–193
17. Bibert, S., Liu, C. C., Figtree, G. A., Garcia, A., Hamilton, E. J., Marassi, F. M., Sweadner, K. J., Cornelius, F., Geering, K., and Rasmussen, H. H. (2011) FXYD proteins reverse inhibition of the Na-K pump mediated by glutathionylation of its β1 subunit. *J. Biol. Chem.* **286,** 18562–18572
18. Jørgensen, P. L. (1988) Purification of Na^+,K^+-ATPase. Enzyme sources, preparative problems, and preparation from mammalian kidney. *Methods Enzymol.* **156,** 29–43
19. Smith, T. W. (1988) Purification of Na^+,K^+-ATPase from the supraorbital salt gland of the duck. *Methods Enzymol.* **156,** 46–48
20. Kaneko, M., Elimban, V., and Dhalla, N. S. (1989) Mechanism for depression of heart sarcolemmal Ca^{2+} pump by oxygen free radicals. *Am. J. Physiol.* **257,** H804–H811
21. Rathbun, W. B., and Betlach, M. V. (1969) Estimation of enzymically produced orthophosphate in the presence of cysteine and adenosine triphosphate. *Anal. Biochem.* **28,** 436–445
22. Cortés, A., Cascante, M., Cárdenas, M. L., and Cornish-Bowden, A. (2001) Relationships between inhibition constants, inhibitor concentrations for 50% inhibition and types of inhibition. New ways of analyzing data. *Biochem. J.* **357,** 263–268
23. Mitkevich, V. A., Kononenko, A. V., Petrushanko, I. Y., Yanvarev, D. V., Makarov, A. A., and Kisselev, L. L. (2006) Termination of translation in eukaryotes is mediated by the quaternary eRF1·eRF3·GTP·Mg^{2+} complex. The biological roles of eRF3 and prokaryotic RF3 are profoundly distinct. *Nucleic Acids Res.* **34,** 3947–3954
24. Shevchenko, A., Tomas, H., Havlis, J., Olsen, J. V., and Mann, M. (2006) In-gel digestion for mass spectrometric characterization of proteins and proteomes. *Nat. Protoc.* **1,** 2856–2860
25. Morth, J. P., Pedersen, B. P., Toustrup-Jensen, M. S., Sørensen, T. L., Petersen, J., Andersen, J. P., Vilsen, B., and Nissen, P. (2007) Crystal structure of the sodium-potassium pump. *Nature* **450,** 1043–1049
26. Grycova, L., Sklenovsky, P., Lansky, Z., Janovska, M., Otyepka, M., Amler, E., Teisinger, J., and Kubala, M. (2009) ATP and magnesium drive conformational changes of the Na^+/K^+-ATPase cytoplasmic headpiece. *Biochim. Biophys. Acta* **1788,** 1081–1091
27. Xu, K. Y., Zweier, J. L., and Becker, L. C. (1997) Oxygen free radicals directly attack the ATP-binding site of the cardiac Na^+,K^+-ATPase. *Ann. N.Y. Acad. Sci.* **834,** 680–683
28. Lancel, S., Zhang, J., Evangelista, A., Trucillo, M. P., Tong, X., Siwik, D. A., Cohen, R. A., and Colucci, W. S. (2009) Nitroxyl activates SERCA in cardiac myocytes via glutathiolation of cysteine 674. *Circ. Res.* **104,** 720–723
29. Aracena-Parks, P., Goonasekera, S. A., Gilman, C. P., Dirksen, R. T., Hidalgo, C., and Hamilton, S. L. (2006) Identification of cysteines involved in *S*-nitrosylation, *S*-glutathionylation, and oxidation to disulfides in ryanodine receptor type 1. *J. Biol. Chem.* **281,** 40354–40368
30. Gallogly, M. M., and Mieyal, J. J. (2007) Mechanisms of reversible protein glutathionylation in redox signaling and oxidative stress. *Curr. Opin. Pharmacol.* **7,** 381–391
31. Schafer, F. Q., and Buettner, G. R. (2001) Redox environment of the cell as viewed through the redox state of the glutathione disulfide/glutathione couple. *Free Radic. Biol. Med.* **30,** 1191–1212
32. Bogdanova, A. Y., Ogunshola, O. O., Bauer, C., and Gassmann, M. (2003) Pivotal role of reduced glutathione in oxygen-induced regulation of the Na^+/K^+ pump in mouse erythrocyte membranes. *J. Membr. Biol.* **195,** 33–42
33. Klatt, P., and Lamas, S. (2000) Regulation of protein function by *S*-glutathiolation in response to oxidative and nitrosative stress. *Eur. J. Biochem.* **267,** 4928–4944
34. Cappiello, M., Voltarelli, M., Cecconi, I., Vilardo, P. G., Dal Monte, M., Marini, I., Del Corso, A., Wilson, D. K., Quiocho, F. A., Petrash, J. M., and Mura, U. (1996) Specifically targeted modification of human aldose reductase by physiological disulfides. *J. Biol. Chem.* **271,** 33539–33544
35. Shelton, M. D., Chock, P. B., and Mieyal, J. J. (2005) Glutaredoxin. Role in reversible protein *S*-glutathionylation and regulation of redox signal transduction and protein translocation. *Antioxid. Redox. Signal.* **7,** 348–366

36. Despa, S., and Bers, D. M. (2007) Functional analysis of Na^+/K^+-ATPase isoform distribution in rat ventricular myocytes. *Am. J. Physiol. Cell Physiol* **293,** C321–C327
37. Swift, F., Birkeland, J. A., Tovsrud, N., Enger, U. H., Aronsen, J. M., Louch, W. E., Sjaastad, I., and Sejersted, O. M. (2008) Altered Na^+/Ca^{2+} exchanger activity due to down-regulation of Na^+/K^+-ATPase α2-isoform in heart failure. *Cardiovasc. Res.* **78,** 71–78
38. Cappel, R. E., Bremer, J. W., Timmons, T. M., Nelson, T. E., and Gilbert, H. F. (1986) Thiol/disulfide redox equilibrium between glutathione and glycogen debranching enzyme (amylo-1,6-glucosidase/4-α-glucanotransferase) from rabbit muscle. *J. Biol. Chem.* **261,** 15385–15389
39. Bers, D. M., and Despa, S. (2006) Cardiac myocytes Ca^{2+} and Na^+ regulation in normal and failing hearts. *J. Pharmacol. Sci.* **100,** 315–322
40. Shi, H. G., Mikhaylova, L., Zichittella, A. E., and Argüello, J. M. (2000) Functional role of cysteine residues in the (Na,K)-ATPase α subunit. *Biochim. Biophys. Acta* **1464,** 177–187

Manuscript 3

Interventricular heterogeneity in rat heart responses to hypoxia: the tuning of glucose metabolism, ion gradients, and function

Milena Segato Komniski, Sergej Yakushev, Nikolai Bogdanov, Max Gassmann, and Anna Bogdanova

Submitted 3 March 2010. Accepted in final form 3 March 2011. Published online before print March 11, 2011, doi: 10.1152/ajpheart.00220.2010
AJP - Heart May 1, 2011 vol. 300 no. 5 H1645-H1652

Am J Physiol Heart Circ Physiol 300: H1645–H1652, 2011.
First published March 11, 2011; doi:10.1152/ajpheart.00220.2010.

Interventricular heterogeneity in rat heart responses to hypoxia: the tuning of glucose metabolism, ion gradients, and function

Milena Segato Komniski,[1] Sergej Yakushev,[1,2] Nikolai Bogdanov,[1] Max Gassmann,[1,2] and Anna Bogdanova[1,2]

[1]*Institute of Veterinary Physiology, Vetsuisse Faculty and* [2]*Zurich Center for Integrative Human Physiology (ZIHP), University of Zurich, Zurich, Switzerland*

Submitted 3 March 2010; accepted in final form 3 March 2011

Segato Komniski M, Yakushev S, Bogdanov N, Gassmann M, Bogdanova A. Interventricular heterogeneity in rat heart responses to hypoxia: the tuning of glucose metabolism, ion gradients, and function. *Am J Physiol Heart Circ Physiol* 300: H1645–H1652, 2011. First published March 11, 2011; doi:10.1152/ajpheart.00220.2010.—The matching of energy supply and demand under hypoxic conditions is critical for sustaining myocardial function. Numerous reports indicate that basal energy requirements and ion handling may differ between the ventricles. We hypothesized that ventricular response to hypoxia shows interventricular differences caused by the heterogeneity in glucose metabolism and expression and activity of ion transporters. Thus we assessed glucose utilization rate, ATP, sodium and potassium concentrations, Na, K-ATPase activity, and tissue reduced:oxidized glutathione (GSH/GSSG) content in the right and left ventricles before and after the exposure of either the whole animals or isolated blood-perfused hearts to hypoxia. The hypoxia-induced boost in glucose utilization was more pronounced in the left ventricle compared with the right one. ATP levels in the right ventricle of hypoxic heart were lower than those in the left ventricle. Left ventricular sodium content was higher, and hydrolytic Na, K-ATPase activity was reduced compared with the right ventricle. Administration of the Na, K-ATPase blocker ouabain caused rapid increase in the right ventricular Na^+ and elimination of the interventricular Na^+ gradients. Exposure of the hearts to hypoxia made the interventricular heterogeneity in the Na^+ distribution even more pronounced. Furthermore, systemic hypoxia caused oxidative stress that was more pronounced in the right ventricle as revealed by GSH/GSSG ratios. On the basis of these findings, we suggest that the right ventricle is more prone to hypoxic damage, as it is less efficient in recruiting glucose as an alternative fuel and is particularly dependent on the efficient Na, K-ATPase function.

glucose utilization; redox state; ventricles

BOTH THE LEFT VENTRICLE (LV) and the right ventricle (RV) possess structural, biochemical, and metabolic differences that meet their functional requirements. The LV has approximately three times the mass and twice the wall thickness of the RV and can be viewed as a "pressure pump" whose cavity resembles an elongated cone. The RV, which pumps at a lower pressure and operates as a "volume pump" is crescent-shaped (26). The double-peaked waveform of both the right ventricular pressure and the right ventricular outflow recorded using the electrically isolated right ventricular free-wall preparation, revealed the presence of two components in the RV contractile function (26). The first is attributed to the contraction of the free wall of the RV, whereas the second is related to the LV and its septal contraction. Analysis of numerical data suggests that ~30% of the stroke output of the RV was generated by the LV (15).

These differences in the generation of force are mirrored by differences in the properties of the force-generating proteins. The distribution of myosin heavy-chain (MHC) isoforms between the ventricles supports this functional asymmetry. The RV of the rodent heart is enriched with a fast α-MHC isoform that exhibits higher levels of myosin ATPase activity than the slow β-MHC isoform (8, 31, 42). The slow muscle fiber-specific energy-saving β-MHC isoform, which requires less energy to generate cross-bridge force, is correspondingly more abundant in the LV than in the RV (21, 34).

Heterogeneity in ventricular force-generation capacity is further supported by the differences in sarcoplasmic reticulum Ca^{2+} reserve (27) between the two ventricles. Excitation propagation differs between the ventricles as do Ca^{2+}-dependent outward transient $I_{to,f}$ currents(36) and ATP-dependent, non-voltage-gated rectified K^+ currents (2, 19). These differences stem from heterogeneity in channel expression levels [e.g., that of Kv4.2, Kv4.3, KChIP2, Kv1.5, and Kv2.1 (9, 25)], densities, amplitudes, and their sensitivity to agonists (1, 25, 27, 35, 41). Loss of heterogeneity in ion-current densities after myocardial infarction results in the development of arrhythmias (25). Interventricular differences in channel-mediated passive K^+ transport imply that active transport of K^+ mediated by the Na, K-ATPase also varies between the ventricles to sustain transmembrane ion gradients. However, local differences in the abundance and activity of Na, K-ATPase in ventricular tissue have never been studied.

Heterogeneity in energy demand required for sustaining the contractile force and ion gradient preservation suggests asymmetry in energy production in the ventricles. A local difference in oxygen extraction (60–75% by the LV and 50–51% by the RV) was observed during coronary venous blood sampling in open-chest dogs (28, 49). The right and left resting coronary venous P_{O_2} is ~30 and ~20 mmHg (4.0 and 2.7 kPa), respectively, indicating higher demand for energy in the LV (49). Under resting conditions, oxygen supply is controlled by coronary blood flow, which is higher in the left coronary artery than in the right.

What happens when the oxygen supply becomes limited? Severe local or global hypoxia results in "myocardial hibernation" followed by reduction in heart rate and myocardial contractility (17). Suppression of oxidative phosphorylation fuelled mainly by fatty acid metabolism is at least partially compensated for by an increase in anaerobic glycolysis to avoid irreversible ATP deprivation (11, 12, 20, 44). In a single study, autoradiography was used to assess local glucose utilization rates in the ventricles of conscious rats (29). Data

Address for reprint requests and other correspondence: A. Bogdanova, Institute of Veterinary Physiology, Univ. of Zurich, Vetsuisse Faculty, Winterthurerstrasse 260, CH-8057, Zurich, Switzerland (e-mail: annab@access.uzh.ch).

obtained in these in vivo settings indicate the existence of LV-to-RV heterogeneity in glucose utilization, which cannot be statistically resolved because of high interindividual variation. The present study explores the mechanisms of interventricular heterogeneity in response to acute hypoxic challenge in rat hearts. Acute challenge (1 h) was employed to exclude the effects driven by the changes in gene expression. We hypothesized that the differences in oxygen supply and anaerobic metabolism, as well as those in expression and activity of ion transport systems, will result in differential sensitivity of ventricles to oxygen deprivation.

In vivo and ex vivo experimental models were used to compare systemic and autonomous responses of the ventricular tissue to reduced oxygen supply, respectively. Data obtained in animals exposed to hypoxia for 1 h were compared with those generated in isolated rat hearts perfused with hypoxic autonomous blood passing through a hollow fiber oxygenator. By the reduction of the complexity of the system, this ex vivo model offered greater precision and reproducibility. We have monitored the interventricular heterogeneity and hypoxia- sensitivity of glucose utilization, tissue ion content, and redox state. Resulting data revealed substantial differences in glucose utilization capacity and maintenance of Na^+/K^+ gradient between the LV and RV.

MATERIALS AND METHODS

Organ harvesting procedure. Male Wistar rats (180–250 g) were purchased from Janvier (Le Genest, St Isle, France). All animal experiments were approved by the Federal Veterinary Office and performed in accordance with Swiss animal protection laws and institutional guidelines that comply with guidelines of the American Physiological Society and the Institute of Laboratory Animal Resources.

In vivo hypoxic model. Rats exposed to systemic hypoxia were placed in an InVIVO$_2$ 1000 hypoxic cabinet (Ruskinn Technology/Ruskinn Life Sciences, Bridgend, UK) in standard cages. Food and water were provided ad libitum. Ten percent oxygen was used in the in vivo hypoxic settings because conscious rats can tolerate this O_2 levels well and show a prominent hypoxic response (46, 47). During the experiments, rats showed no signs of distress except for reduced activity and moderate hyperventilation. The reduction of O_2 content in the hypoxic chamber from 20% to 10% was performed gradually, reducing oxygen in 2% increments with adaptation periods of 10 min at each pO_2 level. The animals remained in the hypoxic chamber for 1 h and were euthanized immediately upon removal from the chamber. The hearts were quickly harvested and chilled in an ice-cold sucrose washing solution [300 mM of sucrose and 20 mM of a HEPES-TRIS buffer (pH 7.4 at 0°C)]. Blood from the coronary vessels was then removed by perfusion with the same sucrose solution and processed as described below. The control animals from the normoxic group spent 2 h in the air-filled InVIVO$_2$ hypoxic cabinet, and tissues were processed as described above.

Ex vivo blood-perfused rat-heart model. Before blood harvesting, animals were anesthetized using isoflurane (3% in a 1:1 mixture of O_2 and N_2O). The abdomen was opened and heparin (100 μl of 10,000 U/ml heparin; Braun, Grenchen, Switzerland) injected into the caudal vein. Blood (5–8 ml) was then collected from the caudal vein, and the animals were euthanized. Immediately after, the heart was removed and cooled down in an ice-cold physiological solution containing (in mM): 120 NaCl, 25 $NaHCO_3$, 1 $CaCl_2$, 0.15 $MgCl_2$, 10 glucose, 0.1 L-arginine, 10 TRIS-HCl, pH 7,4. The ex vivo organ perfusion circuit constructed by Dr. J. Vogel consisting of a minioxygenator, a thermostated organ chamber, and a peristaltic pump (for details see Ref. 6 and Supplemental Fig. S1; supplemental material for this article is available online at the *American Journal of Physiology Heart and Circulatory Physiology* website) filled with blood at room temperature. The heart was mounted onto a perfusion cannula and perfused via the aorta. Blood perfusion was initiated at a rate of 3 ml/min, and the temperature of the water jacket was gradually increased to 37°C. The time between tissue harvesting and the onset of the perfusion never exceeded 5 min. Blood was equilibrated with a precalibrated humidified gas mixture containing 20% O_2 (normoxia) or 5% O_2 (hypoxia), 5% CO_2, and balanced with N_2 (PanGas, Basel, Switzerland). This concentration of oxygen in hypoxic gas mixture has been chosen on the basis of our previous findings as the one causing a pronounced autonomous response of the isolated heart but does not cause irreversible damage within 1 h of exposure to it (6). Blood gases, SO_2, hematocrit, glucose, and the pH level were all controlled during the perfusion, using the Stat Profile pOX Plus Blood Analyser (Nova Biomedical, Waltham, MA). In addition, hematocrit was assessed by means of microcapillary centrifugation. Glucose consumption by erythrocytes and water loss from the organ chamber were compensated for by supplementation of 1.1 mmol/l glucose (40 μl from 140 mM stock solution) every 20 min. Blood pH, glucose concentration, and hematocrit values (pH 7.42 ± 0.02, plasma glucose 5.5 ± 1 mM plasma glucose, hematocrit 25–30%) were stable during the 60 min of perfusion. Heart rate and ECG (aVL projection) were continuously recorded with a Heart Rate Module (Hugo Sachs Elektronik-Harvard Apparatus, March-Hugstetten, Germany) connected to an analog-digital transducer (Power Lab; ADInstruments, Oxfordshire, UK). Perfusion of the coronary vessels with hypoxic blood for 60 min caused a progressive decrease in the spontaneous heart rate (Supplemental Fig. S2*B*), whereas heart rate of those perfused with normoxic blood increased by 9%. An example of the original ECG recordings from normoxic and hypoxic hearts is shown in Supplemental Fig. S2*C*.

After a 20-min restitution period, during which the contractile function has been shown to stabilize, hearts were perfused for 1 h with normoxic or hypoxic blood (So_2 98% or 35%, respectively, Supplemental Fig. S2*A*). Hearts were then cooled and the blood washed away with ice-cold sucrose washing solution. Ventricular tissue was subsequently frozen in liquid nitrogen and later used to assess tissue Na, K-ATPase activity, ATP, and reduced (GSH) and oxidized (GSSG) glutathione levels. Samples were also collected for the analysis of the tissue ion concentrations and water content in preweighed, predried tubes and processed as described below.

Tissue ion and water content. Tissue water content and ion concentrations were monitored in blood-free ventricular samples. Gravimetric measurement of tissue water content was performed by assessing wet and dry (80°C, for 72 h) weight of each sample and reporting result as the percentage of water per wet weight. After being dried, the samples were wet burned with ultrapure concentrated HNO_3. The tissue Na^+ and K^+ content was then determined using flame photometry (IL-943; Instrumentation Laboratory, Bedford, MA). Results were normalized to the dry weight of a sample.

Na, K-ATPase activity in ventricular tissue homogenates. Hydrolytic activity of the Na, K-ATPase was determined in ventricular tissue homogenates from isolated blood-perfused hearts exposed to normoxia or hypoxia (20 or 5% O_2 in a gas phase) for 60 min. The Na, K-ATPase hydrolytic activity was assayed as previously described (39). Briefly, the ventricular tissue was homogenized in KCl-MOPS buffer and was added to media containing 130 mM NaCl, 20 mM KCl, 3 mM $MgCl_2$, and 1 mM ouabain, according to experimental protocol at 37°C for 10 min. In the presence of the saturating concentrations of Na, K-ATPase substrate and ligands, the measured enzymatic activity corresponded to the pseudomaximal ATP cleavage rate, pseudo V_{max}. The enzymatic ATP hydrolysis was initiated by adding an ATP-HEPES-NaOH mixture at final concentrations of 3 mM and 30 mM, respectively, and allowed to proceed for 7 min. The reaction was then stopped by adding ice-cold 4% formaldehyde in a 1.3 M sodium acetate solution buffered with acetic acid to pH 4.3.

Samples were mixed with 100 μl of a $SnCl_2$ solution (15 mg of $SnCl_2$ in 5 ml of 0.002% acetic acid) and 100 μl of a 2% $(NH_4)_2MoO_4$ solution in distilled water. After 15 min, a colored complex of phosphate with Sn^{2+} and $(MoO_4)^{2-}$ was formed and evaluated by measuring the optical density (660 nm, Lambda 25 spectrophotometer; Perkin Elmer, Waltham, MA). Blank samples were either free of cell lysates, or the lysates were added after the ATP hydrolysis was stopped. Hydrolytic activity of Na, K-ATPase was calculated as a difference in the rate of phosphate production in corresponding ouabain-free and ouabain-containing sample pairs. Activity was normalized to the amount of protein in the homogenate quantified using a Bio-Rad protein assay (Bio-Rad Laboratories, Hercules, CA).

Ex vivo assessment of the glucose utilization rate. The autoradiography method used to assess the local rate of glucose utilization was initially developed by Kuschinsky et al. (29) for in vivo studies. A 5-μl aliquot of the radiolabeled nonmetabolizible glucose derivative ^{14}C-2-deoxyglucose (^{14}C-2-DOG; Amersham International, Cardiff, UK) from the stock (of 200 μCi/ml) was added to blood. Aliquots (25 μl) of blood were collected at 5, 10, 20, 30, and 45 min of perfusion and centrifuged (4,000 *g* for 3 min). Total plasma glucose content was assessed in plasma samples (3 μl) using a blood Glucose Meter (Ascensia Elite; Bayer, Basel, Switzerland). Also, plasma (10 μl) was added to scintillation fluid (10 ml), and the amount of ^{14}C-2-DOG was determined using a scintillation β-counter (Tricarb 1000; Packard Bioscience, Downers Grove, IL). After 45-min perfusion, the heart was frozen in isopentane and kept at −20°C. Cryosections (20 μm) were mounted on glass coverslips, thawed immediately, dried on a hot plate (60°C), and exposed to film (MIN-R; Kodak, Jena, Germany) for 2 wk together with standards (American radio-labeled chemicals) described in Ref. 29. The distribution of ^{14}C-2-DOG within and between the ventricles was determined using a densitometry camera (cool SNAP camera from Sigma DG macro D), and the images were processed using the Local Cerebral Glucose Utilization module of MCID image analysis software (Cambridge, UK).

Assessment of local tissue calcium uptake. Calcium accumulation in ventricular tissue was assessed by means of autoradiography. Radioactive tracer (30 μl, ^{45}Ca, specific activity >80.5 mCi/mmol, ~0.5 mCi/ml; Perkin Elmer) was added to blood at the onset of perfusion. At the end of the perfusion period (60 min), hearts were snap frozen in chilled isopentane (−20°C). Another experimental set included the addition of ouabain (1 μM) and ^{45}Ca to blood used to perfuse the coronary vessels. After the 60 min of perfusion, the blood was briefly washed out of the heart with an ice-cold sucrose-TRIS solution, and the heart was snap frozen in chilled isopentane. The heart was cut into sections (20 μm) and treated similarly to those perfused with ^{14}C-DOG and exposed to the film for 3 wk. The ^{45}Ca distribution fingerprints were analyzed as described above for ^{14}C-DOG.

GSH, GSSG, and ATP levels in myocardium. Tissue GSH, GSSG, and ATP levels were assessed in blood-free ventricular tissue preparations. Frozen ventricular fragments (~0.1 g) were homogenized on ice in KCl-MOPS buffer (100 mM KCl and 10 mM MOPS, pH 7.4 and deproteinized with 5% trichloracetic acid). After centrifugation (5 min, 9,000 *g*, at 4°C), an aliquot of the protein-free supernatant was neutralized to a pH of ~7 with TRIS-OH powder, and ATP was assessed using an ATP Bioluminescent Assay Kit (FLAA; Sigma, St. Louis, MO). The luminescence intensity in heart tissue samples and in standard samples of known ATP content was monitored using a Sirius luminometer (Berthold Detection Systems, Pforzheim, Germany). Values were normalized to tissue wet weight. GSH and GSSG were assessed in the protein-free supernatant using Ellmann's reagent and also normalized to sample wet weight (for details see Ref. 45).

Statistics and data analysis. Data are presented as means ± SE, and GraphPad Instat v.3.0 (GraphPad Software, San Diego, CA) was used for statistical analyses. Data were analyzed using one-way ANOVA followed by Bonferroni post hoc test. Because of the substantial differences between the ventricles, the values obtained for the RV and LV of the same heart were treated as independent entities. Significance was accepted at $P < 0.05$.

RESULTS

The anaerobic metabolic capacity of the ventricular tissue. Glucose utilization rates in the ventricles of isolated rat hearts perfused with normoxic and hypoxic blood were assessed using autoradiography as exemplified in Fig. 1*A*. Somewhat higher rates of glucose utilization were observed in LV than RV (20.2 ± 1.8 vs. 15.6 ± 1.9 μmol·100 g^{-1}·min^{-1}, respectively), in hearts perfused with normoxic blood (Fig. 1*B*).

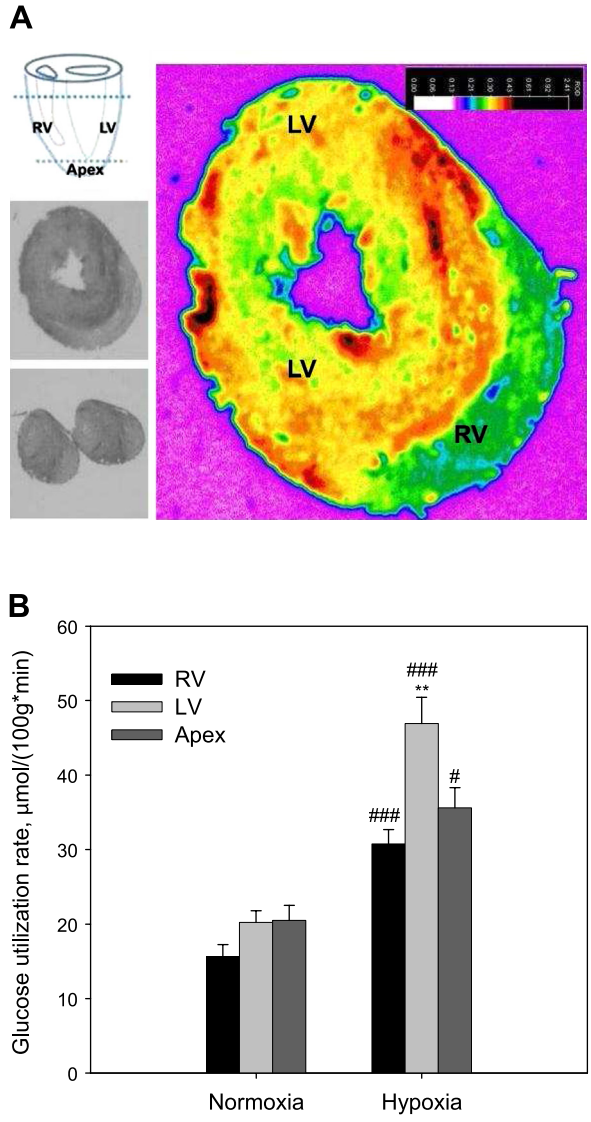

Fig. 1. Local glucose utilization rates in different regions of normoxic and hypoxic rat hearts were evaluated by autoradiography. *A*: *left*: scheme of tissue sampling with the original results of ^{14}C-2-DOG autoradiography in the ventricles and apex as well as the organ-sectioning scheme. *Right*: exemplifies the quantification of ^{14}C-2-DOG in the ventricles using densitometric image analysis software. The fire scale reveals regions of low (blue and green) and high (yellow and red) ^{14}C-2-DOG content. *B*: glucose utilization rates in the ventricles and apex of isolated hearts perfused with normoxic (20% O_2) or hypoxic (5% O_2,) blood for 1 h. $^{**}P < 0.01$ when compared with right ventricle (RV) exposed to the same percent oxygen (n = 5–7 per group). $^{\#}P < 0.05$ and $^{\#\#\#}P < 0.001$ when compared with normoxic control tissue from the same region. LV, left ventricle.

These values were lower, but within the range of mean rates previously reported in the hearts of normoxic conscious rats (53 μmol·100 g^{-1}·min^{-1} LV and 30 μmol·100 g^{-1}·min^{-1} RV) (29). Although hypoxia increased glucose utilization rates in both ventricles, utilization rates were greatest in LV compared with RV and apex (Fig. 1*B*).

Interventricular differences in glucose utilization rates in hypoxic myocardium were mirrored by heterogeneity in ATP content. Basal tissue ATP levels in the hearts obtained fresh from normoxic in vivo and ex vivo preparations did not differ between the ventricles. However, hypoxia caused selective depletion of the tissue ATP in the RV, but not in the LV (Fig. 2).

The redox state of ventricular tissue. Reduced and oxidized glutathione were used as markers of the tissue redox state. Tissue GSH content and the half-cell redox potential E_{hc} for the GSH/GSSG couple {$E_{hc} = -240 - (59.55/2)\log([GSH]^2/[GSSG])$} showed no interventricular variation in normoxic hearts (Fig. 3, *A* and *B*). Exposure of rats for 1 h to 10% O_2 resulted in development of oxidative stress in the RV but not the LV because of GSH depletion and a positive shift of the E_{hc} (Fig. 3*A*). On the other hand, perfusion of the isolated rat hearts with hypoxic blood was not accompanied by oxidation. On the contrary, it caused a slight insignificant shift ($P = 0.062$ for the LV) in the GSH and E_{hc} levels toward a more reduced state (Fig. 3*B*).

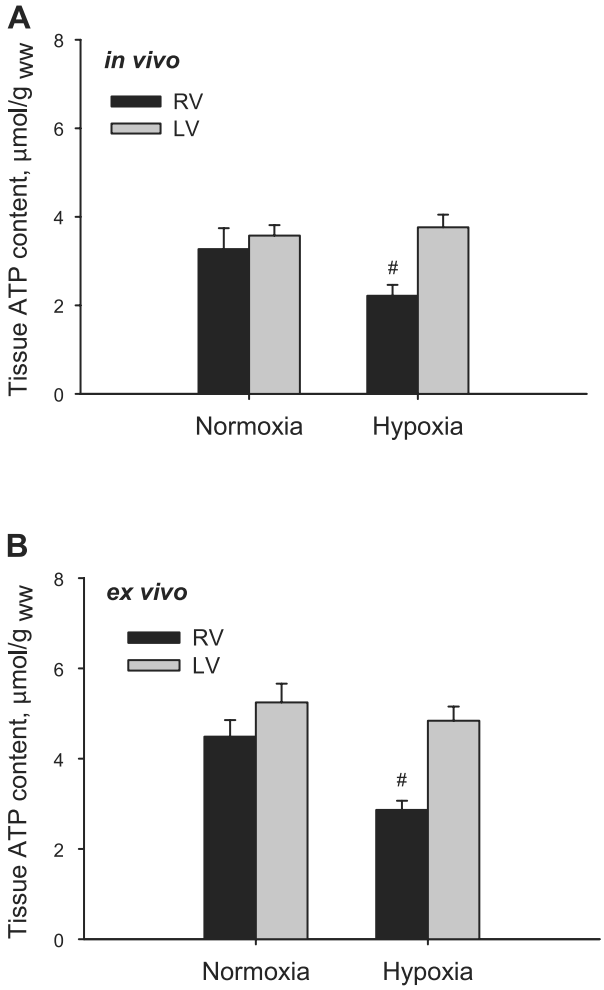

Fig. 2. Tissue ATP content was determined in differing regions of normoxic and hypoxic rat hearts, in vivo and ex vitro. *A*: ATP concentration of the RV and LV heart tissue homogenates obtained from rats after 1 h of exposure to normoxia, (20% O_2, $n = 5$) or hypoxia (10% O_2, $n = 5$). *B*: ATP concentration in the ventricles of isolated rat hearts perfused with normoxic (20% O_2, $n = 15$ per group) and hypoxic (5% O_2, $n = 5$ per group) blood for 45 min. #$P < 0.05$ when compared with LV exposed to the same percent oxygen. ww, wet weight.

Ion and water balance in myocardial tissue. Ventricular tissue Na^+ content was measured in ventricles of hearts harvested from rats exposed to normoxia (air) or hypoxia (10% O_2) for 1 h and in isolated hearts perfused with normoxic or hypoxic (5% O_2) blood for 1 h (Fig. 4*A*). Tissue sodium content in normoxic hearts in vivo was greater in the LV compared with the RV. Hypoxia had no effect on the tissue Na^+ content in LV or RV (Fig. 4*A*). Sodium levels in the LV of ex vivo hearts perfused with normoxic blood trended higher but were not significantly higher than those in the RV (Fig. 4*B*). Hypoxia caused a significant rise in LV sodium content, such that it was greater in LV compared with normoxic LV and RV as well as hypoxic RV (Fig. 4*B*). Sodium accumulation in the hypoxic LV was associated with K^+ loss in both ventricles ex vivo (Supplemental Fig. S3). However, there was no difference between RV and LV K^+ during normoxia or hypoxia. In accordance, tissue water content in the hypoxic heart did not differ from that of normoxic heart (72.68 ± 0.62 and 73.77 ± 0.96% H_2O/wet weight in normoxic and hypoxic hearts, respectively, $n = 8$).

In search for the mechanism underlying heterogeneous ion distribution between the ventricles, we have investigated the contribution of Na, K-ATPase to the ion balance ex vivo. Perfusion of hearts with normoxic blood containing low doses (1 μM) of the Na, K-ATPase blocker, ouabain, caused selective accumulation of Na^+ in the RV, suggesting that the latter expresses higher levels of Na, K-ATPase, or at least its ouabain-sensitive α2 isozyme (Fig. 5*A*). In ouabain-treated hearts the existing interventricular differences in Na^+ content were eliminated. To confirm these observations, Na, K-ATPase hydrolytic activity was assessed in tissue homogenates prepared from RV and LV of rat hearts perfused with normoxic blood. As shown in Fig. 5*B*, the rate of ATP cleavage by Na, K-ATPase in the RV homogenate significantly exceeded that in the LV. Hypoxia caused a massive reduction of Na, K-ATPase activity in both ventricles and associated with Na^+ accumulation in the RV (Fig. 4*B*).

Increased myocardial sodium content triggers secondary Ca^{2+} uptake by cardiomyocytes (40). We have observed intracellular calcium accumulation associated with increase in the RV Na^+ content in ouabain-treated hearts using $^{45}Ca^{2+}$ as a tracer. Distribution of the tracer in the ventricles was homogeneous in control hearts but shifted after perfusion with the Na, K-ATPase blocker. In ouabain-treated hearts, $^{45}Ca^{2+}$ levels in the RV exceeded those in the LV by 8.8 ± 2.2% ($n = 5$, $P < 0.001$). Furthermore, ouabain-induced sodium accumulation in the RV was associated with massive RV infarctions in 4 out of 12 hearts, whereas LV infarction was not observed.

DISCUSSION

Our data provide evidence for heterogeneity in the maintenance glucose utilization and ion and redox balance in rat heart ventricles, rendering the RV more sensitive to the hypoxia. The observed heterogeneity likely originated from the differences

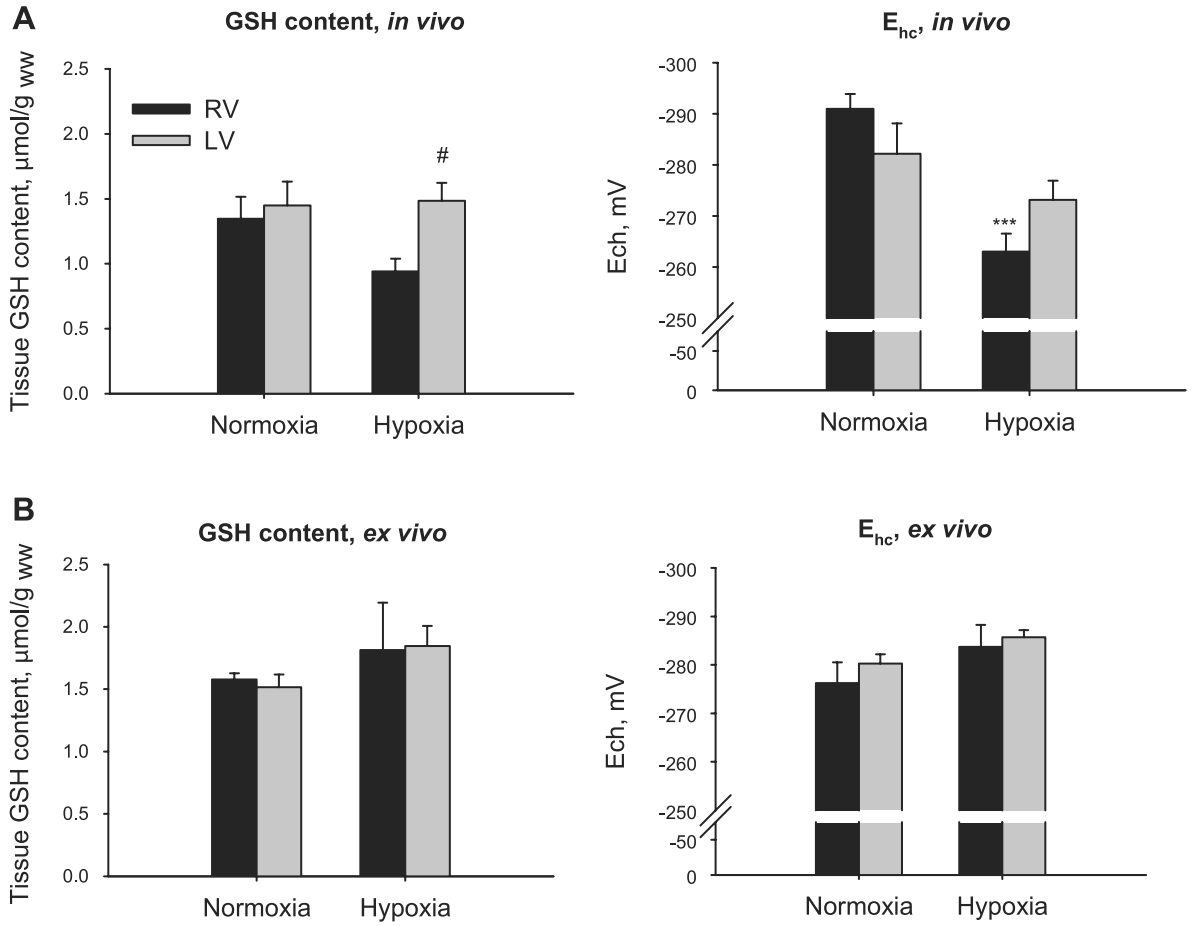

Fig. 3. GSH content and half-cell redox potential E_{hc} for the GSH/GSSG couple was calculated from the following equation: $Ehc(\text{mV}) = -240 - (59.55/2)\log([\text{GSH}]^2/[\text{GSSG}])$ in ventricular tissue. *A*: redox state parameters measured in the hearts of rats exposed to normoxia (air, $n = 5$–7) or hypoxia (10% O_2, $n = 5$–7) for 1 h before heart tissue was harvested. #$P < 0.05$ compared with the corresponding RV and ***$P < 0.001$ compared with the corresponding normoxic control. *B*: tissue GSH content and E_{hc} values obtained for isolated hearts perfused with normoxic or hypoxic blood ($n = 5$–12 per group).

in developmental origin of the ventricular cardiomyocytes (7, 10) and from the different functional requirements these cells present in an adult heart. Interventricular differences became particularly pronounced under conditions of hypoxic stress owing to the fact that the LV was less sensitive to hypoxic insult than RV. Interventricular heterogeneity in hypoxic responses is rarely taken into account when designing therapeutic strategies for the treatment of ischemic heart disease.

Effective glucose utilization is decisive for the preservation of ATP levels in hypoxic myocardium (11, 12, 20, 44). We have demonstrated limited capacity of the RV and apex for upregulation of glucose utilization upon hypoxic stimulation (Fig. 1). This limitation results in the inability of the RV to maintain the ATP level in response to hypoxia (Fig. 2). Because of the short period of hypoxic exposure, it is unlikely that the observed increase in glucose utilization rate was linked to the hypoxia-inducible factor-1-driven stimulation of de novo production of glycolytic enzymes. Rapid increase in glucose uptake in the LV could be mediated by recruitment of the GLUT-4 glucose transporters to the sarcolemma. Further investigations are required to prove whether this is the case and to delineate which of the factors listed in the recent review of Patterson et al. (37) are mediating the response.

Apex-to-LV differences in glucose utilization rates similar to those we have observed in hypoxic rat myocardium have been reported in the hearts of patients during RV pacing (38). In contrast to the RV-to-LV differences, those between the LV and apex cannot be explained on the basis of the differences in origin of cells. Cells contributing to the formation of the apex mainly originate from the same precursor as the cells that make up the LV, the cardiac crescent cells (10).

Anaerobic glycolysis does not only provide ATP for sarcolemmal enzymes such as Na, K-ATPase (48) but also contributes to the replenishment of NADH and NADPH pools. The latter is used to maintain GSH levels and to convert GSSG back into GSH in a reaction that is catalyzed by glutathione reductase. Suppression of the glycolytic NADPH production by pharmacological inhibition of glucose-6-phosphate dehydrogenase was shown to cause GSH depletion in isolated rat cardiomyocytes (22). Reduction in GSH content was observed in the RV of freshly harvested hearts where glucose utilization rates are lower compared with the LV (Figs. 3 and 5*A*, and Ref. 24). We did not assess local changes in free radical production in the ventricles directly and therefore can only speculate on the heterogeneity in generation of prooxidative equivalents in the ventricles under hypoxic stress conditions. The origin of oxidative stress in hypoxic myocardium is still debated. Mitochondrial uncoupling (18) and reduction in NO production (30) have been suggested to contribute to an increase in the H_2O_2 production under hypoxic conditions. Exposure of rats to

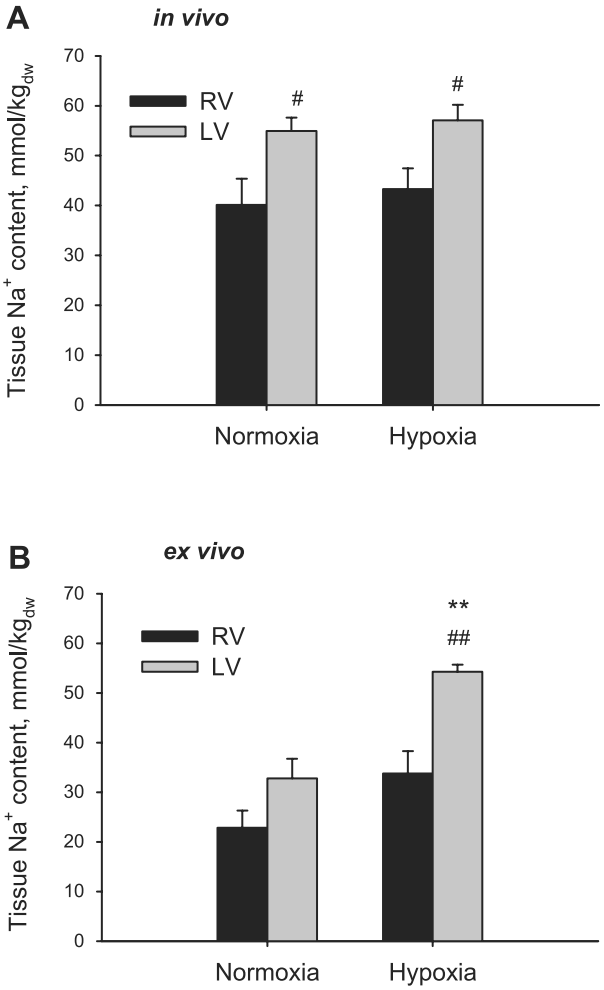

Fig. 4. Sodium and potassium concentrations were evaluated in different regions of normoxic and hypoxic rat hearts in vivo and ex vivo. *A*: Na^+ content in the LV and RV of hearts isolated from the rats exposed to air (normoxia) or 10% O_2 (hypoxia) for 1 h before the heart was harvested (n = 6–10 per condition). #$P < 0.05$ when compared with RV exposed to the same percent oxygen. *B*: Na^+ concentrations in the RV and LV of isolated rat hearts perfused with normoxic (20% O_2) or hypoxic (5% O_2) blood for 1 h (n = 6 per group). **$P < 0.01$ when compared with normoxic LV, ##$P < 0.01$ when compared with hypoxic RV. dw, dry weight.

systemic hypoxia increases the myocardial mechanical load, thereby boosting oxygen consumption (16). Pulmonary vasoconstriction in response to hypoxia could contribute to the oxidative stress observed in the RV in vivo, but not ex vivo. In addition lower glucose utilization rates in RV could result in lower NADH and NADPH production rates if our observations on the glucose utilization ex vivo are also found in vivo.

One of the interesting and unexpected findings of the present study is the heterogeneity of Na^+ levels and Na, K-ATPase activity in the ventricles. The basal Na^+ content reflects a balance between the contribution of passive transporters to the uptake of Na^+ and that of the Na, K-ATPase in mediating the active Na^+ extrusion. So far, interventricular heterogeneity in ion channel expression has only been reported for K^+ channels (2, 19, 25), but not for Na^+ channels. In the present study we have not evaluated Na, K-ATPase expression levels but focused on its functional characteristics. The activity of this enzyme depends on its isozyme composition, the phosphorylation, tyrosine nitration, *S*-nitrosylation, and *S*-glutathionylation of the catalytic and regulatory subunits, as well as the availability of substrates and ligands (5). Our data indicate that higher activity of Na, K-ATPase in the RV (Fig. 1*C*) is responsible for the RV-to-LV heterogeneity in tissue Na^+ content. LV-to-RV Na^+ gradient collapses in the heart perfused with ouabain, which is primarily blocking the ouabain-sensitive α2-isozyme (IC_{50} 1–5 × 10^{-7} M for the α2-β1 vs. 1–5 × 10^{-5} M for the α1-β1) in rodent myocardium (4, 24). The α2-β1 isozyme plays a key role in Ca^{2+} handling in the heart muscle (23). Its inhibition by perfusion with ouabain resulted in Na^+ and Ca^{2+} accumulation in the RV (Fig. 1*B*). Further studies are required to verify whether the interventricular differences we have reported in rat heart are present in human myocardium in which affinity of the α1 and α2 isoforms to ouabain differs by about fivefold (33). If results are similar in human and rat tissue, caution should be taken when

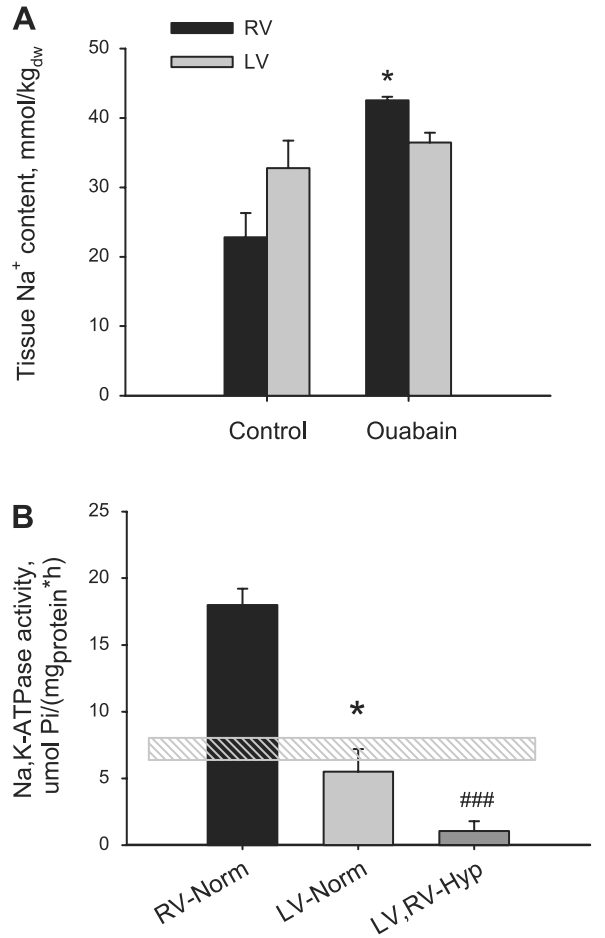

Fig. 5. The role of Na, K-ATPase in ventricular heterogeneity of ion concentrations was evaluated in isolated perfused hearts. *A*: ouabain (1 μM) was added to normoxic (Norm) blood perfusate to inhibit Na, K-ATPase, and sodium concentrations were evaluated in RV and LV, (n = 5–6 per group). *$P < 0.05$ when compared with normoxic RV. *B*: Na, K-ATPase activity was evaluated in crude homogenates prepared from the RV and LV of hearts perfused with normoxic blood (20% O_2, n = 14) and from both ventricles of hearts perfused with hypoxic (Hyp) blood (5% O_2, n = 6). The corresponding Na, K-ATPase activity range assessed in both ventricles of the normoxic heart is shown as a hatched horizontal bar. The values are means ± SE. *$P < 0.01$ compared with the values in normoxic RV. ###$P < 0.001$ compared with values in normoxic ventricular tissue homogenate.

using cardiac glycosides such as digitalis for the treatment of heart failure and atrial fibrillation (32).

Coupling of the transmembrane Na^+ gradients with the size of the Ca^{2+} stores in sarcoplasmic reticulum of cardiomyocytes, and hence with the contractile force amplitude, provides a possible explanation for the observed transventricular differences in the tissue Na^+ content. Changes in the ventricular tissue Na^+ levels were reported to result in a secondary alteration of the potential for force generation (3, 43). Our experiments were designed to assess the interventricular heterogeneity in short-term Ca^{2+} uptake. We observed greater Ca^{2+} accumulation in the RV of the ouabain-treated hearts. However, live imaging of Ca^{2+} transients in cardiomyocytes isolated from the RV and LV revealed that Ca^{2+} reserves of the RV and the LV differ (27). Furthermore, greater expression of the Na^+/Ca^{2+} exchanger was reported in LV compared with the RV in rat heart (14). Thus we hypothesize that interventricular asymmetry in basal ventricular Na^+ concentrations contributes to the RV-to-LV differences in developed peak systole pressure (13).

Our findings, together with those reported in the literature, reveal the existence of a delicate balance between the local functional requirements, metabolic processes, and activity of the Na, K-ATPase in rat cardiac tissue. The observed interventricular differences indicate that the rat RV may be more prone to hypoxic damage because of its inability to recruit sufficient amounts of glucose as an alternative source of energy and reducing equivalents. Conditions that suppress Na, K-ATPase enzyme activity, such as hypoxia, have a greater effect on RV stability because the RV is more reliant on the Na, K-ATPase than the LV. Inability to match passive and active cation flux components results in Na^+ overload.

ACKNOWLEDGMENTS

We are grateful to Dr. J. Vogel for providing us with the hollow-fiber minioxygenator manufacturing technology and for help in establishing the autoradiography assay. We thank Dr. M. Tissot van Patot for discussions and careful reading of the manuscript.

GRANTS

This work was supported by the 3R Research foundation and Swiss National Science Foundation (no. 310030-124970/1) to A. Bogdanova.

DISCLOSURES

No conflicts of interest, financial or otherwise, are declared by the authors.

REFERENCES

1. **Antzelevitch C, Sicouri S, Litovsky SH, Lukas A, Krishnan SC, Di Diego JM, Gintant GA, Liu DW.** Heterogeneity within the ventricular wall. Electrophysiology and pharmacology of epicardial, endocardial, and M cells. *Circ Res* 69: 1427–1449, 1991.
2. **Ashford ML, Bond CT, Blair TA, Adelman JP.** Cloning and functional expression of a rat heart KATP channel. *Nature* 370: 456–459, 1994.
3. **Bers DM, Barry WH, Despa S.** Intracellular Na+ regulation in cardiac myocytes. *Cardiovasc Res* 57: 897–912, 2003.
4. **Blanco G, Mercer RW.** Isozymes of the Na-K-ATPase: heterogeneity in structure, diversity in function. *Am J Physiol Renal Physiol* 275: F633–F650, 1998.
5. **Bogdanova A, Petrushanko I, Boldyrev A, Gassmann M.** Oxygen- and redox-induced regulation of the Na/K ATPase. *Curr Enzyme Inhib* 2: 37–59, 2006.
6. **Bogdanova A, Vogel J.** Isolated autologous blood-perfused heart: replacement of heterotopic heart transplantation. *ALTEX* 24: 75–76, 2007.
7. **Boukens BJ, Christoffels VM, Coronel R, Moorman AF.** Developmental basis for electrophysiological heterogeneity in the ventricular and outflow tract myocardium as a substrate for life-threatening ventricular arrhythmias. *Circ Res* 104: 19–31, 2009.
8. **Brooks WW, Bing OH, Blaustein AS, Allen PD.** Comparison of contractile state and myosin isozymes of rat right and left ventricular myocardium. *J Mol Cell Cardiol* 19: 433–440, 1987.
9. **Brunet S, Aimond F, Li H, Guo W, Eldstrom J, Fedida D, Yamada KA, Nerbonne JM.** Heterogeneous expression of repolarizing, voltage-gated K+ currents in adult mouse ventricles. *J Physiol* 559: 103–120, 2004.
10. **Buckingham M, Meilhac S, Zaffran S.** Building the mammalian heart from two sources of myocardial cells. *Nat Rev Genet* 6: 826–835, 2005.
11. **Cartee GD, Douen AG, Ramlal T, Klip A, Holloszy JO.** Stimulation of glucose transport in skeletal muscle by hypoxia. *J Appl Physiol* 70: 1593–1600, 1991.
12. **Chen CH, Liu YF, Lee SD, Huang CY, Lee WC, Tsai YL, Hou CW, Chan YS, Kuo CH.** Altitude hypoxia increases glucose uptake in human heart. *High Alt Med Biol* 10: 83–86, 2009.
13. **Correia-Pinto J, Henriques-Coelho T, Magalhaes S, and Leite-Moreira AF.** Pattern of right ventricular pressure fall and its modulation by afterload. *Physiol Res* 53: 19–26, 2004.
14. **Correia Pinto J, Henriques-Coelho T, Roncon-Albuquerque R Jr, and Leite-Moreira AF.** Differential right and left ventricular diastolic tolerance to acute afterload and NCX gene expression in Wistar rats. *Physiol Res* 55: 513–526, 2006.
15. **Damiano RJ Jr, La Follette P Jr, Cox JL, Lowe JE, and Santamore WP.** Significant left ventricular contribution to right ventricular systolic function. *Am J Physiol Heart Circ Physiol* 261: H1514–H1524, 1991.
16. **De Angelis C, Haupert GT Jr.** Hypoxia triggers release of an endogenous inhibitor of Na(+)-K(+)-ATPase from midbrain and adrenal. *Am J Physiol Renal Physiol* 274: F182–F188, 1998.
17. **Depre C, Vatner SF.** Cardioprotection in stunned and hibernating myocardium. *Heart Fail Rev* 12: 307–317, 2007.
18. **Duranteau J, Chandel NS, Kulisz A, Shao Z, Schumacker PT.** Intracellular signaling by reactive oxygen species during hypoxia in cardiomyocytes. *J Biol Chem* 273: 11619–11624, 1998.
19. **Flagg TP, Kurata HT, Masia R, Caputa G, Magnuson MA, Lefer DJ, Coetzee WA, Nichols CG.** Differential structure of atrial and ventricular KATP: atrial KATP channels require SUR1. *Circ Res* 103: 1458–1465, 2008.
20. **Fraser H, Lopaschuk GD, Clanachan AS.** Assessment of glycogen turnover in aerobic, ischemic, and reperfused working rat hearts. *Am J Physiol Heart Circ Physiol* 275: H1533–H1541, 1998.
21. **Harris DE, Work SS, Wright RK, Alpert NR, Warshaw DM.** Smooth, cardiac and skeletal muscle myosin force and motion generation assessed by cross-bridge mechanical interactions in vitro. *J Muscle Res Cell Motil* 15: 11–19, 1994.
22. **Jain M, Brenner DA, Cui L, Lim CC, Wang B, Pimentel DR, Koh S, Sawyer DB, Leopold JA, Handy DE, Loscalzo J, Apstein CS, Liao R.** Glucose-6-phosphate dehydrogenase modulates cytosolic redox status and contractile phenotype in adult cardiomyocytes. *Circ Res* 93: e9–e16, 2003.
23. **James PF, Grupp IL, Grupp G, Woo AL, Askew GR, Croyle ML, Walsh RA, Lingrel JB.** Identification of a specific role for the Na,K-ATPase alpha 2 isoform as a regulator of calcium in the heart. *Mol Cell* 3: 555–563, 1999.
24. **Jewell EA, Lingrel JB.** Comparison of the substrate dependence properties of the rat Na,K-ATPase alpha 1, alpha 2, and alpha 3 isoforms expressed in HeLa cells. *J Biol Chem* 266: 16925–16930, 1991.
25. **Kaprielian R, Sah R, Nguyen T, Wickenden AD, Backx PH.** Myocardial infarction in rat eliminates regional heterogeneity of AP profiles, I_{to} K^+ currents, and $[Ca^{2+}]_i$ transients. *Am J Physiol Heart Circ Physiol* 283: H1157–H1168, 2002.
26. **Katz AM.** *Physiology of the Heart,* 4th ed. Lippincott Williamson and Wilkins: Philadelphia, PA, 2006.
27. **Kondo RP, Dederko DA, Teutsch C, Chrast J, Catalucci D, Chien KR, Giles WR.** Comparison of contraction and calcium handling between right and left ventricular myocytes from adult mouse heart: a role for repolarization waveform. *J Physiol* 571: 131–146, 2006.
28. **Kusachi S, Nishiyama O, Yasuhara K, Saito D, Haraoka S, Nagashima H.** Right and left ventricular oxygen metabolism in open-chest dogs. *Am J Physiol Heart Circ Physiol* 243: H761–H766, 1982.
29. **Kuschinsky W, Bunger R, Schrock H, Mallet RT, Sokoloff L.** Local glucose utilization and local blood flow in hearts of awake rats. *Basic Res Cardiol* 88: 233–249, 1993.

30. **Lopez-Barneo J, Nurse CA, Nilsson GE, Buck LT, Gassmann M, Bogdanova AY.** First aid kit for hypoxic survival: sensors and strategies. *Physiol Biochem Zool* 83: 753–763, 2010.
31. **Martin AF, Robinson DC, Dowell RT.** Isomyosin and thyroid hormone levels in pressure-overloaded weanling and adult rat hearts. *Am J Physiol Heart Circ Physiol* 248: H305–H310, 1985.
32. **Morike K, Sindermann JR.** Drug treatment for chronic systolic heart failure. *Thorac Cardiovasc Surg*, 58 *Suppl* 2: S170–S172, 2010.
33. **Muller-Ehmsen J, Juvvadi P, Thompson CB, Tumyan L, Croyle M, Lingrel JB, Schwinger RH, McDonough AA, Farley RA.** Ouabain and substrate affinities of human Na^+-K^+-ATPase $\alpha_1\beta_1$, $\alpha_2\beta_1$, and $\alpha_3\beta_1$ when expressed separately in yeast cells. *Am J Physiol Cell Physiol* 281: C1355–C1364, 2001.
34. **Narolska NA, van Loon RB, Boontje NM, Zaremba R, Penas SE, Russell J, Spiegelenberg SR, Huybregts MA, Visser FC, de Jong JW, van der Velden J, Stienen GJ.** Myocardial contraction is 5-fold more economical in ventricular than in atrial human tissue. *Cardiovasc Res* 65: 221–229, 2005.
35. **Nerbonne JM, Guo W.** Heterogeneous expression of voltage-gated potassium channels in the heart: roles in normal excitation and arrhythmias. *J Cardiovasc Electrophysiol* 13: 406–409, 2002.
36. **Nerbonne JM, Kass RS.** Molecular physiology of cardiac repolarization. *Physiol Rev* 85: 1205–1253, 2005.
37. **Patterson B, Fields AV, Shannon RP.** New insights into myocardial glucose metabolism: surviving under stress. *Curr Opin Clin Nutr Metab Care* 12: 424–430, 2009.
38. **Preumont N, Jansens JL, Berkenboom G, van de Borne P, Stoupel E, Goldman S.** Effects of right ventricular pacing on regional myocardial glucose metabolism. *Eur Arch Otorhinolaryngol* 7: 584–591, 2005.
39. **Rathbun WB, Betlach MV.** Estimation of enzymically produced orthophosphate in the presence of cysteine and adenosine triphosphate. *Anal Biochem* 28: 436–445, 1969.
40. **Saini HK, Dhalla NS.** Sarcolemmal cation channels and exchangers modify the increase in intracellular calcium in cardiomyocytes on inhibiting Na+-K+-ATPase. *Am J Physiol Heart Circ Physiol* 293: H169–H181, 2007.
41. **Schram G, Pourrier M, Melnyk P, Nattel S.** Differential distribution of cardiac ion channel expression as a basis for regional specialization in electrical function. *Circ Res* 90: 939–950, 2002.
42. **Sharma S, Razeghi P, Shakir A, Keneson BJ 2nd, Clubb F, Taegtmeyer H.** Regional heterogeneity in gene expression profiles: a transcript analysis in human and rat heart. *Cardiology* 100: 73–79, 2003.
43. **Shigekawa M, Iwamoto T.** Cardiac Na(+)-Ca(2+) exchange: molecular and pharmacological aspects. *Circ Res* 88: 864–876, 2001.
44. **Stanley WC, Recchia FA, Lopaschuk GD.** Myocardial substrate metabolism in the normal and failing heart. *Physiol Rev* 85: 1093–1129, 2005.
45. **Tietze F.** Enzymic method for quantitative determination of nanogram amounts of total and oxidized glutathione: applications to mammalian blood and other tissues. *Anal Biochem* 27: 502–522, 1969.
46. **Toporsian M, Govindaraju K, Nagi M, Eidelman D, Thibault G, Ward ME.** Downregulation of endothelial nitric oxide synthase in rat aorta after prolonged hypoxia in vivo. *Circ Res* 86: 671–675, 2000.
47. **Wodopia R, Ko HS, Billian J, Wiesner R, Bartsch P, Mairbaurl H.** Hypoxia decreases proteins involved in epithelial electrolyte transport in A549 cells and rat lung. *Am J Physiol Lung Cell Mol Physiol* 279: L1110–L1119, 2000.
48. **Ziegelhoffer A, Kjeldsen K, Bundgaard H, Breier A, Vrbjar N, Dzurba A.** Na,K-ATPase in the myocardium: molecular principles, functional and clinical aspects. *Gen Physiol Biophys* 19: 9–47, 2000.
49. **Zong P, Tune JD, Downey HF.** Mechanisms of oxygen demand/supply balance in the right ventricle. *Exp Biol Med (Maywood)* 230: 507–519, 2005.

Abstract 1

Manuscript number: K719F0024

Hypoxic heart: be a trout, not a rat

Bogdanova Anna, Vogel Johannes, Yakushev Sergej, Segato Komniski Milena, Makhro Asya, Bogdanov Nikolaj, Gassmann M.

2008, 4th CBP Meeting in Africa: MARA 2008, Molecules to Migration: The Pressures of Life

Hypoxic heart: be a trout, not a rat

[1]Bogdanova Anna, [1]Vogel Johannes, [1,2]Yakushev Sergej, [1]Segato Komniski Milena, [1,2]Makhro Asya, [1]Bogdanov Nikolaj, [1]Gassmann M.
[1] Institute of Veterinary Physiology and Zurich Center for Integrative Humar Physiology, University of Zurich, Zurich, Switzerland, [2] Department of Biochemistry, M.V. Lomonosov Moscow State University, Moscow, Russia

Summary

This study was designed to compare hypoxic responses of the Na/K ATPase and oxygen-dependence of nitric oxide production in rat and trout myocardium. The obtained results indicate that Na/K ATPase in rat ventricular tissue is highly sensitive to even minor changes in blood oxygenation whereas in trout myocardium activity of this ion gradient-keeping enzyme is essentially oxygen-insensitive. Furthermore, reduction in oxygenation triggers oxidative stress and reduction in NO production in rat myocardium whereas in trout heart tissue redox state is maintained and NO levels up-regulated in response to hypoxia.

Introduction

Vertebrates show a marked variety of myocardial responses to hypoxia. Whereas the majority of mammals fail to sustain cardiac output under hypoxic conditions fishes are capable to maintain it transiently (from 20 min to weeks) even when anoxic. This profound resistance results from a balance between optimisation of the myocardial performance in order to provide oxygen delivery from the lungs/gills to the periphery and efficient protection of the myocardial tissue from the hypoxia-induced damage. In mammals reduction in oxygenation observed e.g. during local low-flow ischemia shifts the balance towards the local organ-based defence response resulting in condition known as myocardial hibernation [1]. Reduction in cardiac output following this pathological state may be life-threatening; however it allows rapid restoration of the myocardial function upon reoxygenation. Fishes on the contrary are able to maintain cardiac output for minutes to weeks even under conditions of severe hypoxia/anoxia up to several-fold (3-fold in rainbow trout heart) increase in stroke volume compensates the reduction in heart rate [2] [3]. This physiological difference results from a remarkable elasticity of fish myocardium molecular basis of which remain obscure. Nothing is known about the structure and elasticity of fish titin the major lontitudal elastic

element. Cardiac myomesin contributing to the vertical elastic axis appears to be longer in cardiac muscle compared to that in skeletal muscle of adult rainbow trout whereas in adult healthy mammals both muscles contain a single myomesin isoform [4] [5]. This is achieved by a remarkable increase in stroke volume along with reflex bradycardia [3,2]. Along with remarkable elasticity fish myocardial sarcomeres, although not different in size from those of mammals when inactive, are capable to generate contractile force over significantly broader stretching distance compared to mammalian ones [6]. Peak tension generated by trout cardiac muscle increases greatly under hypoxic conditions whereas only modest increase is reported in rat myocardial tissue [7]. Recent studies indicate that this increase in contractile force in fish heart results from the corresponding regulation of calcium handling and hypoxia-inducible calcium sensitization of contractile elements [8,9,6]. Mammalian hearts on the contrary respond do hypoxia (local or global) with acute reduction of contractile force and, when global, of heart rate. This adaptive response known as hibernating myocardium protects the heart from acute damage and enables rapid restoration of the myocardial function upon reoxygenation [1]. Being protective for the heart, myocardial hibernation may become the cause of death as oxygen supply of the peripheral organs including the brain is thus endangered during hypoxic period.

Molecular basis of these hypoxic responses remains unclear. One of the key players in control of electrical activity, calcium handling, and energy balance in the heart muscle is the Na/K ATPase. This ion transporter is oxygen- and redox-sensitive in mammalian excitable tissues [10]. Inhibition of the Na/K ATPase in hypoxic mammalian heart is well-documented but the mechanisms involved in oxygen sensing by the transporter are unclear [11]. In ventricular tissue of crucian carp the Na/K ATPase activity is maintained during prolonged hypoxic treatment (weeks, [12,13]) with no information available for acute responses of the transporter to deoxygenation and no clues on the mechanism of this sound hypoxia tolerance of the enzyme.

One of the possible trigger of hypoxia-induced suppression of the Na/K ATPase function is progressive oxidative stress in embryonic chicken cardiomyocytes [14,15]. Our recent studies show that nitric oxide plays a role of second messenger messenger rendering the Na/K ATPase oxygen-sensitive in rat cerebellar neurons [16]. Oxygen-induced responses of the Na/K ATPase in various cell types in both mammals and fishes are not associated with ATP depletion suggesting that changes in the intracellular ATP are not involved in oxygen-driven regulation of the transporter [16] [17] [18] .

This study was designed to compare oxygen-sensitivity of the Na/K ATPase in trout and rat myocardium. We furthermore assessed the changes in tissue redox state and NO production in trout and rat ventricular tissue and plasma in response to the acute changes in oxygenation.

Materials and Methods

Animals

Wistar rats (250-350 g (young animals) or 450-600 g (aged animals) were purchased from Janvier Breeding Center and kept on a commercial diet in the breeding facilities of the Institute of Veterinary Physiology. All experiments were performed in accordance with the Swiss animal protection laws and institutional guidelines. Animals were anesthetized with 5-3% halothane and heparinised. Thereafter 5-8 ml blood was collected from the vena cava and heart was harvested and placed in ice-cold phosphate buffer after the animals were killed by decapitation. Closed circuit containing self-constructed mini-oxygenator (for details see [19]) was filled with blood and the heart perfused via aorta with blood oxygenated with either humidified normoxic (20%O_2, 5% CO_2 and 75% N_2) or hypoxic (5% O_2, 5% CO_2 and 90% N_2, when not stated otherwise) gas mixture at 37°C. Normoxic pre-equilibration lasting for 20 min was followed by 1 h of normoxic/hypoxic perfusion. For left ventricular pressure measurements balloon catheter was inserted into the left ventricle and connected to a pressure transducer with signal recoded using PowerLab data acquisition system (AD Instruments). Ventricular tissue was harvested after perfusion protocol was completed and used for measurement of the Na/K ATPase.

Primary cultures of neonatal rat ventricular myocytes were prepared as described elsewhere [20]. Briefly, the hearts were harvested from the rats at postnatal days 3-4 and digested with a mixture of collagenase (11 kU/100 ml, Worthington, type IV) and pancreatin (0.1g/100 ml, Sigma). After separation from myocardial fibroblasts using Percol gradient centrifugation the cardiomyocytes were plated on collagen-coated dishes and maintained in culture for 1-3 days.

Rainbow trout (~ 300 g) were obtained from a local private fish farm (Andreas Zollinger, Riedikon, Zurich). Animals were randomly divided into two groups. One group of 6 fishes was used for the blood and heart

harvest when fresh-captured and stunned by a sharp blow into the head whereas the second group of 6 fishes was kept in a tank with water flow stopped for 1 h and sampled thereafter serving as a hypoxic group [21].

Tissue redox state assessment, detection of plasma NO_2^- levels and measurements

Samples for plasma NO_2^- measurement were collected after centrifugation of ice-cooled heparinised blood and stored at -20°C. Nitrite detection was performed using chemiluminiscence detector (CLD-88, EcoMedica, Switzerland, for details see [22]). Reduced and oxidized glutathione (GSH and GSSG respectively) were assessed in ventricular tissue homogenates prepared on ice using 150 mM KCl-10 mM MOPS-KOH solution (pH 7.4), deproteininsed with 1:1volume of 5% trichloracetic acid and using Ellmann's reagent as described elsewhere [17].

Assessment of the hydrolytic function of the Na/K ATPase in myocardial tissue

Ventricular tissue was homogenised in homogenisation solution (0.25 M sucrose and 30 mM histidine, pH 7.1, tissue: buffer ratio 1:10) and used fresh or stored in liquid nitrogen. The rate of ATP cleavage by the Na/K ATPase was determined as a difference in inorganic phosphate (Pi) production in the presence and in the absence of 2 mM ouabain in the medium containing (mM): 130 NaCl, 20 KCl, 3 mM ATP, 3 mM $MgCl_2$, 0.09% saponin 30 imidazol (pH 7.5 at 37°C). The amount of Pi was assessed photometrically as it was quantitatively converted into coloured complexes with Sn^{2+} and molybdate (for details see [23]). The obtained values were related to the amount of protein in homogenate. Protein content was measured using Folin phenol reagent [24].

Results and Discussion

Na/K ATPase and contractile force responses to hypoxia

In rat myocardium hydrolytic activity of the Na/K ATPase is profoundly dependent on oxygen saturation of the circulating blood (Fig 1A). About 5-fold reduction in hydrolytic function of the enzyme in hypoxic rat myocardium occurring as oxygen saturation of hemoglobin reduced from 96% to 35% was observed. In trout hearts hydrolytic activity of the Na/K ATPase remained unaffected by an hour of gradual hypoxic treatment when measured both at 13°C and 37°C (Fig 1B). Of note, absolute values of the ATPase hydrolytic activity in trout ventricular homogenate when measured at 37°C were about 10-fold lower than those in rat tissue under

the same conditions. Decreasing the temperature of the ATPase activity assay to 13°C, which is considered normal environmental temperature for trout caused further two-fold reduction in activity of the enzyme. This low activity of the Na/K ATPase probably matches lower passive permeability of the trout membrane for Na^+ and K^+ concurring with the heart rate of 80-100 beats/minute in trout vs 300-400 beats/minute in rat. Unfortunately, no data are available on the temperature-sensitivity of the Na/K ATPase function in trout heart. In crucian carp brain Q10 for the ATPase varied between 2 and 4 depending on the season [25]. Studies performed on the enzyme isolated from shark rectal gland and ox brain and kidney showed that the shark ATPase retained about 10% of its maximal activity at 13°C whereas the enzyme isolated from ox was fully suppressed at that temperature. At 37°C the Na/K ATPase isolated from the shark rectal glands was functioning with 95 % of maximal ATP cleavage rate whereas that of ox showed ~75% of maximal activity [26].

Decrease in activity of the Na/K ATPase in response to administration of low doses of cardiac glycosides is known to increase contractile force due to the accumulation of the intracellular calcium [27]. Hypoxia-induced deactivation of the Na/K ATPase in rat myocardium on the contrary was followed by a rapid decrease in left ventricular pressure which may be rapidly reversed upon reoxygenation (Fig 2). Trout heart in contrast respond to hypoxic with an increase in contractile force and consequently of stroke volume [27]. Fishes were shown to increase developed force and stroke volume dramatically when exposed to hypoxia [2] . This response was partially caused by hypoxia-induced calcium sensitization [6]. Reduction in activity of the Na/K ATPase under hypoxic conditions would render the trout myocardium unstable and gradually depolarizing. This was clearly not the case as its activity occurred to be acutely oxygen-insensitive. Our data on the oxygen-sensitivity of the Na/K ATPase in rat cerebellar granule cells reveal a key importance of nitric oxide production in maintenance of the high enzyme activity[16]. We thus assessed the nitrite levels in trout and rat plasma as well as in rat cardiomyocytes as a function of oxygen availability.

Nitrite pool and myocardial redox state in rat and trout

Plasma and tissue nitrite levels are accepted as a marker of nitric oxide production in the organism [22]. In conscious rats NO_2^- levels range between 150 and 250 nmol/l (our data and [22]) increasing to 522±40 nmol/l when under deep Nembutal anesthesia when respiration is suppressed resulting in systemic hypoxia. Nitrite concentration in trout plasma ranges between 1963±405 nmol/l in normoxic animals to

8591±548 in hypoxic ones. These data are close to the NOx levels reported by others [28]. Circulating nitrite may be rapidly converted into NO by deoxyhemoglobin and deoxymyoglobin comprising a pool of natural NO donor [29,30]. Due to high degree of trabeculation of the fish heart compared to mammalian heart [2] the surface for diffusion of blood-born NO is significantly higher in trout heart compared to that of rodents keeping NO levels in myocardial tissue high particularly under hypoxic conditions.

Nitric oxide synthases (NOS) are expressed in the myocardium contributing to the endogenous NO formation [31]. When not pathologically up-regulated, NOS may provide potent antioxidant protection to the myocardial tissue in particular exposed to ischemia-reperfusion [32]. From the equations (1)-(4) it becomes evident that nitric oxide competes with superoxide dismutase (SOD) for superoxide anion preventing H_2O_2 and *OH formation:

(1) $O_2 + e^-$ (NAD(P)H oxidases) $\rightarrow$ $*O_2^-$
(2) O_2+L-arginine (NOS) $\rightarrow$ NO + citrulline
(3) NO+$*O_2^-$ $\rightarrow$ $ONOO^-$ $\rightarrow$ NO_3^-
(4) $*O_2^- + e^-$ (SOD) $\rightarrow$ H_2O_2 (Fe^{2+}/Cu^+) $\rightarrow$ *OH + OH^-

Under hypoxic conditions NOS activity is limited as these enzymes require O_2 as a substrate. Instead, nitrite conversion into NO by deoxy-haemoglobin and deoxy-myoglobin is stimulated contributing to the maintenance of blood vessel tone and tissue redox balance.

We assessed oxygen-sensitivity of NO production by neonatal rat cardiac myocytes (NRCs). Nitrite accumulation in the medium was significantly reduced in NRCs incubated at 3 or 1% O_2 for 2h compared to that at 21%O_2 (Fig 3). In trout, nitric oxide production by myocardial tissue was up-regulated in response to hypoxia [33]. Of note, highest levels of NO production in fish ventricle were reported for compacta zone compared to the spongiosa zone (trabeculi) [33].

Measurements of the tissue glutathione levels were performed in ventricular tissue homogenate of hearts exposed to a short-term (1h) hypoxia or normoxia. As follows from the table 1, GSH content remained unchanged in hearts of the young animals although GSSG showed a trend to increase from 3.57±1.0% to 7.85±1.96% in response to hypoxic treatment. Ventricular tissue of the aged animals showed lower GSH compared to the young animals already under normoxic conditions with further substantial GSH deprivation triggered by deoxygenation. In trout

myocardium no hypoxia-induced oxidative stress was observed. In trout ventricular tissue both GSH and GSSG levels were maintained unchanged independent on the state of oxygenation (table 2).

Conclusions

The obtained results suggest that the ability to preserve or up-regulate NO production may play a decisive role in maintenance of redox balance in myocardial tissue under hypoxic conditions. High plasma NO_2^- levels in trout are beneficial as they may be converted to NO when nitric oxide synthases function is jeopardised due to oxygen deficiency. Possible links between oxygen-sensitivity of the myocardial Na/K ATPase in rat, lack of oxygen/-induced regulation in trout myocardium and NO production are currently investigated. Such links have been previously demonstrated in rat cerebellar neurons [16].

Acknowledgements
This study was funded by the Swiss National Science Foundation (#112449).

References

[1]. HEUSCH, G., SCHULZ, R.,RAHIMTOOLA, S.H. Myocardial hibernation: a delicate balance. *Am J Physiol Heart Circ Physiol* 288: H984-999, 2005
[2]. FARRELL, A.P. Tribute to P. L. Lutz: a message from the heart--why hypoxic bradycardia in fishes? *The Journal of experimental biology* 210: 1715-1725, 2007
[3]. FARRELL, A. From hagfish to tuna: a perspective on cardiac function in fish. *Physiol Zool* 64: 1137-1164, 1991
[4]. AGARKOVA, I., AUERBACH, D., EHLER, E.,PERRIARD, J.C. A novel marker for vertebrate embryonic heart, the EH-myomesin isoform. *The Journal of biological chemistry* 275: 10256-10264, 2000
[5]. SCHOENAUER, R., BERTONCINI, P., MACHAIDZE, G., AEBI, U., PERRIARD, J.C., HEGNER, M.,AGARKOVA, I. Myomesin is a molecular spring with adaptable elasticity. *Journal of molecular biology* 349: 367-379, 2005
[6]. SHIELS, H.A., CALAGHAN, S.C.,WHITE, E. The cellular basis for enhanced volume-modulated cardiac output in fish hearts. *The Journal of general physiology* 128: 37-44, 2006

[7]. NIELSEN, K.E.,GESSER, H. Effects of [Ca2+]o on contractility in the anoxic cardiac muscle of mammal and fish. *Life sciences* 32: 1437-1442, 1983

[8]. DEGN, P.,GESSER, H. Ca2+ activated myosin-ATPase in cardiac myofibrils of rainbow trout, freshwater turtle, and rat. *The Journal of experimental zoology* 278: 381-390, 1997

[9]. VORNANEN, M.,PAAJANEN, V. Seasonality of dihydropyridine receptor binding in the heart of an anoxia-tolerant vertebrate, the crucian carp (Carassius carassius L.). *American journal of physiology* 287: R1263-1269, 2004

[10]. BOGDANOVA, A., PETRUSHANKO, I., BOLDYREV, A., GASSMANN, M. Oxygen- and redox-induced regulation of the Na/K ATPase. *Curr Enzyme Inhibition* 2: 37-59, 2006

[11]. ZIEGELHOFFER, A., KJELDSEN, K., BUNDGAARD, H., BREIER, A., VRBJAR, N.,DZURBA, A. Na,K-ATPase in the myocardium: molecular principles, functional and clinical aspects. *General physiology and biophysics* 19: 9-47, 2000

[12]. PAAJANEN, V.,VORNANEN, M. Effects of chronic hypoxia on inward rectifier K(+) current (I(K1)) in ventricular myocytes of crucian carp (Carassius carassius) heart. *The Journal of membrane biology* 194: 119-127, 2003

[13]. STECYK, J.A., STENSLOKKEN, K.O., FARRELL, A.P.,NILSSON, G.E. Maintained cardiac pumping in anoxic crucian carp. *Science (New York, NY* 306: 77, 2004

[14]. VANDEN HOEK, T.L., LI, C., SHAO, Z., SCHUMACKER, P.T.,BECKER, L.B. Significant levels of oxidants are generated by isolated cardiomyocytes during ischemia prior to reperfusion. *Journal of molecular and cellular cardiology* 29: 2571-2583, 1997

[15]. VANDEN HOEK, T.L., BECKER, L.B., SHAO, Z., LI, C.,SCHUMACKER, P.T. Reactive oxygen species released from mitochondria during brief hypoxia induce preconditioning in cardiomyocytes. *The Journal of biological chemistry* 273: 18092-18098, 1998

[16]. PETRUSHANKO, I.Y., BOGDANOV, N.B., LAPINA, N., BOLDYREV, A.A., GASSMANN, M.,BOGDANOVA, A.Y. Oxygen-induced Regulation of Na/K ATPase in cerebellar granule cells. *The Journal of general physiology* 130: 389-398, 2007

[17]. BOGDANOVA, A., OGUNSHOLA, O., BAUER, C.,GASSMANN, M. Pivotal role of reduced glutathione in oxygen-

induced regulation of the Na+/K+ pump in mouse erythrocyte membranes. *J Membrane Biol* 195: 1-10, 2003

[18]. BOGDANOVA, A., GRENACHER, B., NIKINMAA, M.,GASSMANN, M. Hypoxic responses of Na+/K+ ATPase in trout hepatocytes. *The Journal of experimental biology* 208: 1793-1801, 2005
[19]. BOGDANOVA, A.,VOGEL, J. Isolated, autologous blood-perfused heart: replacement of heterotopic heart transplantation *ALTEX* 24: 75-76, 2007
[20]. SEN, A., DUNNMON, P., HENDERSON, S.A., GERARD, R.D.,CHIEN, K.R. Terminally differentiated neonatal rat myocardial cells proliferate and maintain specific differentiated functions following expression of SV40 large T antigen. *The Journal of biological chemistry* 263: 19132-19136, 1988
[21]. WOOD, C.M.,SHELTON, G. The reflex control of heart rate and cardiac output in the rainbow trout: interactive influences of hypoxia, haemorrhage, and systemic vasomotor tone. *The Journal of experimental biology* 87: 271-284, 1980
[22]. KLEINBONGARD, P., DEJAM, A., LAUER, T., RASSAF, T., SCHINDLER, A., PICKER, O., SCHEEREN, T., GODECKE, A., SCHRADER, J., SCHULZ, R., HEUSCH, G., SCHAUB, G.A., BRYAN, N.S., FEELISCH, M.,KELM, M. Plasma nitrite reflects constitutive nitric oxide synthase activity in mammals. *Free radical biology & medicine* 35: 790-796, 2003
[23]. RATHBUN, W.B.,BETLACH, M.V. Estimation of enzymically produced orthophosphate in the presence of cysteine and adenosine triphosphate. *Anal Biochem* 28: 436-445, 1969
[24]. LOWRY, O.H., ROSEBROUGH, N.J., FARR, A.L.,RANDALL, R.J. Protein measurement with the Folin phenol reagent. *The Journal of biological chemistry* 193: 265-275, 1951
[25]. VORNANEN, M.,PAAJANEN, V. Seasonal changes in glycogen content and Na+-K+-ATPase activity in the brain of crucian carp. *American journal of physiology* 291: R1482-1489, 2006
[26]. ESMANN, M.,SKOU, J.C. Temperature-dependencies of various catalytic activities of membrane-bound Na+/K+-ATPase from ox brain, ox kidney and shark rectal gland and of C12E8-solubilized shark Na+/K+-ATPase. *Biochimica et biophysica acta* 944: 344-350, 1988
[27]. VON LEWINSKI, D., BISPING, E., ELGNER, A., KOCKSKAMPER, J.,PIESKE, B. Mechanistic insight into the functional and toxic effects of Strophanthidin in the failing human myocardium. *Eur J Heart Fail* 9: 1086-1094, 2007

[28]. MCNEILL, B.,PERRY, S.F. The interactive effects of hypoxia and nitric oxide on catecholamine secretion in rainbow trout (Oncorhynchus mykiss). *The Journal of experimental biology* 209: 4214-4223, 2006
[29]. GLADWIN, M.T. Role of the red blood cell in nitric oxide homeostasis and hypoxic vasodilation. *Advances in experimental medicine and biology* 588: 189-205, 2006
[30]. RASSAF, T., FLOGEL, U., DREXHAGE, C., HENDGEN-COTTA, U., KELM, M.,SCHRADER, J. Nitrite reductase function of deoxymyoglobin: oxygen sensor and regulator of cardiac energetics and function. *Circulation research* 100: 1749-1754, 2007
[31]. BAROUCH, L.A., HARRISON, R.W., SKAF, M.W., ROSAS, G.O., CAPPOLA, T.P., KOBEISSI, Z.A., HOBAI, I.A., LEMMON, C.A., BURNETT, A.L., O'ROURKE, B., RODRIGUEZ, E.R., HUANG, P.L., LIMA, J.A., BERKOWITZ, D.E.,HARE, J.M. Nitric oxide regulates the heart by spatial confinement of nitric oxide synthase isoforms. *Nature* 416: 337-339, 2002
[32]. IWASE, H., ROBIN, E., GUZY, R.D., MUNGAI, P.T., VANDEN HOEK, T.L., CHANDEL, N.S., LEVRAUT, J.,SCHUMACKER, P.T. Nitric oxide during ischemia attenuates oxidant stress and cell death during ischemia and reperfusion in cardiomyocytes. *Free radical biology & medicine* 43: 590-599, 2007
[33]. AGNISOLA, C. Role of nitric oxide in the control of coronary resistance in teleosts. *Comparative biochemistry and physiology* 142: 178-187, 2005

Figure 1. Oxygen-sensitivity of the Na/K ATPase in rat and trout myocardium
A: Rat hearts were excised and perfused with autologous blood equilibrated with gas containing 5% CO_2; 3, 5, 10, 15 or 20% O_2 in N_2 for one hour. Hemoglobin oxygen saturation in blood used for perfusion was measured using CO-oximeter (IL-492, Instrumentation Laboratory AG). Thereafter hydrolytic activity of the Na/K ATPase was determined in crude homogenate at 37°C (for details see Materials and methods). The obtained data were plotted against the SO_2 values and curve fitting was performed using the following equation: $y=(a+b)/(b+cx)$ with $a=129\pm7.0$, $b=-116.95\pm13.9$, $c=1.16\pm0.13$, $y(1/2)=90.2$. Each point represents the mean of 5-8 experiments ± SD. B: Rainbow trout were exposed to a gradual hypoxia for one hour and hydrolytic activity of the Na/K ATPase was assessed in crude myocardial homogenate at 13°C and 37°C. Data are means of 4-6 independent heart samples ±SD.

Figure 2. Original recording of the left ventricular pressure (LVP) in isolated blood-perfused heart

Balloon catheter was inserted into the left ventricle of the isolated rat heart perfused with autologous blood via aorta and LVP recorded continuously. Prior to entering the coronaries blood was warmed to 37°C and equilibrated with gas phase consisting of 20% O_2, 5% CO_2, the rest N_2 resulting in haemoglobin oxygen saturation (SO_2) of 98%. Arrows mark the time points when oxygen level in gas phase was reduced to 5% (SO_2 of 35%) and thereafter restored to the original 20% O_2.

Figure 3. Oxygen-dependence of nitrite production by neonatal rat cardiomyocytes

Cells were exposed to either 21% O_2 (normoxia) or 1% O_2 (hypoxia) for two hours. Accumulation of nitrite in the incubation medium was used as a marker of nitric oxide production. Data are means ± SD for 6 independent experiments. * denotes $p<0.05$ and *** stands for $p<0.001$ compared to normoxic conditions (pO_2 20 kPa)

Table 1.GSH content in rat ventricular tissue

Values are means of 5-8 experiments expressed in μmol/mg wet weight ±SD. * denotes $p<0.01$ compared to the corresponding normoxic control; # indicates $p<0.01$ between the old and the young animals.

Table 2. GSH and GSSG content in trout ventricular tissue

Fig 1

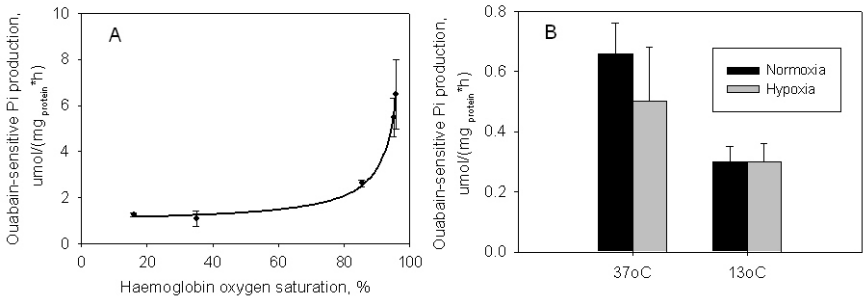
A
Ouabain-sensitive Pi production, umol/(mg protein *h)
Haemoglobin oxygen saturation, %
0
2
4
6
8
10
0
20
40
60
80
100
B
Normoxia
Hypoxia
37oC
13oC
0.0
0.2
0.4
0.6
0.8

Fig 2

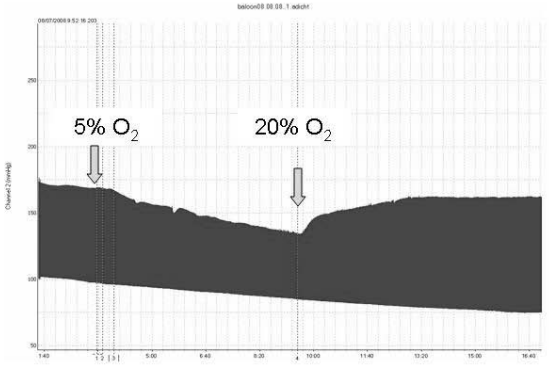
5% O2
20% O2

Fig 3

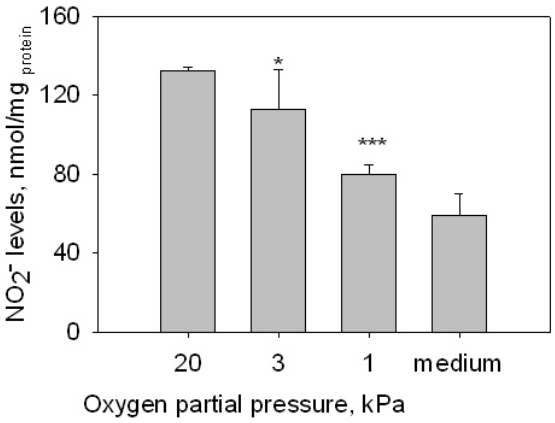

Table 1 GSH content in ventricular tissue

Age group	20% O_2	5% O_2
Young(6-10 weeks)	1.73±0.08	1.77±0.13
Old (≥20 weeks)	1.51±0.02$^{\#}$	0.82±0.05$^{\#*}$

Values are expressed in μmol/mg ww. * denotes $p<0.01$ compared to the corresponding normoxic control, # indicates $p<0.01$ between young and old animals

Table 2
GSH and GSSG levels in trout ventricular tissue

	Normoxia	Hypoxia
GSH, nmol/mg protein	3.10±0.97	3.28±0.73
GSSG, %	3.00±0.88	3.81±1.90

Curriculum Vitae

- YAKUSHEV
- Sergey Sergeevich
- Born in November 28th, 1982 in Moscow (Russia)
- Russian
- Married, 1 child

- **Education**

- **2000-2005**, student, M.V. Lomonosov Moscow State University, Faculty of Biology, Biochemistry department, Moscow, Russia
- **2005**, Diploma in Biochemistry with Honor
    - Diploma subject: biochemistry
    - Title of diploma thesis: "Comparative analysis of properties of Na,K-ATPase from rabbit kidney and duck salt gland"
- **2005-2008**, junior researcher fellow, M.V. Lomonosov Moscow State University, Faculty of Biology, Biochemistry department, Moscow, Russia
- **2008-2012**, PhD student, University of Zurich, Institute of Veterinary Physiology, Zurich, Switzerland

- **Publications, abstracts and manuscripts**

Publications and abstracts:

1. Petrushanko I., **Yakushev S**., Mitkevich V., Kamanina Y., Ziganshin R., Meng Xian Yu, Anashkina A., Makhro A., Lopina O., Gassmann M, Makarov A., Bogdanova A., 2012, "Catalytic subunit S-glutathionylation of the Na,K-ATPase as a determinant of the enzyme oxygen-sensitivity", JBC (submitted)

2. **S. Yakushev**, M. Band, M. Tissot van Patot, M. Gassmann, A. Avivi, A. Bogdanova, 2012, "Cross-talk between S-nitrosylation and S-glutathionylation in control of the Na,K-ATPase regulation in hypoxic heart", Am J Physiol Heart Circ Physiol. (submitted)

3. Komniski M., Yakushev S., Bogdanov N., Gassmann M., Bogdanova A., 2011, "Interventricular heterogeneity in rat heart responses to hypoxia: the tuning of glucose metabolism, ion gradients, and function", Am J Physiol Heart Circ Physiol. 300(5):H1645-52

4. **Yakushev S**, Petrushanko I, A. Makhro, M. Segato Komniski, Mit'kevich VA, Lopina OD, Makarov AA, M Gassmann, and A Bogdanova, 2010, "Molecular mechanisms in control of Na,K-ATPase function in hypoxic heart", Cardiovasc Res. 2010 Jul 15;87 Suppl 1:S103

5. A. Bogdanova, D. Mihov, P. Mocharla, **S. Yakushev**, J. Vogel, M. Gassmann, R. Tavakoli, 2010, "Two faces of nitric oxide: behind cardioprotective effects of erythropoietin." Cardiovasc Res. 2010 Jul 15;87 Suppl 1:S85

6. Bogdanova Anna, Vogel Johannes, **Yakushev Sergej**, Segato Komniski Milena, Makhro Asya, Bogdanov Nikolaj, Gassmann M., 2008, "Hypoxic heart: be a trout, not a rat", 4th CBP Meeting in Africa: MARA 2008, Molecules to Migration: The Pressures of Life

7. Petrushanko I., Mit'kevich V., Borzova V., **Yakushev S**., Lopina O., Makarov A., 2009, "Different domain organization of two main conformational states of Na+/K+-ATPase", Biofizika; 54(6):1019-25.

8. **Yakushev SS**, Kumskova EM, Rubtsov AM, Lopina OD, 2008, "Effect of colchicine on sensitivity of duck salt gland Na,K-ATPase to Na+", Biochemistry (Mosc). 2008 Sep;73(9):990-4.

Manuscripts in preparation:
- Yakushev S., Mikhov D., Bogdanova A., Grenacher B., Vogel J., Tavakoli R., Gassmann M., Bogdanova A. "Coronary vessels as a target for cardioprotection by erythropoietin"

- **Grants and Awards**

- Personal Forschungskredit: Candoc, 2011-2012, 53820CHF

Acknowledgements

I would like to thank Professor Dr. Max Gassmann for giving me the opportunity to be a part of his team and to do my PhD work in one of his labs.
In addition I would like to thank Dr. Bogdanova Anna for her outstanding support as a thesis supervisor and for her patience and guidance through these four years.
My special thanks to Prof. Dr. Carsten Wagner and to Prof. Dr. Kaethi Geering for their tutorship as members of my PhD thesis committee.
I would like to thank also rulers of the lab: Beat Grenacher, Daniela Gerst, Mikola Bogdanov, Olga Vogel and Michaela Bednar for technical assistance.
Also I would like to express my thanks to Prof. Dr. Johannes Vogel, Dr. Lara Ogunshola, Dr. Louise Ostergaard, Dr. Thomas Gorr, Dr. Jorge Soliz, Dr. Abraham Al Ahmad, Dr. Deyan Mikhov and Dr. Arezoo Daryadel for sharing scientific knowledge and perfect teamwork.
Many thanks to all my colleagues and friends Robert Jacobs, Dr. Milena Komniski, Dr. Edith Schneider, Dr. Markus Thiersh, Maria Alvarez, Victor Diaz, Sarah Duermueller, Sabrina Engelhardt, Manuela Gianella, Tanja Guentert, Dr. Thomas Haider, Asya Makhro, Daniela Nizzari, Caroline Leuenberger, Dr. Elena Gammella, Dheeraj Shinde and Dr. Junmin Hu for the best scientific and friendly atmosphere.
I would like to express my special gratitude to my wife Nele Sprekeler and my daughter Runa for understanding, love and motivation.
Finally I would like to thank my family, my parents and grandparents for their encourage and support.